PROCEEDINGS OF THE SCHOOL OF UNDERGROUND MINING, DNIPROPETROVS'K/YALTA, UKRAINE, 2-8 OCTOBER 2011

Technical and Geoinformational Systems in Mining

Editors

Genadiy Pivnyak
Rector of National Mining University, Ukraine

Volodymyr Bondarenko
Department of Underground Mining, National Mining University, Ukraine

Iryna Kovalevs'ka
Department of Underground Mining, National Mining University, Ukraine

CRC Press
Taylor & Francis Group
Boca Raton London New York Leiden

CRC Press is an imprint of the
Taylor & Francis Group, an Informa business
A BALKEMA BOOK

CRC Press/Balkema is an imprint of the Taylor & Francis Group, an informa business

Typeset by Olga Malova & Kostiantyn Ganushevych, Department of Underground Mining, National Mining University, Dnipropetrovs'k, Ukraine
Printed and bound in LizunovPress Ltd, Dnipropetrovs'k, Ukraine

Published by: CRC Press/Balkema
P.O. Box 447, 2300 AK Leiden,The Netherlands
e-mail: Pub.NL@taylorandfrancis.com
www.crcpress.com – www.taylorandfrancis.co.uk – www.balkema.nl

ISBN: 978-0-415-68877-2 (Hbk)
ISBN: 978-0-203-33266-5 (eBook)

Technical and Geoinformational Systems in Mining – Pivnyak, Bondarenko & Kovalevs'ka (eds)
© 2011 Taylor & Francis Group, London, ISBN 978-0-415-68877-2

Table of contents

Technical and Geoinformational Systems in Mining – Pivnyak, Bondarenko & Kovalevs'ka (eds)
© 2011 Taylor & Francis Group, London, ISBN 978-0-415-68877-2

Preface

The second collection of articles dedicated to the "School of Underground Mining" conference embraces many important scientific trends such as implementation of new mining methods to extract mineral deposits with high methane content together with new methods of roof management during high rates of the longwall advance. Specific attention is given to mathematical simulation of the support functioning in the development mine workings, creation of 3-D modeling to study stress-strain state of the rock massif and development of new bolt support designs.

Much of work is done in order to simulate and assess economic and ecological risks during undermining land surface together with forecast of dynamic phenomena in regional zones of the Donbass mines. Geoinformational systems in mining, electro-stimulation of chemical reactions in coal and new methods of mine wastes utilization are scrutinized as well.

Consideration is given to rational parameters of ventilation and degassing at production units of deep mines with use of air cooling complex systems.

Taking into account worsening of the mining-geological conditions for conventional extraction of coal, there is much of attention dedicated to borehole underground coal gasification technology at Ukraine's coal deposits. Very intriguing topic is connected with one of the most perspective and abundant sources of energy on the planet – gas hydrates. The question of their prospecting, properties and ways of extraction is also covered in this book.

Examination is given to financial conditions of work and financial strategy of mining industry in Poland Ukraine and other countries.

Genadiy Pivnyak
Volodymyr Bondarenko
Iryna Kovalevs'ka
Dnipropetrovs'k
October 2011

Technical and Geoinformational Systems in Mining – Pivnyak, Bondarenko & Kovalevs'ka (eds)

Induction heating in electrotechnology of machine parts dismantling

G. Pivnyak & N. Dreshpak
National Mining University, Dnipropetrovs'k, Ukraine

ABSTRACT: General requirements for induction heating of machine parts connections with a purpose of their dismantling are substantiated. The methodology for the specific surface power and other mode parameters determining that meet formulated requirements is developed. The influence of electromagnetic field parameters on the character of thermal process development is shown.

1 FORMULATING THE PROBLEM

Cylindrical steel connections of machine parts (bushings to a shaft) made with an interference fit are widely used in machine-building and mining. Bushings fittings on the shaft are often made as piles and bandages that fix the position of other parts on the shaft, and prevent their axial movement. Such type connections also include internal bearing rings fittings on the shaft.

While repairing and testing machines it is necessary to perform dismantling. Connections dismantling realized by means of the axial loads using removers accompanied with damage surfaces as emerging surface scratches. After several repairs the shaft becomes unusable. Large numbers of dismantling result in substantial material losses.

Heating details connections permit avoiding undesirable consequences. While heating bushing enlargers and it can be easily removed from the shaft without any surfaces damages. One of the most effective methods of dismantling is induction heating of details connections. Dismantling is realized with minimum time and energy costs to be typical for direct heating systems.

At the same time connections heating modes that lead to interference liquidation and conditions necessary to dismantle the site are not studied enough. Induction heating of cylindrical part connections is characterized by the fact that along with electromagnetic and thermal processes there are temperature deformation processes in the system which results in the bushing extension. This significantly affects the conditions of heat transfer between the bushing and shaft, and determines the level of temperature. Lack of theoretically substantiated mode parameters results in practical use of induction heating systems with unsuccessful constructive decisions and relatively low technical and economic factors.

Thus there is a need for the research aimed at defining the parameters of rational heating mode, providing on this basis with efficient connections dismantling and improve technical and economic factors of induction units (reducing mass, size, and cost).

There is determined basic structure of an investigated object (Figure 1).

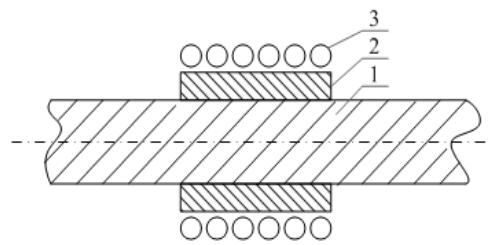

Figure 1. System "inductor-collection": 1 – shaft; 2 – bushing; 3 – coil winding.

A coil winding 1 of an induction installation is located on the surface of the thin-walled equal thickness bushing 2, which is connected to the shaft with interference. Heating modes should be connected to the temperature deformation processes that result in interference liquidation and create conditions for the connection dismantling. In the presence of interference fit a direct contact between the bushing and shaft is possible owing to the protruding hard surfaces. During the heating process of the bushing and its extension the interference is gradually liquidated. In this context the area of direct contact of solids decreases following by significant changes in thermal transfer conditions. The feature of details connection dismantling associated with the contact thermal conductivity changing between the bushing and shaft should be taken into account when analyz-

ing the process of heating.

Specific literature analysis shows that interconnected electromagnetic, thermal and mechanical processes in such system were not previously considered. The criteria of dismantling operation efficiency are not determined. Therefore it is necessary to specify the requirements for the heating process and to determine the conditions for their implementation. It is required to identify available dependences between the parameters of electromagnetic fields and temperature of heating as well as the influence of individual parameters field on the nature of the heating process. This will allow establishing rational heating modes, will provide them with efficient connection dismantling, and will improve technical and economic factors of an induction setup.

Induction heating process control can be done by changing the parameters of inductor current. Variants of sinusoidal and pulsed current are considered. Under such conditions it is expedient to focus on variant implying changing the frequency of current repetition. To consider the variant it is necessary to guarantee a possibility of thermal process modeling under heat sources impulsive effect on the bushing surface.

2 INDUCTION HEATING REQUIREMENT FOR MACHINE PARTS DISMANTLING

Selected heating mode should ensure the reliability of dismantling operation. Attention is paid to temperature conditions of heating in connection area of the shaft and bushing as the process of interference liquidation takes place while the bushing extension. It is important to consider not only individual local areas of the connection but also the whole surface as dismantling implies interference liquidation within the area of the contact surface. Unsuccessfully selected mode may lead to the fact that in some local areas or the within the whole connection surface the interference will not be liquidated and dismantling will not be performed. Thermal heating mode is determined by configuration and parameters of the current magnetic field. Therefore the problem should be solved by means of substantiating the required characteristics of the magnetic field and determination of the heating mode conditions.

Modern tools of dismantling connections have to guarantee high technology of operation primarily determined by time spent for its implementation. This characteristic is particularly important if there repair time is limited. The time of parts heating reduction results in energy saving by means of increasing heating power i.e. the use of high power rated source. This way of the problem solving leads to increased cost of power and lowering its technical and economic factors. This is especially important when using devices of power transforming equipment (frequency converters). Therefore selecting a mode it is necessary to find a compromise that will ensure an acceptable rate of nominal power of energy source with negligible heating time.

Ensuring reliability, feasibility and energy efficiency of the dismantling process, reducing the rate of nominal power of the supply are the requirements that should be met to improve technical and economic factors of induction heating; besides they determine its high performance characteristics. The general requirements for induction heating imply the determining the conditions and ways of their implementation. It can be done on the basis of analyzing the temperature modes of interference liquidation, and studying the picture of magnetic field.

Taking into consideration the variety of fitting types as well as properties of steel products it is determined the required temperature difference ΔT_R between the internal bushing the shaft surfaces.

Depending upon the axial symmetry of the system (symmetry axis of the shaft) it is expedient to obtain required value of the temperature difference simultaneously in all points of mating surfaces. It prevents overheating of certain areas of a connection, and reduces time for interference liquidation across its surface. Hence a need for uniform distribution of heat sources on the surface of a bushing is obvious. Magnetic field with the same intensity at all points of the surface of the shaft is the solution. In the system of induction heating of cylindrical parts connections the size of the bushing heated is limited. Therefore there are end effects that distort magnetic field. Getting the necessary field picture is possible by changing coil winding step. The task is to define the necessary change of this parameter. Considering the variety of design solutions offers conducting physical modeling of electromagnetic processes directly in real objects. It helps to obtain required magnetic field configuration based on the specific measurements of field tension on the heated surface. Measurements are carried out by sectional winding located on the surface of bushings. The values of EMF (electromotive force) induced in each section of a measuring winding allow to estimate the field tension of a bushing area where a curtain section is located. Under equality of EMF each section receives a homogeneous magnetic field. It is used 50 Hz current in an experiment which flows through the inductor and does not result in significant bushing heating interference liquidation. This heating mode applies to use relatively cheap simple low-power equipment. The method of magnetic field

forming is developed to reveal the idea and sequence of actions carried out during the experiment. This field application in the active induction setup for connection dismantling ensures constant for the whole surface of the bushing surface value of specific power, and allows using one-dimensional models that simplifies the modeling of either electromagnetic or thermal processes.

3 THE METHODOLOGY FOR HEATING MODE PARAMETERS DETERMINING

It is shown that choice of P_0 level significantly influences the thermal process character (Vypanasenko 2008). It is proposed to set the value of P_0 to provide the required level of ΔT_R in transient heating mode. Herewith, required temperature conditions for connections dismantle are stored in a stationary mode. This requirement for P_0 determination is important for the heating time reduction, increased reliability and efficiency of technological operations.

The modeling of electromagnetic processes in the heating system is performed (Dreshpak 2009). The modeling of method is substantiated, the algorithm of the specific surface power, current frequency and other settings definition that provide the conditions necessary for the connection dismantling are developed.

It is shown that under conditions typical for the induction heating of parts connections with the purpose of their dismantling it is necessary to consider a one-dimensional longitudinal magnetic field that operates in a continuous cylinder (Vypanasenko 2008). It is proved the expediency of analytical method of electromagnetic processes calculation in the system. The method takes into account the features of connections induction heating technology (the one-dimensional electromagnetic field, the limitation of penetration depth with a bushing thickness Δ_b) and provides highly informative and accurate results. In the process of analytical dependences formation for the specific surface power calculating P_0 the assumptions is introduced: heat losses from the external and lateral surfaces are not available.

The value of P_0 is received from the formula

$$P_0 = \alpha_i \cdot \Delta T_R \cdot \frac{R_2}{R_1}, \quad (1)$$

where R_1 and R_2 – external and internal bushing radii.

Contact thermal conductivity between the bushing and the shaft α_i is defined experimentally identifying its value directly on the object to be dismantled (Patent 43365). During low-temperature (without interference liquidation) stationary heating measurements are made on the lateral surface of internal T_i and external T_e temperatures of its surfaces. Also surface temperature of the shaft T_s is taken. Figure 2 illustrates the points of temperature T measurement.

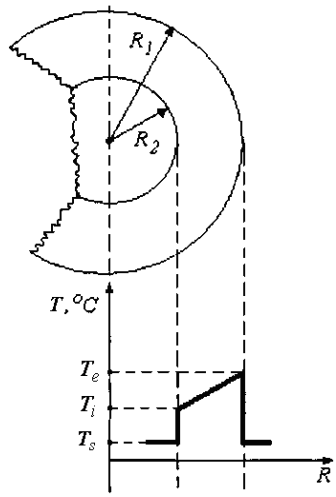

Figure 2. The characteristic of temperature in a stationary connection heating mode.

The value of α_i is received from the formula

$$\alpha_i = \frac{(T_e - T_i)\lambda_{st}}{(T_i - T_s)(R_1 - R_2)}, \quad (2)$$

where λ_{st} – factor of thermal conductivity of steel.

When choosing the current frequency of induction installation it is offered to consider high energy efficiency of the heating process, limiting the penetration of electromagnetic field trough the shaft and taking into account the default output values of power supplies frequency. Complete attenuation of electromagnetic waves accounting the dependence of relative magnetic permeability μ of the field strength H is at a distance from the surface of a bushing $X_n = 1.68 \cdot \Delta_e$. Then the formulated condition corresponds inequalities

$$X_n \le \Delta_b;\ \Delta_e \le \Delta_b / 1.68, \quad (3)$$

where Δ_b – bushing thickness; Δ_e – depth of penetration of electromagnetic waves, calculated on the

basis of the value of μ – bushing surface (μ_e). To limit mode $\Delta_e = \Delta_b / 1.68$ "deep" bushing heating is typical. This mode corresponds to the lower recommended value of inductor current frequency. Figure 3 shows the dependence $f_L(P_0)$.

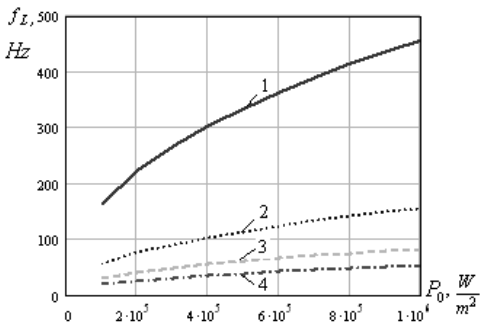

Figure 3. $f_L(P_0)$ dependencies: 1 – Δ_b = 0.005 m; 2 – Δ_b = 0.01 m; 3 – Δ_b = 0.015 m; 4 – Δ_b = 0.02 m.

The initial frequency of the power source is chosen in view of its common values and the condition $f_g \geq f_L$. Figure 3 shows that at the bushing thickness being less than 2 cm it is possible to carry out heating with the industrial current frequency of 50 Hz. Under lower thickness values and also under size restrictions in design it is reasonable to use high frequencies (kHz).

Developed mathematical model is focused on determining the mode parameters P_0, f_g, H_e (H_e is the value of magnetic field tension on the bushing surface). The parameters guarantee temperature conditions for connection dismantling and are used for inductor calculation, nominal power of energy source selection applying known methods.

4 THE INFLUENCE OF ELECTROMAGNETIC FIELD PARAMETERS ON THE CHARACTER OF THERMAL PROCESS DEVELOPMENT

The parts connections dismantling process is directly connected with thermal heating modes. Therefore there was a need to evaluate the effects of electromagnetic parameters on the thermal process, and to confirm their eligibility for the technological operation. This led to a mathematical model creation to study transient and stationary thermal processes that take place in a cross-section of the bushing. The implementation of the one-dimensional longitudinal magnetic field acting in the bushing allow describing the non-stationary process of connection induction heating with the one-dimensional heat-conduction equation in second order partial derivatives. The impact of the bushing extension on the value of the contact thermal conductivity α_i of the parts connection is taken into account and also the possibility of the process calculating in the presence of pulsed current in an inductor is realized.

The modeling pulse current of the inductor is done by periodic input and output of heating sources concentrated in the active layer of the bushing that allows analyzing the possibility of pulse-frequency control for heating.

There are a number of factors that affect the nature of thermal process in the bushing: the specific surface power P_0, the current frequency of inductor f_g, the value of the contact thermal conductivity α_i. A heating modeling indicates that on the increased current frequency of inductor the necessary value of ΔT_R for dismantling realization is achieved at the higher level of temperature on the external surface of the bushing to be explained by more vivid surface effects. This dependence should be considered determining the rational value of current frequency. It is shown that the current frequency influence on the character of the thermal process it is manifested in different values of ΔT delays relative to the start of heating because of the character of heat sources location in a cross-section of the bushing. With $\alpha_i = const$ the increase of a specific surface capacity reduces heating cycle time t_c of details connection. The non-linear characteristic of this dependency with a significant time increase with low capacity values (Figure 4) is distinctive. Here $n = P_d / P_0$ (P_d –estimated power). The reduction during the heating process of the value of α_i is equivalent to the high surface capacity action which ensures heating cycle time reduction.

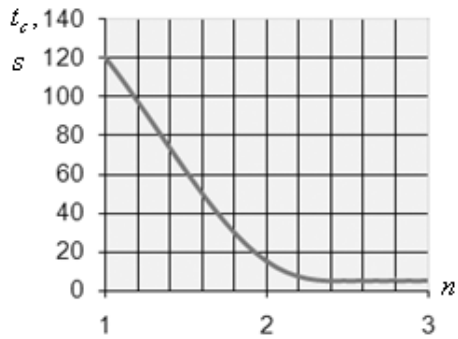

Figure 4. $t_c(n)$ dependence.

The thermal contact conductivity α_i reduction significantly modifies the character of temperature distribution in a cross-section of the bushing. There is a leveling of temperature in the area close to its internal surface (Figure 5). The value of $\Delta T = \Delta T_R$ necessary for dismantling realization is achieved under lower values of surface temperature of the bushing. The increase of heating time is followed by the increase of the speed growth rate of ΔT owing to thermal deformation of the bushing (Figure 6).

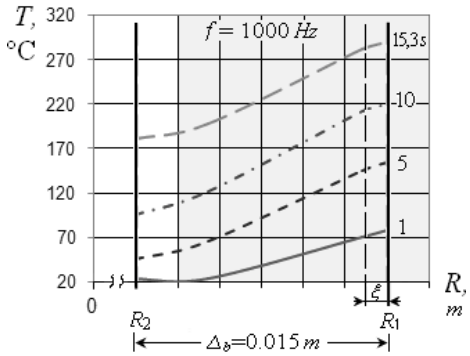

Figure 5. The temperature distribution taking into account $\alpha_b(\Delta T)$ dependences.

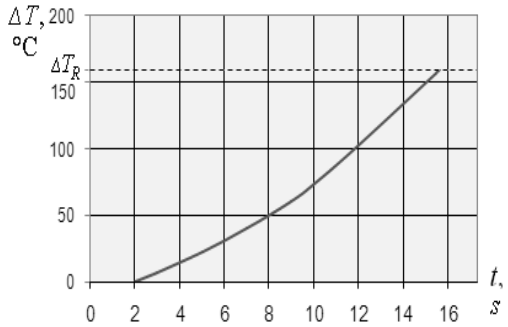

Figure 6. $\Delta T(t)$ Dependence during α_i changing in the heating process.

The slowing-down of ΔT growth at the initial stage of heating depends on significant α_i that corresponds to close contact between the bushing and shaft. The dependence in Figure 6 is obtained by the estimated value of the specific power P_0 that confirms the fact of a thermal mode necessary for dismantling occurrence in a transitional mode of heating. It is shown that decreasing the thickness of the bushing Δ_b the heating cycle time t_c decreases. The increase of P_0 results in more sizeable t_c reduction. The character of these dependences is the result of a contact thermal conductivity action in steel. As a result of inductor current pulse modeling it is shown that the increase of sinusoidal pulses frequency results in the increase of the temperature difference ΔT indicating the possibility of heating temperature conditions operation.

To identify the value of the contact thermal conductivity of the connection area between the bushing and shaft α_i by means of the experimental setup the low temperature (50 °C) heating of the bushing surface was performed. In the stationary heating mode by means of a non-contact pyrometer the temperatures on the lateral surface of the bushing and the shaft surface were measured. The values of α_i were calculated using dependence (2).

The value of α_i obtained experimentally indicates that when there is a tight interference fitting there are favorable conditions for the transfer of heat from the bushing to the shaft. The value of α_i significantly (in two orders) exceeds the value of a heating transfer index from the external surface of the bushing.

If it is necessary to reduce the heating cycle time t_c significantly the use of forced heating mode of details connections is required (Patent 43339). To realize the forced heating mode the frequency of current pulse repetition keeps stable in the period of time that corresponds to the surface temperature increase, and its value is changed up to complete dismantling the connection. The control method allows reducing the heating cycle time by 30 per cent.

5 CONCLUSIONS

The development of methodology for the specific surface power P_0 and other mode parameters on the surface of the bushing determining allows making a reasonable choice of inductor and power source parameters, and abandon the existing in induction heating practice of over-rated power source usage. If the method is available the savings for one installation purchasing is several thousand dollars. The weight and dimensions of power source reduce significantly (by tens of per cent) indicating improved overall parameters of an induction setup.

REFERENCES

Vypanasenko, N.S. 2008. *The specific surface power of induction heating of parts connections made by interference fit determining.* Bulletin of Azov State Technical University. Mariupol: Azov State Technical University. Edition 18. Part 2: 131-136.

Dreshpak, N.S. 2009. Induction *heating modes of cylindrical details connected with interference fit.* Technical Electrodynamics. Kyiv: National Academy of Sciences of Ukraine.Edition, 6: 61-66.

Patent 43365 Ukraine. 2009. IPC B23P19/02 Pivnyak, G.G. & Dreshpak, N.S. *Device for induction dismantling of details*, 15: 4.

Patent 43339 Ukraine. 2009. IPC B23P19/02 Pivnyak, G.G. & Dreshpak, N.S. *The way of induction details dismantling control*, 15: 4.

Technical and Geoinformational Systems in Mining – Pivnyak, Bondarenko & Kovalevs'ka (eds)

Mechanism of force interaction of "rock bolt-rocks" system

V. Bondarenko, G. Simanovich & A. Laguta
National Mining University, Dnipropetrovs'k, Ukraine

Y. Cherednychenko
Ministry of Coal Industry of Ukraine

ABSTRACT: The interaction of rock bolts with the blast-hole walls is given. The mechanism of interaction during rock bolt installation and the process of further work based on the load resistance from a rock mass side are described. Analytical-experimental description of four modes of rock bolt (without any expansion shell) interaction with the blast-hole walls, and fully characterized process of rock bolt deformation under influence of an axle load are given. The main criterion of optimal power parameter selection during rock bolt installation is developed.

1 INTRODUCTION

Despite variety of lockless rock bolt's designs, they are characterized (except screw-threaded bolts) by a number of the general principles of force interaction with blast-hole walls:

– bolt fastening is basically carried out by means of friction and cohesion (adhesion) forces. So, the main role of tubular rock bolt's fastening belongs to friction forces; ferro-concrete, polymeric and ferro-polymeric bolts have cohesion forces; and a tubular bolt with a fastening layer has friction and cohesion forces, when extending mixture is applied;

– bearing element (a rod, a cylinder, etc.) of a rock bolt perceives the basic tensile load, directly or through the fastening layer, contacting with blast-hole walls. On these contacts the tangential stresses are operated due to friction and cohesion forces, or their combination;

– lockless rock bolt's interaction with a rock is characterized not only by a direct, but also by a reverse connection of normal tensile stresses in the bearing element with tangential stresses, operating along contact surface of the bearing element with blast-hole walls or the fastening layer, and also fastening layer with blast-hole walls. It is explained that during the deformation process of mine working's bolted mass the bearing element of a bolt is loaded by axial tensile stresses through the rock contact. It leads to changing of the existing stress field of the "bolt-rock" system.

The similarity of main features of bolt force interaction with blast-hole walls is in the very idea of fastening rock mass by lockless rock bolts. It substantiates the single deformation mechanism of bolts with blast-hole walls under the axial loading influence.

2 THE MAIN IDEA

Based on a number of experimental researches (Melnikov 1980; Skobtsov 1973; Shirokov 1971; Roginsky 1968 & Yemelyanov 1978) of rock bolt deformation under the axial loading influence, it is possible to highlight four consecutive modes of bolt interaction with blast-hole walls. The first mode, or the mode of elastic interaction, is characterized by the full contact of a bearing element with rocks (a bearing element with fastening layer, or fastening layer with rocks) along a bolt. In this mode, the displacement of the rock bolt's loaded end is negligible, and maximum of tangential τ_{rz} stresses is on the bolt's loaded end. When limiting state occurs, breaking of a less strong contact, connecting the bearing element with blast-hole walls, happens.

When contact is broken, the second mode takes place – the mode of increasing resistance to axial loading. The maximum of tangential τ_{rz} stresses moves to the sunken bolt end. The tangential stresses operate in the place of lost contact, provided by rough surface of broken contact. There are also stresses of friction in the presence of radial pressure upon the contact, therefore total tangential stress action is raised and increases resistance of the bearing element to axial load. The U displacement of loaded bolt end is grown due to increase of working area of normal tensile σ_z stresses of the bearing element.

As the maximum τ_{rz} moves towards the sunken bolt's end, gradual growth of its resistance to axial loadings occurs, till the moment, when the loss of

total tangential stresses will not exceed the total tangential stresses increase on the broken contact area. With equality of these forces, maximum bolt resistance to axial loads will take place.

During further displacement of the maximum τ_{rz} towards the sunken bolt's end, the intensive decrease of bolt resistance to axial loads occurs, because total outgoing tangential stresses on the elastic deformation area considerably exceed the growth of total tangential stresses on a failure contact site. This process characterizes the third mode – the mode of the intensive reduction of bolt resistance to axial load, which finishes when one of the contacts along the full bolt length is broken.

The fourth mode – the sliding mode – causes considerable displacement of a rock bolt, which resists to axial loads due to friction forces along the surface of the broken contacts. The resistance reduction to axial loads in the sliding mode occurs slowly enough since contact sections of bolt's loaded end are gone out of operation in the first place, where the tangential stress value is insignificant.

The revealed modes of the "bolt-rock" system interaction have their peculiarities, and this has to find a reflection in corresponding analytical models for calculation of parameters of rock bolts without expansion shell.

3 THE CALCULATION OF ROCK BOLTS WITHOUT EXTENSION SHELL

For lockless bolt calculation it is necessary to have original data parameters of their installation. There are geometrical, strength and strain parameters of rock bolt elements, and also constructive-technological features of their installation. If the first group of parameters is known in advance and is defined by the material properties, used in different lockless rock bolt constructions, then the second group of parameters has to be defined by the process of their installation in a blast-hole. Thus, it means to install the rock bolts with initial radial P pressure along the contacts (bearing element – fastening layer – blast-hole walls). Ferro-concrete and ferro-polymeric rock bolts, with expanding (during solidification) hardening layer, and also tubular bolts are related to such constructions.

Installation of bolts without extension shell and with initial radial stresses $\sigma_z = P$ along the contact, with the blast-hole walls, in some constructions promotes increase of the bolt fastening in a blast-hole (ferro-concrete and ferro-polymeric rock bolts), and in others it is the main force connection providing bearing capacity (a tubular bolt). Therefore the problem is to make correct choice of initial radial pressures during the bolting process and, correspondingly, their constructive realization.

As the basis of criterion of calculation of bolt design parameters that provide required initial radial stresses, the condition of achievement of the maximum fastening strength of a bolt in a blast-hole is supposed, which directly depend on radial stresses along the bolt contact with blast-hole walls. The greater radial σ_r stresses along the contact, the greater friction forces that resist to axial load on the bolt. However, it is impossible to infinitely increase radial stresses, as it will lead to blast-hole walls macrodestruction and to abrupt falling of bolt's bearing capacity. Therefore, during the process of radial strain of a bolt, the maximum of radial stresses $\sigma_r = P_{max}$, reaching during bolting, must not exceed the value which creates blast-hole walls macrodestruction. On the other hand, radial stresses along the contact are inevitably decreasing to established P_∞ pressure under influence of rheological factor and due to peculiarities of rock bolt design. That is why, in order to choose rational value of initial radial σ_r stresses on the contact, it is necessary to consider the mechanism of "bolt-rock" system deformation in radial direction.

4 RADIAL DEFORMATION PROCESS OF THE "BOLT-ROCK" SYSTEM

Radial process of deformation of the "bolt-rock" system is visually illustrated in the diagram of stresses (in coordinates of σ stresses – radial strain ε_r) of a bolt material and blast-hole walls (Figure 1). During influence of radial pressures on contact of the $\sigma_r = P$ system, in blast-hole walls triaxial non-uniform stress state occurs, characterized by radial σ_r, tangential σ_θ and axial σ_z components of stresses. As axial component σ_z is average and according to the Mohr's theory of strength does not essentially effect limiting state of rock, then the process of components σ_r and σ_θ changing in blast-hole walls is considered. At a stage of elastic and elastic-plastic deformation, component σ_r is a compressing type, and tangential σ_θ is a stretching type (Baklashov & Kartoziya 1975). As rocks resist to stretching loads poorly, when component σ_θ reaches ultimate rock strength on σ_p tensile (see Figure 1, point 2), discontinuity and radial micro-cracks formation occur in blast-hole walls.

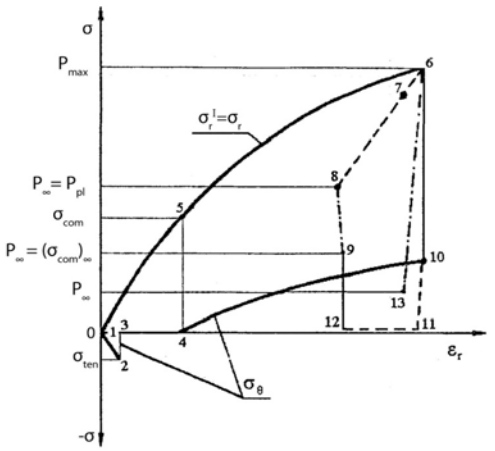

Figure 1. The diagram of lockless bolt interaction with blast-hole walls: ——— loading; – – – – unloading at $(\sigma_{com})_\infty \geq P_{pl}$ and – · – · – at $(\sigma_{com})_\infty < P_{pl}$.

Tangential stresses disappear (area 2-3) and during the further loading process of blast-hole walls a tangential component equals to zero (area 3-4). Radial stresses simultaneously increase. Therefore, ultimate rock strength on uniaxial compression σ_{com} and blast-hole walls transfer into limiting state (point 5). Thus dilatation process of blast-hole walls is intensively developed, areas 5-6 and 4-10, which are characterized by the occurrence of compression tangential stresses. The essence of this process consists in the following. During compressing of rocks in radial direction, limited by radial microcracks, its (rocks) expansion occurs (according to Poisson law) in tangential direction and that characterizes tendency of closing microcracks. The tangential strain's value of closing radial microcrack $(\varepsilon_\theta)_з$ equals to

$$(\varepsilon_\theta)_з = 2\mu\varepsilon_r ,$$

where μ – coefficient of rock transversal strain; ε_r – radial strain of blast-hole walls.

It is also important to know tangential strain of opening microcrack $(\varepsilon_\theta)_p$. It equals to the plastic strain of the rocks around the cylinder hole (Baklashov & Kartosiya 1975) of radial strain ε_r, that is

$$(\varepsilon_\theta)_p = -\varepsilon_r .$$

Total tangential strain is

$$\varepsilon_\theta = (2\mu - 1)\varepsilon_r . \qquad (1)$$

From the formula 1 it follows that when $\mu = 0.5$ (plastic state of blast-hole walls), tangential strain equals to zero and opening microcrack remains constant. However, in limiting rock state (points 4 and 5) the dilatation effect is observed (Baklashov & Kartosiya 1975). It is characterized by coefficient μ of intersection deformation can significantly exceed 0.5, as the complex of experimental investigations (Baklashov 1975 & Bridgeman 1955) of loading of different rock samples has shown. In this case, according to formula (1), positive tangential strain appears, providing closure of earlier formed radial microcracks and leading to occurrence of compressing tangential stresses. And, therefore, it promotes the increase of abrupt resistance to radial loads (points 5-6 and 4-10) without macrodestruction of blast-hole walls.

At a definite stage the process of the bolt's radial strain finishes and the balance state of "bolt-rock" system occurs, during which radial stresses along the contact reach their maximum $\sigma_r = P_{max}$ (point 6). Further, the unloading process of the "bolt-rock" system begins. For ferro-concrete and ferro-polymeric rock bolts this process is identified by unloading blast-hole walls. That is why the unloading process of a tubular bolt is considered, as the most common process for "bolt-rock" system.

At the moment of reaching maximum P_{max} by radial stresses, a rock bolt is loaded by external compressive radial stresses. And its material is under tensile tangential stresses, appearing when a bolt is extended due to explosion power, or pressure inside of a rock bolt. Such state is unstable and in the next moment anchor elastic compression to its own axis begins. The process of which can be divided into two serial stages. At the first stage tangential tensile stresses σ_θ^I of a rock bolt are reduced to zero, blast-hole walls are simultaneously unloaded and radial stresses are reducing on the contact of a system. At the second stage, elastic compression of a bolt by tangential compressive stresses occurs under influence of the remained tangential stresses. So, during this process, three cases of "bolt-rock" system's unloading take place.

In the first and second cases, value P_{max} of maximum radial stresses on the contact is such as even when the system is elastically unloaded (site 6-7), remaining radial compressive stresses exceed value P_{pl}, with which a rock bolt transfers into plastic state due to external pressure. (Pisarenko 1979)

$$P_{pl} = \frac{r_2^2 - r_1^2}{2r_2^2}\sigma_T^I , \qquad (2)$$

where σ_T^I – ultimate flow material of the bearing element; r_1 and r_2 – inner and outer radiuses of a tubular bolt.

Plastic deformation of a bolt's bearing element towards its axis begins and unloading of blast-hole walls takes place also (area 7-8). When radial stresses on the contact are reduced to value P_{pl}, then the process of bolt plastic compression ends.

The mechanism of blast-hole walls' unloading process is considered as well. In the works (Bridgeman 1955 & Stavrogin 1979) the dependence of a rock sample volume's change, during uniaxial loading, has been experimentally received. One of the features of such diagram is when a sample is unloaded, that was in a limiting stress state, its volume does not increase at a primary stage but decreases. Therefore, during unloading the increase of sample volume in direction to main stress action is lower, than the decrease of sample volume in lateral direction. This phenomenon can be explained by the fact that during loading-up to limiting state of a sample, a row of microcracks (dilatation) appears in the sample. At the primary stage of unloading, a rock of sample, striving to take initial position, fills part of a volume of these microcracks, and after this the sample is unloaded as a solid body. That is, both during the loading process and unloading process, a rock sample goes through three sequential states: elastic-plastic (decrease of volume during loading and increase – during unloading), plastic (volume is constant) and limiting (increase of volume during loading and decrease – during unloading).

Using mentioned regularities it is possible to make a conclusion that in primary stage of unloading of blast-hole walls from radial σ_r stresses, tangential strain exceeds radial. The opening of rupture radial microcracks occurs and tangential σ_θ stresses disappear (see Figure 1, area 10-11). Stress state of blast-hole walls turns to biaxial again. Their resistance to pressure from rock bolt side is dramatically fallen and causes unstable state appearance. Rock bolt material has the same condition, if radial stresses exceed value P_{pl}, as a result unloading process of the system continues to develop. If ultimate axial σ_{com} compression of rock strength is greater or equals to value P_{pl}, then when $\sigma_r = P_{pl}$, the balance state at the system's contact establishes. Further this state is disturbed by the influence of rheological factors, in particular, by the factor of reduction of ultimate rock compression strength with time. In connection with this, the first case of unloading of the blast-hole walls rocks is characterized by the fact that ultimate long-time rock strength of uniaxial $(\sigma_{com})_\infty$ compression is greater or equals to P_{pl}. Because, when $\sigma_r = P_{pl}$, longtime balance state of "bolt-rock" system occurs. Thus, at $(\sigma_{com})_\infty \geq P_{pl}$ established P_∞ pressure on the system contact equals to

$$P_\infty = \frac{r_2^2 - r_1^2}{2r_2^2}\sigma_T^I . \quad (3)$$

The second case is characterized by the fact that longtime ultimate compression strength $(\sigma_{com})_\infty$ is lower than P_∞. In this case during the decrease of radial stresses to value P_∞ "bolt-rock" system does not turn into balance state. Blast-hole walls are plastically deformed, being in limiting state, the surface of a contact moves towards their side, therefore a rock bolt is elastically unloaded and radial stresses on the contact are reduced to P_∞ (area 8-9), and longtime balance state of the system happens. So, at $(\sigma_{com})_\infty < P_{pl}$ established P_∞ pressure on the system's contact equals to

$$P_\infty = (\sigma_{com})_\infty . \quad (4)$$

The third unloading case of "bolt-rock" system is characterized by the fact that the strain of elastic unloading of the bolt (area 6-7) is enough for unloading of blast-hole walls up to the value of radial stress, which is lower then $(\sigma_{com})_\infty$ and P_{pl} (area 6-13), and system turns into longtime equilibrium state immediately. Settled pressure P_∞ on the contact, for the third unloading case, is determined from formula of radial strain compatibility on the contact of "bolt-rock" system.

For ferro-concrete and ferro-polymeric rock bolts, the settled pressure, as it was mentioned earlier, is determined by unloading process of only blast-hole walls and equals to $P_\infty = (\sigma_{com})_\infty$

Thereby, it is established that radial stresses on the contacts of the "bolt-rock" system's elements, during bolting process, achieve maximum. As a result of rock dilatation this maximum can considerably exceed its uniaxial ultimate compression strength not causing microcracks. Further unloading takes place, during process of which radial stresses are reduced and consequently longtime balance state is settled. It is initial state during studying of static interaction of lockless bolt with a rock mass.

5 RESULTS

Research of the mechanism of "bolt-rock" system's interaction during bolting with initial radial stresses is a basic for the criterion development to choose installation parameters of rock bolts (blasting charge, inner pressure for tubular bolt installation; volume expansion of fastening layer – for ferro-concrete and ferro-polymeric bolts and etc.). A selection of parameters is defined by the method of determination of changing rational interval of required radial pressure on the rock bolt contact with blast-hole walls. Upper boundary of interval is determined by acceptable radial P_{max} pressure, which does not cause microcracks of blast-hole walls taking into account its dilatation. Lower boundary P_{min} equals to settled P_{∞} pressure plus the loss of radial stress under elastic unloading of a bearing element (see Figure 1, site 6-7). Possibility of radial stress changing in certain interval favorably affects on regulation efficiency of bolt installation parameters.

Let us consider the definition of rational interval of changing radial σ_r stresses on top P_{max} and bottom P_{min} pressures, according to above stated requirements. For the calculation of P_{max} the exponential equation of rocks' ultimate state, which was experimentally gotten in (Stavrogin & Protosenya 1979), was used

$$\sigma_r - \sigma_\theta = \sigma_{com} exp\left(T\frac{\sigma_\theta}{\sigma_r}\right), \tag{5}$$

where T – constant coefficient for given rock type (Stavrogin & Protosenya 1979).

Unknown value of tangential stresses in formula (5) is determined by the system of

$$\left.\begin{aligned} &\varepsilon_\theta = (2\mu - 1)\varepsilon_r;\ \varepsilon_\theta = \frac{\sigma_\theta}{E(\varepsilon_i)};\\ &\varepsilon_r = \frac{1}{E(\varepsilon_i)}\left[\sigma_r - \mu(\sigma_\theta + \sigma_z)\right];\\ &\sigma_z = \mu(\sigma_z + \sigma_\theta);\ \mu = \mu_0\, exp\left(-\Gamma\frac{\sigma_\theta}{\sigma_z}\right), \end{aligned}\right\} \tag{6}$$

where μ – coefficient of transversal rock strain; $E(\varepsilon_i)$ – function of dependence of rock's elasticity modulus on strain intensity ε_i; μ_0 and Γ – constant coefficients for given rock type (Stavrogin & Protosenya 1979).

The first equation links radial and tangential strains during the dilatation of blast-hole walls. The second and the third equations are physical, and the fourth describes the condition of flat blast-hole walls' strain in axial direction. The fifth equation defines the dependence of coefficient μ, transversal rock strain, on a type of stress state of a rock sample (Stavrogin & Protosenya 1979). During solving of system (6) it is taken into account that $\frac{\sigma_z}{\sigma_r}$ ratio, as a rule, is bigger, than 0.5, when in line with data work (Kuznetsov 1973) coefficient μ strives to 0.5. As a result formula for the calculation of tangential with radial components $C = \frac{\sigma_z}{\sigma_r}$ is given

$$C = \frac{1.5\mu_0 e^{-2c} - 0.75}{0.75 - 0.5\mu_0 e^{-2c} + 2\mu_0^2 e^{-2\cdot 2c}}. \tag{7}$$

Then maximum acceptable radial pressure on the rock bolt's contact with blast-hole walls is determined by formula

$$P_{max} = \frac{\sigma_{com}}{1\text{-}C} exp\, TC. \tag{8}$$

For the definition of interval's lower boundary of rational changing maximum radial σ_r stresses, the equation of compatibility of radial displacement on the bolt contact with blast-hole walls in the system's unloading process is done

$$U_1 = U_2 + U_3, \tag{9}$$

where U_1, U_2 and U_3 – radial dislocations during unloading of blast-hole walls of a bearing element and elastic loading of a bearing element accordingly.

Taking into account, during the process of unloading blast-hole walls, as a material of a bearing element, elastically deform. For the calculation of dislocations U_1, U_2 and U_3 known formulae were used

$$\left.\begin{aligned} U_1 &= \frac{1+\mu}{E} r_3\left[P_{min} - P_\infty\right];\\ U_2 &= \frac{1-(\mu^I)^2}{E^I} r_2\left[\sigma_T^I + \frac{2r_2^2}{r_2^2 - r_1^2} P_{min}\right];\\ U_3 &= \frac{1-(\mu^I)^2}{E^I} r_3\left[2(1-\mu^I)\frac{r_2^2}{r_2^2 - r_1^2}\right] P_\infty, \end{aligned}\right\} \tag{10}$$

where E^I and μ^I – module of elasticity and Pois-

son coefficient of a bearing element's material.

Jointly solving the equation (9) with the system (10), formula for the calculation of P_{min} is received

$$P_{min} = \left(\frac{1-\left(\mu^I\right)^2}{E^I} r^2 \sigma_T^I + P_\infty \left\{ \frac{1+\mu}{E} r_3 + \frac{1+\mu^I}{E^I} r_2 \times \right.\right.$$

$$\left.\left. \times \left[2\left(1-\mu^I\right) \frac{r_2^2}{r_2^2 - r_1^2} - 1 \right] \right\} \right) \times$$

$$\times \left[\frac{1+\mu}{E} r_3 - 2 \frac{1-\left(\mu^I\right)^2}{E^I} \cdot \frac{r_2^3}{r_2^2 - r_1^2} \right]^{-1} \qquad (11)$$

Formula (11) is just for the determination of P_{min} parameter in the first and second cases of "bolt-rock" system's unloading, i.e. when settled P_∞ pressure on the contact is defined by formula (3) or formula (4). If mechanical parameters of "bolt-rock" system are such that settled pressure P_∞ is less than value of longtime rock compression strength $\left(\sigma_{com}\right)_\infty$ and the beginning of plastic bolt's phase P_{pl}, then P_{min} should be defined by formula

$$P_{min} = \left\{ P_{max} \left[\frac{1+\mu}{E} r_3 - 2 \frac{1-\left(\mu^I\right)^2}{E^I} \cdot \frac{r_2^3}{r_2^2 - r_1^2} \right] - \right.$$

$$\left. - r_2 \frac{1-\left(\mu^I\right)^2}{E^I} \sigma_T^I \right\} \left[\frac{1+\mu}{E} r_3 + \frac{1+\mu^I}{E^I} r_2 \times \right.$$

$$\left. \times \left(2 r_2^2 \frac{1-\mu^I}{r_2^2 - r_1^2} - 1 \right) \right]^{-1} . \qquad (12)$$

Thus, rational interval of changing $P_{max} - P_{min}$ radial pressure has been defined. It is the main criterion of optimal power parameters in the bolting process.

REFERENCES

Melnikov, N.I. 1980. *A rock bolt*. Moscow: Nedra: 252.

Scobtsov, B.S. & Afanasiev, U.S. 1973. *Research of stresses in ferro-concrete rock bolts.* Physicotechnical mining problems of minerals, 3: 29-34.

Shirokov, A.P. 1971. *Practice and theory of rock bolt application.* Mine working's fastening on the Far East' mines. Prokopyevsk: city topography: 6-51.

Roginskiy, V.M. 1968. *Ferro-concrete rod's testing with strain sensors of resistance*.Mining journal, 12: 69-70.

Yemelyanov, B.I. 1978. *Tensometric investigations of steel-polymeric rock bolt operation*. Stability and fastening of mine workings. Leningrad's mining university, 5: 52-54.

Baklashov, I.V. & Kartosiya, B.A. 1975. *Rock mechanic.* Moscow: Nedra: 271.

Bridgeman, P. 1955. *Research of big plastic deformations and rupture*. Moscow: 350.

Pisarenko, G.S. *Resistance of materials*. 1979. Kiev: High school: 696.

Stavrogin, V.N. & Protosenya, A.G. 1979. *Rock's plasticity*. Moscow: Nedra: 300.

Kuznetsov, V.I. 1973. *About breaking of metallic rings in plastic state*, 4: 567-571.

Technical and Geoinformational Systems in Mining – Pivnyak, Bondarenko & Kovalevs'ka (eds)
© 2011 Taylor & Francis Group, London, ISBN 978-0-415-68877-2

Results of realized new concept of complex coal-gas deposit development

A. Bulat, V. Lukinov & V. Perepelitsa
M.S. Polyakov's Institute of Geotechnical Mechanics, Dnipropetrovs'k, Ukraine

ABSTRACT: The authors have created a new concept of the coal-gas deposit development according to which a combined degassing of both natural and man-caused methane accumulations increases the productivity of the coal mining thanks to the captured coal-mine methane used to produce electric and thermal energy, and improves effectiveness of nature-conservation measures aimed to make ecological situation in the coal-mining region better.

Difficultness of mining-and-geological conditions for the coal seam development in Donetsk coal basin (Donbas) is explained by small thickness of the coal strata, developed small and large erosion, and tectonic deformations. Mining of the deeper horizons in the key industrial geological regions of Donbas folding is complicated by high rock pressure, high gas content, sudden outbursts of coal, rocks and gas, methane blowers and complicated geothermal conditions (Lukinov & Pimonenko 2008). More than 25% of active mines are referred to the highest risk categories by methane content (more than 15 m^3 per 1 ton of daily coal production). Only 12% of active mines are referred to the gas-free mines, and they produce mainly non-gaseous anthracites (Dolzhansk-Rovenetsk and Shahtinsk-Nesvetaevsk regions).

Today, gas composition in the Donbas coal deposits accounts 16 components and includes methane, ethane, nitrogen and carbon dioxide content of which is more than 1%. Trace contaminants in the gas mixture with content less than 1% are presented by propane, butane, pentane, hydrogen, hydrogen sulphide, argon, krypton, xenon, helium, neon, oxygen, carbon dioxide.

Most of researchers of the coal-bed gases recognize obviousness of the fact that methane was mainly formed in the process of metamorphism of organic matters in the coal strata and rocks. However, no general consensus has been obtained between the scientists concerning volume of methane formation at the moment when coals transit from one grade of metamorphism to another. According to G.D. Lidin (Lidin 1944), when 1 t of anthracite is created from coal grade D about 200 m^3 of methane is emitted, and according to V.A. Uspensky (Uspenskiy 1954) – only 150 m^3. Kozlov V.P. and Tokarev G.D. (Kozlov & Tokarev 1961) said that volume of emitted methane was 251 m^3 per 1 t of anthracite.

Article (Kravtsov 1968) shows clear dependence of changes of key gas components – methane, nitrogen and carbon dioxide – on the depth of the coal bedding. It should be noted that such clear definability of gas zoning in the coal stratum is explained by counter flows of metamorphogene gases and atmospheric gases and also, as we believe, by physical and chemical peculiarities of the coal structure (coals is a natural sorbent of methane) and its low filtering properties. This our opinion is obviously confirmed by less clearly definable gas zoning in the rocks and different locations of the gas zones in coal strata and adjoining deposits.

Gas composition in the coal seams and rocks is identical though distribution of the gases essentially differs and depends on geological conditions and factors.

By impact on gas content in the coal-bearing thicknesses, main geological factors include the following: 1) gas formation and burial; 2) gas accumulation and reservation; and 3) degassing of the coal-bearing deposits. At the same time, it is obvious that all these factors were under direct or indirect impact of tectonic processes that had happened in the region at various stage of its development.

Long-term researches of gas content in Donbas coal-bearing deposits help us to reveal and study regional and, partially, local changes of gas characteristics in the coal seams and rocks; these changes could have far-reaching impact on organization of degassing processes and methane recovery. It was found (Brizhanev 1979; Dmitriev & Kulikova 1982; Zabigailo & Shirokov 1972; Skochinskiy & Lidin 1948) that gas in the coal seams and rocks could be in free, aqueous and retained states; content of free

gas depends on porosity and fracturing of the rocks and coals and thermodynamic conditions of the coal and rock bedding.

Regional factors include depth of the coal-seam bedding and rate of the seam metamorphism, while local factors include rate and type of tectonic deformations and lithologic and facial characteristics of the rocks.

Articles (Kravtsov 1968; Zabigailo & Shirokov 1972; Kravtsov 1980) describe impact of paloestresses on gas content in the coal-bearing thickness: deformations caused by stretching (faults) are permeable and make degassing of the coal-bearing deposits easier, while in compression zone overthrusts are formed: they are gas-impermeable and force gas to be accumulated and reserved in adjoining zones. According to A.M. Brizhanov (Brizhanev 1979), gas content depends on time when deformations were created and proceeds from the following properties of the deformations: post-sedimentation faults are permeable, and con-sedimentation faults are impermeable; overthrusts are characterized by changeable permeability that depends on lithology of adjoining rocks.

Thus, it is generally recognized that, in regional terms, natural gas content in a massif depends on rate of catagenetic transformations and forms pattern of gas distribution; and, in local terms, gas content depends on 1) lithologic and facial conditions; 2) types, parameters, time and conditions of breaking deformations formation; and 3) local folding.

Recovery of mine methane as a hydrocarbon input plus supported by safety conditions for mining operations, reduced harmful emissions of mine methane into atmosphere and improved ecological situation – all these are the strongest business case for practically each coal-mining regions of the world. To solve this problem, it is necessary to understand impact of natural and man-caused factors on methane resource distribution in the coal-bearing thickness and principles of accumulation of this valuable energy resource in the coal thickness.

Methane resources in the coal-bearing thickness primary depend on geological conditions and factors which form regional patterns of methane-content changes in the rocks and coals. Key methane accumulators in the coal-bearing thickness are coals and sandstones. Character of the gas-content changes in coals and sandstones depends on level of their catagenesis. In coal-bearing thicknesses with weakly-metamorphized coals methane is mainly located in sandstones, and in areas with OS, T and PA coal grades methane is mainly accumulated in the coals.

As opposite to the natural gas deposits, main portion of methane in the coal deposits is not locally concentrated but is widely dispersed throughout the whole coal-rock massif. In the coal strata, coal interlayers, coalified organic sediments and dispersed organic substances, methane is mainly available in retained (but not in sandstones), free or dissolved-in-water state.

By conditions of formation of methane accumulations suitable for commercial recovery, the gas can be divided into the following groups:

– methane in the coal strata and rocks outside the active mine fields;

– methane inside the coal-rock massif of the active mines;

– methane in coal-and-rock massif and tunnels of the closed mines.

Methane from the coal strata outside the mine field can be extracted by various methods: for example, by hydraulic fracturing of the stratum or by directed multilateral drilling of wells with further hydraulic fracturing and dewatering. In international terminology, methane extracted by these methods is called CBM, or coal bed methane. Technology of the CBM extraction is very complicated and required essential funds. In order to provide good effectiveness of this technology it is necessary to drill hundreds of wells that should operate simultaneously. One more problem arises: big volumes of salt water that should be treated and utilized.

Experience of other coal-producing developed countries with commercial recovery of methane shows that for proper extraction of methane it is necessary to increase permeability of the coal-and-rock massif and to disturb sorption balance in order to stimulate desorption of methane from the coal and force the gas to move.

Today, this technology is successfully applied in the USA and Canada though operators in Germany, Russia and Ukraine have failed to obtain expected results.

However, there are some fields in Donbas within western, southern and northern boundaries where weakly-metamorphized coals and, accordingly, sandstones with favourable collecting properties are developed and where methane deposits are available for commercial production with no additional efforts. Actually, the fields can be considered as small deposits of natural gas. They are confined to positive tectonic structures: Leventsovskaya structure in West Donbas, Lavrentievskaya structure in South Donbas geological industrial region, Matrosskaya structure in Lisichansk region and some others, mainly, in northern and southern zones of the small folding. Unfortunately, number of these zones is not great.

Sandstones bedded in the regions with developed medium-metamorphized coals feature low permeability (less than tenth and hundredth fractures of

millidarcy), and such permeability impedes formation of methane accumulations in the sandstones. Here methane is dispersed in the pores, and the only source to extract the gas from without additional measures is tectonically created collecting fracture reservoirs where free methane accumulations could be formed.

In 2005, our Institute IGTM of NASU worked out and approved a as normative document a technique to predict tectonically deformed zones favourable for formation of free-methane accumulations in coal-and-rock massifs not disturbed by mining operations. The technique helps to detect promising areas for methane extraction in boundaries of so-called opened anticline structures with parameters specified by local structure maps made in the form of projections of the stratum hypsometry on approximating surface. We determined some structures promising for preliminary degassing in the Butovskaya Mine field and in one district of Kalmiuskiy Colliery that is a reserve unit of A.F. Zasyadko's Mine. Here, basing on our recommendations, the operators set location of and installed equipment for drilling a 3Г – 2 well.

Ukrainian mines and Donbas coal mines in particular have obtained good experience in methane recovery with simultaneous coal mining through investigating man-caused processes that influence on changes of physical properties of rock-and-coal massif and, in particular, the massif fracturing, permeability and gas-bearing.

When coal is extracted the rock pressure in the coal strata and adjoining rocks is dropped, the coal strata and adjoining rocks become fractured and soft, and, accordingly, permeability increases. These processes are followed by formation of man-caused collecting reservoirs and, consequently, concentrations of free and liberated methane in the reservoirs. This gas is called CMM, or coal mine methane, and it can be extracted by current degassing and drilling of underground and surface wells in the active mine fields.

This is exactly the line that is directly associated with the needs of Ukrainian coal industry and to which our Institute of Geotechnical Mechanics (IGTM) orients our researches. In this filed we closely cooperate with other trade and academic institutes, Safety Department of Ministry of Energy and Coal Industry of Ukraine and some other organizations among which the A.F. Zasyadko's Mine should be specially noted. Only for the last 5 years, we worked out and approved as normative documents: schemes and methods of gas-emission control in the working areas of coals mines (2006); technique to predict man-caused methane accumulations in disturbed coal-and-rock massif (2007); procedure for applying advance degassing method in the coal strata (2010).

Practice of advance coal strata degassing is our absolutely new technology based on the laws of methane flow distribution in the border between mined area of and not-disturbed coal-and-rock massif and makes it possible to capture in advance additional volumes of methane. For example, this practice helped the A.F. Zasyadko's Mine to produce additionally more than 4 mln. m^3 of methane.

Our new degassing technologies increase methane content in composition of gas recovered with the help of underground degassing wells, extend output of methane production, and improve safety of the coal mining.

We also worked out a method to estimate density of methane resources in the roof rocks of the mining coal stratum. The method takes into account geological, mining and technical factors that influence on formation of methane accumulations in the undermined coal-and-rock massif. For example, methane resource density in undermined roof rocks in mines of Makeevugil Company varies between 40 m^3 / m^2 and 140 m^3 / m^2 depending on metamorphism rate of produced coal, extracted coal thickness, depth of mining operations, method of the roof control and some other parameters. Volume of methane resources in these mines is between 9 mln. m^3 and 35 mln. m^3 at mining column with length 1000 m and longwall with length 230 m. Extractable methane reserves are approximately half of estimated resources and vary between 6 mln. m^3 and 17 mln. m^3.

Practice of mining high-productive longwalls with methane content more than 15 m^3 / min. shows that up to 80% and even more methane is emitted into the mining district from the roof undermined coal-and-rock massif. Due to divergent parameters of deformation, behaviour of rocks with different lithologic characteristics is not the same at the similar undermining conditions: undermined rocks with greater ultimate tension deformation are less soft and with lower permeability, and vice versa. Besides, in the process of undermining each geological object in the coal-and-rock massif should be considered from the point of its gas output (in case of gas-bearing rocks) and from the point of gas filtered though it (in case of both gas-bearing and non-gaseous rocks). To estimate possible resources of methane in the roof coal-and-rock massif we worked out a method that 1) specifies interval space for the rock unloading towards the roof when the seam has been extracted; 2) calculates distance to the seams with screening properties and collecting seams; and 3) specifies parameters of degassing zone and zone of gas recovery.

The authors have created an absolutely new concept of combined degassing of the coal-and-rock massif. The concept is based on previously designed

methods, practices and technologies tested in-situ in mines and assumes that these methods, practices and technologies should be applied with taking in account all natural geological, mining and technical conditions. Processes of the coal mining and combined degassing (that ensures safety operation of the mine) are sequenced in time and space. Usage of mine methane to produce electricity and thermal energy essentially reduces methane emissions into atmosphere and serves as nature-conservative measure that improves ecological situation in the coal-producing region.

Concept of combined degassing assumes combination of fully and/or partially applied: "gas horizon" technology; technology of advance degassing; methane capture by degassing wells drilled from the surface and mine tunnels; recovery and usage of methane degassed from the mined longwall faces; estimation of methane resource distribution in coal-and-rock thickness; and maximal utilization of captured methane.

Today, the largest scale application of the concept is realized in the A.F. Zasyadko's Mine (Lukinov, Perepelitsa, Bokiy & Efremov 2010). Here, for the time period of the concept operation from 2006 till 01.01.2011, co-generation plants generated 735312 MW-h of power and 232177 Gcal of heat, and about 210 mln. m^3 of mine methane was used. Besides, from 2004 till 01.01.2011 more than 13 mln. m^3 of methane was used as fuel for cars: this gas was captured through surface degassing wells. Totally, about 223 mln. m^3 of methane were used from 2004 till 01.01.2011 providing reduction of harmful gas emissions in amount equivalent to 3576149 tons of CO_2 which, in accordance with Kyoto Protocol, were officially registered, and the Mine received essential compensation.

Gases received from different sources of degassing feature different qualitative composition. Gas captured through the surface wells contains more than 90% of methane and is used as fuel for cars and igniter for gas reciprocators. Gas from underground wells contains 30-50% of methane and together with gas pumped from the mined districts of the mines with methane content less than 30% is used to generate electrical and thermal energy and in boiler houses.

It should be noted that a strong trend to reduce amount of the coal mines is observed in Europe and in the world, and the same happens in Ukraine. There are a great number of closed old mines in Ukraine, especially in Donbas region, thus, problem of methane extraction from the coal-and-rock massifs and mine tunnels in the closed mines is a question of the day from both economic and ecological points of view.

Methane that escapes from disturbed coal-and-rock massifs into goafs of the mined longwalls and fills mine tunnels in the closed mines is extracted when coal production has been finished; to this end, wells are usually drilled into the old tunnels via which methane is pumped out by vacuum pumps. Such methane is called CAM, or coal abandoned methane. Today, CAM is successfully recovered and utilized in the USA, Germany, United Kingdom and in some other countries where methane-air mixture with methane content more than 50% is used to generate power. Ukraine does not have such good experience in CAM recovery and utilization, however, successful application of this practice in other countries is a witness of its livability as well as economic and ecological effectiveness of CAM recovery and utilization.

Density of remaining methane resources is estimated in each concrete case with taking into account mining and geological conditions and all factors of the deposit development. To our estimates, density could be more than 50% of the mining reserves and could reach 60 mln. m^3 per 1 km^2 of the stripped area in abandoned mine.

Methane that fills tunnels in abandoned mines creates threat of explosion for buildings and objects and poisoning for people in areas where methane escapes to the surface. Coal in Ukraine has been mined for more than 200 years, and hundreds of mines were closed during this period of time especially during the last twenty years resulting in depressive development of the regions.

Realization of the projects on recovery and utilization of methane from the closed mines will, from one hand, involve additional energy resources into fuel-and-power system of Ukraine and, from the other hand, ensure safety life and better ecological situation in the old coal-producing regions of Ukraine.

REFERENCES

Lukinov, V.V. & Pimonenko, L.I. 2008. *Tectonics of Methane-Coal Deposits in Donbas*. Kyiv: Naukova dumka: 352.

Lidin, G.D. 1944. *Zonal Distribution of Natural Gases in Donbas*. News of AS of the USSR, 6: 337-345.

Uspenskiy, V.A. 1954. *Material Balance of the Processes in Metamorphism of the Coal Strata*. News of AS of the USSR, 6: 94-101.

Kozlov, V.P. & Tokarev, L.V. 1961. *Scale of Gas Formation in Sediment Thicknesses (Donetzkiy Basin as an Example)*. Soviet Geology, 7: 19-33.

Kravtsov, A.I. 1968. *Geological Conditions of Gas-Content in Coal, Ore and Non-Metallic Mineral Deposits.*

Moscow: Nedra: 331.
Brizhanev, A.M. 1979. *Regularity of Gas-Content Changes with Changed Depth of Mining in Donbas*. Gas-Content of the Coal Basins and Deposits in the USSR. Moscow: 98-101.
Dmitriev, A.M. Kulikova, N.N. & Bodnya G.V. 1982. *Problems of Gas-Content in the Coal Deposits*. Moscow: Nedra: 263.
Zabigailo, V.E. & Shirokov A.Z. 1972. *Geological Problems of Gases from the Coal Deposits*. Kyiv: Naukova dumka: 172.
Skochinskiy, A.A. & Lidin, G.D. 1948. *Classification of Emitted Methane from the Coal Mines*. News of AS of the USSR, OTNH, 11: 1741-1751.
Kravtsov, A.I. 1980. *Impact of Geological Factors on Natural Gases Distributed in the Coal Seams and Adjoining Rocks*. Gas-Content of the Coal Basins and Deposits in the USSR. Moscow: Nedra. V.3: 74-101.
Lukinov, V.V., Perepelitsa, V.G., Bokiy, B.V. & Efremov, I.A.. 2010. *Creation of Effective Energetic Complex on Mine Methane Recovery and Utilization*. Geotechnical Mechanics. Dnipropetrovs'k: Issue 88: 3-8.

Technical and Geoinformational Systems in Mining – Pivnyak, Bondarenko & Kovalevs'ka (eds)
© 2011 Taylor & Francis Group, London, ISBN 978-0-415-68877-2

Substantiation of chamber parameters under combined open-cast and underground mining of graphite ore deposits

V. Buzilo, T. Savelieva, V. Saveliev & T. Morozova
National Mining University, Dnipropetrovs'k, Ukraine

ABSTRACT: The move from open-cast to combined mining method of developing Zavalyevsky deposit of graphite is considered in the paper. The selection of chamber dimension satisfying conditions of long-term stability is one of the questions for scientific substantiation of the move to combined mining method of deposit development. With this purpose physical and mechanical properties of graphite and enclosing rocks are determined. Stress and strain condition of rocks around the chambers using the method of finite elements is studied.

1 INTRODUCTION

The main consumers of graphite are enterprises of metallurgical, electrical engineering, mechanical engineering, aircraft and other branches of industry. One of the most important raw material base supplying graphite is Zavalyevsky deposit of graphite (Ukraine).

Nowadays the development of deposit is carried out by the open-cast method. The Southern-Eastern part of the deposit is worked-out. The depth of the quarry is 100 m and it is very close to its boundaries.

A great part of commercial reserves is within the pillars under the bed of the Yuzhny Bug river, dressing mill and the village. While deepening a quarry it's boundaries should be moved. Besides, it is necessary to move aside dressing mill and the bed of the Yuzhny Bug river. For further open-cast mining operations it is required to construct a dam and offtake bed channel, relocate dressing mill and amortize the land of 400 ha. Total cost of underground mining of graphite is muck higher then it was expected. Therefore, it is required to work-out the deposit by combined mining method, e. i. to carry out further development of the quarry up to the level of 19 m. For further deepening reserves of graphite ores are worked-out in designed contour of Southern-Eastern quarry without wall cutback. After that the transition to underground mining with dressing mill reconstruction is performed. It's capacity is up to 62.0 thousand ton of graphite per year. At the same time the thickest and the richest ore bodies of the Northern part of Zavalyevsky deposit are worked-out.

Taking into account the demands as for Earth surface protection, steep dip of ore body, available information concerning mechanical properties of ore and enclosing rock, attempts to avoid significant losses and delution under the safe condition of stoping, it is recommended to apply level and chamber mining method. In this case ore is broken by deep boreholes and subsequent filling of worked-out area is carried out by consolidating stowing.

At the same time three chambers are worked-out. Chamber stowing is carried out after finishing extraction. There are three stages of filling worked-out chambers by consolidated stowing:

– filling chamber bottom with the mixture of higher content of binding substance with the aim to obtain hardened stowing on the level of the dam;

– filling chamber from the bottom till the top stopping on the level of the dam;

– additional chamber stowing with higher content of binding substance.

Applying chamber method of mining determines the necessity of substantiating chamber and pillar dimension meeting the requirements of long-term strength. For this purpose it is required to carry out the study of physical and mechanical properties of graphite and enclosing rock.

2 DETERMINING PHYSICAL AND MECHANICAL PROPERTIES OF GRAPHITE AND ENCLOSING ROCK

Study concerning determination of breaking stress under one-axle compression and on tension was carried out on regular form samples according to the standard methodic (Baron, Loguntsov & Nozin 1962).

According to this methodic cylindrical form sam-

ples with the diameter and height ratio equal one were used during the study. Diameter of the samples was from 50 till 51 mm for graphite and from 57 till 58 mm for enclosing rock. Sample processing was carried out in such a way that fluctuation from the end parallelism was not more than 0.05 mm, from end perpendicularity to the cylinder element was also 0.05 mm. Tests were performed on the press PG-100A.Ball centering device was used for strict load centering. Loading was performed gradually increasing the load up to sample destruction .Value of destructive load was fixed.

Strength under tension is determined by Brazil method on regular form samples: diameter of the cores is 57-58 mm. Height of the cores is equal to the diameter. Determination was carried out by the method of diametrical compression. It means that cylindrical samples were broken by the forces applied along diametrically opposite elements.

Characteristic of the rock hardness under displacement is its shift resistance created by two physical factors: internal friction and cohesion. Internal friction can be comparatively easy calculated as it represents the interacting force under deformation taking place between mineral particles. This deformation is proportional to regular stresses caused by external load.

Cohesion is that part of shift resistance which is not connected with stresses caused by external load. It is determined by only molecular binding forces and cannot be constant value.

So, complete resistance of the rock to the shift is expressed by the sum of internal friction caused by external forces and cohesion. It was determined on the regular form samples (Turchaninov, Medvedev & Panin 1967). Sample test was carried out on the press with the help of inclined cores with angles of $a_1 = 35^\circ$ and $\alpha_2 = 55^\circ$.

It is known that the rate of distributing elastic waves depends on the module of material elasticity. Therefore, nowadays method of determining rate of compression and cross elastic wave distribution – sound dynamic method – is widely used to determine elastic values of rock properties (elasticity module and Puasson coefficient).

At present this method is one of the most perspective as it is much cheaper and simpler then other well-known methods (particular statistic ones).Besides, it enables to determine rock properties within massif. That makes it unique while performing field operations. Elastic values of rock properties obtained under statistic and dynamic loads are different due to various character of rock deformation.

Ultrasound defectoscope UK-10P, selective amplifier EGU-60, audio generator LEG-60, vacuum tube voltmeter, conductors made of zirconate-titanate barium with $\delta = 10000$ were used to determine Yung module and Puasson coefficient using dynamic method. Resonance of compression and cross waves were determined with the help of these devices. The rate of compression and cross wave transmission was determined according to this resonance.

The value of dynamic elasticity module was determined after finding out the rate of compression and cross wave transmission within the samples.

Table 1 shows averages of determining physical and mechanical rock properties.

Estimation of result reliability of experimental study using the method of Monte-Karlo probability theory was carried out (Ventsel 1972).It was stated that the level of confidence is equal to 0.84-0.99. It enables to confirm that the amount of tests taking into account while determining physical and mechanical rock properties is enough to be considered as a true one.

Table 1. Mechanical properties and elastic characteristics of graphite ore and enclosing rock.

No	Rock	Compression		Extension		Dynamic method			Module of shifting, 10^{-10} Pa
		Amount of samples	σ_{com}, MPa	Amount of samples	σ_{ten}, MPa	Amount of samples	Elasticity module, 10^4 MPa	Puasson coefficient	
1	Graphite	9	20.2	6	1.0	8	1.55	0.26	0.61
2	Quartzite	8	60.3	7	8.8	8	5.42	0.21	2.24
3	Calciphyre	8	40.1	7	6.7	8	4.79	0.25	1.81
4	Gneiss	7	31.4	6	6.8	8	4.51	0.32	1.68
5	Calc-silicate hornfels	8	64.1	7	10.3	6	7.10	0.22	2.92

3 SUBSTATIATING PARAMETERS OF HEADING-AND-STALL MINING METHOD

Development with consolidated stowing means that sizable chambers are worked-out beforehand. After that worked-out chambers are filled in consolidated stowing. The areas (pillars) left between chambers are worked out in three months after complete stowing consolidation. Pillar size is usually equal to the chamber size.

The study of rock stress-strain condition using the method of finite elements was carried out to substantiate chamber and pillar sizes (Zienkiewicz & Taylor 2000).

Ore and enclosing rock are considered as elastic body and the problem is described in terms of elasticity theory. Chamber roof and interchamber pillars are loaded by the press force of overlying rock. These forces are perpendicular to chamber direct axis. All cross-sections are in the same conditions and there is no shifting in longitudinal direction. As cross-section conditions are the same, it's enough to consider thin layer between two sections. The distance between them is equal to one. The system is in condition of the plane deformation.

Chamber location is periodic in both sides. Due to the symmetry only the area between symmetry axis is considered.

The problem was solved under the following boundary conditions:

– the absence of horizontal point shifting of the left and the right boundaries due to the symmetry;

– external forces are not applied to the right and the left boundaries as well as to the internal points (gravity forces are not taken into account), rigid fixing prevents area turning as a whole one;

– the weight of overlying rock is replaced by concentrated forces applied to the points of horizontal line.

Study of stresses within chambers and chamber roof was carried out to the following tasks.

Task 1. Chamber width is 10 m, height is 48 m, pillar width is 10 m. Chamber shape is symmetric. Due to the calculation stresses in the gravity center finite elements were obtained. Stress epures were build according to them (Figure 1).

Maximal tension stresses in the center of chamber width is $7 \cdot 10^5$ Pa. Strength margin in the center of the roof is 1.4.

Maximal compression stresses within the chamber is – $44.1 \cdot 10^5$ Pa. So, strength margin is 4.5.

Task 2. Chamber width is 10 m and the height is 48 m, pillar width is 10 m. Chamber shape is not symmetric. Stress epures are built taking into account the results of calculation (Figure 2).

Maximal tension stress in the center of the chamber roof is $7.5 \cdot 10^5$ Pa. Strength margin is 1.3. Maximal compression stresses is – $43.2 \cdot 10^5$ Pa. Strength margin is – 4.6.

Task 3. This strength margin within the roof is insufficient for durable construction stability. The change which the roof in the shape of basket described by two radius brings in to the stress field is considered. Pillar width and chamber span are the same – 10 m. Stress epures are built according to the calculation data (Figure 3). In this case strength margin is sufficiently increased and it is 5 in the center of the roof as well as within the pillars.

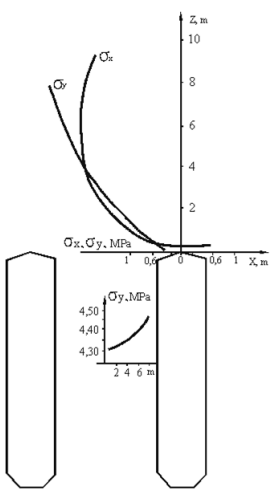

Figure 1. Stress epures around the chambers. Variant 1.

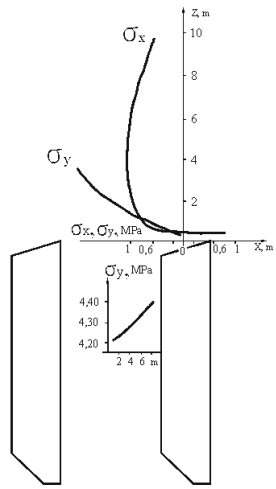

Figure 2. Stress epures around chambers. Variant 2.

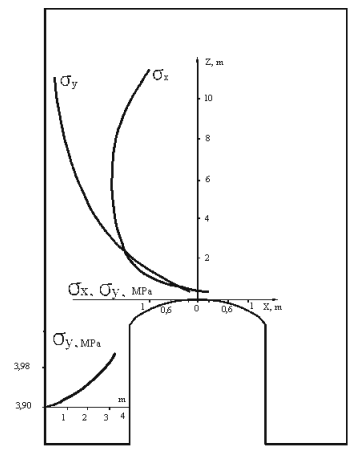

Figure 3. Stress epures around chambers. Variant 3.

Task 4. The width of chambers and pillars should be chosen to ensure safe support of the roof with the help of enterchamber pillars.It is required to find out optimal size and shape of the roof meeting the demand of stability as well as increased graphite extraction.

Stress distribution around chambers with the width of 14 m and pillars with the width of 6 m were considered to choose optimal pillar and chamber sizes Stress epures were build taking into account calculation (Figure 4). In this case tension stresses in the center of the roof is $2.99 \cdot 10^5$ Pa, that corresponds to the strength margin equal to 3.3. Compression stresses within the pillars is $52.47 \cdot 10^5$ Pa, strength margin is 3.7.

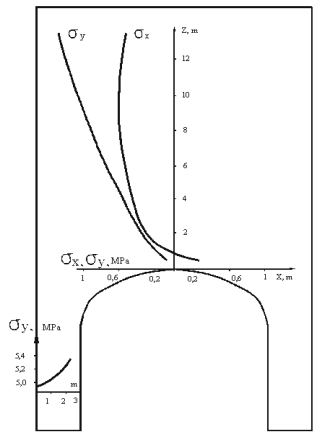

Figure 4. Stress epures around chambers. Variant 4.

4 CONCLUSIONS

It is recommended to work-out the deposit using combined method, that is, to carry out further quarry development up to the point of 19 m and transition to level-chamber mining method filling the goaf with consolidated stowing.

The choice of system development parameters was based on the study of stress distribution character according to four schemes in Figure 1, 2, 3, 4 in the form of epures. Two first calculation schemes showed that strength margin within the roof was 1.5 that is not enough for long-term construction reliability. That is why these schemes cannot be recommended to apply. According to the third scheme where distance between chambers is 10 m and arch is outlined by the basket curve, strength margin within roof and pillars is sufficiently increased and is 5. According to the fourth scheme where distance between chambers is 14 m and pillar width is 6 m, strength margin correspondingly is 3.3 and 3.7.

Taking into account that heading-and stall method with stowing worked-out area will be used in the quarry and to increase graphite extraction it can be recommended to apply the following parameters: chamber width is 14 m, pillar width is 6 m, chamber height is 48 m, the shape of the roof is basket.

REFERENCES

Baron, L.E., Logutsov, V.M. & Nozin, E.Z. 1962. *Determining rock properties.* Moscow: Gosgornehizdat: 332.

Turchaninov, E.A., Medvedev, R.V. & Panin, V.E. 1967. *Up-to-date methods of complex determining physical rock properties*. Moscow: Nedra: 199.

Ventsel, E.S. 1972. *Operation study.* Publish house. Sovetskoe Radio: 306.

Zienkiewicz, O.C. & Taylor, R.L. 2000. *Finite Element Method*. Volume 1 – The Basis. London: Butterworth Heinemann: 712.

Zienkiewicz, O.C. & Taylor, R.L. 2000. *Finite Element Method*. Volume 2 – Solid Mechanics. London: Butterworth Heinemann: 480.

Technical and Geoinformational Systems in Mining – Pivnyak, Bondarenko & Kovalevs'ka (eds)
© 2011 Taylor & Francis Group, London, ISBN 978-0-415-68877-2

The problem with increasing metal-content of a development working's combined support

I. Kovalevska & V. Fomichev
National Mining University, Dnipropetrovs'k, Ukraine

V. Chervatuk
OJSK "Pavlogradugol", Pavlograd, Ukraine

ABSTRACT: The results of researches of prolonged flexible hip-roof support (PFHS) combining with roof bolts in the in-seam working are given. The character of distribution of vertical and horizontal components of stresses in the elements of "rock mass-support" system, involving two specific profiles of PFHS (SVP-27 and SVP-19) was examined by computer modeling, using finite element method. Inessential difference of components' values of stresses in load-bearing elements of the system was detected by analyze of stress diagrams. That caused to substitute specific profile of a frame to SVP-19 and to successfully carrying out mine tests with decreasing up to 30% metal-content of a support.

1 INTRODUCTION

The problem of decreasing combined support's metal-content of mine workings is considerably linked with the fullest accounting of laws of changing strain-stress state (SSS) both for rock-contained mine opening and directly for support elements, depending on constructive, technical and force parameters of its interaction. Therefore, using finite element method in geomechanical models the investigations of influence of PFHS specific profile's nominal size in combination with roof bolts, strengthening the roof of a working, were carried out (Bondarenko 2006 & Bondarenko 2007). Comparison of two frame-support specific profiles, SVP-27 and SVP-19, has been done, based on SSS analyze of "layered massive-support of mine working" system. It is done due to vertical σ_y and horizontal σ_x stresses with analyze of stress field in pairs with SVP-27 frame and SVP-19 frame, to determine significant differences and to explain reasons of their appearance. At first, comparison of σ_y field was carried out in near-the-contour rock mass, and then in the frame support and bolts. So far, the level of stresses in mentioned elements of the system differ by one order, so two colored σ_y scales were separately used for near-the-contour rocks and for a support, with illustration of them by diagrams for SVP-19 profile.

2 RESULTS

Directly in the roof of mine working the zone of unloading occurs, similar to the shape of Protod'yakonov's arch of natural balance (Figure 1a). The zone size of rock ultimate state is usually evaluated by the condition of appearing tensile stresses ($\sigma_y \approx 0$). Every mine rocks can badly resist to this stresses, especially layered and weak rocks. Following mentioned condition the sizes of ultimate state area of roof rocks are practically even: 2.02 m width and 0.43 m height for SVP-27; 2.09 m width and 0.44 m height for SVP-19. So, if to change from SVP-27 frame to SVP-19 frame zone's width will be increased only in 3.5%, and height – 2.3%. In both versions quite limited areas are observed (till 0.2…0.3 m), actions of tensile σ_y reach up to 1 MPa in places between neighboring bolts. Enumerated facts can prove almost similar diagram of vertical σ_y stress distribution in the roof, both as qualitative and quantitative meanings.

In the walls of mine working the zone of abutment pressure with increased compressing σ_y stresses is formed. These stresses exceed resistance to compression of mudstone (13 MPa) and siltstone (13.5 MPa) directly in the roof and in the foot of C_6 coal-seam accordingly. Sizes of this zone are enough wide and reach the whole layer of siltstone in depth, directly in the foot (both for SVP-27, and as for SVP-19). Height of zone (from opening's

foot) is 2.48 m for SVP-27 and 2.54 m for SVP-19 (increasing till 2.4%), zone's width of distribution is about 2.04 m for SVP-27 and 2.08 m for SVP-19 (increasing till 2.0%).

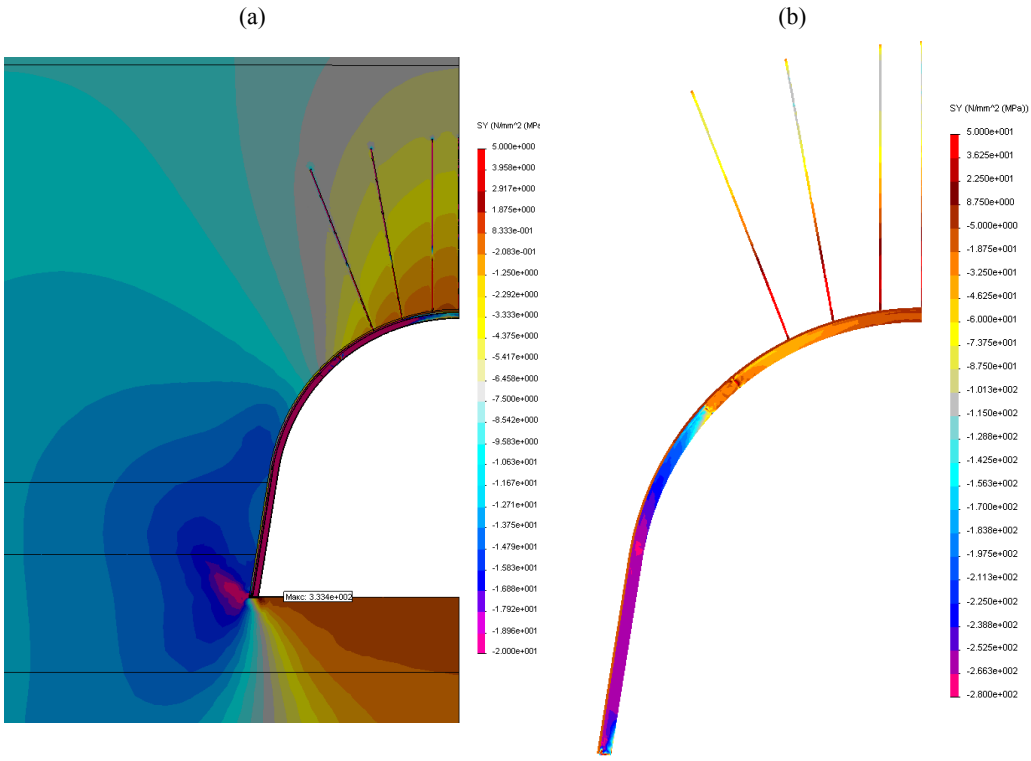

Figure 1. Diagram of vertical σ_y stresses in the "layered massive-working's support" system (a) and in the frame support with bolts (b), especially for SVP-19 using.

Maximum σ_y, about 20…25 MPa, is created in the area of a frame-leg and has local character. Thereby, in the lateral part of a working the field of compressive σ_y stresses is almost identical for both nominal sizes of SVP profile.

The zone of unloading is located in the foot of a working, achieving not only siltstone layer in depth, but and lower layer of sandstone. Tensile σ_y stresses, up to 3 MPa, forms the zone of unstable rocks as the opposite shape of arch along all immediate foot. Ultimate state zone with $\sigma_y \approx 0$ criterion is expanded in the whole width of a working, and is 2.13 m for SVP-27 and 2.17 m for SVP-19 in depth (increasing till 1.9%). Therefore, any considerable differences of σ_y diagrams between both versions of SVP are not observed in working's foot.

Analyze of σ_y diagram in the frame and rock bolts of SVP-27 and SVP-19 profiles led to following results. In the roof bar of a frame reduced compressing σ_y (till 40…60 MPa) operate with passing in the tensile area (till 10 MPa) in the lock of an arch only. This picture (both in qualitative and in quantitative meanings) is almost identical for both versions of SVP. It points to influence of relatively not great load in the roof, making conditional stable state of a roof bar (Figure 1b).

Frame legs are under influence by higher compressing σ_y stresses: in the part of yieldability-lock, of 0.8 m long, σ_y is increased from 115 MPa to 240 MPa; further, in the rectilinear part of a bar σ_y is exceeded ultimate tensile strength of steel St.5 ($\sigma_T = 270$ MPa), reaching 280 MPa; in the lower part of a frame-leg, of 0.4 m high, σ_y is decreased to 150…240 MPa, and in the contact with a step-bearing the maximum occurs again, $\sigma_y = 231.1$ MPa for SVP-27 and 333.4 MPa for

SVP-19. However, an action area of contact stresses is limited in the leg's end and a step-bearing. And sufficient σ_y difference is explained by far lower area of contact for SVP-19. Given sufficient difference is single in σ_y diagrams of a frame support, made of SVP-27 and SVP-19, and whole contour of a frame has almost constant strain state, with factor of vertical σ_y stress action.

The analogous conclusion can be drawn due to analyze of σ_y in a rock bolt support. For both SVP versions the transformation of compressing stresses $\sigma_y = 60...110$ MPa (in the sunken part of a bolt) to tensile $\sigma_y = 0...50$ MPa, in closer-to-mine working part of a bolt, is clearly observed. This fact points to bolt resistance to movements of near-the-contour rocks in direction to working interior. These rocks are in ultimate state and fully coordinated with existent researches of rock strengthening by bolts. σ_y value is far away from ultimate tensile strength of bolt armature ($\sigma_T = 240$ MPa), that highlights to its steady state, because of vertical σ_y stresses.

Thereby, due to results of comparison of σ_y diagrams for SVP-27 and SVP-19 it is enough to affirm about its identity. Increased contact stresses, in the connection of a frame end and a step-bearing, can not considerably influence on bearing capacity of a SVP-19 frame, and single local plastic zone is self-balanced due to well-known fact of load redistribution to elastic areas during plastic material flow because of local contact stress action.

Comparative analyze of distribution field of horizontal σ_x stresses of near-the-contour rocks during installing frames, made from SVP-27 and SVP-19 (Figure 2), gave following results. In the roof of mine working an area of increased compressing σ_x stresses (with concentration coefficient 1.3…1.9) is formed lengthwise bolt and on width is quiet exceeded the distance between locks of yieldability. But, σ_x value is far lower than resistance to rock compression of an immediate roof. These rocks are totally in steady state, following to action factor of σ_x. Attract attention local σ_x concentration in the place of yieldability's lock, which can be explained by the process of its actuation.

In the walls of working (mainly in C_6 coal seam) along height up to 2 m and about 1 m wide an area of unloading with changing σ_x range of compressing 1 MPa value and tensile 1 MPa value is situated. Tensile σ_x intensifies an area of ultimate state, however, due to short depth of this area (till 1 m) sufficient blowing up of foot rocks should not be expected. All mentioned characteristics of σ_x distribution in near-the-contour rocks are almost the same as in qualitative and in quantitative meanings for frames, made of SVP-27 and SVP-19.

Features of σ_x stress field in a frame support lead to following. In the roof bar compressing σ_x act from 90 MPa, in the place of lock of yieldability, to 145…160 MPa in the place of lock of support's arch, made of SVP-27. For SVP-19 specific profile (Figure 2b) increased $\sigma_x = 180...200$ MPa work in the central part of exterior side of arch. It points out more intensive unloading of light-weight specific profile from roof side. However, level of σ_x is far from ultimate tensile strength of St.5 and a roof-bar is in elastic state. The lock of yieldability is most unloaded ($\sigma_x = 20...35$ MPa), as it should be when it goes off. The top (curvilinear) part of a frame is under relatively insignificant compressing ($\sigma_x = 40...75$ MPa) stresses, and its rectilinear part is almost fully unloaded with converting from little compressing σ_x stresses to tensile about 20 MPa.

Given combination of high σ_y and low σ_x (opposite symbol) leads to growth of current σ stress values (or intensity of σ stresses). It favors appearing an area of plastic material state in the rectilinear part of a frame. In the place of supporting a quite limited area of contact tensile $\sigma_x = 30...50$ MPa actions is formed. Also these actions increase current σ stresses and generate appearance of plastic zone. Point contact of frame-leg end with a step-bearing causes appearing maximum of tensile stresses $\sigma_x = 335.3$ MPa (SVP-27) and $\sigma_x = 252.2$ MPa (SVP-19). Steel St.5 is in the area of strengthening and can fully resist on given stresses. However, extremely small volume of action of contact maximum values contributes to load redistribution to elastic areas and considerably not to influence on bearing capacity of a frame. Overall, except to increased stresses in the exterior side of the central roof-bar part (SVP-19), σ_x field has almost the same qualitative and quantitative measures for SVP-27 and SVP-19.

Not great horizontal σ_x stresses effect rock bolts: in sunken part – generally compressing stresses about 20…35 MPa, in the near-the-contour – tensile stresses about 15…20 MPa, because of more intensive moving of near-the-contour massive inside the mine working, and bolts resist to this process.

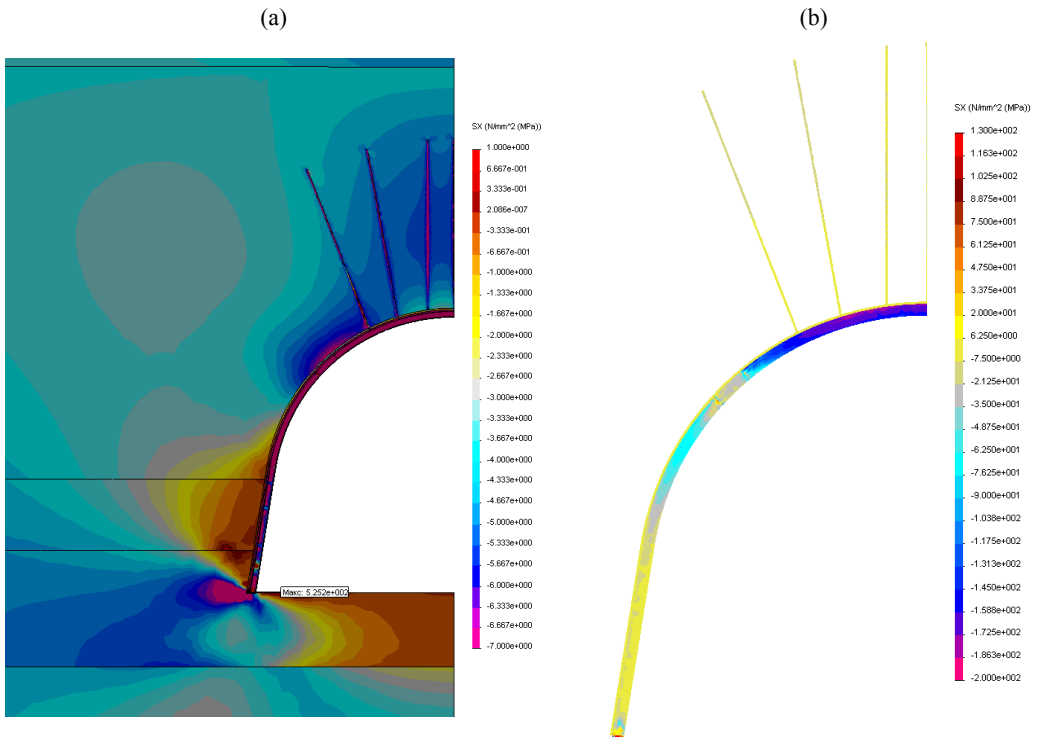

Figure 2. Diagram of horizontal σ_x stresses in "layered massive-support" system (a) and in frame support with bolts (b) for using SVP-19 specific profile.

Figure 3. General view of "Ubileinaya" mine's joining #2, supported by PFHS-15 made of SVP-19 profile in combination with rock bolt support in the roof of mine working.

Therefore, analyze of distribution of horizontal σ_x stresses field in "layered massive-working's support" system does not detect (except of some quite limited areas) sufficient differences for frames, made of SVP-27 and SVP-19 specific profiles.

Mine testing (Figure 3) allows to appreciate in detail rock pressure manifestations in development workings, driven along the C_6 seam of "Ubileinaya" mine. These workings are supported by combination of rock bolts with frame supports, made from SVP-27 (base version), and using the same combination, duy to installing light-weight PFHS-15.0 frame support made of SVP-19.

The fact of increased rock pressure and rock contour displacements of working's walls was experimentally determined by computer modeling and mine researches and geomechanical explanation was given. The most important thing is in over 3.5 times increase of rock movements in the opening's walls. It is more than value of approaching a roof with a foot, that is explained by specific process of weak lateral rock extrusion of Western Donbass. These rocks are located between load-bearing rock plate, strengthened by bolts in the roof and harder (about 3 times) coal bed in the foot.

Comparison of results of modeling and mine measurements is confirmed by validity and reliability of researches of geomechanical processes in "layered massive-working's support" system. So, non-loading of frame roof-bars and absence of any considerable activation of yieldability's locks are confirmed, and disagreement of calculated and measured values of approaching a roof and a foot is 7.4…10.7%. Also increased lateral loading on frame-legs is experimentally confirmed – divergence of mine measurements of horizontal rock contour movements and results of modeling are 13.2% on the level of frame's arch end and 23.4% in the place of lower frame-leg part, that is full satisfactory inaccuracy of geomechanical process calculations in "layered massive-working's support" system.

3 CONCLUSIONS

Results of computer modeling of "layered massive-working's support" system's SSS allow to investigate the mechanism of frame support and bolts operation due to existing scheme of layered working maintenance. The main point of which is formation of reinforced-rock plate in the roof of mine working for increased rock pressure in its walls, leading to appearing areas of plastic state in frame-legs.

Analyze of "layered massive-working's support" system's SSS revealed little differences (as rule, about several percents) of vertical and horizontal stress component values during installation SVP-27 and SVP-19 frames in combination with rock bolt support in the opening's roof. Installation of more light-weight profile allows to reduce till 30% metal-content of frames and to decrease labor-content to installing it.

In the frame-legs two areas (in the place of arch ends and in lower frame-leg part) of plastic material state are created independently on SVP-number. For removing these areas, strengthening lateral working sides by rock bolts is required to do.

REFERENCES

Bondarenko, V.I., Kovalevska, I.A., Simanovich, G.A. & Fomichev V.V. 2006. *Computer modeling of stress-strain state of fine-layered rock mass around an in-seam working*. Preultimate stage of "rock-support" system deformation. Book 1. Dnipropetrovs'k: System technologies: 172.

Bondarenko, V.I., Kovalevska, I.A., Simanovich, G.A. & Fomichev, V.V. 2007. *Computer modeling of stress-strain state of fine-layered rock mass around an in-seam working*. Ultimate and behind-ultimate states of "rock-support" system. Book 2. Dnipropetrovs'k: System technologies: 198.

Technical and Geoinformational Systems in Mining – Pivnyak, Bondarenko & Kovalevs'ka (eds)
© 2011 Taylor & Francis Group, London, ISBN 978-0-415-68877-2

Energy saving approaches for mine drainage systems

O. Beshta, D. Beshta, O. Balakhontsev & S. Khudoliy
National Mining University, Dnipropetrovs'k, Ukraine

ABSTRACT: The article is devoted to optimization of mine drainage facilities operation for reducing of energy consumption. Specific features of pumps electric drives and their operating modes are described. Basing on drainage pumps requirements the new approach for energy saving operation is developed. Experimental results proving approach adequacy are given.

1 INTRODUCTION

Energy saving is stated to be a key trend in Ukrainian industry. It is especially important for coal and ore mining enterprises which being the basis of GDP in Ukraine meanwhile suffer severe competition on international market. The main reason for low competitiveness of Ukrainian raw materials is high level of specific energy cost in final product.

Privatization of mining enterprises made their owners thoroughly revise management principles. Modern resource planning strategies are being applied instead of obsolete soviet approaches. The need for energy consumption assessment is realized to be the key factor for energy saving. Only "administrative" measures i.e. rational organization of equipment maintenance brought about 10% energy consumption reduction during the first decade since optimization. Now the potential for furtheir energy saving due to only rational planning is believed to be depleted. It is time to improve technology.

The chart (Figure 1) illustrates energy consumption distribution among main facilities of a coal mine. Obviously exact numbers depend on many factors like water content, temperature and humidity. The distribution pattern varies from mine to mine and even within a day for a certain mines.

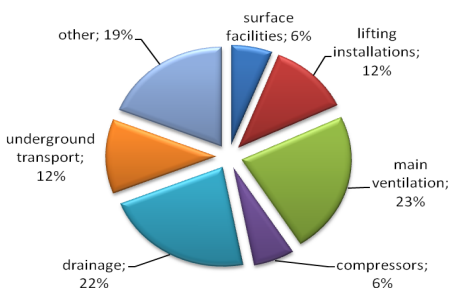

Figure 1. Typical coal mine energy consumption chart.

Amazingly, the share of "useful" energy i.e. connected with coal extraction and underground transportation and lifting it to the surface is only about 30%. The rest of total energy is consumed with "auxiliary" but nevertheless necessary loads – ventilation, drainage, compressors and other facilities.

Mine ventilation and drainage are the most important consumers at any mine. Ventilation must provide necessary oxygen content and methane rarefaction down to safe level. It mainly depends on mine structure and its energy consumption cannot be significantly decreased for safety reasons. And fault of pumping system can cause almost immediate mine flood. So these two facilities must operate stable despite on production level.

Authors had carried out a series of field research at several coal and ore mines of Dnipropetrovs'k and Zaporizhya region. Preliminary results show that mine drainage systems being the key energy consumers are maintained in inefficient modes. So these systems possess the highest potential for energy saving.

2 APPROACH DESCRIPTION

The key concept describing any pumping system is a QH-curve, it shows dependence of pump's flow rate (supply) Q from head H. The dewatering line is characterized with same values – pressure drop as a function of flow rate. The head pressure contains two components: static pressure (simply, the height you need to deliver water on) and dynamic (connected with friction between liquid and tube and other hydraulic phenomena like turbulence) (Pivnyak 2010; report by Xenergy 1998).

Mine dewatering lines are featured with high static pressure and low dynamic component. Another specific feature of mine systems is parallel operation of the pumps. In order to estimate operation

points of each pump under parallel operation one must build a resulting pumps' QH-curve and superimpose it to the mains curve.

Figure 2 illustrates scheme and typical QH-curves for mine drainage system in case of parallel pumps' connection.

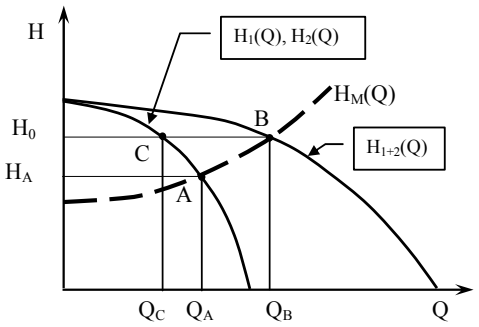

Figure 2. Parallel pumps operation in mine drainage: QH-curves and operation points.

$H_1(Q)$ and $H_2(Q)$ represent individual pumps' characteristics, $H_{1+2}(Q)$ – the resulting curve. $H_M(Q)$ stands for the characteristic of the water mains (the whole dewatering system).

If the pumps have absolutely coinciding characteristics, as it shown at Figure 2, they provide equal flow rates, defined by the resulting head H_0. The value of H_0, in turn, depends on resulting flow rate Q_0 and hydraulic line's characteristic. The "B" point is found as intersection between the resulting pumps' $H_{1+2}(Q)$ and mains $H_M(Q)$ characteristic. Thus, point "A" shows each pump's standalone operation, point "B" represents resulting H and Q under parallel operation. This case each pump operates at its "C" point due to the rise of output head from H_A to H_0 value.

Operating at "C" point means less flow rate for each pump. The maintenance area of each pump must be wide enough to provide stable operation. It also means the increase of hydraulic drop and hence, specific energy consumption. So, the more pumps operates simultaneously the more expensive dewatering is.

The situation becomes even more strained when pumps have different QH-curves (Figure 3).

The "2" curve is peculiar to the worn out pump – it produces less flow under the same backpressure. Simultaneous operation of pumps with different QH-curves results in shifting of operation point of the "weaker" pump down to low flow rate area Q_{B2}. In extreme case it can produce zero supply meanwhile consuming electric power. Therefore, specific energy consumption in dewatering depends not only on pumps' general condition but also on their "matching".

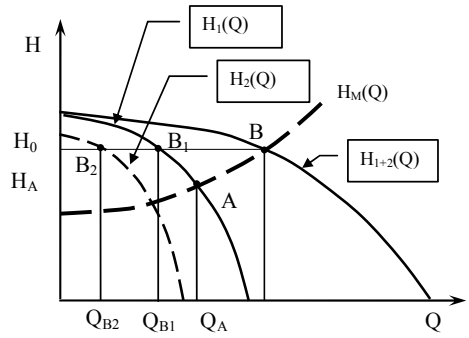

Figure 3. Parallel operation of pumps with different QH-curves.

All the mentioned gives us realization of two major energy saving principles for dewatering systems:

- rational pumps' operation time planning according to inflow rate and time-of-day tariff;
- rational pumps' combination in case of their parallel operation for minimal specific energy consumption.

Implementation of both tasks requires introduction of mine monitoring system for constant survey of hydraulic and mechanic factors. The inflow rate, electric motors' and pumps' and dewatering line condition should be monitored (Europump and Hydraulic Institute 2001).

3 EXPERIMENTAL RESULTS

To estimate energy saving potential in mine dewatering the preliminary experiments were carried out at several coal mines of Dnepropetrovsk region.

The dewatering horizon -225 m contained ten pumps of CSP 300×290 type in three sunk basins (CSP stands for "centrifugal sectional pump", correspondent Russian abbreviation is CNS; 300 represents rated head, m, 290 – rated supply, m^3 / hr).

Special measuring equipment was installed, including autonomous data acquisition systems (ADA) at each pump. ADA has internal power supply and memory storage, providing continuous data collection for 48 hours. Each ADA was synchronized with the rest ones and the basic acquisition module.

Measuring of the flow rate caused certain problems. Ultrasonic flowmeter produced error up to 40% when flow rate reached 1000 m3/hr because of turbulence effect. A special approach was developed basing on water level at the inlet header on the surface. The approach is based on the Bernulli equation

$$Q = \mu \cdot S_0 \cdot (2g \cdot k_0 \cdot (L - h_0))^{\alpha},$$

where μ, α – nonlinear coefficients depending on liquid's viscosity and other parameters; S_0 – area of the inlet; $g = 9.81$ – acceleration of gravity; k_0, h_0 – scale gains; L – level of water in the inlet header.

The actual flow rate was estimated by ratio $\Delta V / \Delta t$, where ΔV is the gain of water volume in the water precipitation pool (measured rather simply) and ΔV is the time period. Thus flowmeter was replaced with much cheaper hydrometric float level meter.

Figure 4 illustrates measuring scheme for each pump and dewatering mains.

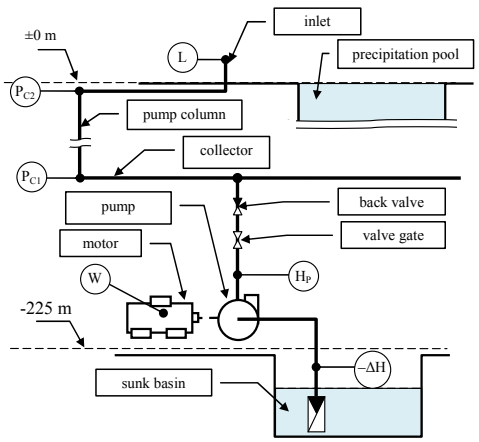

Figure 4. Measuring scheme for a pump and dewatering line.

The following parameters were measured:

- total flow rate Q (measured via water level L);
- each pump's input depression – ΔH;
- each pump's head H_P;
- pressure at the dewatering collector P_{C1} (underground);
- pressure at the pump column P_{C2} (surface);
- electric power consumption W.

During several testing sessions the individual pumps' QH-curves were obtained. Then energy consumption under each pump standalone operation and their various combinations was estimated. As was expected, actual QH-curves and pump's efficiencies differed from each other and from rated values. Figure 5 shows rated and actual QH-curve of one pump under standalone and parallel operation.

The actual QH-curve lies lower than the rated one. It means that for the same backpressure the pump produce less flow rate. For example, under rated backpressure of 290 m the pump produce 210 m^3 / hr instead of rated value of 300 m^3 / hr.

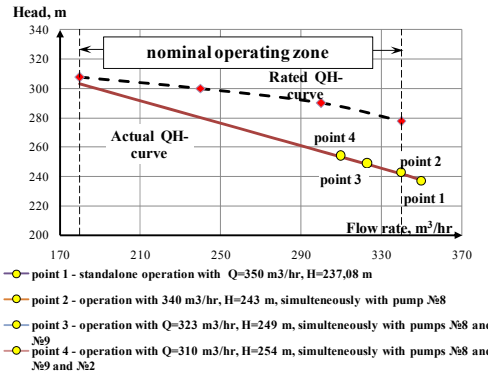

Figure 5. QH-curves and operating points under standalone and parallel operation.

Operating point #1 (standalone maintenance) lies beyond the zone of normal functioning in the area of extra supply, which is can cause cavitation effect.

Point 4 indicates simultaneous operation of four pumps – maximal number of parallel operating pumps. Even at this point the pump has a good reserve to stay in the rated operating zone.

Lower supply under required head means less pump efficiency. Figure 6 illustrates pumps' efficiencies under standalone operation. The value of "total efficiency" includes efficiencies of the pumps themselves and their drive motors.

Obviously, actual efficiency is always lower than the rated value. It depends of how worn the pump is. The pump #2, for example, posses the lowest efficiency of 29%.

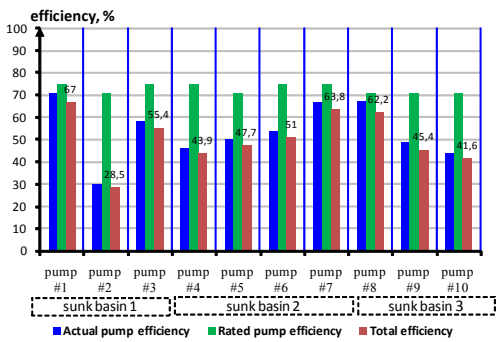

Figure 6. Estimated efficiencies of the pumps.

Meanwhile, most of duty cycle pumps operate in parallel. The resulting efficiency and thus, specific energy consumption, depends not only of these parameters in standalone operation, but also on individual QH-curves.

The energetic performances of dewatering system under all possible combinations of the pumps in-

stalled cannot be determined experimentally. Certain restrictions should also be considered – the allowable number of gear starting, the pumps under repair and so on. So, in order to forecast specific energy consumption under pumps' parallel operation, simulation is required.

Table 1 shows specific energy consumption (kWh / m^3) under parallel operation of two of possible ten pumps.

Table 1. Specific energy consumption under operation of pumps in pairs.

pump #	#1	#2	#3	#4	#5	#6	#7	#8	#9	#10
#1	1.0									
#2	2.5	2.2								
#3	1.2	2.6	1.1							
#4	1.5	2.7	1.5	1.4						
#5	1.4	2.5	1.4	1.6	1.3					
#6	1.5	2.7	1.5	1.6	1.6	1.4				
#7	1.2	2.3	1.2	1.6	1.4	1.6	1.0			
#8	1.1	2.4	1.2	1.6	1.4	1.6	1.2	1.0		
#9	1.5	2.6	1.5	1.6	1.6	1.6	1.7	1.5	1.4	
#10	1.6	2.8	1.7	1.7	1.7	1.7	1.8	1.7	1.7	1.5

The diagonal of the table shows specific energy under standalone pumps operation. The cell with coordinates, for instance, 3, 2 indicates specific energy consumed by dewatering system when pumps #2 and #3 are operating simultaneously and so on.

The pump #2, possessing the lowest efficiency in standalone operation, "spoils" the system being launched together with any of the rest of pumps. Generally, the level of specific energy demand varies within 1.1-2.8 kWh / m^3, showing us how important is to chose correct combination of the pumps. Considering average water inflow of about 20000 m^3 / day gives us a huge potential for energy saving.

Forecasting of specific energy consumption for combinations of three or four pumps cannot be presented graphically. Nevertheless, the need for intelligent selection of what pump to launch is obvious.

4 FURTHER RESEARCH

A special system should be developed to assist dewatering dispatcher service. It should later be transformed in automated control system implementing energy saving principles.

It should be taken into account that individual QH-curves of pumps are not stable since wearing goes continuously. Faults occur, pumps and electric motors and shutoff valves are being replaced for certain technological reasons. So, the system to be developed must be adaptive to variations of industrial conditions.

5 CONCLUSIONS

Dewatering systems being the key consumers in mine production posses the highest potential for energy saving. Two basic principles must be implemented: rational pumps' operation time planning according to inflow rate and time-of-day tariff and rational pumps' combination in case of their parallel operation for minimal specific energy consumption.

REFERENCES

Pivnyak, G., Beshta, A. & Balakhontsev, A. 2010. *Efficiency of water supply regulation principles*. New Techniques and Technologies in Mining. Proceedings of the school of underground mining. © CRC Press/Balkema, Taylor & Francis Group, London.

United States Industrial Motor Systems Market Opportunities Assessment, report by Xenergy for Oak Ridge National Laboratory and the U.S. Department of Energy. 1998. http://www.oit.doe.gov/bestpractices/pdfs/mtrmkt.pdf.

Pump Lifecycle Costs: A Guide to LCC Analysis for Pumping Systems, Europump and Hydraulic Institute. 2001. http://www.oit.doe.gov/bestpractices/pdfs/pumplcc_100.pdf.

Technical and Geoinformational Systems in Mining – Pivnyak, Bondarenko & Kovalevs'ka (eds)

Development of methods for utilization of thermal energy in the underground gasification of coal mining

G. Gayko & V. Zayev
Donbass State Technical University, Alchevsk, Ukraine

ABSTRACT: The methods of heat extracting out of the coal layer combustion zone and surrounding rocks during underground coal gasification are developed. New technology allows obtaining additional electricity another than generating gas by using a liquid coolant.

1 INTRODUCTION

Global trends in energy indicate expansion of underground coal gasification, and actively seeking ways to improve the effectiveness of these technologies. In today's world there are about 20 major stations of the underground gasification of coal, and every year we introduce 1-2 new stations. Leader in this technology is China (in 2007 in the country 6 stations worked and 4 more were built) (Kondyrev 2007), 1-2 stations operate in Australia, Canada, USA, South Africa, Uzbekistan (in Angren lignite mine – since 1963). Interest in introducing technology of underground thermochemical conversion of coal comes from such countries as Belarus, Bulgaria, Britain, India, Kazakhstan, Poland and Ukraine, where the evaluations of coal deposits were made in terms of their prospects for the gasification, the projects of building new plants were justified.

It is noteworthy that the Ukraine in the last century has been a pioneer in the development of technology of underground gasification of coal seams; Lisichansk and Gorlovka for decades successfully operated Podzemgaz stations. In the 80th years of the twentieth century the special geological surveys were conducted, and coal gasification projects were designed foe Dneprovskiy lignite basin, as well as a comprehensive assessment of the suitability of Donbass fields for underground gasification was given (Kolokolov 2000). Significant contribution to the development of new technologies have been made by schools of the Russian Federation (Vladimir Rzhevskii, W. J. Ahrens, J. D. Dyad'kin, A. Ruban, etc.), but using of rich deposits of natural gas has weakened the practical interest to the construction of underground coal gasification plants on Russian territory.

Despite the obvious advantages of underground thermochemical conversion of coal (exploitation of deserted fields, involvement in the development of off-balance sheet inventory, solving a number of environmental problems), the global experience of operating stations "Podzemgaz" identified a number of unresolved issues that impede widespread use of these technologies. Disadvantages include: relatively low heat of combustion of the resulting gas generator, the difficulty in control of the processes of gasification and significant (up to 30-50%) loss of heat in the interior (Gluzberg & Serov 1985). The latter factor causes the lack of effectiveness of the technologies and simultaneously indicates significant opportunities to improve it.

One of the areas of recycling thermal energy at the thermochemical processing of coal seam gas is the use of coolant (water vapor), which fillsburnt-out space after (or during) gasification (development SPGGI). Unstable characteristics of the coolant caused its use only in the heat exchangers, and the complexity of the extraction and separation of steam from the generator gas impede widespread use of this method.

The original method for extracting heat from the combustion zone of the coal face is proposed in KuzGTU (Kemerovo) (Patent RF #2278254). Method is based on building coal-fired units and their burning with the simultaneous selection of the burning heat of bed by steam generators, which should move the slope after the fiery front. Scope of this method involves mining method burning coal seams, however, to ensure the movement of steam generators for biases is extremely difficult due to the uncertainty of the line of fire and slaughter of the complexity of maintenance of slopes directly adjacent to the combustion zone.

2 DISPOSAL OF THE USE OF LIQUID COOLANT

In DonSTU concept of mine-power station, assuming an underground combustion (gasification) coal seams with a liquid coolant circulating in the collector pipe in the ground coal seam is designed (Gayko & Kasyanov 2008). Recent advances in the field of geothermal energy technologies open up entirely new opportunities for electricity generation using a liquid coolant, bringing the efficiency of hydro turbines and high-temperature steam power plant units. Modern modular geothermal power plants are used as the working fluid superheated water ($T = 110 - 250$ ºC), have compact dimensions (for "Tuman-2"– $10.5 \times 3 \times 3.5$ m) and consume the amount of coolant from 10 to 40 m^3 per hour. Method of DonSTU first combined the principle of the circulation of hot water in a sealed tube collector, placed in the soil of burnt coal seam using hydro turbines to generate electricity for the modular stations. The developed concept could be rather promising for mine thermochemical conversion of coal seams, or their parts (whole, areas in difficult GSU, etc.).

Since the highest prevalence and cost-effectiveness of downhole are demonstrated by ways of underground gasification of coal seams, the authors posed the problem of adaptation of technical ideas embodied in the concept (Gayko & Kasyanov 2008), for downhole technology. For this purpose, we developed methods of utilization of thermal energy for the horizontal (flat) (Gayko & Zayev 2010) and steep-slope (Patent Ukrainy #54138) coal layers.

On flat layers the method is carried out as follows (Figure 1). In accordance with the method of gasification (or burning) coal layers from the surface there are drilled air-supplying system and gas-escape holes 1, which reach the coal layer 2. Additionally, there drill penetrating wells 3 with pass cavity 4, and the wells are in the soil of the coal layer and come to the surface. In penetrating wells three tight line 5 are brought, which are formed by the connection (for example, by welding) hard segments of the pipeline 6 with flexible intermediate elements 7 made in the form of corrugated hoses. Length of straight rigid pipe section 6 is determined considering the curvature of the penetrating hole 3 and the size of the pass cavity 4 in which the transition of the pipeline in the plane of the soil carbon reservoir is performed.

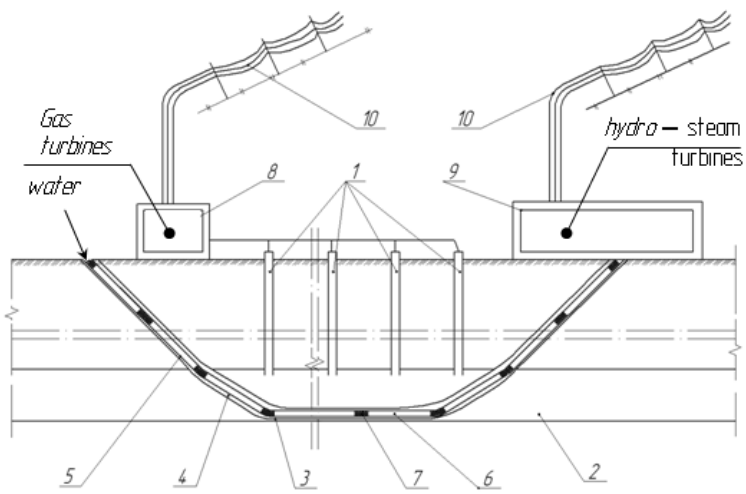

Figure 1. Scheme of utilizing method of heat power.

After installation of the pipeline the process of gasification of coal layer is performed, removing the resulting producer gas for gas turbine 8. Simultaneously, fluid (water) heat transfer is brought to the input of the pipeline 5, adjusting the pump speed of the coolant, whose temperature at the outlet should be 150-200 ºC (the optimal parameters for hydro turbine 9). Electricity obtained on the gas and hydro turbines is fed through power lines to 10 users.

For steep-slope layers a method of generating electricity (Figure 2, 3) is developed. On the surface coal layer 3 air-supplying 1, gas-outlet 2, and heat exhaust wells 4 are drilled. The latter are drilled in the soil layer 3 and are equipped with airtight stand-

pipe 5 with a closed end. In the standpipe they place five feeding sleeves 6, forming a system of "pipe in pipe". Using the supply hose 6 liquid heat-carrier is fed to the bottom of the standpipe and going through it the heat-carrier passes combustion zone reservoir 7 in which the coolant is heated to a temperature of 250-300 ºC and transported to the wellhead, where it is fed to hydroturbines with electric generators 8.

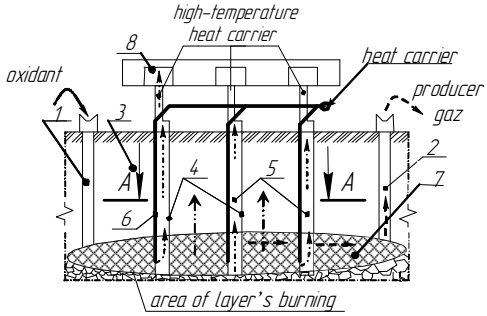

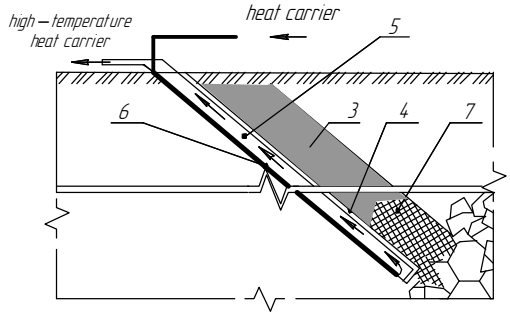

Figure 2. General scheme of providing the method.

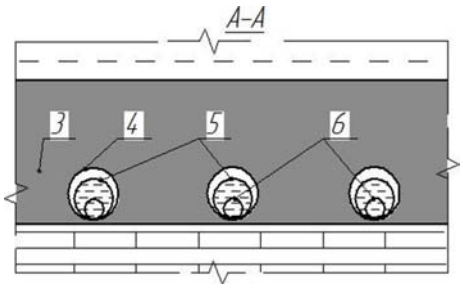

Figure 3. Cross section of a coal layer with a heat-wells, tube set and the supply hose.

Thus, in addition to the produced generator gas from underground coal gasification, the developed methods allow to extract a great part of thermal energy from the combustion zone, which is transported using a liquid coolant along airtight pipes to hydro turbines. This allows us greatly improve the general efficiency of power production and develop new perspectives for the introduction of borehole technology at "Podzemgaz" stations.

3 CONCLUSIONS

1. Global trends in power industry indicate expansion of underground coal gasification, and actively seeking ways to improve the efficiency of these technologies, primarily aimed at reducing heat losses in the subsoil.

2. In DonSTU for utilization of thermal power from underground gas generator it was first proposed to use liquid heat-carrier (overheated water) circulating in airtight pipe or sewer system in high temperature combustion zone of a layer.

3. Advances of previous decades in the field of geothermal energy technologies have opened new possibilities for power generation using liquid coolant, bringing the efficiency of new hydro turbines (water at $T = 110 - 250$ ºC) to the traditional high-temperature steam-power units (steam at $T = 700$ ºC). This allowed us to combine the methods developed by recycling heat from power generation at hydro turbines.

4. The expected economic effect from introducing the new technology when developing one coal block with the dimensions: on the gradient – 200 meters, on stretching – 300 m, seam thickness – 2.5 m will be not less $ 4 million. These money should be considered as an addition to the cost of generator gas obtained by gasification of coal block.

REFERENCES

Kondyrev, B.I., Belov, A.V. & Mannangolov, D.Sh. 2007. *Developing the technology of underground coal gasification.* Perspectives of coal deposits development in the Far East. Mining informational and analytical bulletin (scientific and technical journal), 1: 297-300.

Kolokolov, O.V. 2000. *Theory and practice of thermochemical technology of producing and conversion of coal.* Dnepropetrovsk: NMU: 281.

Gluzberg, Ye.I. & Serov, V.A. 1985. *Assessment of heat losses from fire area into surrounding massif.* Mining Journal, 11: 59-64.

Patent RF #2278254, MPK E21B 43/295 (2006.01). *Sposob poluczenia elektroenergii pri podziemnem ugleszyganii*. S.A. Prokopienko; Zajawl. 21.12.2004; Opubl. 20.06.2006. Bul. 17.

Gayko, G. & Kasyanov, V. 2008. *The Concept of Mine-*

Power-Station Involving the Underground Burning of Coal Strata. 21st World Mining Congress. New Technologies in Mining. Krakow: AGH: 199-204.

Gayko, G.I. & Zayev, V.V. 2010. *New method for producing power during underground coal seam gasification (burning)*. Donetsk Bulletin of Shevchenko Scientific society. Donetsk: Schidnyj wydawnyczyj dim, 29: 64-67.

Patent Ukrainy #54138, MPK E21B 43/00. *Sposib otrymannia elektroenergii pri bezszachtnomu spalenni plastiw pochylogo zaliagannia* / G. Gayko, V. Zayev. – Zajawl. 07.05.2010. Opubl. 25.10.2010. Bul. 20.

Technical and Geoinformational Systems in Mining – Pivnyak, Bondarenko & Kovalevs'ka (eds)

Engineering support of BUCG process in Solenovsk coal deposits

V. Falshtynskyi & R. Dychkovskyi
National Mining University, Dnipropetrovs'k, Ukraine

M. Illiashov
SC "Donetsksteel", Donetsk, Ukraine

ABSTRACT: In the article characteristics of fitness criteria to BUCG for thin Solenovsk seams are grounded. The calculations of thermal and material balance for coal seam gasification process are executed. The construction, method of underground gas generator preparation, and sequence of coal seam gasification for area №1 are designed.

1 INTRODUCTION

The technology of borehole underground coal gasification (BUCG) is an enterprise for the generation of electric and thermal energy, passing chemical products, fuel and fluid gases in place of coal seams location. Installation of this technology will give a capability to explore uneconomical coal reserves and local deposits of solid fuel in difficult geological conditions.

As compared to traditional mining during BUCG it is possible to except hard work of miners, use uneconomical and unconditional coal reserves. The products of gas combustion are not contained by the oxides of carbon, particulate matters, sulphurous anhydrite.

The methods, technological schemes and constructions of underground gas generators designed in the National mining university allow to manage the process of underground coal gasification, providing remaining the thermo-chemical balance of conversions and physical processes at coal seam gasification. Enterprises using the BUCG technology provide automation of production processes. The final product of such generation becomes not coal, as a feed for further conversion, but kilowatts of thermal, electric energy and chemical row materials. Closed-circuit operation in chemical manufacturing effects a substantial saving in starting materials and utilities.

Industrial enterprises on BUCG technology was first built and exploited in the USSR in 1928. (Lisichanska, Gorlovska, Yuzhno-Abenska, Podmoskovn, Shatska and Angrenska station of "Pidzemgaz"). The stations after a closing were blocked at the end of 1960, Yuzhno-Abenskay – 1996. Angrenskaya works from 1964 until present time.

On the modern stage of underground coal gasification development the leader in this direction is China (8 experimental and experimentally-industrial underground gas generators) Such country as Australia, Poland, South Africa, USA, Spain, Belgium, England, Slovakia also conducted several experiments.

2 CRITERIA OF COAL SEAM FITNESS TO BUCG IN THE AREA #1

Based on the evaluation of practical material of coal seam gasification on the "Pidzemgaz" stations (Lisichanska, Gorlovska and Yuzhno-Abinska), conducted investigations on an experimental mine gas generator and stand unit options, the generalized dependences of criteria are certain for 12 area of Solenovsk coal deposit, for the carrying out industrial experiment the area #1 was chosen (Kolokolov 2000 & Skafa 1960).

Area #1 located on the field of Solenovsk coal deposits – 1, 2, 3, Krasnoarmiysk coal district, Donetsk region, joins to the north-eastern bent of the Ukrainian crystalline rock mass and extends along on a southeast beads of the Donetsk ridge. A department presents a C_6^1, C_6, C_5^1, C_5, C_4^2.

To the down-dip and to the rise the series of strata are limited by Shevchenkivskiy fault #1 and Kirillovskiy fault, along the strike – Shevchenkivskiy fault #3. The size of area to the down-dip $H = 1410$ m, on the rise southward $S = 827$ m. on

the north $S = 3000$ m. General productive coal reserves make $Z = 4786.8$ thousand tons. The stratification depth of coal seams $H = 72 - 221$ m, power $m = 0.5 - 0.9$ m, angle of inclination $\alpha = 10 - 19^{\circ}$.

The criteria of strata formation fitness located in area №1 for underground coal gasification covered on basal factors: to mining-and-geological, hydrogeological and technical. The scopes of area condition the presence of natural screens (disjunctive dislocations). The stratification depth of coal seams enables to provide efficiency and fail-safety working. Coal seam power are within the limits of 0.7-0.9 m, that is conditioned by a lower bound in the criteria of fitness of coal seams to BUCG. Containing rocks (77.4% claystone and siltstone), penetration capabilities within the limits 0.71-1.06 Darcy, providing impermeability and efficiency of process at the penetration capability of coal seams 0.38-0.62 Darcy.

In these terms the expected inflow of water in an underground gas generator will make 1.2-3.4 m^3 / t (on a hydrogeological factor this area requires supplementary explorations).

At existing technological and engineering developments assurance of effective and fail-safety of coal seam gasification process is possible on this area.

The criteria of fitness to in-situ coal seam gasification on the area #1 resulted in Table. 1.

Table 1. Basic suitability criteria of hard coal seams underground gasification within the area #1 (C_6^1, C_6, C_5^1, C_5, C_4^2).

Coal grade G	Seam thickness, m	Coal seam ash content, A^C, %	Wall rocks (roof, bottom); total			Sulphur content in the seam, S, %
			Thickness of clays or other low permeable rocks in roof; h^1, m $h^1/m > H$	Thickness of clays or other low-permeable rocks in bottom; h, m $H \geq 2.0$ m	Distance from the seam roof to separate highpermeable layers or undrained water-bearing horizons h_2; $h_2 > h$ h – height of the fractures zone, m	
C_6^1	0.9	6.9-12	14.3 > 8.1	9.6 > 2	24.5 > 10.8	1.9
C_6	0.7	6.2-18	12.5 > 6.3	7.3 > 2	11.2 > 8.4	1.9
C_5^1	0.75	10-21	13.2 > 6.8	5.5 > 2	15.75 > 9.0	1.1
C_5	0.7	5.9-16	10.1 > 6.3	6.2 > 2	11.4 > 8.4	1.9
C_4^2	0.55	9.2-17	18.4 > 5.5	7.8 > 2	22.6 > 67	2.5

Continuation of Table 1

Coal grade G	Minimal safe mining depth (H, m) and seam dip angle from $\alpha = 0^{\circ}$ to 45° (wings, mould); $H/m \geq 15$, $n = 1$ $H \geq m \cdot n$	Tectonic abnormalities; $L_n \geq L_g$	Specific water inflow, m^3 / t into reaction channel of the gas generator considering BUCG process intensity, (not more than 1.6-3.4 m^3 / t)		Moisture content of BUCG gas, g / m^3		Ratio of coal and rock gas-permeability
			Q_{air}	Q_{oxygen}	Q_{air}	Q_{oxygen}	
C_6^1	69.8 m > 15; $H = 15$ m	Boundaries of the area. Disjunctive abnormalities	4.4 t / h	2.8 t / h	445	238	21-38
C_6			4.15	2.17	429	234	17-29
C_5^1			4.23	2.25	387	231	18-34
C_5			4.04	2.2	375	220	18-36
C_4^2			3.6	1.98	411	235	20-37

3 MATERIALLY-THERMAL BALANCE OF COAL SEAM GASIFICATION PROCESS, AREA #1

For the calculation of materially-thermal balance of BUCG the program MTBalanse SPGU is utillized designed by the employees of underground mining department from the National mining university (Lavrov 1957 & Falshtynskyi 2010). The algorithm of calculation includes thermochemical conversions of solid fuel in a gas and condensed fluid in the conditions of elementary composition of coal seam, external water inflow and thermal balance of underground gas generator is foreseen in it. A program algorithm is presented on a Figure 1.

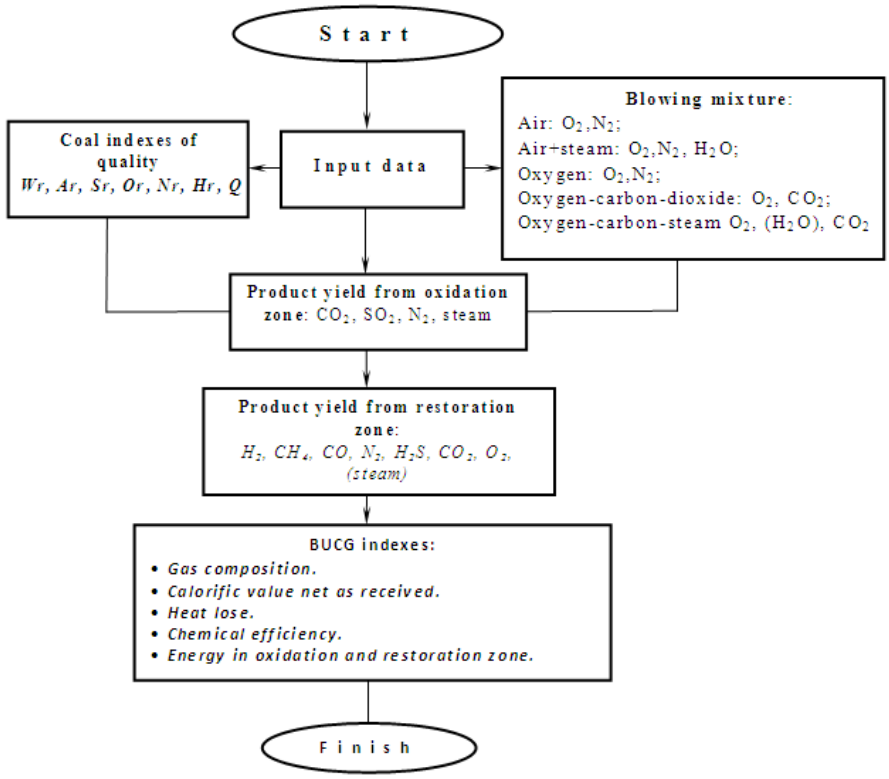

Figure 1. Algorithm of the program for material and thermal balance calculation.

The program of calculation takes into account such terms of process:

1. A change a technogenic situation in rock masss which contain a underground gas generator taking into account mine and geological conditions and technological characteristics of process;

2. Specifics of blowing composition and effect them on the process of coal seam gasification;

3. Change of high-quality and quantitative coefficients of BUCG gas from the grade of coal seam and blowing mixture;

4. Influence of geometrical characteristics of oxidizing and restoration zone of reactionary conduit of gas generator on balance of coefficients of chemical conversions and physical speeds;

5 Influence on thermal balance at coal seam gasification;

6. Effect of ballast gas of gasification process on the high-quality coefficients of underground gas generator;

Technological coefficients of underground gas generator and escape of basic chemical products at BUCG, presented in Tables 2 and 3, characteristics of materially-thermal balance on the area for SPGU #1 presented in Tables 4, 5, 6, 7.

Table 2. Technological indexes of underground gas generator.

Indexes of underground gas generator	COMPOSITION OF BLOWING					
	Air	Oxygen	Oxygen + CO_2 + steam	Oxygen + CO_2	Air + steam	Oxygen + steam
Thermal power	GKal					
	11.97	23.6	21.7	23.72	14.17	22.1
Electrical power	MVat					
	13.9	27.4	25.2	27.5	16.4	25.6
Capacity on gas	10^6 m^3					
(CH_4, CO; H_2)	26.9	68.4	57	80.7	32.2	571

Table 3. Escape of main chemical products during production activities of underground gas generator.

Types of blowing mixture	Escape of chemical products at BUCG (tons)			
	Coal gum	Benzol	Ammonia	Sulphur
O_2N_2	2649	482.4	1050	153.3
H_2O (steam)+ O_2, N_2	26207	476	1132.6	164.6
O_2 (30-62%) N_2	2829.4	609.4	758.3	286.2
O_2 + steam	2624	578.1	782.6	235.3
$CO_2 + O_2$	2858	621	718.4	293.4
$CO_2 + O_2 + H_2O$ (steam)	2665	588	773	277.2

Table 4. Characteristics of materially-thermal balance on the area #1 (coal seam, C_6^1 – 0.9 m).

Type of blowing mixture	Characteristics of blowing	Gas quantity from a gas generator, %						
	m^3 / h	H_2	CH_4	CO	N_2	H_2S	CO_2	O_2
Air	6957	4.68	4.46	26.13	60.21	0.3	3.68	0.54
Air + steam O_2 N_2 Steam	7026 1266.2 3541.4 2218.4	15.13	15.07	6.31	52.74	0.49	9.30	0.78
Oxygen + steam O_2 N_2 Steam	6323 2856.8 1429.1 2037.1	23.06	22.45	11.05	21.61	0.69	19.98	1.16
Oxygen + carbon dioxide + steam O_2, CO_2 steam	6118 1963.8 911.6 3242.5	26.58	25.24	13.83	0.27-	0.61	32.34	1.14
Oxygen O_2 N_2	6885 4186.1 2698.9	10.27	9.78	37.31	21.46	0.66	10.26	1.19
Oxygen + carbon dioxide O_2 CO_2 N_2	6 506 4 014.2 969.4 1 522.4	11.68	10.17	52.9	11.73	0.69	11.68	1.15

Continuation of Table 4.

Type of lowing mixture	Speed of coal seam gasification	Efficiency	Lower heat of combustion	Gas discharge from gasgenerator	The humidity of BUCG gas	Quantity of coal gasification
	m / day	%	Mj / m^3	m^3 / kg of coal	g / m^3	t / h
Air	1.94	62.87	4.71	2.84	372	2.5
Air + steam O_2, N_2, steam	2.04	68.21	5.82	2.94	473	2.62
Oxygen + steam O_2, N_2, steam	2.63	78.4	8.5	2.12	369	4.25
Oxygen + carbon dioxide + steam O_2, CO_2, steam	2.3	79.12	9.28	2.19	320	4.2
Oxygen O_2, N_2	2.5	80.5	9.84	1.95	238	5.06
Oxygen + carbon dioxide O_2, CO_2, N_2	2.25	80.03	9.36	2.08	274	4.26

Table 5. Technological characteristics of BUCG process (area #1, coal seam, C_6^1 – 0.9 m).

Type of blowing mixture	Expenditure of blowing, thousand				Escape of BUCG gas, thousand			
	m^3 / h	m^3 / d	m^3 / m	m^3 / y	m^3 / h	m^3 / d	m^3 / m	m^3 / y
Air	6.96	167	5011.2	60134.4	8.83	212	6360	76320
Air + steam	7.03	168.7	5061	60732	9.2	221	6630	79560
Oxygen	6.88	165.1	4953.6	59443	12	288	8640	103680
Oxygen steam	6.32	151.2	4536	54432	10.5	252	7560	90720
Oxygen + carbon dioxide	6.5	156	4680	56160	12.5	300	9000	108000
Oxygen + carbon dioxide + steam	6.12	146.9	4406.4	52876.8	10.1	242.4	7272	87264

Continuation of Table 5.

Type ob blowing mixture	Quantity of coal gasify for set time:				Time of gasification, days	Quantity of gas at expluatation 10^6 m^3
	t / hour	t / day	t / year	kg / for the time of gasgenerator expluatation		
Air	2.5	60	21 900	15 330	256.6	53.4
Air + steam	2.62	62.88	22 951.2	16 754.4	240.5	59.6
Oxygen	5.06	1214	44 311	13 293.3	105	31.1
Oxygen +steam	4.25	102	37 230	13 075.3	128.5	33.2
Oxygen + carbon dioxide	4.26	102.2	37 303	13 802	135	40
Oxygen + carbon dioxide + steam	4.2	100.8	66 792	15 452.6	152	36.7

At the oxygen blowing in the range O_2 = 45-62% (4186.13 m / h), the capacity of underground gas generator is provided gas production $8.4 \cdot 10^6$ m^3 / h and electrical power 27.4 MWt, with efficiency equal 80.5% and by the temperature in production borehole $T = 534$ °C.

Blowing carbon dioxide CO_2 – 379.3 – 969.4 m^3 / h, provides in combination with oxygen (2092.4 – 4014.2 m^3 / h) and steam (1863.8 m^3 / h) the receipt of power gas with high-quality coefficients: escape of burning gases of 50 – 80.7·10^6 m^3 / y, electrical power 25.2 – 27.5 MWt, with Efficiency equal 79.12 – 80.3% and by the temperature gas in outlet borehole $T = 529$ °C.

Arrangement of blowing mixture O_2 (2856.8 m^3 / h) + steam (2037.1 m^3 / h), provides gas $57.1 \cdot 10^6$ m^3 / y

with N_2 – 23.06%, CH_4 – 22.45 and CO – 11.05%, such arrangement of burning gases, at oxygen + steam and air + steam blowing (steam = 2218.4 m^3 / h, N_2 – 15.13%, CO – 6.31%), enables to provide a technological gas discharge suitable for synthetic gas.

The coefficients of the air blowing provide a power gas discharge with coefficients: escape of burning gases $26.9 \cdot 10^6$ m^3 / h, and electrical power 13.9 MWt, with efficiency equal 62.9% and by the temperature gas in outlet borehole $T = 366$ °C, at the heat of combustion of power gas 4.71 MJ / m^3.

The pressure in a gas generator at the air and air + steam blowing $P = 0.24 - 0.57$ MPa, at blowing, enriched O_2 ; CO_2 ; H_2O (steam) $P = 0.38 - 1.2$ MPa.

Table 6. Thermal balance of underground coal gasification on the area #1 (coal seam, C_6^1 – 0.9 m).

Indexes	COMPOSITION OF BLOWING											
	Air		Oxygen		$O_2 + CO_2$ + steam		Oxygen + carbon dioxide		Air + steam		Oxygen +steam	
	Mj/kg	%	Mj/kg	%	Mj/kg	%	Mj/kg	%	Mj/kg	%	Mj/kg	%
Heat of combustion on a working fuel	35.04	97.64	35.04	91.25	35.04	91.25	35.04	91.25	35.04	92.79	35.04	91.25
Entalphy in oxidation zone	0.636	1.772	1.272	3.312	1.272	3.313	1.272	3.312	0.636	1.684	1.272	3.312
Entalphy in blowing	0.208	0.580	2.087	5.434	2.087	5.434	2.087	5.434	2.087	5.526	2.087	5.434
In all:	35.88	100	38.40	100	38.4	100	38.4	100	37.76	100	38.4	100
Heat of gas combustion	13.37	38.32	19.09	49.70	20.12	51.96	19.47	50.83	17.1	44.40	18.02	46.88
Heat lose: Heating of ash and slag, MJ	0.095	0.272	0.095	0.247	0.095	0.245	0.095	0.248	0.095	0.247	0.095	0.247
Warming evaporation of moisture, MJ	0.375	1.074	0.375	0976	0.375	0.965	0.375	0.979	0.375	0.974	0.375	0.974
Heating of containing rocks (roof, ground), MJ	6.310	18.079	5.562	14.482	5.510	14.23	5.146	13.435	5.915	15.365	5.967	15.5
Entalphy of generator gas.	14.74	42.25	13.28	34.59	12.62	32.6	13.21	34.5	15.01	39.0	14.0	36.39
In all:	34.903	100	38407	100	38.724	100	38.304	100	38.495	100	38.497	100
Outlet temperature in gasgenerator °C	522		803		798		767		652		705	
Outlet temperature in production borehole °C	346		441		436		421		360		378	

4 TECHNOLOGICAL SCHEME AND ORDER OF UNDERGROUND GAS GENERATOR PREPARATION IN AREA #1

The gas generator preparation is carried out from a surface. The order of gasification of coal seam descending (Figure 2). For assurance the efficiency of gasification process in area #1 the construction of underground gas generator (Figure 3) is used with long coal walls. The system of gasification by long columns to up-dip $L = 400$ m. The distance between the boreholes, $l = 30$ m.

Preparation of gasgenerator providing by in-seam directional drilling (Figure 3).

Coal seam ignition is porvided through the directional boreholes by binary explosives (Falshtynskyi 2008). Ignitions of coal at application of this method

possibly at presence of underwaters and does not require investments on the generation of ignition boreholes.

Control of blowing mixture direction is carried out by flexible pipeline Figure 3. The selective discharge of blowing mixture will provide interference of blowing with fire combustion face. For intensification of process the six arrangements of blowing mixture and heating of blowing are foreseen before a discharge in a underground gas generator to 200 °C, and also the impulsive discharge of main chemical agents (oxygen, steam, carbon dioxide) is provided on combustion face with different time duration. With the purpose of equal combustion face advance the reverse direction of gasification is foreseen.

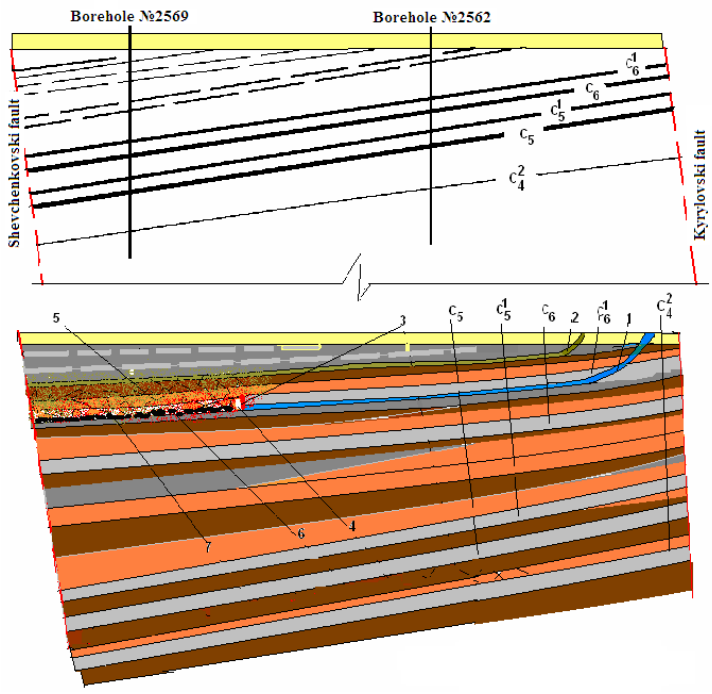

Figure 2. Technological scheme of coal seams on area #1: 1 – inlet borehole, 2 – stowing borehole; 3 – combustion face; 4 – reaction channel of underground gas generator; 5 – a stowing rock mass; 6 – goaf, 7 – ash and slag.

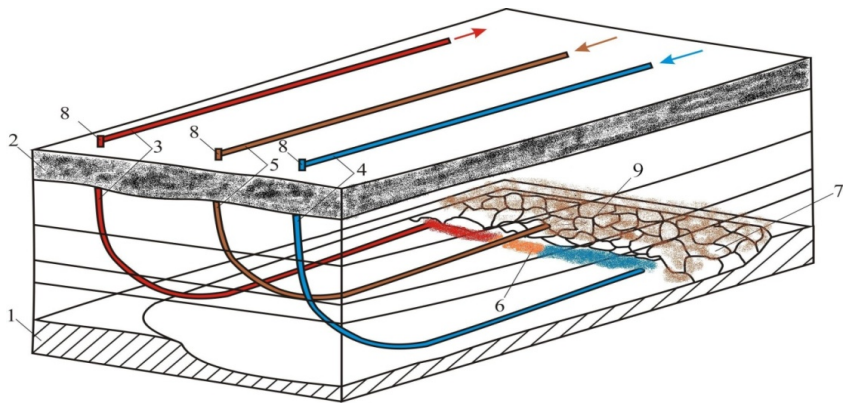

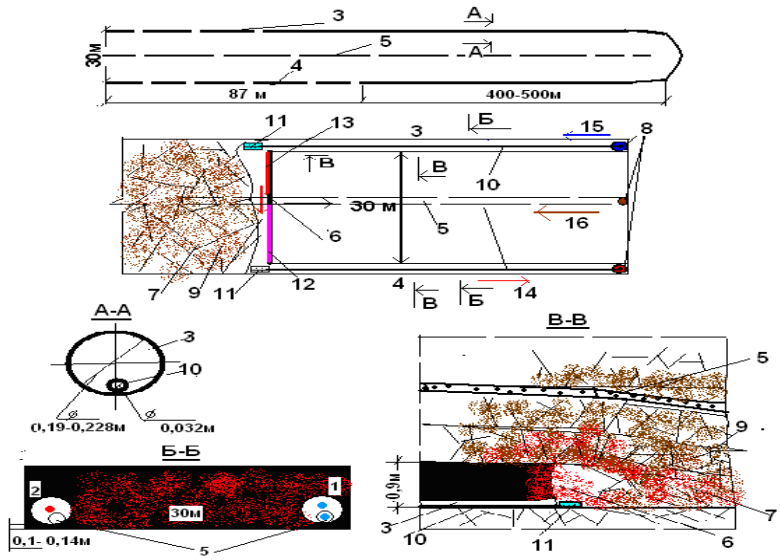

Figure 3. Technological scheme of underground gas generator in the conditions of area #1: 1 – coal seam; 2 – surface; 3 – gas outlet borehole, 4 – inlet borehole; 5 – stowing pipeline; 6 – reaction channel (oxidation zone (blue), restoration (red)); 7 – goaf; 8 – casing head tool; 9 – stowing rock mass; 10 – flexible pipeline; 11 – heat-resistant nose (0.4 m); 12 – restoration zone of reaction channel; 13 – oxidation zone of reaction channel; 14 – direction of BUCG gas; 15 – direction of blowing mixture; 16 – direction of stowing material.

CONCLUSIONS

Efficiency of BUCG is related to the seasonal expenditure of products, so the complex use of BUCG products has to be reached. That foresees the receive of chemical products from the condensed fluid, use the generator gas for the receipt of chemical agents by thermal conversion, and also thermal and generator gas for electric energy on power installations.

The heat recuperation from rocks containing a gas generator and products of BUCG provided by recuperational collections (Falshtynskyi 2010 & Brand 2008) for receipt of electric power. A remaining heat is utillized for engineerings (heating of blowing, process of catalytic conversion) and domestic needs.

Chemical raw material, got from the condensed fluid of power gas of underground gasification can be released chemical enterprises as a feed (coal gum, benzene, ammoniac water, phenols, acetylene, pyridines et.c.) or processed in place in the finished good (grey, surface active agents, solvents, carbon, dyes, polymer cements, naphthalene et.c.) (Falshtynskyi 2009).

Utilization of outcoming smoke from power station is on a principle of the closed cycle. Combustion gases CO_2 act from power-station back in an underground gas generator, where at co-operating with a burning hot carbon passes to burning gas – carbon monoxide (CO) and oxygen of O_2 . Adding CO_2 to blowing calorie content of gas, will not yield to conventional gas.

In an underground gas generator direct oxides SO_n and nitrogen NO_n and other toxic components of smoke escape from power station.

Noncombustible mineral particles at coal gasification and carboniferous rocks remain in goaf, because they are not exposed to thermal decomposition.

Sufficient impermeability of underground gas generator is provided by injection stowing of the deformed rocks containing a gas generator and goaf (Falshtynskyi 2010).

As an stowing material can be used offcuts from coal power station. That will provide safety of landscape, fail-safety and efficiency of gasification process.

At building and production activity of underground gas generator on the area #1 on coal seam C_6^1 the investigations are foreseen on the audit of engineer decisions and technological characteristics of rock mass behavior at gasification. Varying the parameters of gasification process with the purpose of receipt the complex-industrial product of gasification from coal seam.

REFERENCES

Kolokolov, O.V. 2000. *Theory and practice of thermochemical coal process*. Dnipropetrovs'k: NMU Ukraine: 281.

Skafa, P.V. 1960. *Underground coal gasification*. Moscow: 169.

Lavrov, N.V. 1957. *Physical and chemical combustion of coal*. Moscow: 40.

Falshtynskyi, V.S. 2010. Analytical *determination of parameters of material and thermal balance and physical parameters of coal seam work-out on mine "Barbara", Poland*. Dnipropetrovs'k/Yalta: Proceedings of the school of underground mining: 157-161.

Falshtynsky, V.S., Dychkovskyi, R.O. & Tabachenko, M.M. Patent №35883 UA (2006) E21B 43/25. *Coal seam ignition* #200805265; Pub. 10.10.2008, Bjul. 19.

Liu, SQ, Li, J, Mei, M., & Dong, D. 2007. G*roundwater Pollution from Underground Coal Gasification*. Journal of China University of Mining & Technology, 4. Vol.17.

Falshtynskyi, V.S, Dychkovskyi, R.O. & Tabachenko, M.M. Patent №50867. *Heat recuperation at coal seam gasification* (UA) Pub. 25.06.2010. Bjul. 12.

Brand, J.F. 2008. *UCG pilot study in Secunda, South Africa – the experimental design and operating parameters for the demonstration of the UCG technology and verification of models.* In: Proceedings of the 2008 Pittsburgh coal conference. 30 Sep-2 Oct 2008, Pittsburgh, PA, USA, CD-ROM, Pittsburgh, PA, USA, University of Pittsburgh: 11.

Falshtynskyi, V.S. 2009. *Underground coal gasification technology*. Dnipropetrovsk: NMU: 131.

Falshtynskyi, V.S., Dychkovskyi, R.O. & Lozynskyi, V.G. 2010. *Economical justification of effectiveness the sealing rockmass above the gas generator for borehole coal gasification*. Praze naukowe GIG, Gornictwo i srodowisko, kwartalnik, 3. Katowice: GIG: 51-59.

Technical and Geoinformational Systems in Mining – Pivnyak, Bondarenko & Kovalevs'ka (eds)

Improvement of technology of the gold- and diamond-contained ores concentration with the help of a new highly-effective disintegration and thin screening by using of dynamically active band sieves (DABS)

A. Bulat & V. Morus
M.S. Polyakov's Institute of Geotechnical Mechanics, Dnipropetrovs'k, Ukraine

ABSTRACT: Basing on many years' fundamental researches the N.S. Polyakov's Institute of Geotechnical Mechanics of National Academy of Science of Ukraine (IGTM of NAS of Ukraine) has created a new special technology of disintegration and thin screening of 0.3-5.0 mm size by using of rubber dynamically-active band sieves (DABS). Numorous experiments and our long-term practical experience in industries shows that technical and technological parameters of the technology helps to effectively recover fine-class gold and diamonds with 1.5-2 better productivity of the washing machine.

A.S. Polyakov's Institute of Geotechnical Mechanics of National Academy of Science of Ukraine (IGTM of NAS of Ukraine) works for many years in order to study, create, manufacture and widely introduce technologically highly-effective and long-lasting mineral processing equipment with working faces made of wear-resistant rubber and dynamically active band sieving surfaces (DABS) (Chervonenko 1997; Morus 1998). One of the directions of this research work that is currently intensively developed is to create a special highly effective equipment which could essentially improve technology of gold- and diamond-ore concentration. Keeping in mind, as our key objective, the task to increase output and, at the same time, to improve effectiveness of disintegration and thin screening by screening surfaces that operate with the streams of inputs containing great amount of lumpy ores we have developed scientific base for designing a new equipment for ore-washing and preparing plants in gold- and diamond-mining factories. The equipment is presented in two types of washing-and-classifying machines:

– scrubber-trommels with extended scrubbers for the difficult-to-disintegrate and difficult-to-wash materials;

– drum screens of a "dredging barrel" type that simultaneously disintegrate and separate materials by several size classes.

One of the examples of aggregates of the first type can be a scrubber-trommel СБР-100 (Figure 1) consisting of the following assemblies: scrubber, sludge separator, intermediate drum and classifying trommel and drive, supporting driving wheels, pressing wheels, stop wheel that are located on the platform.

Figure 1. General view of the СБР-100 scrubber-trommel.

The layout of the aggregates and assemblies should:

– disintegrate and wash off the crushed materials with size less than 100mm from the difficult-to-wash materials including kaolin clay;

– separate and discharge, during the flushing stage, clay sludge with size -0.5 mm;

– combine quartzite final washing with classification by size 5 mm.

The scrubber is a thick-wall cylinder drum edges of which are the flanges; there are bandages on the outer sides of the scrubber by which the scrubber rests against the wheels with rubber studs. One of the wheels is a traction one, three wheels are supporting and one wheel is stop. Besides, pressing wheels are installed on the hinged cross beams over the bandages. Pressing wheel installed over the driving bandage can be used to increase pulling force of

the traction wheel in friction transmission in adverse weather conditions (rain, icing) and as a stopper for cross travels of the working member at the start moment. Pressing wheel located over the stop wheels serves to prevent tilting of the working member in case of center of gravity shifts towards discharge end when the load is re-transferred.

The scrubber has an edge wall in the charge sector of the scrubber, with round central hole in to which a feeding chute enters at a regulated slope angle. Entire inside surface of the scrubber is lined (Figure 2) by special rubber plates of different shapes and purposes and is equipped with a system of ring thresholds of different heights that form a line of reservoirs along the length of the working member.

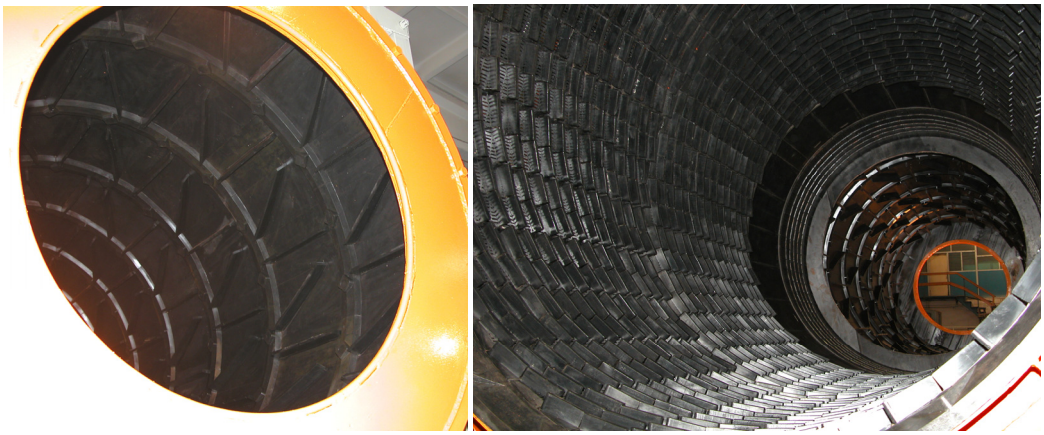

Figure 2. Inside working faces of the СБР-100 scrubber-trommel.

Usage of exclusively rubber lining elements ensures efficient protection of the thin-wall cylinder drum and other key assemblies of the scrubber against dynamic and impact loads and abrasive wear, and also helps to solve a problem of maximal reduction of the working member weight and, consequently, cut operational costs. The lining plates are installed on the working face with straight and return lifters. The lifters and ring thresholds located inside the scrubber drum provide, at feeding a proper quantity of water, highly effective disintegration and clay washing off. All lining plates are fastened inside the scrubber by special clinching without any additional fastening items or glues.

Speed of the material run in the scrubber can be regulated by changing the scrubber longitudinal slope. Slope is regulated by changing tilt angel of the bearing platform with the help of special screw jack.
Material after washing in the scrubber drum, together with the sludge, run over the first from the top ring threshold to the sludge separator. The sludge separator is flange-mounted in the discharge sector of the scrubber and is made in the form of a "squirrel's cage" inside surface of which is equipped with rubber DABS for screening 0.5 mm size class. Here, in the area with length 600mm, thin fractions of the dispersed clay are separated from material washed at the first stage; the washed material is further classified and finally washed in the wet-screening section. Totally, the wet-screening sector of the СБР-type scrubber-trommels is made in the form of modular trommel system that could be formed and varied depending on required washing and classification parameters. At the QUARTZITE DM, Ltd., the sludge separator was followed by a blind drum (lined by the rubber) and two-section trommel with special rubber DABS-type sieving surfaces with the cells 5 x 30 mm.

The blind drum of this design option functions as a reserve section. If output of the sludge separation is not enough it is possible to install an additional section of the sludge-separating sieves. As another option, if it is necessary to get better separation by sizes an additional screening section can be installed instead of the blind drum.

Structure of the screening section is similar to the sludge separator – it is a drum with the length 2.2 m in the form of a "squirrel's cage". All ring elements of the drum – flanges, supports for the rubber sieves, parts of the band-holders – are made bent, with no additional mechanical treatment. On the inside surface of the screening section, rubber DABS-type sieves with multiturn transporting spirals are installed with the help of which material continuously travels along the sieve surface with a certain speed actually independently on the trommel axis ti-

tling. The rubber multiturn transporting spirals have one more very important function. Their top ribs (space between them is 80 mm) accept impact load from the big lumps and form a surface over which these fractions are transported to the discharge sector having no contact with the screening sieves for thin fractions. So, the thinnest rubber sieves are efficiently protected against the big lumps whose size multiply exceed the utmost screening size. The discharge sector of the trommel ends with a cap with special rubber-lined bars. The screening section can be designed with two sieves. We have already designed and manufactured first pilot two-sieve trommels with diameter of outside sections up to 3.3 m and DABS rubber working sieving faces for thin, fine and coarse screening of fractions with sizes from 0.5 mm to 300 mm. Trommel modules of such systems can include both existing proved sieving surfaces and new sieving elements with the cell profiles, protectors and special transporting spirals adapted to concrete industrial conditions. Each key working-member assembly and part of the scrubber and screening sections are made by bending method only, with no additional mechanical treatment providing easy maintenance and repair.

If compare technical and economic results of the СБР-100 operation observed during more than 6 years with operation of well-known equipment (Stepanenko; Vysotin 2006; Pyatokov) it is worth to note that usage of wear-resistant rubber in all disintegrating and sieving working faces in the scrubber-trommels helps to create machines with similar productivity but with 1.3-1.6 times less weight and less (up to 1.5 times) energy consumption. Weight of the assemblies and parts could be reduced to the extent when reliable operation of a new machine drive could be provided, in some cases, by a single electric engine against two engines in other similar existing machines. This aspect essentially simplifies design, reduces price of the scrubber-trommels and cut expenditures for their operation and repair.

These projects and technological and operational results, as well as our many-year's tests in the industries allowed us to apply the modular method in designing scrubbers with the widest range of application. To get effective dispersion of difficult-to-wash kaolin clays we recommend to use scrubbers with 6-10 m length. We worked out a concept and principles of designing any models of the scrubbers with diameters ranging between 1.5 m and 3.0 m and length ranging between 2.0 m and 10.0 m and with highly-elastic wear-resistant rubber lining. Some our scrubber-trommel models designed by individual orders of different enterprises are shown on the Figure 3. Mounting of classifying trommels with greater length on the large-size disintegration aggregates causes no technological problems thanks to modular structure of the trommels. Trommels with sieving drum length 4-5 m provide the highest technological effectiveness of screening sizes from 0.5 mm up to 300.0 mm. Very important is the fact that our DABS sieving elements for fine screening the smallest cells (0.5-3.0 mm) are designed for contacting with the lumps sizes of which are 500-800 times bigger than utmost screening size. For example, basing on our 5-year operational experience in industries we modernized our special DABS sieving elements for screening 0.5; 1.0; 2.0; 3.0 and 5.0 mm size classes that can form working faces of the trommels for interacting with the lump size 300-400 mm. It should be noted that reliability of the sieve fastening, strength and wear-resistance is designed for not less than one season of operation. This is especially important for solving such pressing problem as obtaining a high effectiveness of thin productive class separation at the head of technological processes and, in particular, for treating material from the placers and man-caused deposits that includes thin mineral inclusions and productive classes with particle minimal sizes 0.5-1.0 mm. This problem is mostly characteristic for new technological concentration schemes of diamond- and gold-mining industries.

Our scrubber-trommel СБР 2.2 x 8/2 (Figure 4) is an example of an aggregate with longer disintegration sector for dispersing difficult-to-wash clays and trommel with rubber sieving elements for screening sizes 80 mm. This scrubber-trommel is designed to treat minerals with clay content up to 90% and to prepare diamond-contained inputs from placers for further concentration. This scrubber-trommel was installed in a flushing complex of URAL-ALMAZ Company.

Aggregates of our another design line are drum screens of the "dredging barrel" type that are widely used in processing less difficult-to-wash and easy washable minerals. The design is based on our experience in creating special highly-productive machines for dry separation of fine and thin classes from mined and supplied for further concentration ordinary coals with natural humidity between 6% and 12%. It is well known that screening of coal with such humidity content is always a very difficult, actually unsolvable problem. An example of our first successful solving of this problem is our design of a drum screen ГБК (Figure 5) with the DABS-type rubber sieves used for dry separation of the fine -3 mm classes at the head of technological line in Kievskaya Factory (Mine named after A.F. Zasyadko) with output capacity up to 400 t / h by base supply.

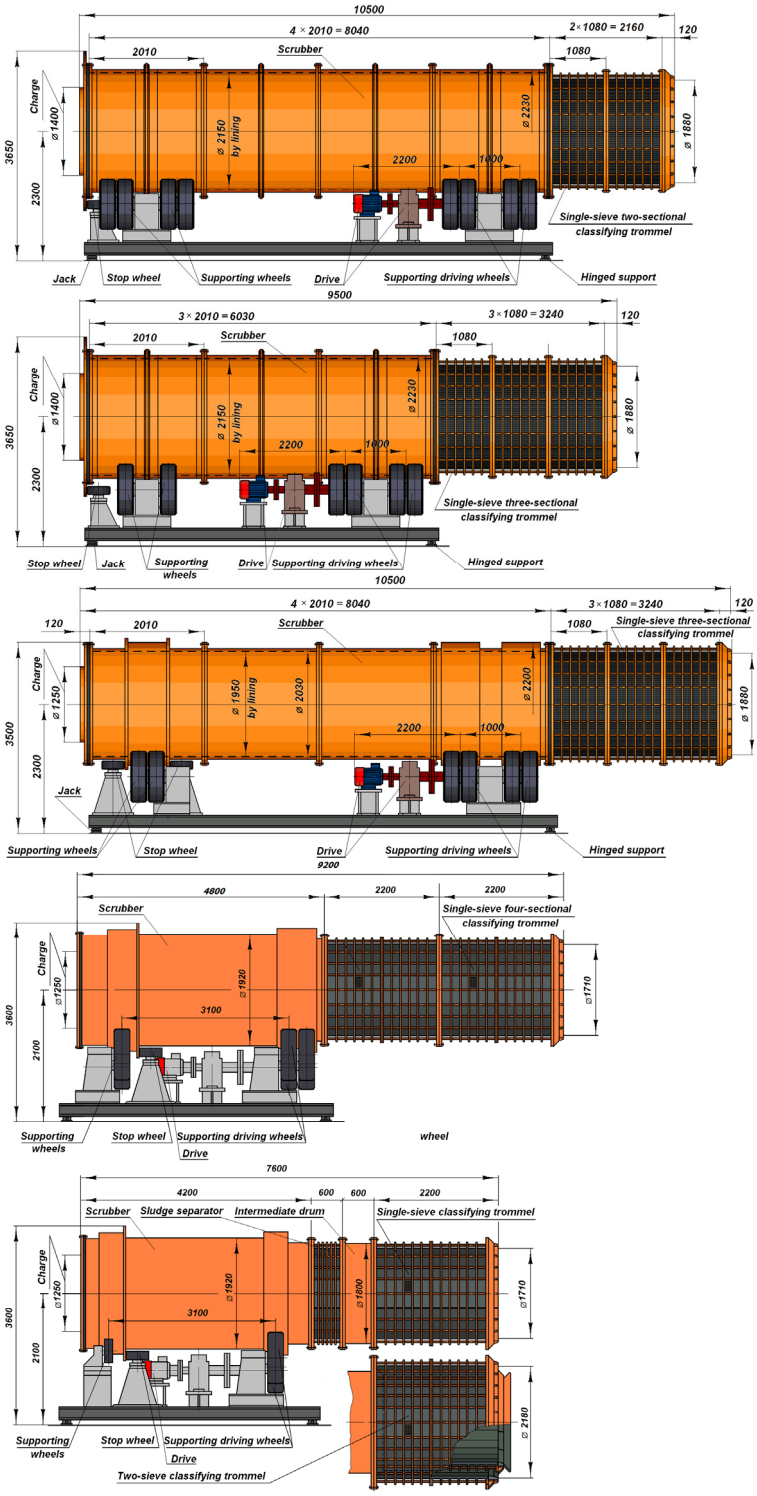

Figure 3. Examples of designed models of the scrubber-trommels.

Technical characteristics of scrubber-trommel СБР 2.2 × 8/2.

Type – scrubber-trommel, modular, 4 – sectional scrubber and 2 – sectional trommel, rubber lifter-threshold lining, with DABS sieves;		Drive type – electromechanical, friction	
		Electric engine – asynchronous; 220/380 V; 50 Hz	
Design feeding output, t / h	up to 400	Installed power, kW	2 x 30.0
Number of sieving elements	2	Frequency of the engine shaft rotation, min^{-1}	735
DABS cells size of the trommel, mm	80 x 80	Reducer type	cylinder
Diameter of the sieving surface, mm	1710	Driving wheels – rubber, big, highly elastic tyres (МВЭ)	
Total area of the sieve, m^2	16.8	Dimensions L x W x H, mm	7350 x 3290 x 2875
Angle of the drum axis slop, to horizon, degrees	2-10	Drum weight, t	13.5
Frequency of the drum rotation, min^{-1}	11-15	Weight, t	28.9

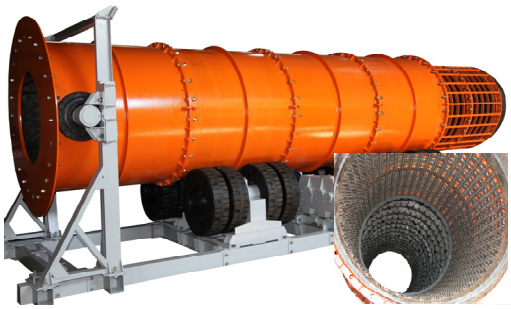

Figure 4. СБР 2.2 x 8/2 scrubber-trommel for flushing complex of URAL-ALMAZ.

Figure 5. General view of the ГБК screen at the bench tests.

Our seven-year experience of industrial testing and exploiting of the ГБК in technological line of the Kievskaya Factory helped us to improve our ГБК and create a dimension series of the drum screens with improved structures of the sieving sections and the drum itself and of assemblies and aggregates of the drive (Figure 6). According to the designers, this dimension series should include machines with maximal design capacity of 100 t / h; 200 t / h; 400 t / h and 600 t / h. These parameters are achievable through the properly specified length and diameter of the drum. Dimension series shown on the Figure 6 is extended by screens with the following working diameters of the drum: 1500 mm; 2000 mm; 2300 mm; 2500 mm and 300 mm.

However, in order to solve specific problems of the main screening in other factories it is possible to apply other variants of the key structural and technological parameters and other individually designed models of the drum screens with taking into account in-situ specific peculiarities of transporting and loading facilities and different building objects.

An example of design with “two-arm” drive and two electric engines is our screen ГБА (Figure 7). It was designed on the basis of the ГБК screen for flushing complexes used in the new technological practices for fine natural gold recovery and preparation.

Additionally to the above features of the support platform with drive, design of this screen differs by 1) longer charging sector that, thanks to special rubber lifting liner, functions as a short receiving scrubber; and 2) specific layout of discharge sector and interacting assembly between drum and stop cross arm. DABS sieves for the thin screening of sizes 2.0 mm, 3.0 and 5.0 mm with slotted drum cells are oriented across the drum rotation axis. Critical requirements to the sieve design for such technologies is their high effectiveness by separation of undersized classes, reliable fastening and their long life at heavy loads caused by feeding material contained up to 40-80% of clay and lumps (300-500 mm and bigger).

The ГБА screen is in operation in technological line of the fine and thin gold recovery in the PIKAN deposit (Amur oblast, Russia) of the AMUR-DORE Company since 2009. General view of the main technological aggregate of mobile flushing machine with ГБА screen is shown on the Figure 8. The screen installed on the sledge platform provides highly effective disintegration, flushing and extraction of gold-contained minerals with size -2.0 + 2.0 mm; -0.3 + 2.0 mm; and -0.5 + 3.0 mm that are

supplied from the undersized fraction receiving hopper to the lock sector for fine material where natural gold of appropriate sizes is extracted. Productivity of the machine is up to 140 t / h, and water consumption is about 400 m^3 / h. It was the first experience of the Company in executing a practice of highly effective extraction of thin-class gold in the mobile plants with the drum screens of the dredging-barrel type. This experience has demonstrated that employing of highly effective facilities for the thin screening in the gold separating-and-flushing machines reduces amount of lost fine mineral particles and, in particular, particles of the flaky form giving a good chance to increase output of the flushing machines and complexes by 1.5-2 times.

Following the review of these results we managed to put our new technology in to operation in four other production units of this Company and in technological lines of other gold- and diamond-mining companies.

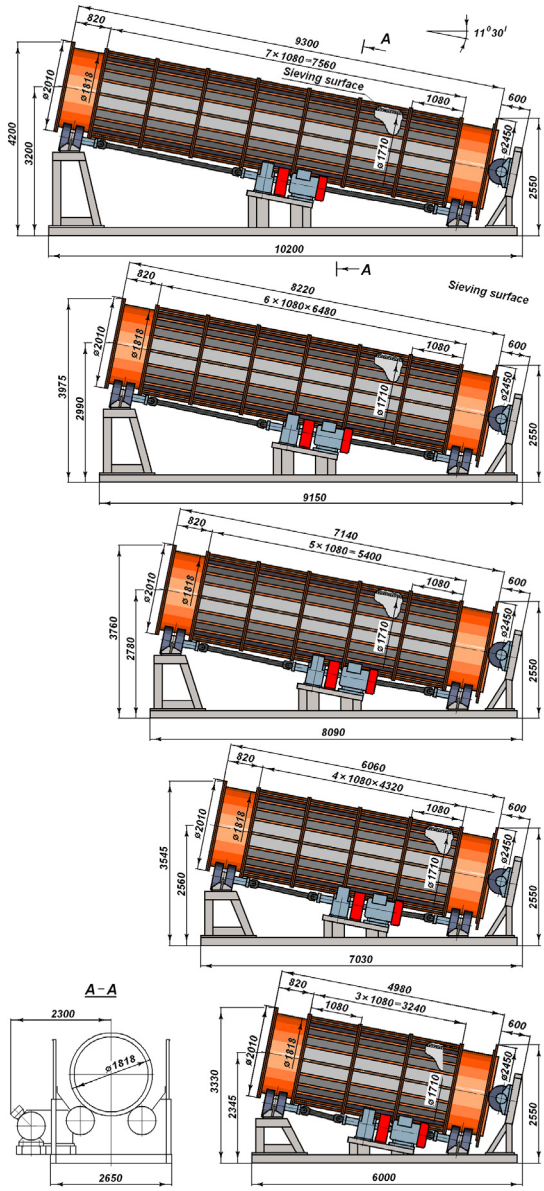

Figure 6. Dimension series of the drum screens with two-arm drives, one electric engine and DABS working surfaces.

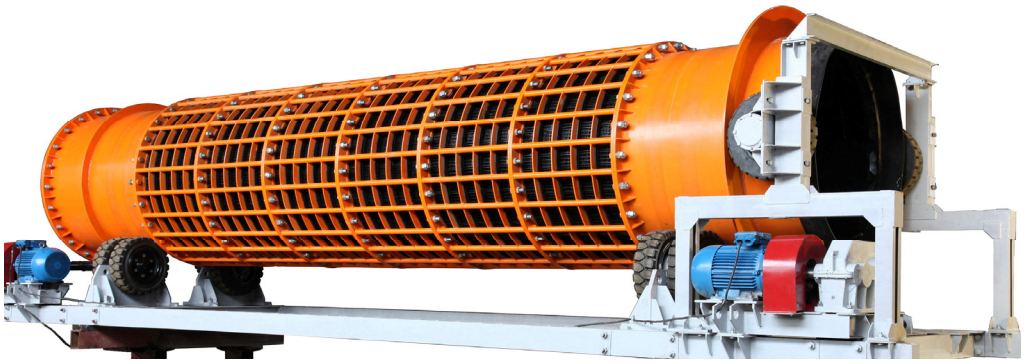

Figure 7. Screen ГБА for the gold-recovery technologies.

Figure 8. ГБА screen in the flushing plant for mining thin-size gold.

REFERENCES

Chervonenko, A.G. & Morus, V.L. 1997. *Wear-Resistant Dynamically Active Band Sieving Elastomeric Surfaces For Separating Loose Materials and Pulps*. Proceedings of the II International Symposium on Mechanics of Elastomers. Dnipropetrovs'k. V.1: 296-309.

Morus, V.L. & Nikutov, A.V. 1998. *New Wear-Resistant Rubber Working Surfaces for Drum-Type Screens,* Regularity of Material Movements inside of Cylinders with Multiturn Transporting Spirals. In the book "Geotechnical Mechanics". Interorganization Collected Scientific Papers. Edition 7. Dnipropetrovs'k: 125-132.

Stepanenko, A.I. *Up-to-date Disintegrating Equipment.* Novosibirsk: httm: //gmexp.ru/about/.

Vysotin, A.V. & Stepanenko, A.I. 2006. *Concentration of Glass-Making Sand*. Novosibirsk: httm://gmexp.ru/about/.

Pyatokov, Vl.G (IrGTU) & Pyatakov, Vik.G. (Irgiredmet). *Light-Weight Scrubber Aggregate.* Mining Magazine, 2.

Technical and Geoinformational Systems in Mining – Pivnyak, Bondarenko & Kovalevs'ka (eds)

Development of gas hydrates in the Black sea

V. Bondarenko, K. Ganushevych, K. Sai & A. Tyshchenko
National Mining University, Dnipropetrovs'k, Ukraine

ABSTRACT: Given work presents urgency of the alternative sources of energy development, in particular, gas hydrates. Evaluation is given to the Black sea's gas hydrates amount and volume of methane in them. Also gas hydrates formation conditions are scrutinized. Leading technologies of gas recovery from gas hydrates are considered. Special attention is paid to CH_4 into CO_2 exchange within the gas hydrate deposit. Calculations for substantiation of the gases exchange parameters are presented with following conclusions.

1 INTRODUCTION

Standard of life of the most countries is directly proportional to their energy consumption (Guliyants 2010). This is substantiated by the fact that at modern consumption rates of standard energy carriers such as oil, coal and gas, according to the leading scientists, their amount will be enough for 150-300 years of world use. Thus, prospects of such minerals development lose their relevance with every year. In connection with that, all developed countries understanding hopelessness of the situation, begin to pay a lot of attention to development of alternative sources of energy. At present, the main and most perspective of such sources is gas hydrates. Scientific and practical interest for gas hydrates development i.e. extraction of natural gas from them has significantly increased during the last decade.

Such increased attention to gas hydrates is substantiated by their wide distribution in the oceans and seas that wash coasts of leading countries-importers of natural gas. Also, very interesting fact is that hydrates possess a very high specific concentration of gas – up to 200 m^3 / m^3 and are deposited relatively not deep (starting from the depth of 300-500 m under the sea bottom). Understanding all importance of the given prospect, the leading scientists of Ukraine do not set themselves aside from this trend, especially considering the fact that Ukraine has a great source of gas hydrates – the Black sea. The Black sea represents an ideal place for gas hydrates research because its annual average temperature allows to conduct studies practically all year round. In 1974 exactly from the bottom sediments of the Black sea the first samples of gas hydrates were received for the first time ever (Yefremova & Zhizchenko 1974).

2 NUMBER OF GAS HYDRATES IN THE BLACK SEA

In 2002 the studies conducted by Bulgarian scientists showed that the average depth at which the hydrates begin to form is 620 m embracing territory of about 288100 km^2 that presents near 68.5% of the Black sea total area (Vassilev & Dimitrov 2002).

Based upon the research of the same scientists, thickness of the hydrate stability zone (HSZ) in the Black sea reaches 160 m at depth of 1000 m. At depth of 1500 m the layer thickness makes up 260 m in average (from 110 to 650 m) and at 2000 m-depth – 350 m. If to calculate the amount of gas contained in gas hydrates of the Black sea (volume of gas hydrates makes up about 0.35 $\times 10^{12}$ m^3) then this number would make 40-50$\times 10^{12}$ m^3 of methane! (Korsakov 1989).

Based upon the expeditions conducted in the 90's in the USSR, the amount of methane in the whole Black sea resulting from drilling and lifting samples of the sea bottom soil in more than 400 cores is not less than 100 trillion m^3 (Solov'yov 2003).

The amount of natural gas in the Black sea's hydrates really impresses and based on the calculations of Ukrainian specialists in this field, given amount of gas will be enough for Ukraine for 1500-3000 years (http://www.goodvin.info/news/biznes/13432v_ukraine_naydeno_novoe_mestorozhdenie_gaza_metana.html). With that, regions of the Sea of Azov still remain to be unexplored.

Map of the Black sea showing gas hydrates forming places is presented on Figure 1.

As seen on Figure 1, basic mass of gas hydrates is located in Ukraine and Romania, less in Turkey, Bulgaria and Russia, there are deposits in Abkhazia and Georgia.

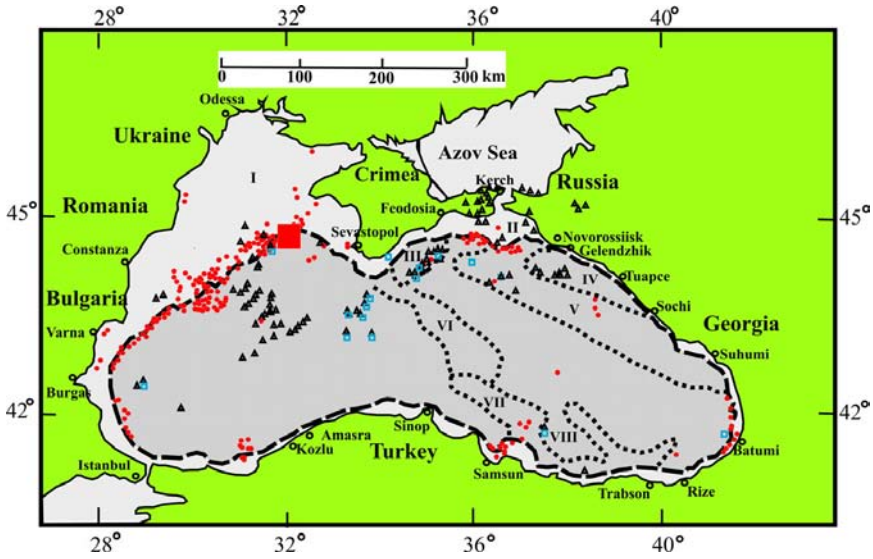

Figure 1. Location of methane hydrates in the Black sea (Starostenko 2010).

3 FORMATION CONDITIONS OF GAS HYDRATES IN THE BLACK SEA

When talking about formation conditions of gas hydrates the attention should be paid to composition of gas forming the hydrate, temperature and pressure of the forming media, sediment porosity and other.

Usually, hydrates form under temperature below +30 °C and high pressure. For example, at 0 °C methane hydrate forms at pressure of 3 MPa, and carbon dioxide at 1 MPa. If the temperature is +25 °C, methane hydrate forms at pressure of 40 MPa. Density of the Black sea's gas hydrates is within 0.9-1.1 g / cm^3.

Water temperature in the Black sea below the seasonal temperature variations increases with depth and consequently the water surface temperature grows from 8.7 to 8.8 °C at sea depth being 400-500 m; and at sea depth of 2100-2200 m – to 9.05-9.1 °C. It allows to make a conclusion that in bottom sediments at sea depth of 620-650 m, favorable thermobaric conditions exist all over the place for formation and stable existence of methane hydrates (Kutas 2005).

The Black sea water, especially in shallow layers is far less salty than the oceans water. In average, 1000 grams of the Black sea water contains 18 grams of salt. Whereas, in Atlantic ocean 1000 grams of water contains 35 grams of salt, Red sea water contains 39 grams of salt. So, exactly relatively low content of salt in the Black sea has a favorable influence on gas hydrates formation (http: //www.crimeazoo.narod.ru /crimea/text3_1.htm).

4 EXTRACTION TECHNOLOGIES

If to consider methods of gas hydrates extraction, then, at present, there are several technologies in the world using which it is possible to receive gas from gas hydrates. Among them are the following ones: artificial lowering of pressure in the gas hydrate layer, pumping vapor or warm water into the gas hydrate deposit, pumping various inhibitors and salts, electromagnetic influence and other.

The most perspective method, according to the leading scientists of the world, is an exchange of methane to carbon dioxide captured from industrial enterprises. Such technology will solve three problems: 1. Methane production and its further industrial utilization; 2. Sequestration of carbon dioxide within the sea bottom "cementing" it by means of formation of more stable hydrate – carbon dioxide hydrate (this hydrate represents by itself more stable compound since it is less subjected to temperature and pressure variations); 3. Reduction of global warming as carbon dioxide captured from the enterprises does not go into the atmosphere but gets deposited under the bottom.

5 STUDIES IN THE NATIONAL MINING UNIVERSITY OF UKRAINE

A lot of attention to development of this technology is paid by the research staff of the Underground Mining Department. The second, modernized unit for gas hydrates receive was created this year at the department

which allows to receive video surveillance during formation of hydrates created by various gases.

In 2011 the scholars of this department submitted patent "Method of gas methane extraction from sea gas hydrate deposits" that aims at improvement of gas recovery technology from gas hydrate deposits.

The essence of the technology consists of carbon dioxide delivery in gaseous state with temperature of +10 °C (±2 °C) along the inner pipeline with diameter of 200 mm (5) from the reservoir (2) located on the platform (3) to the depth of 100 m below the bottom of the sea that makes 600 m below the water surface, substitution of methane by carbon dioxide and formation of carbon dioxide hydrate with simultaneous methane recovery into the reservoir (1).

Methane is pumped out along the outer pipe with diameter of 400 mm (4) (Figure 2). Exchange process is conducted layer-wise (6) from the bottom to the top: radius from the borehole wall and height of the dissociation zone of each layer make up 3.5 m after 100 days that has been confirmed by the researches. After formation of the first CO_2-hydrate layer the pipe is raised up on the height of 3.5 m and a new layer development begins. Following layers are worked out by the same way up to the upper boundary of the hydrate deposit (3). After development of all the layers is over, the next borehole is drilled at a distance of 7 m from the worked-out area and methane recovery process begins by analogy.

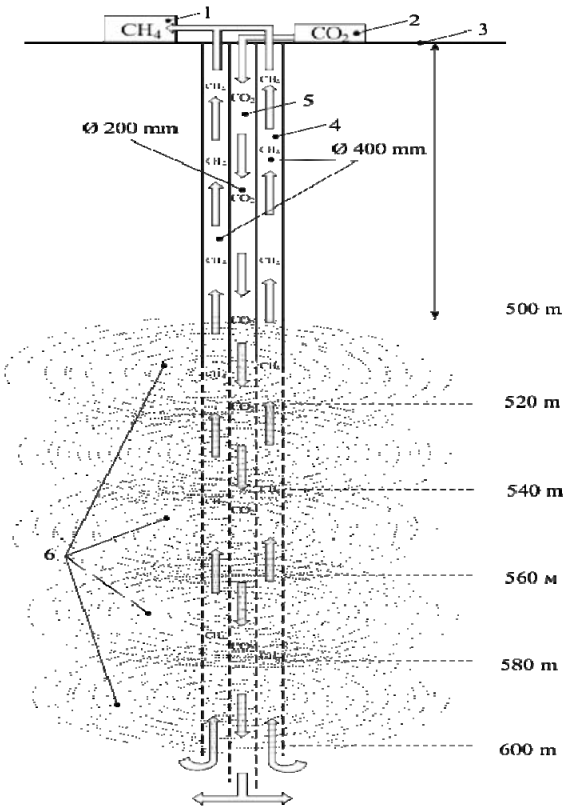

Figure 2. Scheme of CH_4 into CO_2 exchange in natural gas hydrates.

Phase transition temperature of the hydrate at 600m-depth was calculated to substantiate the above-mentioned technology:

$$T_{p.t.} = 9.75 \cdot ln(P) - 0.7 \quad (1)$$

Where pressure (P) is taken to be equal to 4 MPa, since critical pressure for gas methane is 4.641 MPa (Chukhareva 2010). (Critical pressure is a pressure at which gas does not yet transfer into liquid state regardless the temperature).

$$T_{f.t.} = 9.75 \cdot ln\,4 - 0.7 = 9.75 \cdot 1.39 - 0.7 = 12.82\ ^{o}\text{C} \quad (2)$$

Given temperature contributes to prevention of CH_4 transfer into liquid (4 MPa < 4.6 MPa). That

is, if the temperature exceeds 12.82 ºC then CH_4 will transfer into liquid. Based on these data, the pressure in natural gas hydrate is artificially lowered down to 4 MPa and the temperature of hydrate deposit does not raise above 12.82 ºC. This is done in order to control the process of exchange.

There is an interesting fact that during methane hydrate decomposition, 2.2 kJ / mole of heat releases at temperature of 0 ºC, whereas during carbon dioxide hydrate formation the amount of 1.1 kJ / mole of heat gets absorbed (Moelwyn-Hughes 1975). Based on this, it can be concluded that CH_4 into CO_2 exchange will be conducted with ratio of 1:2. Hence, the following calculations can be made:

1 mole of $CH_4 = 16$ kg of CH_4;

1 mole of $CO_2 = 44$ kg of CO_2.

In terms of kilograms, the ratio will have the following look:

16 kg of CH_4 :(44 × 2)kg of CO_2;

16 kg of CH_4 :88 kg of CO_2;

1 kg of CH_4 :5.5 kg of CO_2. (3)

That is, in order to pump out 1 kg of CH_4 from gas hydrate it is required to pump down 5.5 kg of CO_2 into this hydrate that undoubtedly expresses very important positive aspect of given technology: deposition of a big volume of green gas and, consequently, fight against global warming.

Further, using Mendeleev's-Clapeyron equation – $P \cdot V = \frac{m}{M} \cdot RT$, the mass of injected CH_4 can be calculated for the pipe height of 600 m with diameter of 400 mm. Initially, the volume of injected CO_2 for the depth of 600 m from the sea surface is calculated by the following equation:

$$V = h \cdot S = h \cdot \pi \cdot r^2 = 600 \cdot 3.14 \cdot 0.1^2 = 18.84 \text{ m}^3 \quad (4)$$

Having expressed the mass "m" from the Mendeleev's-Clapeyron equation and substituting the volume "V" value, we will receive:

$$m = \frac{P \cdot V \cdot M}{R \cdot T} = \frac{4 \cdot 10^6 \cdot 5.5 \cdot 18.84 \cdot 44}{8.31 \cdot 283} = 7750 \text{ т} \quad (5)$$

Based on the above-stated gases exchange equation (3), the volume of recovered CH_4 will make up 7750 t/5.5=1409 t.

The next stage is calculation of speed of CO_2 injection and CH_4 pumping-out. These values are calculated by the Reynolds number:

$$R_e = \frac{D \cdot U \cdot \rho}{\mu}, \quad (6)$$

where D – pipe diameter, m; U – flow speed, m / s; μ – dynamic viscosity of medium, Pa·s; ρ – density of medium, kg / s.

Having expressed the value of flow speed "U" from the given equation, we will receive the following:

$$U = \frac{R_e \cdot \mu}{D \cdot \rho}. \quad (7)$$

Now, in order to calculate the "U" value, the other values contained in the equation must be defined, taking into account that flow mode is laminar (such flow at which liquid or gas move by layers without mixing with each other). Thus, R_e value is accepted to be 2000.

Further, in order to calculate gases viscosity change "μ" depending on the temperature and pressure, the Sutherland's equation is used:

$$\mu = \mu_0 \cdot (273 + C) \cdot \frac{\left(\frac{T}{273}\right)^{1.5}}{T + C}, \quad (8)$$

where μ_0 – gas viscosity under normal conditions, Pa·s. According to the conducted studies (Chukhareva 2010), gases viscosity does not depend on pressure when its value is not greater than 5-6 MPa. Hence, the following gases viscosity values are accepted: for CO_2 – $137 \cdot 10^{-7}$ Pa·s, for CH_4 – $104 \cdot 10^{-7}$ Pa·s; C – Sutherland's coefficient, for CO_2 – 254, for CH_4 – 162.

Having substituted these values, it is possible to calculate viscosity of these gases:

$$\mu_{CO_2} = 137 \cdot 10^{-7} (273 + 254) \times$$

$$\times \frac{\left(\frac{283}{273}\right)^{1.5}}{283 + 254} = 141.9 \cdot 10^{-7} \text{ Pa·s}$$

$$\mu_{CH_4} = 104 \cdot 10^{-7} (273 + 162) \times$$

$$\times \frac{\left(\frac{283}{273}\right)^{1.5}}{283 + 162} = 107.3 \cdot 10^{-7} \text{ Pa·s}$$

Densities of the gases depending on pressure and temperature can be defined by the following equation:

$$\rho = \frac{M \cdot P}{R \cdot T}. \quad (8)$$

Substituting needed values, we will receive the following:

$$\rho_{CO_2} = \frac{44 \cdot 10^{-3} \cdot 4 \cdot 10^6}{8.31 \cdot 283} = 74.84 \ \text{kg/m}^3$$

$$\rho_{CH_4} = \frac{16 \cdot 10^{-3} \cdot 4 \cdot 10^6}{8.31 \cdot 283} = 27.21 \ \text{kg/m}^3$$

Now, CO_2 injection speed can be defined:

$$U_{CO_2} = \frac{2000 \cdot 141{,}9 \cdot 10^{-7}}{0.2 \cdot 74.84} = 0.002 \ \text{m/s}$$

CH_4 pumping-out speed will be as follows:

$$U_{CH_4} = \frac{2000 \cdot 107.3 \cdot 10^{-7}}{0.2 \cdot 27.21} = \frac{0.02146}{5.442} = 0.004 \ \text{m/s}$$

As it is seen by the last two equations, methane pumping-out speed is 2 times greater than carbon dioxide injection speed.

Having summarized the calculations results, it can be concluded that using given technology consisting of CH_4 into CO_2 exchange with formation of carbon dioxide hydrate, the mass of CO_2 injected into the natural hydrate is 5.5 times greater than the mass of pumped-out CH_4 and methane pumping-out rate is 2 times higher than injection rate of carbon dioxide.

6 CONCLUSIONS

Extraction of natural gas from the Black sea's gas hydrates is a real task which has the place in modern scientific society.

Technology allowing to not only recover methane from gas hydrates of the Black sea but also to sequester captured from industrial enterprises carbon dioxide into the sea bottom is the most perspective and reasonable one because it provides methane recovery, formation of a more stable gas hydrate and reduction of global warming by means of CO_2 emissions reduction into the atmosphere;

The calculations result have shown that CH_4 recovery rate from the hydrate is 2 times higher than CO_2 injection rate and, with that, mass of the injected gas is 5.5 times greater than that of the recovered one.

Methane recovery is controlled by variation of pressure and temperature in hydrate deposit that prevents spontaneous abrupt dissociation of the hydrate leading to a sudden blowup. That is why, the following studies should be directed to improvement of this technology, and substantiation that this method is safe in terms of the environment influence.

REFERENCES

Guliyants, S.T., Egorova, G.I. & Aksent'yev, A.A. 2010. *Physico-chemical features of chemical hydrates*. Tumen, 2010.

Yefremova & Zhizchenko. 1974. Academy of Sciences. Volume 214. #5:1179-1181.

Vassilev, A. & Dimitrov, L. 2002. *Model evaluation of the Black sea gas hydrates*. Volume 56.

Korsakov, O., Byakov, U. & Stupak, S. 1989. *Sov. Geologia*, 12:3-10.

Solov'yov, V.A. 2003. *Natural gas hydrates as potential mineral*. Russian chemical magazine. Volume 48:59-69.

http://www.goodvin.info/news/biznes/13432v_ukraine_naydeno_novoe_mestorozhdenie_gaza_metana.html

Starostenko, V.I., Rusakov, O.M., Shnyukov, E.F., Kobolev, V.P. & Kutas, R.I. 2010. *Methane in the northern Black Sea: characterization of its geomorphological and geological environments*. The Geological Society of London.

Kutas, R.I., Kravchyuk, O.P. & Bevzyuk M.I. 2005. *Diagnosis of gas hydrates in near-bottom layer of sediments as the results of their heat conductivity measurement in situ.* Kiev: Institute of geophysics NAS of Ukraine.

http://www.crimeazoo.narod.ru/crimea/text3_1.htm

Chukhareva, N.V., Rudachenko, A.V. & Polyakov, V.A. 2010. *Definition of quantitative characteristics of oil and gas in a system of main pipelines: tutorial*. Tomsk polytechnic university: 311.

Moelwyn-Hughes, E.A. 1975. *The kinetics of reactions in solution. Moscow*: Chemistry.

Technical and Geoinformational Systems in Mining – Pivnyak, Bondarenko & Kovalevs'ka (eds)

The influence of performance funding strategy on capital cost of mining enterprises in Poland

M. Turek
Central Mining Institute, Katowice, Poland

A. Michalak
University of Technology, Faculty of Organization and Management, Zabrze, Poland

ABSTRACT: The problem of performance funding is very complex and multi-thread, especially regarding such specific companies as mining enterprises. They perform in a situation which is called crisis situation in the industry. In the hereby study the structure of funding two mining enterprises is presented. The structure is not typical for market conditions, it mainly bases on outside funding sources and results in alarming level of many financial ratios. Therefore, the proposal of building new funding structures of mining enterprises performance is described concerning various strategies of finance management and studying their influence on capital cost.

1 INTRODUCTION

Business functioning in the market requires adapting and conducting a specified funding strategy. It consists of a set of rules that in an ordered way determine assets structure and funding sources in order to allow company gain its aimed goals (Wawryszuk-Misztal 2007).

In the literature of finance discipline three kinds of performance funding strategy are distinguished (Tokarski 2006):

- aggressive strategy;
- conservative strategy;
- moderate strategy.

Aggressive strategy bases on assumption that floating and fixed[1] current assets and a part of fixed assets are funded by short-term outside capital. Other fixed assets are funded by fixed capital. There is a negative level of current net capital in this situation that means a low level of assets funded by fixed capital. Aggressive strategy aims to maximize income in relation to equity capital and accepts a higher financial level risk and also gives opportunity of using significant effects of financial leverage and tax cover (Kołosowska et al. 2006). According to aforementioned strategy, financial liquidity is low which may indicate danger for company debts settling (Krzemińska 2005).

Conservative strategy deems that fixed capital funds involves not only fixed assets but also a fixed part of current assets. A conservative strategy is the opposite of aggressive funding performance strategy. Then a positive amount of current net capital appears. The financial risk is low in this case but nevertheless, considering a big share of long-term capital in company funding, including bank loans, funding costs are high. Financial liquidity is maintained on a high level. On the other hand, equity capital profitability is low due to high involvement of costly fixed assets in current performance (Krzemińska 2005).

The company conducting a **moderate strategy** funds its fixed assets by fixed capital and total current assets by short-term sources. A moderate strategy is an indirect strategy between aggressive and conservative strategy (Kołosowska et al. 2006). Current net capital floats around zero.

[1]Businesses observation indicates that the amount of current assets demand changes in time. This is caused by strong seasonal production and stock fluctuations. According to this, current assets may be differed into fixed not prone to changes and floating in the periods of high season. See: Z. Dobosiewicz, *Wprowadzenie do finansów i bankowości*, Wydawnictwo Naukowe PWN, Warszawa, 2005, pp.105.

2 CONTEMPORARY FUNDING STRATEGIES OF MINING ENTERPRISES IN POLAND AND THEIR FINANCIAL RESULTS

There were researched two out of five mining enterprises performing in Poland (determined in the article as I and II). They were created as a result of consolidation process in mining industry in the previous decade and consist in their structures of several to dozens of hard coal mines. The companies are sole stock corporations of National Treasury. The financial condition under which the researched mining enterprises perform may be considered as critical. The research conducted for the period of 2003-2009 indicates that capital structures in researched enterprises are consistent with aggressive strategy. There are presented contemporary funding structure strategies of researched enterprises in a simplified way in Table 1 and 2.

Table 1. Funding structure of mining enterprise I [%].

The kind of capital	years						
	2003	2004	2005	2006	2007	2008	2009
Own equity	3.93	12.12	17.48	14.67	14.63	14.44	14.24
Provisions	15.47	21.96	25.24	31.17	36.15	41.52	42.27
Long-term liabilities	22.30	18.12	15.69	14.53	10.31	10.43	9.27
Short-term liabilities	33.33	28.71	25.56	29.32	33.45	32.15	33.17
Accruals	24.97	19.09	16.03	10.31	5.46	1.46	1.05

Source: own study.

Table 2. Funding structure of mining enterprise II [%].

The kind of capital	years						
	2003	2004	2005	2006	2007	2008	2009
Own equity	53.10	39.95	40.44	36.19	34.38	32.66	29.10
Provisions	9.82	27.33	31.55	35.01	33.04	26.47	25.59
Long-term liabilities	1.54	0.74	0.38	0.40	0.38	2.94	3.66
Short-term liabilities	34.88	31.47	26.98	27.87	31.72	37.55	41.26
Accruals	0.66	0.51	0.64	0.53	0.47	0.37	0.39

Source: own study.

Funding structures presented above break most of funding rules. For example, in the first of researched enterprises own equity does not exceed the level of 20% in total liabilities which implicates the lack of gold balance rule fulfillment. A very high financial risk is also proved by the level of equity capital debt. In 2003 liabilities and provisions exceed the value of equity capital 24 times. In the subsequent years the value of this rate gains a considerable decrease to the level of 5-6, however, it is still high in relation to safety norm which is value of 1. This financial pathology is deteriorated by the fact that among outside capital short-term liabilities dominate.

A bad financial situation in coal industry also stresses the financial analysis of a second researched enterprise. In this case, the share of equity capital in funding structure oscillates around 40% and in addition, it presents a decreasing dynamics. Similarly to the first researched enterprise, short-term liabilities are on a significant position in outside capital structure.

When analyzing this untypical financial structure for market conditions additionally, attention should be aimed at the fact that analyzed enterprises, regarding their performance profile, characterize a highly stranded assets of a big amount that is practically impossible to cash (buildings and underground objects, excavation pits, professional mining machines etc.). Such assets should be funded by equity capital. Then in researched mining enterprises a negative net capital is observed proving that a considerable part of fixed assets is founded by outside capital and this situation is even more disturbing if, similarly to analyzed enterprises, it is a short-term outside capital. Such funding model, as we deal with in researched mining enterprises, results in an alarming level of most of financial ratios. Especially worrying are liquidity ratios of researched enterprises.

In the whole examined period, current financial liquidity of the first enterprise is on the much lower level than the normative value. Thus the enterprise in the analyzed period does not have the ability to regulate current liabilities by current assets in the light of adapted norms. Even when considering industry specificity, a systematic decrease of ability to

settle current liabilities is alarming. In year 2006 it is the lowest in the researched period and allows only to settle 40% of current liabilities by current assets (Turek & Jonek-Kowalska 2008).

In the second of researched enterprises, where funding structure is better formed due to higher share of equity capital, situation is not satisfactory either. In the whole examined period this enterprise, similarly to previous one, does not have current financial liquidity. The ratios are much below standard norms. The problem of these two enterprises is a high level of current liabilities that exposes them to risk of financial liquidity loss and at the same time to settle these liabilities disability[2].

According to the results of analysis conducted it is possible to summarize that current strategies of mining enterprises funding cannot exist in the conditions of completely free market for mining activities. The financial situation of mining enterprises hereby described is a basic reason to build new funding strategies.

3 THE RULES OF BUILDING NEW FUNDING STRATEGIES OF MINING ENTERPRISES

When building funding strategies a basic assumption has been made that funding grounds on **dominant capital.** The share of dominant capital is the highest in funding structure. This feature do not possess other kinds of capital, called **supplementary** (Michalak 2007).

Dominant capital and supplementary capital(s) consist in some kind of funding structure. As there are many possible combinations of dominant and supplementary capital, there are also many options of funding strategies.

When considering financial situation of mining enterprises described above as **dominant capital** in funding performance of mining enterprises, it concerns equity capital. It may come from many sources, such as inner sources like income, amortization, rent etc. and outer sources like shares issue. On the other hand, **supplementary capital** is thought to be an outside capital coming from any source e.g. (Michalak 2007):

– bank loan (possibly consortium loans);
– capital coming from shares issue;
– support capital (e.g. from European Union funds);
– short-term securities;
– leasing;
– short-term liabilities and others.

There are assigned example supplementary capitals for a dominant capital in each strategy. Then it is possible to construct many options of performance funding strategy for mining enterprise, choosing various standards of dominant capital and various combinations of supplementary capitals.

In the conditions of mining enterprises functioning, when willing to build an optimal strategy of funding it has been assumed that in capital structure equity capital should dominate which derives from various sources and they are altogether combined for calculating the level of equity capital and its share in funding structure. It was estimated that the level of equity capital will not be lower than 50% of total capital. As fixed assets constitute about 80% of examined assets in mining enterprises, it is possible to envisage that regarding their unstable financial situation, these assets will be covered by fixed capital i.e. equity capital and current liabilities. Such funding structure is a demanded structure in mining enterprises, nevertheless, it is not possible to obtain in each enterprise and thus there will also be other options analyzed of performance funding in mining enterprises. The structure that will be established on the grounds of at least 50% share of equity capital and at least 80% share of fixed capital in capital structure will be the type consistent with **conservative** or **moderate strategy**. Some of mining enterprises that are in a better financial situation than in researched enterprises may adapt a more **aggressive** funding strategy of its assets, choosing funding structure resulting in negative net working capital, that is lower than 80% share of fixed capital in capital structure, however, the elementary assumption concerning minimum of 50% share of equity capital should be strictly retained.

While making analysis of contemporary funding structures in examined mining enterprises it should be stressed that the income significance in equity capital structure is not high and it cannot bear self-funding duty.

[2]More on this matter in: A. Michalak, M. Turek, Analiza struktury kapitału w kontekście źródeł finansowania przedsiębiorstw górniczych. Wyd. Sigmie PAN, Warszawa 2009, pp. 99-113; M.Turek, I.Jonek-Kowalska, Ocena płynności finansowej jako kryterium podejmowania decyzji zarządczych w przedsiębiorstwach górniczych, Wydawnictwo IGSMiE PAN, Warszawa 2009, pp. 115-125; M. Turek, A. Michalak, Uwarunkowania budowy modeli finansowania działalności operacyjnej przedsiębiorstw górniczych. Szkoła Ekonomiki i Zarządzania w Górnictwie, AGH Kraków, Przegląd Górniczy 2010, pp. 20-23.

It is necessary to complement equity capital from other sources. Current situation on coal market (restricted possibilities of generating income) and current public finances state (low probability of obtaining funds from current owner – National Treasury) should force the government to adopt activities leading to developing performance effectiveness.

One of the ways is privatization or additional shares issue. It is easy to notice that in both cases the share of equity capital in funding structure is low and in the second enterprise it is close to assumed value of 50% liabilities, however, its share in funding structure indicates a decreasing tendency. To retain proper functioning, this capital should be increased to the assumed level of 50% and that proves a need to issue shares. A remaining part of funding structure will constitute a suitable combination of long- and short-term outside capitals. These are so called supplementary capitals in separate funding models. Notwithstanding, there are bank loans and shares issue among long-term outside capitals and short-term outside capitals that consist of non-interest short-term liabilities (purchase debts, pays due to be paid liabilities, tax liability etc.) and roll-over credit. According to the assumption of equity capital dominance, it may be stated that the level of outside capital should not exceed 50% of total capital. However, it is advisable to differentiate additionally outside capitals structure, especially regarding the relation of long- and short-term liabilities that influence the level of fixed capital.

Considering assumptions described above, example performance funding structures for mining enterprises may be offered, consistent with conservative, moderate and aggressive types. Examples of conservative performance funding structures for mining enterprises are presented in graphic form in Figure 1.

Conservative funding strategy – option 1 (data in %)					
fixed capital	EQUITY CAPITAL	Contemporary equity capital	25		80
		Additional shares issue	25		
	Long-term liabilities	Long-term loan	15	30	
		Bonds issue	15		
	Short-term liabilities	Non-interest liabilities	18	20	
		Loans and credits	2		
Conservative funding strategy – option 2 (data in %)					
fixed capital	EQUITY CAPITAL	Contemporary equity capital	25		80
		Additional shares issue	25		
	Long-term liabilities	Long-term loan	30		
	Short-term liabilities	Non-interest liabilities	18	20	
		Loans and credits	2		
Conservative funding strategy – option 3 (data in %)					
fixed capital	EQUITY CAPITAL	Contemporary equity capital	25		80
		Additional shares issue	25		
	Long-term liabilities	Bonds issue	30		
	Short-term liabilities	Non-interest liabilities	18	20	
		Loans and credits	2		

Figure 1. Example conservative operational activity funding strategies in mining enterprises Source: own study.

If the mining enterprise for which performance funding strategy is being built is in an unfavorable financial situation then it should adapt a **conservative** funding strategy. It means that equity capital in a certain model should cover fixed assets. It will provide a low financial risk level. Mining industry, as mentioned earlier, is specified by a high degree of assets blockage. In assets structure of mining enterprises fixed assets are dominating and a huge part of them is practically impossible to cash. The share of fixed assets in assets structure equals in the examined enterprises, a similar amount to the whole industry, about 80%. In such conditions fixed capital that consists of equity capital and long-term liabilities should constitute about 80% of all funding sources. If such thing is supposed that the share of equity capital should equal at least 50%, then the share of long-term liabilities in funding structure should oscillate about 30%. An optimistic forecast has been made in such models that the equity capital coming from incomes gained will obtain a share of 7% in total capital structure (it is an average value based on historic data of two researched mining enterprises). On the other hand, other company capital reaches the level of almost 18% of total liabilities. A contemporary equity capital includes about 25% of total capital. In order to obtain the assumed level of 50% liabilities for equity capital, additional company capital should constitute 25% of total liabilities. According to aforementioned, it may be assumed that mining enterprises will gain an additional equity capital by shares issue. Other implications regarding outside long-term capital indicate that in a conservative model should equal 30% of total capital. In the first option it has been supposed that 15% of total capital derives from long-term loan and 15% from bonds issue and in the following options it has been assumed that the total needed long-term outside capital comes from one or another source.

<table>
<tr><td colspan="6">Aggressive funding strategy – option 4 (data in %)</td></tr>
<tr><td rowspan="5">fixed capital</td><td rowspan="2">EQUITY CAPITAL</td><td>Contemporary equity capital</td><td colspan="2">25</td><td rowspan="3">60</td></tr>
<tr><td>Additional shares issue</td><td colspan="2">25</td></tr>
<tr><td rowspan="2">Long-term liabilities</td><td>Long-term loan</td><td>5</td><td rowspan="2">10</td></tr>
<tr><td>Bonds issue</td><td>5</td></tr>
<tr><td rowspan="2"></td><td rowspan="2">Short-term liabilities</td><td>Non-interest liabilities</td><td>25</td><td rowspan="2">40</td><td rowspan="2"></td></tr>
<tr><td>Loans and credits</td><td>15</td></tr>
<tr><td colspan="6">Aggressive funding strategy – option 5 (data in %)</td></tr>
<tr><td rowspan="4">fixed capital</td><td rowspan="2">EQUITY CAPITAL</td><td>Contemporary equity capital</td><td colspan="2">25</td><td rowspan="3">60</td></tr>
<tr><td>Additional shares issue</td><td colspan="2">25</td></tr>
<tr><td>Long-term liabilities</td><td>Long-term loan</td><td colspan="2">10</td></tr>
<tr><td></td><td>Short-term liabilities</td><td>Non-interest liabilities</td><td>25</td><td>40</td><td></td></tr>
<tr><td colspan="2"></td><td>Loans and credits</td><td>15</td><td colspan="2"></td></tr>
<tr><td colspan="6">Aggressive funding strategy – option 6 (data in %)</td></tr>
<tr><td rowspan="4">fixed capital</td><td rowspan="2">EQUITY CAPITAL</td><td>Contemporary equity capital</td><td colspan="2">25</td><td rowspan="3">60</td></tr>
<tr><td>Additional shares issue</td><td colspan="2">25</td></tr>
<tr><td>Long-term liabilities</td><td>Bonds issue</td><td colspan="2">10</td></tr>
<tr><td></td><td rowspan="2">Short-term liabilities</td><td>Non-interest liabilities</td><td>25</td><td rowspan="2">40</td><td rowspan="2"></td></tr>
<tr><td colspan="2"></td><td>Loans and credits</td><td>15</td></tr>
</table>

Figure 2. Example aggressive structures of mining enterprises operational activity funding. Source: own study.

If the mining enterprise which has performance funding strategy being built and uses and **aggressive** funding strategy then it may be estimated that in funding structure equity capital will still dominate (on the level of approx. 50% liabilities), however, complementary long-term liabilities will have a lower share than 30%. In this way fixed capital will not cover assumed 80% of assets in conservative models that consists of fixed assets. Example aggressive performance funding structures of mining enterprises are presented in Figure 2.

A **moderate** strategy will result in an intermediary situation between aforementioned strategy types. Example structure options consistent with this strategy are shown in Figure 3.

<table>
<tr><td colspan="6">Moderate funding strategy – option 7 (data in %)</td></tr>
<tr><td rowspan="5">fixed capital</td><td rowspan="3">EQUITY CAPITAL</td><td>Contemporary equity capital</td><td colspan="2">25</td><td rowspan="3">70</td></tr>
<tr><td>Additional shares issue</td><td colspan="2">25</td></tr>
<tr><td rowspan="2">Long-term liabilities</td><td>Long-term loan</td><td>10</td><td rowspan="2">20</td></tr>
<tr><td>Bonds issue</td><td>10</td></tr>
<tr><td rowspan="2"></td><td rowspan="2">Short-term liabilities</td><td>Non-interest liabilities</td><td>20</td><td rowspan="2">30</td><td rowspan="2"></td></tr>
<tr><td>Loans and credits</td><td>10</td></tr>
<tr><td colspan="6">Moderate funding strategy – option 8 (data in %)</td></tr>
<tr><td rowspan="3">fixed capital</td><td rowspan="2">EQUITY CAPITAL</td><td>Contemporary equity capital</td><td colspan="2">25</td><td rowspan="3">70</td></tr>
<tr><td>Additional shares issue</td><td colspan="2">25</td></tr>
<tr><td>Long-term liabilities</td><td>Long-term loan</td><td colspan="2">20</td></tr>
<tr><td rowspan="2"></td><td rowspan="2">Short-term liabilities</td><td>Non-interest liabilities</td><td>20</td><td rowspan="2">30</td><td rowspan="2"></td></tr>
<tr><td>Loans and credits</td><td>10</td></tr>
<tr><td colspan="6">Moderate funding strategy – option 9 (data in %)</td></tr>
<tr><td rowspan="3">fixed capital</td><td rowspan="2">EQUITY CAPITAL</td><td>Contemporary equity capital</td><td colspan="2">25</td><td rowspan="3">70</td></tr>
<tr><td>Additional shares issue</td><td colspan="2">25</td></tr>
<tr><td>Long-term liabilities</td><td>Bonds issue</td><td colspan="2">20</td></tr>
<tr><td rowspan="2"></td><td rowspan="2">Short-term liabilities</td><td>Non-interest liabilities</td><td>20</td><td rowspan="2">30</td><td rowspan="2"></td></tr>
<tr><td>Loans and credits</td><td>10</td></tr>
</table>

Figure 3. Example moderate performance funding structures of mining enterprises Source: own study.

4 CAPITAL COST IN SEPARATE FUNDING STRATEGIES OF MINING ENTERPRISES

Each of presented example funding structures in mining enterprises is specified by a different weighted average cost of capital (WACC). It is calculated by the following formula (Turek & Jonek-Kowalska 2009):

$$WACC = \sum_{i=1}^{n} w_i K_i ,$$

where w_i – the share of subsequent sources in investment funding structure, K_i – the cost of capital deriving from subsequent sources; n – the number of capital sources in investment funding structure.

In order to indicate weighted average cost of capital there should be known capital costs from several sources establishing funding structure. To carry analysis, average market capital cost values were adapted from several sources[3]. The calculations of WACC for funding structures of conservative type are presented in tables 3-5.

Table 3. WACC for a conservative strategy – option 1.

FUNDING SOURCES	SHARE IN THE STRUCTURE [%]	CAPITAL COST [%]	WACC COMPONENTS	WACC [%]
Income	7	10.28	0.07*0.1028	10.41
Shares issue	25	14.98	0.25*0.1498	
Other company capital	18	10.28	0.18*0.1028	
Long-term loans	15	8.99	0.15*0.0899	
Bonds issue	15	16.54	0.15*0.1654	
Non-interest liabilities	18	0	0.18*0	
Short-term loans and credits	2	13.52	0.02*0.1352	

Table 4. WACC for a conservative strategy – option 2.

FUNDING SOURCES	SHARE IN THE STRUCTURE [%]	CAPITAL COST [%]	WACC COMPONENTS	WACC [%]
Income	7	10.28	0.07*0.1028	9.28
Shares issue	25	14.98	0.25*0.1498	
Other company capital	18	10.28	0.18*0.1028	
Long-term loans	30	8.99	0.30*0.0899	
Non-interest liabilities	18	0	0.18*0	
Short-term loans and credits	2	13.52	0.02*0.1352	

Table 5. WACC for a conservative strategy – option 3.

FUNDING SOURCES	SHARE IN THE STRUCTURE [%]	CAPITAL COST [%]	WACC COMPONENTS	WACC [%]
Income	7	10.28	0.07*0.1028	11.55
Shares issue	25	14.98	0.25*0.1498	
Other company capital	18	10.28	0.18*0.1028	
Bonds issue	30	16.54	0.30*0.1654	
Non-interest liabilities	18	0	0.18*0	
Short-term loans and credits	2	13.52	0.02*0.1352	

Table 6. WACC for an aggressive strategy – option 4.

FUNDING SOURCES	SHARE IN THE STRUCTURE [%]	CAPITAL COST [%]	WACC COMPONENTS	WACC [%]
Income	7	10.28	0.07*0.1028	9.61
Shares issue	25	14.98	0.25*0.1498	
Other company capital	18	10.28	0.18*0.1028	
Long-term loans	5	8.99	0.05*0.0899	
Bonds issue	5	16.54	0.05*0.1654	
Non-interest liabilities	25	0	0.25*0	
Short-term loans and credits	15	13.52	0.15*0.1352	

[3] Values from 2010, more on that matter in: M. Turek, A. Michalak, Uwarunkowania budowy modeli finansowania działalności operacyjnej przedsiębiorstw górniczych, Przegląd Górniczy 2010, pp. 20-23.

The most beneficial conservative strategy among the presented examples is option 2. It is characteristic for the lowest weighted average cost of capital which in this case equals 9.28%.

The calculations of WACC for an aggressive type of strategy is presented in Tables 6-8.

The most gainful option among the example aggressive options of funding structures is number 5. This option shows the lowest weighted average cost of capital which equals 9.24%.

The calculations of WACC for a moderate strategy is presented in tables 9-11.

The most profitable option among the example moderate strategies is option 8. This model is characteristic for the lowest weighted average cost of capital which equals 9.46.

Table 7. WACC for an aggressive strategy – option 5.

FUNDING SOURCES	SHARE IN THE STRUCTURE [%]	CAPITAL COST [%]	WACC COMPONENTS	WACC [%]
Income	7	10.28	0.07*0.1028	9.24
Shares issue	25	14.98	0.25*0.1498	
Other company capital	18	10.28	0.18*0.1028	
Long-term loans	10	8.99	0.10*0.0899	
Non-interest liabilities	25	0	0.25*0	
Short-term loans and credits	15	13.52	0.15*0.1352	

Table 8. WACC for an aggressive strategy – option 6.

FUNDING SOURCES	SHARE IN THE STRUCTURE [%]	CAPITAL COST [%]	WACC COMPONENTS	WACC [%]
Income	7	10.28	0.07*0.1028	9.99
Shares issue	25	14.98	0.25*0.1498	
Other company capital	18	10.28	0.18*0.1028	
Bonds issue	10	16.54	0.10*0.1654	
Non-interest liabilities	25	0	0.25*0	
Short-term loans and credits	15	13.52	0.15*0.1352	

Table 9. WACC for a moderate strategy – option 7.

FUNDING SOURCES	SHARE IN THE STRUCTURE [%]	CAPITAL COST [%]	WACC COMPONENTS	WACC [%]
Income	7	10.28	0.07*0.1028	10.22
Shares issue	25	14.98	0.25*0.1498	
Other company capital	18	10.28	0.18*0.1028	
Long-term loans	10	8.99	0.10*0.0899	
Bonds issue	10	16.54	0.10*0.1654	
Non-interest liabilities	20	0	0.20*0	
Short-term loans and credits	10	13.52	0.10*0.1352	

Table 10. WACC for a moderate strategy – option 8.

FUNDING SOURCES	SHARE IN THE STRUCTURE [%]	CAPITAL COST [%]	WACC COMPONENTS	WACC [%]
Income	7	10.28	0.07*0.1028	9.46
Shares issue	25	14.98	0.25*0.1498	
Other company capital	18	10.28	0.18*0.1028	
Long-term loans	20	8.99	0.20*0.0899	
Non-interest liabilities	20	0	0.20*0	
Short-term loans and credits	10	13.52	0.10*0.1352	

Table 11. WACC for a moderate strategy – option 9.

FUNDING SOURCES	SHARE IN THE STRUCTURE [%]	CAPITAL COST [%]	WACC COMPONENTS	WACC [%]
Income	7	10.28	0.07*0.1028	10.97
Shares issue	25	14.98	0.25*0.1498	
Other company capital	18	10.28	0.18*0.1028	
Bonds issue	20	16.54	0.20*0.1654	
Non-interest liabilities	20	0	0.20*0	
Short-term loans and credits	10	13.52	0.10*0.1352	

6 CONCLUSIONS

Basing on the analysis of example options of conservative, aggressive and moderate strategy it is visible that the most profitable funding sources models are combinations that do not include shares issue. Among most gainful models of separate funding structure types a long-term loan becomes the only source of long-term outside capital. In general, the most profitable are aggressive models from the point of view regarding capital cost decrease. Their fixed capital consists of equity capital and capital from a long-term loan. These models are specific for a negative working capital. Apart from low capital cost, their characteristic feature is high financial risk triggering threat of financial liquidity loss.

The presented research was conducted in the frames of the project by Ministry of Science and Higher Education entitled *Investments in coal mining industry in terms of their financing* (N N524 464836) conducted by Silesian University of Technology.

REFERENCES

Dobosiewicz, Z. 2005. *Wprowadzenie do finansów i bankowości*. Warszawa: Wydawnictwo Naukowe PWN.

Kołosowska, B., Tokarski, A., Tokarski, M. & Chojnacka, E. 2006. *Strategie finansowania działalności przedsiębiorstw*. Kraków: Oficyna Ekonomiczna.

Krzemińska, D. 2005. *Finanse przedsiębiorstwa*. Poznań: Wydawnictwo Wyższej Szkoły Bankowej.

Michalak, A. 2007. *Finansowanie inwestycji w teorii i praktyce*. Warszawa: Wydawnictwo Naukowe PWN.

Michalak, A. & Turek, M. 2009. *Analiza struktury kapitału w kontekście źródeł finansowania przedsiębiorstw górniczych*. Warszawa: Wydawnictwo: Sigmie PAN.

Tokarski, A. 2006. *Strategie finansowania działalności przedsiębiorstw produkcyjnych*. Toruń Wydawnictwo Adam Marszałek.

Turek, M. & Jonek-Kowalska, I. 2009. *Dylematy kalkulacji kosztu kapitału w przedsiębiorstwie górniczym.* Szkoła Ekonomiki i Zarządzania w Górnictwie, Przegląd Górniczy, 9/20.

Turek, M. & Jonek-Kowalska, I. 2009. *Ocena efektywności finansowej jako kryterium podejmowania decyzji zarządczych w przedsiębiorstwach górniczych*. Kraków: Szkoła Eksploatacji Podziemnej 2009, Instytut Gospodarki Surowcami Mineralnymi i Energią Polskiej Akademii Nauk, Sympozja i Konferencje, 74.

Turek, M. & Jonek-Kowalska, I. 2009. *Ocena płynności finansowej jako kryterium podejmowania decyzji zarządczych w przedsiębiorstwach górniczych*. Warszawa: Wydawnictwo IGSMiE PAN.

Turek, M. & Michalak, A. 2010. *Uwarunkowania budowy modeli finansowania działalności operacyjnej przedsiębiorstw górniczych.* Kraków: Szkoła Ekonomiki i Zarządzania w Górnictwie, AGH, Przegląd Górniczy.

Wawryszuk-Misztal, A. 2007. *Strategie zarządzania kapitałem obrotowym netto w przedsiębiorstwach.* Lublin: Wydawnictwo Uniwersytetu M.Curie-Skłodowskie.

Technical and Geoinformational Systems in Mining – Pivnyak, Bondarenko & Kovalevs'ka (eds)
© 2011 Taylor & Francis Group, London, ISBN 978-0-415-68877-2

Analysis of combined support behavior of development openings with criteria of resource-saving technologies

I. Kovalevska & A. Laguta
National Mining University, Dnipropetrovs'k, Ukraine

O. Vivcharenko
OJSK "Pavlogradugol", Pavlograd, Ukraine

O. Koval
GP "Sverdlovantracite", Sverdlovsk, Ukraine

ABSTRACT: The mechanism of interaction of main load-bearing elements of various combined support constructions (a frame and rock bolts) is examined. Due to the analysis of support behaviors, computing experiments are based on finite element method and mine researches, the technology of development opening maintenance by frame-bolt supports is justified. This technology is more fitted to resource-saving criteria. The described support has spatial flexible mechanical connections of frame-legs and bolts as a one load-bearing system, with ability to redistribute loads on bearing elements while the process of its loading.

1 INTRODUCTION

By present time the huge experience of opening's exploitation, maintaining by combined supports has been accumulated. This supports include both positive and as negative evaluation of technical and economical aspects of its application in different mine-geological and mine-technical conditions. That is why we pay attention to development workings, which are situated in layered rock mass of Western Donbass weak rocks. There is high rate of rock pressure, which can be seen in the cross-section of an operation and along its length. Therefore, the spatial irregularity of force massive interaction with any type of support (even with a combined support) is taken place. So, the analysis of effectiveness of behavior of various constructions of such supports (combining pliable frames and bolts) is performed with evaluation of adaptation degree of its designs to spatial manifestations of rock pressure in development openings. From other side, a resource-saving factor of the rock mass near the contour involved in resistance to rock pressure is also important. That is required to evaluate the effectiveness of neighboring rocks to form something like a load-bearing construction around the opening, with high rebuff reaction. Thirdly, combined support installation and different elements, which are included in this support, must be worked together to resist to the displacement of a coal-containing rock mass. Fourthly, the strength balance of a construction directly influences on the resource-saving that is important when considerable load variation occurs in space and time. Therefore the evaluation of combined support ability to self-regulate loads in proportional to bearing capacity of main load-bearing elements is put to the fore.

Thus, taking attention to resource-saving factor the analysis of effectiveness of present constructions of the frame support, combined with rock bolts, is done with following criteria of low cost maintaining of development openings in the weak coal-containing rock mass:

– the highest level of a rock mass near the contour involved to resist to rock pressure manifestations;

– the maximum adaptation degree of such combined support to the character of rock pressure manifestations in time and space;

– the coordination level (or level of synchronism) of main bearing element behavior of a combined support;

– the maximum strength balance degree of a combined support in longitudinal section and cross-section of an operation due to the self-regulation of loading on main bearing elements.

There are constructive and technological solutions of development operation maintaining of coal mines. And it is reasonable to divide the combination of a flexible frame with rock bolts, having analysis of its behavior, into three major groups:

– the combination of the pliable frame support (the metal three-link support is made from specific profile SVP, MFFS-3L ("metallic flexible three-linked frame

support") and PFHS ("prolonged flexible hip-roof support") series are more widespread used) and the rock bolt systems, which are installed in order to opening shape. Rock bolt systems and the frame are not linked with each other (Bulat 2002);

– a frame and a rock bolt (all the bolt set in cross section of an operation or just one part of them) are linked with each other by the hard link that does not allow sufficient moving of main support elements (a frame, a rock bolt) from one another (Vygodin 1989);

– a frame and rock bolts are linked by flexible links, that allows to move together during sufficient rock pressure manifestations as in cross section and as in longitudinal section of maintaining operation (Kovalevska 1995).

Preliminary, to make it clear "frame-rock bolt support" term is objectively conformed only to the second and the third construction groups. There is the mechanical link of two main load-bearing elements – the frame and rock bolts. Constructions of the first group are just combination of two different types of support.

World and domestic practice of combined support application to maintain mine workings are well-know (Bulat 2002). The major aim is to decrease loading on a frame (that promotes the decrease of its metal-content) due to strengthening some volumes of massive near the contour, and to limit the volume of unstable rocks, perceived by a frame support. The functions of a frame and a bolt supports are considerably different from each other here, although can realize one task – ensure the stability of an opening. These constructions of first group are more widespread, even in Western Donbass mines, where combination of PFHS with polymeric-resin rock bolts is used to maintain development openings.

2 PRELIMINARY RESULTS

From the viewpoint of the resource-saving criterion the maximum inclusion level of rocks to resist to rock pressure manifestations is realized by the analyzed constructions of the first group (and even two other groups). The modeling of rock bolt's strengthening action shows that limited area is formed around bolts, where the bolt influence aims to avoid rock separation due to armature stretching and influencing reactive efforts of compression on a rock along the bolt axis. These compression efforts increase concerned stability of rock volumes due to conventional Coulomb-Morh strength theory (Borisov 1980). If the distance between rock bolts is short, joining of strengthened areas occurs and the load-bearing construction (a perceiving part) is formed. With increasing distance between bolts the load-bearing construction is not happened, however, the volumes of strengthened rocks around bolts limit the volumes of unstable rocks, forming load on a frame support. That is why, increasing the density of bolting provides for reduction of load on a frame. Therefore, it contributes decrease of frame's metal-content. However, the material-content of bolt support and labor-content of its installation are simultaneously raised. So, it is necessary to find the compromise to provide for required stability of an operation with minimum cost of its installing and maintaining.

Due to considerations of geomechanical features of the loading process and relatively uniform support resistance along an opening, more preferable installation of rock bolts is in the middle between the frames (as it occurs in the first and third construction groups of combined supports). Then unstrengthened rocks load mainly on a frame, but not on the barrier between the frames, which can be maintained by a wire mesh. The influence step of reaction maximums of a support construction along a mine working is also reduced. According to investigations (Kovalevska 2005), it aligns the diagram of loading on a support and creates more favorable conditions for maintaining operations. Constructions of second group do not have mentioned advantages, because rock bolts are situated in cross-section of frame installation, and the interval between them is strengthened by a wire mesh only. Significant ununiform reaction of a support along a mine working, generating (Kovalevska 2005) considerable fluctuations of displacements of the rock contour of ultimate balance zone that contradicts bearing capacity of main load-bearing elements (a frame, a rock bolt and a wire mesh), occurs.

From the viewpoint of the second resource-saving condition of the maximum adaptation level of rock pressure manifestations, the constructions of all three groups have some differences. If in the cross-section of a mine working the adaptation level of construction to the diagram of predictable pressure can be controlled by the density of bolting, then in the longitudinal section of a mine working the problems of ununiform loading on a support construction are happened, by means of the rock mass irregularity and local manifestations, weakening its factors. Such rock pressure manifestations are forecasted difficulty. That is why support parameters are changed sometimes, especially in certain areas of an opening without taking into account local fluctuations of load and displacements of the rock contour.

For visualization of the analysis of support constructions' adaptive properties to local resistance to rock pressure manifestations along a mine working the scheme is given on Figure 1. It explains the resistance mechanism of each of three combined

support groups. The first construction group (Figure 1b) is characterized by absence of mechanical links of frames and bolts, which are separately deformed in the area of resistance to $G(Z)$ loading. In the area of increased displacement of rock contour the redundant movement U causes additional bolt tension that increases its reaction of resistance of certain maximum Q_1^{max} in specific conditions, i.e. rock bolts reinforce resistance to increased rock pressure. Neighboring frame is independently deformed and due to its structural flexibility the frame resistance is little changed in this mode (Kovalevska 2007). And absence of the link with bolts does not allow increasing rebuff reaction of a frame. In result, in the area of increased rock pressure increase the rebuff of a support is only realized by rising resistance of some bolts and partly frames, being caught in this local area. Next to this area rock bolts and frames are not taken part in resistance to local increased loading. That is why, adaptation degree to the character of rock pressure manifestations of the first support group should be evaluated as low degree.

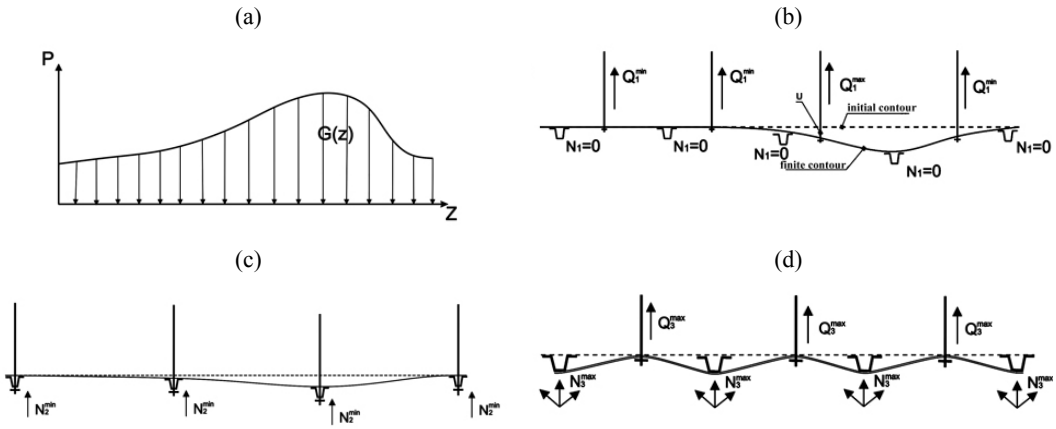

Figure 1. Diagram of $G(Z)$ loading along a mine working (a) and schemes of deforming support constructions are divided into groups of link between a frame and a bolt: (b) without link; (c) rigid link; (d) yielding link.

A frame-bolt support with hard link (Figure 1c) also increases its resistance in the area of local rock pressure manifestations. And the growth of the rebuff reaction is conditional by two components – increasing Q_2^{max} reaction of bolts, a part of which N_2^{max} is transferred to a frame; increasing the bearing capacity of a frame due to appearing additional supports (around the mine working) from the N_2^{max} influence of rock bolts. Given construction group has higher adaptive properties, relatively to previous group, as in the work of resistance to increased rock pressure two major elements – the frame and rock bolts – are included as united load-bearing system. Here the main defect is that changing parameter of force interaction of "rock mass-support of opening" system in the local area of increased rock pressure relates to support constructions only, situated in given area. Beyond it, neither frames nor bolts take part to resist to increased loadings, so the constructive links, between linking elements of supports along a working, are absent.

The third construction group, where bolts and frames are tied by pliable links along an operation, does not have mentioned defects (Figure 1d). There is the highest adaption degree of frame-bolt support to the character of rock pressure manifestations. In the area of higher loading the increased Q_3^{max} reaction of bolts is partly transferred to the frame as N_3^{max} efforts, which promote increase of its bearing capacity. But, all the bars of frame are tied together by pliable links along an opening with possibility of its longitudinal movements relatively to bolts and frame-legs. Then in an area of increased rock pressure the enhanced tension of pliable links is automatically transferred by tie strips behind the limits of local manifestation's area. And sufficient group of frame-bolt supports along a mine working is involved in the work of resistance to increase of local loading that leads to essential reduction of support's loading level at zone of increased pressure.

Therefore, following to the factor of adaptive properties the constructions of frame-bolt supports

with pliable yielding links along an opening are preferable.

The third resource-saving condition of mine working maintenance by means of frame-bolt supports is formulated as the maximum possible degree of coordination of bolts and frames' behavior. It allows "moving away" increased rock pressure from one side, and resisting to pressure manifestations with the maximum rebuff reaction as a single load-bearing system, redistributing load to bearing elements during the process of its unloading, from another side. First of all, let us justify the reasonability (from point view of resource-saving) of frame-bolting combination based on existing geomechanical introductions (Vynogradov 1989; Symanovych 2005) of rock pressure manifestations around an opening during the support interaction with the softening rock mass (Figure 2).

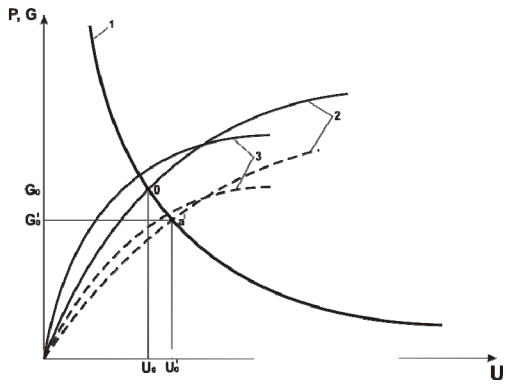

Figure 2. Substantiation of decrease the load on a frame support with combination of bolting: 1 – strain-load characteristic of softening rock mass; 2 – loading of unstable rock's weight; 3 – strain-load characteristic of support; – – – frame support, —— combination of frame support with bolts.

It is generally known that the increase of softening rock in volume causes U displacements of operation's rock contour and further loading on a support by G efforts. If a support has enough constructive pliability it "moves away" increased G loadings that predetermine all-round distribution of pliable supports for unstable rock conditions. Link of G loading on the support with its U pliability (Figure 2, line 1) was proven numerous analytical and experimental researches. Accordingly, G loading is decreased to minimum during sufficient constructive support pliability. But, the "1" dependence characterizes one side of the process only, linked with loosening (exfoliating) of rocks near the contour, which are increased in volume, but saving the stability. Definitely, if not to limit rock contour displacement the resistance reaction to them is not practically happened. However, scientists and specialists point to the second process's side of contained rock mass displacement (Figure 2, line 2). It characterizes growth of unstable rock volumes due to increase of pliability support. These rocks create G loading on a support by its weight. Therefore it is impossible to avoid loading on a support, but other way the value of G loading is increased. Thus, there are two opposite geomechanical tendencies of load formation on a support: 1) softening with loosening and unraveling rock mass; 2) loosing the stability of the part of rocks near the contour with further its caving. Such situation predetermines existence of minimum G_O loading on a support (Figure 2, point O) due to the value of its U_O flexibility. Therefore, strain-load support characteristic (Figure 2, line 3) has to go higher then point O to provide for opening stability during the given period of time. Thereupon the primary bolt task is to decrease the volume of unstable rocks due to its strengthening action. Then Line 2 will be fallen (Figure 2, dotted line) and optimal O^I point will characterize considerably lower G_O^I loading on support. It allows decreasing its minimum enough resistance reaction and material consumption accordingly.

Described mechanism of minimum load formation supposes the condition that is a frame and bolts have to provide for required pliability of support construction and to interactively (synchronously) change resistance reaction during the moving process of opening's rock contour. Obviously, simple combination (without constructive links) of frames and bolts does not allow to realize such condition, because of: 1) a frame support possesses certain flexibility according to its constructive features; 2) a rock bolt forms enough rigid rock load-bearing construction, having lower flexibility. Therefore the majority of loadings will be received by more rigid element. It can lead to breaking element and sufficient loss of general bearing capacity of support construction. If rock bolts do not form rock load-bearing construction, its separate work with a frame does not also suppose any consistency, but it leads to limitation of unstable rock volume according to line 2 in Figure 2.

In our view, the coordination of behaviors of a frame support and bolts is possible due to combining them by constructive links. In this case, it is necessary to analyze the work of a frame-bolt support as a single construction for both rigid and pli-

able links that was realized by means of its strain-load characteristics. During combining by the rigid link in the initial loading period of a frame-bolt support, the components of frames and bolts' reaction are summed up and its total rebuff is increased due to rising bearing capacity of a frame with additional supports (around an operation) from rigid link influence (see Figure 1c). Further, with increasing of rock contour displacement, the resistance of a ferro-polymeric bolt (Samorodov 2001), even in other constructions of rock bolts without expansion ends, is reduced by means of the destruction of the part of the contact of bolt armature with rock bore walls. This process is specified by little flexibility of rock bolts (more spreading in the practice of mine working maintenance), which based on many experiments, does not usually exceed several tens of millimeters. Therefore very limited pliability of a bolt (in few times less, then a frame support has) the total reaction of frame-bolt support is decreased with increase of rock contour displacement. And further, it is stabilized to the level of combination of frame resistance in the flexible mode, plus the action of bolts' reaction during big movements by means of residual friction of the armature to rock bore's walls (Bondarenko 2005).

Potential possibilities of a frame-bolt support (i.e. increasing its resistance reaction in the flexible mode) are fully opened when spatial pliable links of frames and bolts occur. There is also the effect of increase of frame bearing capacity while creating additional supports. But it is increased due to features of flexible link behavior. The essence of the process consists in following. During displacement of rock contour deforming the frame transfers forces to a neighboring rock bolt through pliable (flexible) link. Forces tend to "pull out" this bolt from a borehole. It is called "pulling out" forces. In the given area of the growth of bolt resistance flexible properties of its construction are added by flexibility of pliable link, thus the total value of flexibility is increased and the tension of pliable link becomes weaker. Its N_3^{max} reaction (see Figure 1c) on a frame-leg becomes lower accordingly. But, other rock bolts, which are not reached to "the top" of its resistance reaction, try to prevent to make weaker the tension of pliable link. That is why, the self-regulation of "pulling out" forces between a whole group of bolts, connected by one pliable link, occurs along an opening. Decreasing a part of resistance reaction of separate rock bolt in the flexible behavior is immediately compensated by neighboring bolts and a frame-bolt support generally reaches effective flexible behavior of constant high resistance, exceeding such one for support constructions of previous groups. In result, with the third resource-saving criterion the frame-bolt supports with spatial pliable links have unquestionable advantages.

The fourth criterion of resource saving, concerning the achievement level of the balanced strength condition of main bearing elements, is closely linked with the previous criterion. The essence of the balanced strength condition consists in the redistribution of frame-bolt support's forces in proportion to bearing capacity of every bearing element. And it is reasonable that this redistribution occurs automatically in the process of resistance to rock pressure manifestations. The balanced strength of construction will always have advantage in "bearing capacity-material content" relation. There is sense to compare only two groups of frame-bolt supports – with rigid and flexible links. The rigid link of frames and bolts does not admit any redistribution of forces due to their features. For example, due to small displacements of the rock contour the limited volume of unstable rocks is formed and the frame becomes underloaded. In the same time the given value of displacements is enough to destroy the part of contact of bolt armature with rock walls of a borehole and the rock bolt looses a part of its resistance reaction. So, the one element of construction is underloaded, and the second one is overloaded with partial destruction. From other side, due to increased displacements of the rock contour the frame works in flexible behavior and it is full loaded. Due to the rigid link with rock bolts the frame "pulls out" an armature from the borehole, leading to the bolt destruction partially or fully, that is also undesirable. Therefore, during the whole period of force interaction of the bolt with a frame-leg the maintenance of the process of the self-regulation of forces is required in proportion to the bearing capacity of frames and bolts. It is realized by the creation of spatial pliable links between them. Really, the loading on a separate bolt, in different stages of approaching to the value of its bearing capacity, is redistributed by means of pliable links on neighboring bolts. And this process occurs automatically due to the slipping of connecting element relatively to the tail part of a rock bolt. From other side, the frame, transformed to the flexible behavior, does not "pull out" neighboring bolts due to the stock of the flexibility of pliable links in direction to the displacement of the concerned frame's area. Thus, the analysis of constructions and behaviors of the frame-bolt support confirms the greatest fitness to resource-saving criteria of development opening maintenance by frame-bolt constructions with spatial pliable links, which providing for the self-regulation of behaviors of interaction of main load-bearing elements of "rock mass-opening's support" system.

3 RESULTS

The analysis of computer modeling results of the research of the field of the current σ stresses (Figure 3) has been fixed that the character of distribution σ for the frame-bolt support with pliable links of rib bolts with frame-legs has principal differences from σ field for basic version of the combined support (combination of frames with the bolts without pliable tie strips). So, in the upper part of a support practical constant field σ is installed around an arch, from its U-bolt to the U-bolt of the flexibility of the frame. This field is conformed to the action of even separate bending moment: in the central part of SVP cross-section, nearby its neutral axis, current stresses are minimal ($\sigma = 10...25$ MPa); σ stresses are increased in the upper and the lower part of SVP cross-section, achieving the maximum on the surface of SVP, which equals to 80…100 MPa. Though stresses are in few times less, then the evaluated limit of pliable flow steel St.5 ($\sigma_T = 270$ MPa), and therefore the upper frame part is under quite stable condition.

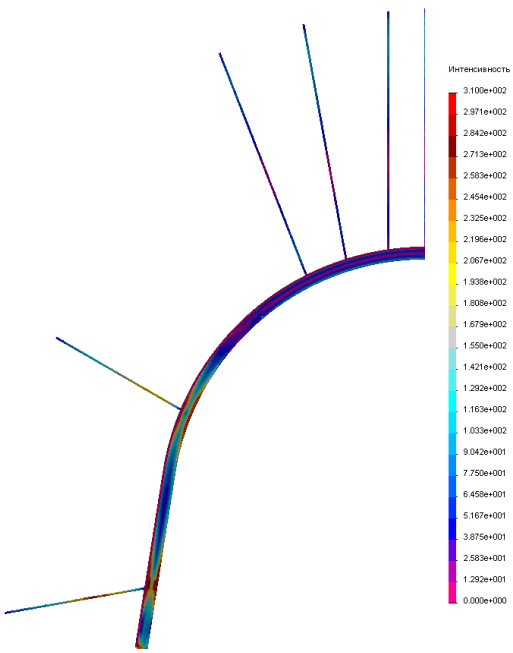

Figure 3. Diagram of current σ stresses in the frame-bolt support with spatial-flexible tie strips.

In the U-bolt of flexibility some changes of the unloading area $\sigma = 10...25$ MPa is observed (it goes to the upper part of SVP cross-section). And behind the limits of this area, up to the SVP surface, the value of current stresses is $\sigma = 25...40$ MPa. That is not enough for achieving the flexibility behavior of a frame and it generally saves the cross-section of the mine working till the ground setting.

In the curvilinear part of a frame-leg, beginning from the flexible U-bolt, the small area (150…200 mm of width) with constant reduced stresses $\sigma = 30...50$ MPa remains. It points to the practical absence of the given area of bending moment. It is fully explained by the neighborhood of the flexible U-bolt, having properties of a quasi-plastic joint. During movement to the upper rib bolt, in the curvilinear part of the frame-leg σ stress is undergone significant changes: 1) current stresses are increased along all area of SVP cross-section, but basically in the upper and lower parts, it points to bending moment action; 2) when stress comes to the upper rib bolt on 200 mm distance, in the surface part of SVP cross-section the σ component reaches 250…275 MPa, that is conformed to the evaluated limit of pliable flow steel St.5. Lower the place of the installation of upper rib bolt the σ stress with local areas of manifestation of pliable steel flow St.5 appears practically and symmetrically. However, areas of pliable condition are quite limited and conditional by contact stresses during the tension of a flexible tie strip and its influence on SVP. Repeated reduction of area measurements of flexible condition is obvious (in comparing with basic version of support) due to only one connection of bolts and frame-legs by the flexible tie strip.

In the curvilinear part of a frame-leg the current stresses are decreased along the height of SVP cross-section: $\sigma = 25...40$ MPa – in the central part; $\sigma = 70...100$ MPa – in the marginal area. During the movement to the lower rib bolt direction the σ stress is changed again, as in the area of the upper rib bolt. The σ component is increased in the all area of SVP cross-section and achieves the 250…275 MPa maximum in the external and internal parts of a cross-section. The quite limited area of pliable steel condition St.5 appears here, which is also conditional by contact stresses of the tie strip and the bottom part of SVP. Downwards along the frame-leg, in the area of its support, σ stresses are decreased and noticeably made even along the height of SVP cross-section up to 40…110 MPa level, except the local area (up to 70 mm) of a frame-leg end. That is also made by contact stresses of the frame-leg with a thrust block. However the σ stresses do not reach the level of pliable condition in the pointed area.

It is also worth that in the area of upper rib bolt, the district of flexible St.5 condition is expanded

along the frame-leg length up to 170 mm and along the height of SVP cross-section up to 35 mm. In the similar area of the basic support version the area's length of flexible SVP condition reaches up to 1120 mm in the frame-leg and the height is up to 90 mm. That is why the sizes of flexible condition of the area of a frame-leg are decreased in 2.6…6.6 times in the district of upper rib bolting, transforming into the local zones of contact stresses, which do not influence on the stability of frame-legs and whole support. In the lower rib bolt area the area length of flexible condition of a frame-leg is not more then 180 mm, and along the height of SVP it is expanded up to 40 mm. In the basic support these sizes are 460 mm and 110 mm accordingly, i.e. are increased in 2.6…2.8 times.

4 CONCLUSIONS

In whole, the major conclusion of the analysis of frame's stress-strain state (SSS) of advanced frame-bolt support consists in assigning the fact of multiple size reduction of pliable condition areas along the leg length till the level of local zones of contact's stresses, situated in the bottom part of SVP. It provides for required stability of the opening's frame. Also the reasonability of technical solution is confirmed in the part of bolts and frames, strengthening by pliable tie strips, with possibility of spatial flexibility. These tie strips provide for original additional support for frame-legs, making them stronger to resist to rock mass displacements inside the opening from the mine working walls. And it does the functions of loading redistribution on bearing elements of a support as in cross-sections, and as in longitudinal-sections of a mine working.

REFERENCES

Bulat, A.F. & Vynogradov, V.V. 2002. *Supporting bolting of the mine openings of coal mines.* Dnipropetrovs'k: Vyl'po: 372.

Vygodin, M.A. & Evtushenko, V.V. 1989. *Increasing methods of mine working stability in the Western Donbass mines.* Mine building, 5: 11-14.

Kovalevska, I.A. 1995. *Rock bolt and combined support interaction with rock mass and development of calculation method of its rational parameters*. Dnipropetrovs'k: National mining academy of Ukraine: 200.

Borisov A.A. 1980. *Mechanic of rocks and rock mass*. Nedra: 360.

Kovalevska, I.A. 2005. *Calculation of parameters of stability management of subsystem "strengthened rocks-support of underground openings".* Dnipropetrovs'k: System technologies: 113.

Kovalevska, I.A. 2007. *General scheme of calculation of loading on subsystem "strengthened rocks-support".* Dnipropetrovsk: Scientific bulletin, 1: 11-12.

Vynogradov, V.V. 1989. *Geomechanics of mass condition management near mine working.* Kyiv: Scientific idea: 192.

Symanovych, G.A. 2005. *Stability of underground mine workings*. Dnipropetrovs'k: System technologies: 164.

Samorodov, B.N., Marysuk, V.P. & Nagovitsyn, U.N. 2001. *Experience of mine working support by ferro-concrete bolts*. Mining journal, 4: 29-31.

Bondarenko, V.I., Kovalevska, I.A., Symanovych, G.A. & Porotnikov, V.V. 2005. *Theory and practice of tubular bolt application.* Dnipropetrovs'k: System technologies: 321.

Technical and Geoinformational Systems in Mining – Pivnyak, Bondarenko & Kovalevs'ka (eds)

Geophysical prospecting of gas hydrate

S. Sunjay
Geophysics, BHU, Varanasi-221005, India

ABSTRACT: Clathrate Gas-Methane Hydrate(White Gold) Crystal Fuel is a crystalline substance composed of water and gas, in which solid lattices of water molecules trap gas molecules in a cage-like structure or clathrate, present in permafrost regions and beneath the sea in outer continental margins. Gas Hydrate are usually inferred on seismic profiles by large amplitude bottom simulating reflector (BSR), which occur near the sea floor; Cutting across underlying dipping strata; The velocity inversion at the BSR caused by moving from high velocity hydrate cemented sediments to low velocity water or gas filled sediments below; The polarity reversal of the BSR with respect to sea floor. The occurrence of a BSR in seismic reflection data is the most important indicator of hydrates in marine sediments. However, hydrates can exist without creating a BSR if there is no underlying free gas or if the hydrates do not appreciably stiffen the sediment matrix. The weak reflectivity observed above the BSR (blanking) acoustic blanking indicates the absence of any signal because of increased transmission and obliteration of sediment impedance structures owing to the general replacement of pore water by hydrate, therefore, the zone with acoustic blanking characteristics is also referred to as the hydrate stability zone which is defined as the sedimentary package which contains the gas hydrates; the degree of blanking is proportional to the amount of hydrate in the pore space. The BSR is conspicuously underlain by transparent zones which are totally devoid of reflections and called as wipeouts. If hydrate layers are thin, tuning effects can occur and make it more difficult to interpret the gas hydrate or determine whether gas hydrates are thin or thick. Therefore, a special approach is required to identify thick high concentration hydrate layers by integrating rock physics modeling, amplitude analysis, and spectral decomposition.

1 INTRODUCTION

Gas Hydrates are detected on seismic section, primarily through identifying an anomalous reflector know as bottom simulating reflector (BSR) that mimics the shape of the sea floor, cuts across the dipping strata and has opposite polarity with respect to the sea-floor event. Third is important manifestation in identifying the BSR is the *polarity reversal* of the wavelet. The abrupt change in the velocity pattern from high velocity zone associated with the gas-hydrates to lower velocity water saturated or gas filled sediments just below the BSR produces a polarity reversal. The velocity configuration produces characteristic reduction in amplitude in the reflector above the BSR. Wave attenuation is an important seismic attribute that contains significant information about physical rock Properties. Seismic reflection techniques are the most important tool for locating gas hydrate zones. Hydrates have very strong effect on the acoustic reflection because of high acoustic impedance contrast, since the cementation of grains by hydrates produces a high velocity velocity (3.3 km / sec), deposit. Sediments below the hydrate-cemented zone if saturated with water will have low velocity and if gas is trapped in these sediments the velocity of the underlying layer will be still lower (1.5-1.7 km / sec). Because the strength of the reflected signal is proportional to the change in acoustic impedance, the base of hydrate-cemented zone produces strong reflections. The degree to which amplitudes are diminished depends on the amount of hydrates present. The phenomenon of amplitude reduction is termed as '*blanking*' –a characteristic feature for identifying gas-hydrates or BSR. It is to be mentioned here that sometimes the *transparency* is caused by homogenization of lithology. Three main manifestations (BSR, Blanking zone, Polarity reversal) have been used to recognize the presence of hydrates in the seismic section. The velocity build-up above the BSR can be used to quantify the amount of hydrates present above BSRs.

2 GEOPHYSICAL EVIDENCES

Gas Hydrate has been recognized in drilled cores but their presence over large areas can be detected more effectively by seismic reflection methods. Gas Hydrate are usually inferred on seismic profiles by Large amplitude bottom simulating reflector (BSR),

which occur near the sea floor, Cutting across underlying dipping strata, The velocity inversion at the BSR caused by moving from high velocity hydrate cemented sediments to low velocity water or gas filled sediments below, The polarity reversal of the BSR with respect to sea floor, Blanking zone above the BSR due to addition of gas hydrates into pore fluids. The occurrence of a BSR in seismic reflection data is the most important indicator of hydrates in marine sediments. However, hydrates can exist without creating a BSR if there is no underlying free gas or if the hydrates do not appreciably stiffen the sediment matrix. The weak reflectivity observed above the BSR (blanking) =Acoustic blanking indicates the absence of any signal because of increased transmission and obliteration of sediment impedance structures owing to the general replacement of pore water by hydrate, therefore, the zone with acoustic blanking characteristics is also referred to as the hydrate stability zone which is defined as the sedimentary package which contains the gas hydrates. Some of the blanking is not obvious, because the acoustic blanking is related to the hydrate cementation in the sediments; the degree of blanking is proportional to the amount of hydrate in the pore space. The BSR is conspicuously underlain by transparent zones which are totally devoid of reflections and called as wipeouts.

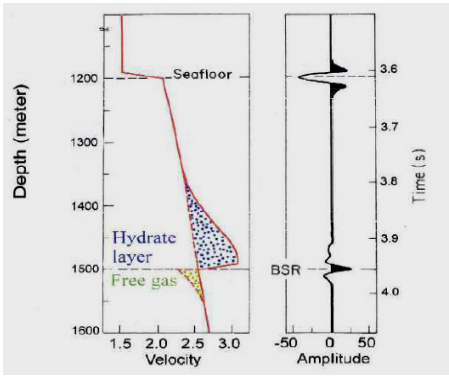

Figure 1. Polarity reversals at the BSR, lower velocities than seawater beneath the BSR perhaps indicating free gas. (Courtesy: http://gsc.nrcan.gc.ca/gashydrates).

In thin-bed interpretation of reflection seismic data, the term stratigraphic interpretation is synonymous with waveform analysis. The objective is to derive from the reflected wavelet as much relevant information as possible about geological formations with thicknesses that are below seismic resolution. For this purpose, the instantaneous amplitude is the least useful, since it is the envelope of the wavelet and masks all subtle waveform changes.

Nevertheless, it offers the advantage of being phase-independent, and is a useful tool for studying the total energy contained in a wavelet or in a wave packet. Because complex attributes separate amplitude information from phase information, any low-amplitude subtle waveform changes can be detected more clearly by instantaneous phase and instantaneous frequency than is evident in the raw data. The complex attributes are useful in that the instantaneous amplitude and the instantaneous frequency both show tuning effects, which indicate the halfway event represents a composite reflection from a thin bed. The instantaneous phase is also useful, although it is slightly less sensitive than the instantaneous frequency. The most unique property of instantaneous frequency is that it can be abnormally high compared to its Fourier frequency components of the wavelet, and it can also be negative. Some of these abnormal values occur around inflection phase anomalies and low-amplitude troughs. Thus, instantaneous frequency and instantaneous phase can be very useful tools to delineate subtle waveform character changes due to thin-bed wavelet interference. Instantaneous frequency is similar to instantaneous phase in that they both illustrate lateral continuity of waveform character and are independent of amplitude. Hence, they are also useful tools for delineating geological features such as pinch outs, angular unconformities, onlaps, faults, and channels etc. Since instantaneous frequency is the derivative of the instantaneous phase, so its section tends to appear slightly noisier than the corresponding phase section due to the high-frequency enhancement property of differentiation. In particular, frequency tuning effects should be investigated further as to how and when they occur. For complex attributes, research should be directed towards linking the qualitative observations to the geological changes.

The reflection amplitude increases as gas hydrate saturation increases. This positive amplitude change suggests phase reversals can occur in these sands if gas hydrate saturation changes laterally. The reflection amplitude is close to zero and between 20% and 40% gas hydrate saturation in these data, which would correspond with what has been described as a "blanking zone" in other gas hydrate systems For free-gas charged sands and hydrate-over-free-gas sands, the dominant reflection amplitudes decrease as gas hydrate or free gas saturation increase. Different concentrations of free gas and gas hydrate over free gas can produce the same reflection coefficient. For example, a given reflection amplitude of -0.35 could be caused by 20% free gas, 32% gas hydrate over 20% free gas, or 52% gas hydrate over 10% free gas (Figure 1). So BSR amplitude interpretation is typically ambiguous for a gas hydrate

layer. Complex Trace Analysis Amplitude analysis with respect to variation of gas hydrate saturation is important.

Seismic properties of thin layers: The normal incidence properties of one layer and two layers are studied in terms of amplitude, frequency, and complex attributes of the composite wavelet. The offset-dependent properties of one layer are also studied. The amplitude results for one-layer models indicate that, as the thickness increases from zero to the (l/8) λ_d value, the amplitude changes quadratically. However, if the two reflection coefficients have equal magnitudes and opposite polarities, the amplitude increases linearly. At (l/4) λ_d thickness, all four models show tuning effect. The amplitude results for two-layered models show that the amplitude changes quadratically as the thickness of one of the two layers increases from zero to the (1/8) λ_d value, with tuning effect occurring at close to the (1/4) λ_d thickness. However, the model with alternating polarities for the three reflection coefficients exhibits a minimum at approximately the (1/16) λ_d thickness, and a maximum at close to the (l/4) λ_d thickness. These properties do not change appreciably as the thickness of one of the two layers increases within a range of five fold. In the frequency study, the results indicate that, as the thickness increases, the peak frequencies of the composite reflections decrease slowly. However, for the one-layered model whose reflection coefficients have unequal magnitude and opposite polarities and the two-layered model whose reflection coefficients have alternating polarities, the peak frequencies increase as the thickness increases from zero to the (1/16) λ_d. Value, and then decrease as the thickness increases further. The complex attributes study indicates that the instantaneous frequency is useful for studying wavelet interference. Amplitude tuning effect combined with frequency tuning effect appears to be a good indicator of the existence of thin layers. However, the use of complex attributes remains largely empirical and a pattern recognition tool. The results of the offset-dependent study show that tuning effect can change drastically the effect of lateral changes in Poisson's ratio in terms of amplitude, peak frequency, and complex attributes. To interpret AVO effect properly in thin-bed interpretation, the effect of offset-dependent tuning must be accounted for.

Tuning effect: A phenomenon of constructive or destructive interference of waves from closely spaced events or reflections. At a spacing of less than one-quarter of the wavelength, reflections undergo constructive interference and produce a single event of high amplitude. At spacing greater than that, the event begins to be resolvable as two separate events. The tuning thickness is the bed thickness at which two events become indistinguishable in time, and knowing this thickness is important to seismic interpreters who wish to study thin reservoirs. The tuning thickness can be expressed by the following formula: $Z = V_I / 2.8 f_{max}$, where $Z =$ tuning thickness of a bed, equal to 1/4 of the wavelength, $V_I =$ interval velocity of the target, $f_{max} =$ maximum frequency in the seismic section. The equation assumes that the interfering wavelets are identical in frequency content and are zero-phase and is useful when planning a survey to determine the maximum frequency needed to resolve a given thickness. Spatial and temporal sampling requirements can then be established for the survey. Tuning thicknesses for both zero-phase and minimum-phase data are slightly less than the Rayleigh resolution limit. Event amplitudes can be better measured from minimum-phase data than from zero-phase data. Amplitude detuning is probably not required for minimum-phase data for bed thicknesses greater than about one-half of the Rayleigh resolution limit. Because event amplitudes in zero-phase data are significantly affected by tuning, amplitude interpretations based on zero-phase data should be calibrated or detuned for correct amplitude analysis.

Resolution: The ability to distinguish between separate points or objects, such as sedimentary sequences in a seismic section. High frequency and short wavelengths provide better vertical and lateral resolution. Seismic processing can greatly affect resolution: deconvolution can improve vertical resolution by producing a broad bandwidth with high frequencies and a relatively compressed wavelet. Migration can improve lateral resolution by reducing the size of the Fresnel zone. Nonlinear seismic imaging enables the end-user to retain the conventional linear seismic images and provides additional nonlinear seismic images that identify the porous and fractured reservoir rocks. In areas where the current seismic fails to map the stratigraphic or fractured hydrocarbon traps, nonlinear seismic technology can provide the useful reservoir information.

Nonlinear Seismic Imaging: In a nonlinear elastic system, the principle of superposition does not hold and the frequency mixing, harmonic generation, and spectral broadening takes place. These changes that add new frequencies to the frequency spectrum provide us with a means of measuring the elastic nonlinearity parameter of the reservoir rocks. This elastic nonlinearity parameter is unique, and

can be effectively used as a seismic attribute to map the rock properties of the reservoirs for improving the results of the exploration and exploitation efforts. The sensitivity of the nonlinear response to the porosity, fracturing, and pore fluids of the reservoir rocks is relatively larger than the linear measurements being used today. Industry needs to take advantage of this additional seismic attribute to reduce the ambiguity of the seismic-based geologic interpretation. Nonlinear seismic imaging enables the end-user to retain the conventional linear seismic images and provides additional nonlinear seismic images that identify the porous and fractured reservoir rocks. In areas where the current seismic fails to map the stratigraphic or fractured hydrocarbon traps, nonlinear seismic technology can provide the useful reservoir information.

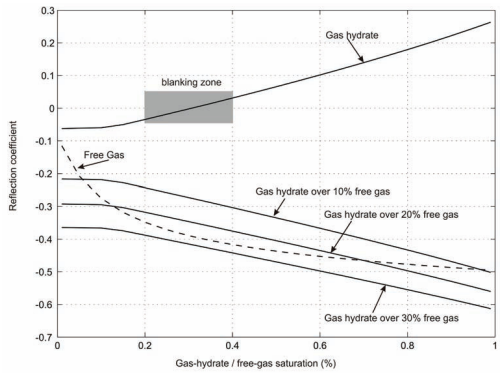

Figure 2. Normal incidence reflection coefficients versus gas hydrate and free gas saturation. The gas hydrate and free gas curves are in sands overlain by clay. The gas hydrate over free gas impedance curves are within a sand. (Courtesy: Zijian Zhang and Dan McConnell, AOA Geophysics).

Here, we focus more on interface responses at gas hydrate and gas contacts using rock physics models based on grain contact theories. To observe the effect of amplitude on different thicknesses of gas hydrate, two sand wedge models, (a) and (b), with various gas hydrate and free gas saturation levels (Figure 3). In model (a), high amplitude occurs with high hydrate saturation in hydrate-bearing sands with the maximum amplitude occurring at $\lambda/5$, where λ is the wavelength. The amplitude starts to decrease at $\lambda/5$ and significantly decreases as the layer thins below $\lambda/10$ (Figures 4a and 4b). Figures 4c and 4d show the results for a variably thick gas.

The strong amplitude can be seen at the interface between gas hydrate and free gas, a type of reflection that could form BSRs. layer of gas hydrate is significantly weaker than at the bottom of the gas hydrate layer (Figure 4c). The weak amplitude could easily be missed by the interpreter as the top of a thick layer of gas hydrate-saturated sand.

Hydrate zone with 30% gas beneath it for model (b).

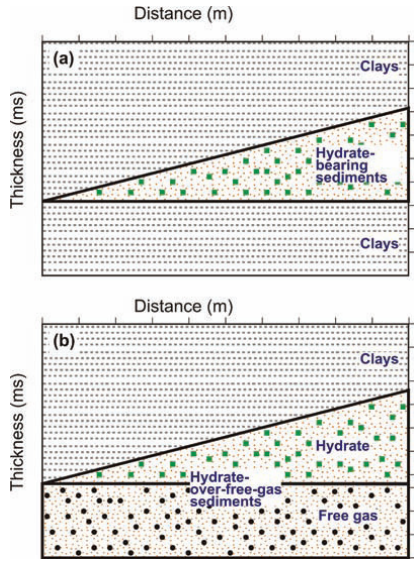

Figure 3. Wedge models for hydrate-bearing sediment (a) and hydrate-over-free-gas sediments (b): (a) three-layer model of a gas hydrate layer in clay; (b) gas hydrate layer with a clay cap and free gas bottom. The thickness of wedge varies from 0 to 30 ms. (Courtesy: Zijian Zhang and Dan McConnell, AOA Geophysics).

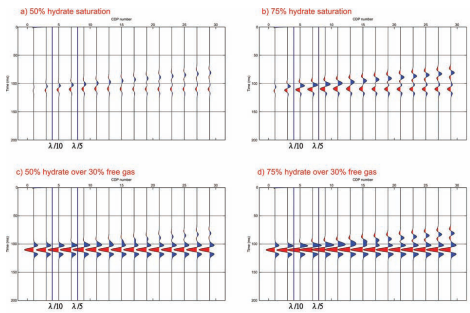

Figure 4. Synthetic seismic from the wedge models for hydrated sediments and hydrate-over-gas sediments. A Ricker wavelet of 50 Hz dominant frequency was chosen to generate zero-offset synthetic seismic data. The P-wave velocity of the clay is 1810 ms and the density is 2.06 g / cc. The properties of wet sand, hydrated sand and gas sand were derived from the well log data and the rock physics model. (Courtesy: Zijian Zhang and Dan McConnell, AOA Geophysics).

Spectral Decomposition. Conventional thickness analysis by picking horizons cannot be used if the peak-trough time separation is less than the tuning thickness (Partyka 1999). The spectral decomposition method, however, is a valuable tool with the ability to map thin beds (Partyka *et al*. 1999; Castagna *et al*. 2003). Partyka (1999) indicates a robust approach to seismic thickness estimation for thin beds showing that thickness can be derived from amplitudes at appropriately low discrete frequencies. The technique may be especially useful for identifying gas hydrate deposits and determining their thickness.

3 CONCLUSIONS

With a view to energy security of the world ,unconventional energy resources: Methane Gas Hydrate, coalbed methane , shale gas, tight gas, oil shale, Basin Centred Gas and heavy oil-exploration and exploitation is pertinent task before geoscientist. Wavelet analysis, known as a mathematical microscope, has scope to cope with nonstationary signal to delve deep into geophysical seismic signal processing and interpretation for hydrocarbon exploration and exploitation. Non-Stationary statistical Geophysical Seismic Signal Processing (GSSP) is of paramount importance for imaging underground geological structures and is being used all over the world to search for petroleum deposits and to probe the deeper portions of the earth. **SeisLab for Matlab** Software for the Analysis of Seismic and Well-Log Data.

REFERENCES

www.journalseek.net.

Fire in the ice http://www.netl.doe.gov/technologies/oil-gas/FutureSupply/MethaneHydrates/newsletter/newsletter.htm

Realizing the energy potential of methane hydrate for the united states, ISBN: 0-309-14890-1, http://www.nap.edu/catalog/12831.html

http://www.mms.gov/revaldiv/GasHydrateAssessment.htm

http://www.netl.doe.gov/technologies/oil-gas/publications/Hydrates/pdf/MethaneHydrate_2007Brochure.pdf; the JIP is managed by Chevron.

http://www.netl.doe.gov/technologies/oil-gas/FutureSupply/MethaneHydrates/projects/DOEProjects/Alaska-41332.html; this cooperative agreement is managed by BP Exploration Alaska,Inc. (BPXA).

www-odp.tamu.edu /publications/citations/cite164.html.

http://iodp.tamu.edu/scienceops/expeditions/exp311.html.

http://energy.usgs.gov/other/gashydrates/india.html.

Castagna, J.P., Sun, S. & Siegfried, R.W. 2003. *Instantaneous spectral analysis. Detection of low-frequency shadows associated with hydrocarbons*. The Leading Edge, 22: 120-127.

Lee, M.W., Collett, T.S. & Inks T.L. 2009. *Seismic-attribute analysis for gas-hydrate and free-gas prospects on the North Slope of Alaska*. Natural gas hydrates – Energy resource potential and associated geologic hazards: AAPG Memoir, 89: 541-554.

Lu, S. & McMechan, G.A., 2002. *Estimation of gas hydrate and free gas saturation, concentration, and distribution from seismic data*. Geophysics, 67: 582-593.

Mavko, G., Mukerji, T., & Dvorkin J. 1998. *The Rock Physics Handbook*. Cambridge, UK: Cambridge University Press.

Partyka, G.A., Gridley, J.A., & Lopez J.A. 1999. *Interpretational aspects of spectral decomposition in reservoir characterization*. The Leading Edge, 18: 353-360.

Technical and Geoinformational Systems in Mining – Pivnyak, Bondarenko & Kovalevs'ka (eds)
© 2011 Taylor & Francis Group, London, ISBN 978-0-415-68877-2

Justification of design parameters of compact load-haul dumper to mine narrow vein heavy pitching deposits

L. Shirin, Y. Korovyaka & L. Tokar
National Mining University, Dnipropetrovs'k, Ukraine

ABSTRACT: Consideration of loading unit performance within the system "rock mass-load-haul equipment-stowing mass" justification of its design parameters covers to mine narrow vein heavy pitching deposits. To intensify the machine performance it is proposed to use vibratory loader while entering ladle into rock mass, and while unloading. Under the same geometrical characteristics of ladle it will help to improve rate of load-haul machine work.

1 INTRODUCTION

From the viewpoint of efficient use of resources the paper uses systematic approach of justification of design parameters of compact load-haul dumper. Considering loading unit performance within "rock mass-loading and hauling equipment-stowing mass" approach justification of parameters of recommended loading equipment is run by means of the three stages.

In the context of method (Korovyaka 2003) stage one determines design dimensions of the loading equipment across the width of working excavation and throughout its height (minimum width of working excavation is $m_{min} = 1.2$ m, unevenness of wall of stope is $b_l = b_h = 0.2 \div 0.25$ m, shift of dynamic axis of working is $\alpha° = 15$ deg., and face movement is $a_1 = 2.0$ m) (Figure 1).

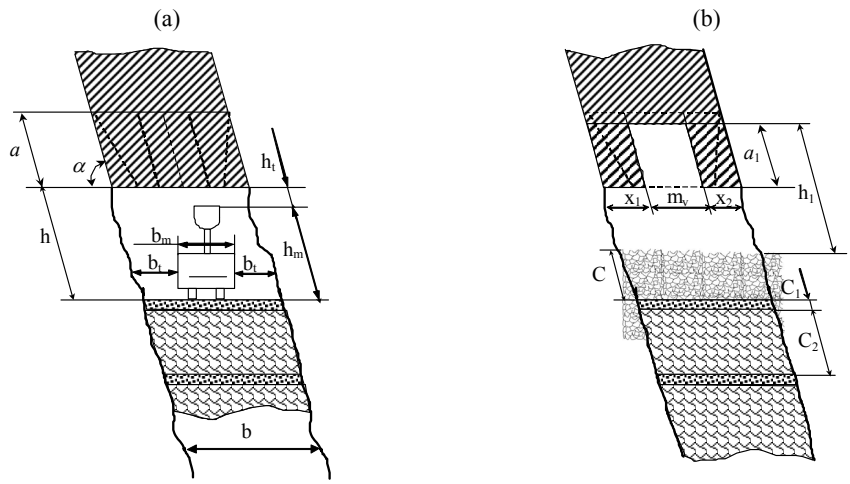

Figure 1. Design model of face space parameters control: b – width of stope, m; a – depth of holes, m; a_1 – face movement, m; h – distance from stowing layer surface up to the top drilled, m; h_l – height of free working space over shot rock, m; α – vein's dip, deg.; m_v – thickness of vein, m; $x = x_1 + x_2$ – width of enclosing roof and floor out-of-seam dilution, m; C – height of shot rock, m; C_1 – a lift of rapid-hardening stowing, m; C_2 – a lift of dry stowing, m; b_t and h_t – manufacturing clearances of width and height according to Safety Rules, m; b_m – minimum constructive width of loading equipment, m; h_m – maximum of loading equipment ladle raise, m.

While ore hauling by means of load-haul dumper making maximum allowable thickness of stowing mass is important process parameter of goaf stowing. It depends on the fact that under raise bench working procedures concerning drilling and charging as well as shot ore loading are performed from consolidating stowing. According to DBO certificate, standard height of face space should be permanent between top and filling mass surface. Under the height, manufacturing clearance h_t being minimum allowable on Safety Rules distance between top and vertical position of loader shovel is kept. Manufacturing clearance h_t is required for free ranging movement of equipment with vertical position of shovel within block (Figure 1a). Manufacturing clearance b_t across the width of face space is the parameter which determines loading equipment adaptability while hauling ore within block.

Taking into account real hypsometry of face space walls and shift of dynamic axis of working obtained as a result of simulation, stage two determines adaptive capacity of loading equipment. That is, minimum length of the equipment is determined for minimum width defined during stage one.

Semitheoretical problem of justification of design parameters of compact load-haul dumper can be solved by means of simulation of its design adaptive capacity within narrow stope which stochastically changes its direction and spatial outline as a result of drilling and blasting, and requirement to follow ore body.

There was performed structural analysis of configuration of side wall and bottom wall of working excavation formed under controlled drilling. Then approximating surfaces of stope were built up, and they had m mining height, $A = 0.2 \div 0.25$ m amplitude of benches and basins, curvatures r_l of side wall and r_h of bottom wall reflecting shift of trend azimuth and vein's dip $\Delta\beta = 15°$ within 5 m segment.

Solving the problem of determining load-haul dumper parameters for its operability assurance in stoping faces which can vary greatly per unit of working's length has been realized in terms of *Poisk bℓ* program (Shirin & Korovyaka 1998).

To describe algorithm and the program of the equipment parameters determination state description of the problem solved with a computer. It is required to find extreme length l of rectangle with fixed width b inscribed in zone D_i limited from left and right by vertical lines $X = x_0$ and $X = x_N$. From above and from below they are limited by certain curves $f_u(X)$ and $f_e(X)$ accordingly (Figure 2):

$$D = \{(X,Y), X \geq X_0; X \leq X_N; Y \leq f_u(X); Y \geq f_e(X)\}.$$

The minimum value is chosen among all l_X values obtained within $[x_0, x_N]$ area of search:

$$\ell = min_{X \in [X_o, X_N]}\{\ell_X\}.$$

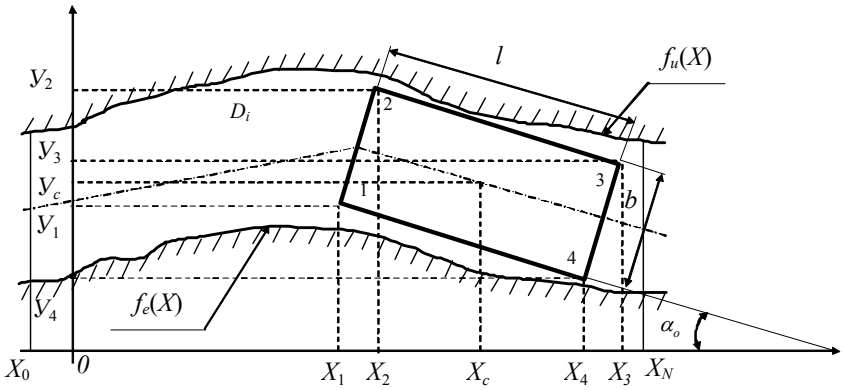

Figure 2. Adaptation of load-haul dumper to shifts of dynamical axis and hypsometry of stope walls: $[x_0, x_N]$ is area of loading equipment optimum length search; X_c, Y_c are coordinates of center of rectangle describing load-haul dumper; (X_1, Y_1), (X_2, Y_2), (X_3, Y_3), (X_4, Y_4) are coordinates of rectangle's vertexes; $f_u(X)$ and $f_e(X)$ are certain curves limiting width of stope.

The value is taken as a length of rectangle (load-haul dumper under study).

Stage three defines constructive parameters of compact load-haul dumper working element under its

minimum structural dimensions (length is $l = 3.0$ m, width is $b = 0.8$ m, height with raised ladle is $h = 1.8$ m).

2 PROBLEM DEFINITION

For compact batch overhead loaders working within narrow stope with variable dynamical axes loading equipment duty cycling is one of the key characteristics of rock mass loading process. Loading equipment (having reduced clearance) with downdip ladle moving from draw hole to rock mass pile at the expense of motional energy being proportional to equipment weight and its velocity squared as well as travel mechanism moving force introduces ladle at a depth of L' into a pile. At the expense of the lift after ladle has been introduced it turns vertically before leaving pile, and dips some rock. Then lifting drive is broken, ladle stops, and equipment moves to draw hole where lift is connected again. With it ladle rises up to maximum upward position, unloads at the expense of handle on buffer, falls, and loading equipment starts its new cycle.

Theoretically, duration of working cycle T_c of batch ladleman loading equipment as it is shown in (Bartashevski, Strashko, Shirin & Shumrikov, 2001) is additive quantity covering timing to perform a number of serial operations:

$$T_c = \sum_{i=1}^{n} t_i, \text{ where } i = 1,2,3,... \quad (1)$$

where t_0 – time to shift a handle (as a rule, 1 to 2 seconds); t_1 – time for equipment to move from a draw hole to a pile; t_2 – time to bring ladle into rock mass pile; t_3 – time for ladle to draw rock mass; t_4 – time for equipment to leave with loaded ladle; t_5 – time for ladle lift to be unloaded; t_6 – time for ladle to be unloaded; t_7 – time to lower ladle into origin return.

As cycle time is a quantity inversely proportional to output then its cutting is connected with increase in theoretical output which reflects loading equipment feasibility. Besides, as (Yevnevich 1975) informs such parameters or factors effect cycle duration: power and mechanical characteristic of drives, reduction ratio of carrier and lift of ladle, equipment weight, shape and dimensions of ladle, physical and mechanical properties of rock mass, and distance from pile to draw hole.

3 ANALYSIS OF THE PROBLEM STATE

Stage one considers factors effecting initial charge of ladle under separate ladling from rock mass pile. Figure 3 shows kinematic chain of ladling rock mass which density is ρ_0. The Figure demonstrates possible motion trajectories of front ladle edge within the pile form. As it is seen, types of the trajectories depends on ladling method, value R_0, rotational center "0" position, and ratio of lift speed and pressure of ladle introduction into rock mass (Poluyanski 1981).

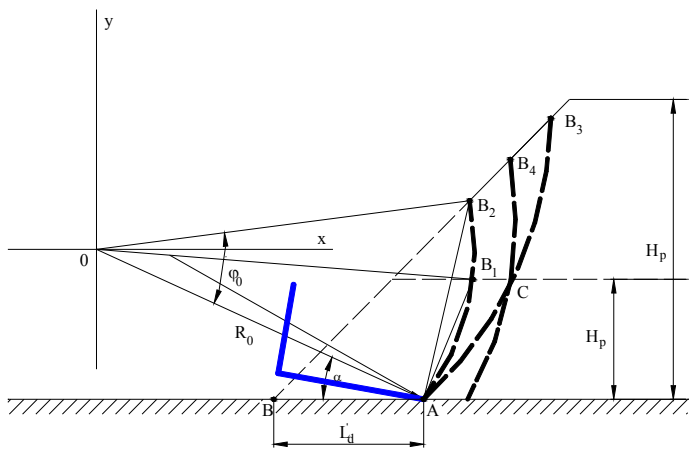

Figure 3. Specified trajectories of front edge of ladle bottom movement within the pile form.

Symbolize introduction depth as L'_d, height of a pile as H_p, and square determining initial loading a ladle as F'. Trajectory of ladle front edge under sequential operation of introduction and loading (when ladle winds) is AB_1 and AB_2 curves. With it (as Figure 4 shows) trajectory may cross form of pile either on horizontal face at B_1 point or on its aslope at B_2 point depending on height of a pile H_p. Theoretically, it can be shown in terms of the inequations:

$H_p \le R_0\left(sin\alpha + sin\left(\varphi_0 - \alpha\right)\right)$ for the first variation, and $H_p > R_0\left(sin\alpha + sin\left(\varphi_0 - \alpha\right)\right)$ for the second variation. (2)

If it is referred to combined ladling method when lift of ladle introduced into some depth keeps pace with continuous introduction then trajectory of ladle front edge will go with AB_3 and AB_4 curves.

Thus, front edge of ladle bottom under its vertical winding separates some volume of rock mass from pile. The volume of rock mass is proportional to involved square F'. When ladle leaves pile the volume of rock mass (separated from the pile), and values of the pile height H_p and introduction depth L'_d are different, the square of polygon $BCDEK$ is separated (Figure 4) and ladle is partially loaded. Theoretically, the figure square is close to square F' value. With it, vertex $D\left(D'\right)$ lies on perpendicular erected to ladle bottom plane form point B (that is front edge).

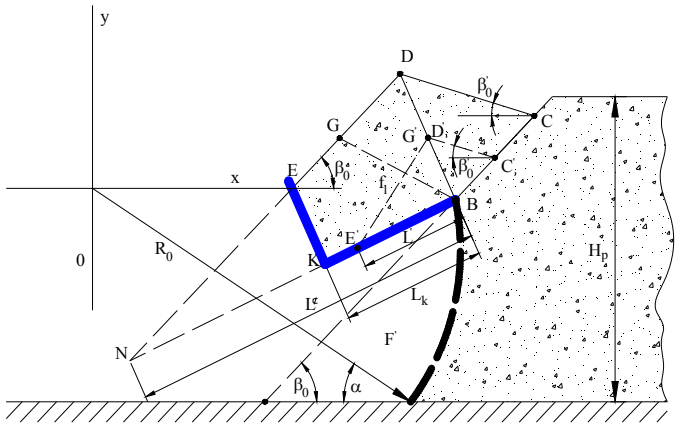

Figure 4. Location of rock mass within ladle at the moment of its leaving the pile.

Inside the ladle rock mass is located on the angle of natural levee β_0 with l' length which in turn may be both more and less than ladle bottom length l_k depending upon introduction depth L'_d.

Rock mass facing a pile with CD slope has slope angle to β'_0 level. Most of all, practical calculations takes the angle as that equal to friction slope, that is $\beta_0 = \beta'_0$.

With it, volume of rock mass taken from a pile in one working cycle is:

$$V_\kappa = f_1 \cdot B_1, \quad (3)$$

where B_1 – ladle width, m; f_1 – square in vertical plane limited by $BGEK$ contour.

While defining square f_1 consider that height is $H_p > R_0\left(sin\alpha + sin\left(\varphi_0 - \alpha\right)\right)$, and introduction depth L_d is equal to ladle bottom length that is $L'_d = l_k$. For the case, (Figure 5) square of $BGEK$ figure is:

$$f_1 = \frac{1}{2}\left[l_k\left(h + h_2\right) - h_1 \cdot l_0\right] \quad (4)$$

But as $\begin{cases} h_2 = h - l_\kappa \cdot tg\left(\beta_0 - \tau\right) \\ h_1 = h \cdot cos\left(\beta_0 - \tau\right) \end{cases}$, then

$l_0 = \left|DG\right| = \left|BC\right|$ will be equal to: (5)

$$l_0 = \frac{cos\left(\beta_0 + \tau\right)}{sin\,2\beta_0}, \text{ where } \tau = \varphi_0 - \alpha_0 \quad (6)$$

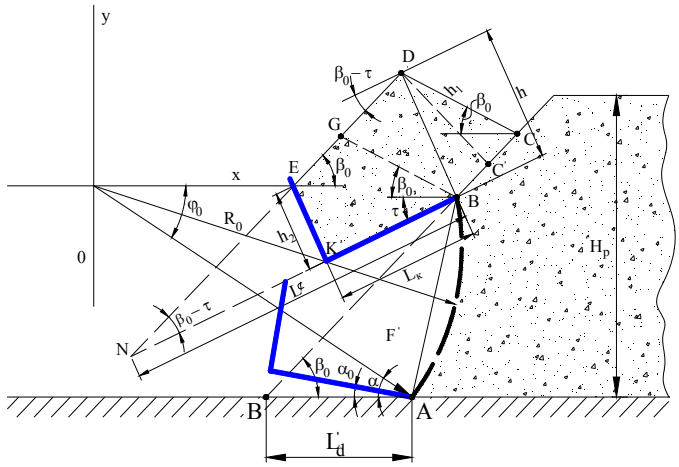

Figure 5. Design diagram for loading ladle with rock mass.

Formula (4) will be:

$$f_1 = \frac{1}{2}\left[2 \cdot h \cdot l_k - \frac{h^2 \cdot cos(\beta_0 + \tau) \cdot cos(\beta_0 - \tau)}{sin\, 2\beta_0} - \right.$$

$$\left. - l_к^2 \cdot tg(\beta_0 - \tau)\right]. \qquad (7)$$

In the formula h is undetermined value. It characterizes location of rock mass at the moment of ladle leaving a pile. While determining it (to simplify the problem) specify approximate equation of squares F' and F'' ($BCDEK$ figure). According to Figure 5:

$$F' = \frac{1}{2}\left[L'_d \frac{1}{ctg\beta_0 - tg\left(\alpha - \frac{\varphi_0}{2}\right)} + \right.$$

$$\left. + R_0^2 \cdot \left(\frac{\pi}{180^0}\varphi_0 - sin\,\varphi_0\right)\right]. \qquad (8)$$

Taking into account

$$R_0 = \frac{L'_d \cdot sin\,\beta_0}{2\, sin\frac{\varphi_0}{2} \cdot cos\left(\beta_0 + \alpha - \frac{\varphi_0}{2}\right)}, \qquad (9)$$

Expression (7) will be:

$$F' = \frac{1}{2} L_d'^2 \left\{ \frac{1}{ctg\beta_0 - tg\left(\alpha - \frac{\varphi_0}{2}\right)} + \right.$$

$$\left. + \frac{\left(\frac{\pi}{180^0}\varphi_0 - sin\,\varphi_0\right) sin^2\,\beta_0}{\left[2\, sin\frac{\varphi_0}{2} \cdot cos\left(\beta_0 + \alpha - \frac{\varphi_0}{2}\right)\right]^2} \right\}. \qquad (10)$$

In turn, from Figure 5 we get:

$$F'' = \frac{1}{2}\left[l_k\left(h + h_2\right) + h_1 \cdot |BC|\right]. \qquad (11)$$

Substituting into (9) values h_1, h_2 and $|BC|$ from Formula (6) we get:

$$F'' = \frac{1}{2}\left[2 \cdot h \cdot l_k + \frac{h^2 \cdot cos(\beta_0 + \tau) \cdot cos(\beta_0 - \tau)}{sin\, 2\beta_0} - \right.$$

$$\left. - l_k^2 \cdot tg(\beta_0 - \tau)\right]. \qquad (12)$$

Equating $F' \approx F''$ if $l_k = L'_d$ determine depth h:

$$h = d_1 \cdot L'_d, \qquad (13)$$

where

$$d_1 = \sqrt{\frac{\sin 2\beta_0}{\cos(\beta_0+\tau)\cdot\cos(\beta_0-\tau)}\left\{\frac{\sin 2\beta_0}{\cos(\beta_0+\tau)\cdot\cos(\beta_0-\tau)}+\frac{1}{ctg\beta_0 - tg\left(\alpha-\frac{\varphi_0}{2}\right)}+\right.} \left.+\frac{\left(\frac{\pi}{180^0}\varphi_0 - \sin\varphi_0\right)\sin^2\beta_0}{\left[2\sin\frac{\varphi_0}{2}\cdot\cos\left(\beta_0+\alpha-\frac{\varphi_0}{2}\right)\right]^2} - tg(\beta_0-\tau)\right\} - \frac{\sin 2\beta_0}{\cos(\beta_0+\tau)\cdot\cos(\beta_0-\tau)}.$$

Finally, substituting value h into Formula (7) and result obtained into (3) find ladle capacity of recommended compact loading equipment:

$$V_\kappa = k_1 \cdot B_{1,} \cdot L_d^2, \tag{14}$$

where

$$k_1 = d_1 - 0.5\cdot d_1 \frac{\cos(\beta_0+\tau)\cdot\cos(\beta_0-\tau)}{\sin 2\beta_0} -$$

$$-0.5\cdot tg(\beta_0-\tau).$$

It results from Formula (14) that under otherwise conditions maximum value of ladle volume is $f\left(k_1 B_1 L_d^2\right)$ function, and $V_{\kappa max}$ if $\beta_0 = \frac{\pi}{2}$. On the other hand, value of ladle loading to the full extent depends on frequency of its introduction into rock mass (Semko 1960).

To determine relationship between ladle loading volume and current time apply directly-proportional dependence of loading time on rock mass being loaded under limiting factors. As a rule, maximum loading volume (Yevnevich 1975) is among them:

$$\frac{dV}{dt} = k\cdot V(b-V), \tag{15}$$

where $\frac{dV}{dt}$ is time of ladle loading, m^3 / s; k is ladle loading factor; V is current value of ladle loading under one-time introduction, m^3; b is maximum ladle loading.

Reduce differential expression (15) to nondimensional values: $V = \frac{V_{min}}{V_{max}}$; $b = 1$ if $t = t_i$.

Then symbolize (15) as:

$$\int \frac{dV}{V(b-V)} = \int k\cdot dt, \tag{16}$$

Separate integral in right member into the two addends, and integrate:

$$\frac{1}{b}\left[\int\frac{dV}{V} + \int\frac{dV}{b-V}\right] = \int k dt. \tag{17}$$

Obtain:

$$\frac{1}{b}\left[lnV - ln(b-V)\right] = kt - C_1. \tag{18}$$

With it, constant of integration C_1 is determined with the help of initial conditions $C_1 = -\frac{1}{b} ln\, a$, where a is starting volume of ladle loading.

(18) helps to get final output:

$$V_{(t)} = \frac{b}{1 + a\cdot e^{-bkt}}. \tag{19}$$

(19) shows that current value of ladle loading depends on values "*a*" and "*k*". Specify $\widetilde{a} = k_1$, then rewrite (19) as:

$$V_{(t)} = \frac{1}{1 + k_1\cdot e^{-kt}}. \tag{20}$$

Values k_1 and k depend on different factors – physical and mechanical properties of rock, its hardness, lumpiness etc. as well on method of ladle introduction into rock mass.

4 RESULTS

To increase efficiency of ladle equipment a number of papers recommend different ways of loading process intensification (Yevnevich 1975 & Poluyanski 1981). For example, Institute of Geotechnical Mechanics of the National Academy of Sciences of Ukraine developed technique of ladle loading intensification with the use of vibration exciter as vibration loader. Hydraulic pulsators or pneumo pulsators with $10 \div 15$ Hz rhythm and $A = 3 \div 5$ mm of ladle loading edge oscillation amplitude. With it, factors k_1 and k increase up to $0.6 \div 0.8$.

Figure 6 shows dependence diagrams of ladle loading on its introduction into rock mass without applying vibration on ladle and with it. Graphical dependences are obtained with the help of *Mathcad* program.

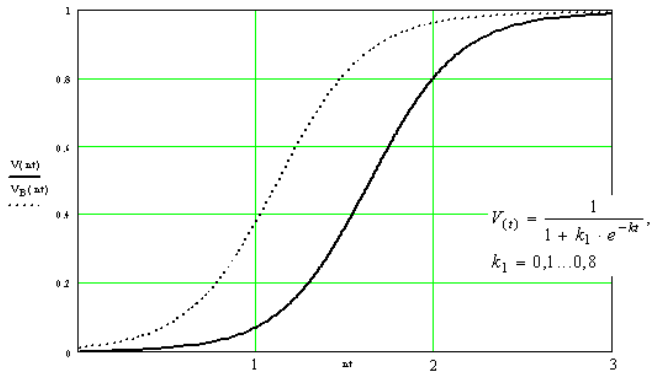

Figure 6. Dependence of ladle loading on its introduction into rock mass frequency: —— conventional ladle; ----- vibrating ladle; $nt = \frac{\bar{t}_u}{t}$, where t_u – average time of cutting cycle; and t – current time of single cutting.

From the dependences it follows that under conventional loading the same volume needs more cuttings to compare with vibrating ladle. Thus, application of vibrating exciter both during introduction into rock mass and during unloading will help to increase efficiency of load-haul-dumper even if geometrical characteristics of ladle stay to be identical.

Hence, according to design model (Figure 1) volume of rock mass to be loaded (if length of semiblock is 25 m, working face movement is 1.8 m, degree of fragmentation is $k_p = 1.5$, and mining power is 1.2 m) will be 81 m^3. Then time to haul gangue to draw hole under continuous operation of compact load-haul-dumper with fixed ladle is about 10 hours, and with vibrating ladle it is about 7 hours.

While determining dimensions of ladle on rolling handle following ratios are taken:

$$l_к = 1.14\sqrt[3]{V_к}, B_к = l_к, h_b \approx 0.4 \cdot l_к, H \approx 1.2 \cdot l_к,$$

where $l_к$ – ladle bottom length; $B_к$ – ladle width; H – ladle height from the front; and h_b – ladle bottom height.

There are identified following design factors for compact load-haul-dumper ladle: $V_к = 0.3$ m^3, $l_к = B_к = 0.76$ m, $H = 0.91$ m, and $h_b = 0.3$ m.

Since cutting is performed by means of pressing loading equipment into rock mass pile then adhesion weight is determined as:

$$G_c = n\frac{P}{\Psi - z(W_m + W_к - W_d)}, \text{ H}$$

where n – reserve coefficient equal to 1.1÷1.15; P_{BH} – rated force of a ladle introduction into a pile, H; Ψ – a coefficient of wheels adhesion with stowing mass; z – the relation between working weight of equipment and its adhesion weight; W_m – running resistance of equipment; $W_к$ – resistance of equipment on curves equal to $(0.25 \div 0.3) \cdot W_m$; $W_d = 0.7 \cdot v^2 / L_d$ – dynamic resistance; and v – stroke speed of equipment, m / s.

Usually, pressure of ladle into pile equal to rock mass reaction when lumpiness is no more than 400 mm is determined as:

$$P = 341 \cdot a \cdot L_d^{1.25} \cdot B_k \cdot k_h \cdot k_f, \text{ кН}$$

where a – a factor taking into account tightness and abrasive properties of rocks and mineral (at average, it is 0.17÷0.2 for iron ore; 0.15 for sandstone and granite, and 0.12 for sandy shale); $k_h = (1.16 \div 1.57) \cdot (2 + lg\, H_p)$ – a factor taking into account influence of pile's height; and k_f – a ladle form factor (roughly, it is taken as that equal to 1.2÷2.0).

5 CONCLUSIONS

From the viewpoint of mining mechanization the area is rather promising while mining ore bodies which thickness is >1.5 m. To cut qualitative losses of minerals while mining seams (to dilute them as a result of mixing with dead rocks) it is necessary to be geared to ore body selective mining and diluted rock walls. It depends on the fact that ore dilution and losses, and cripples economy greatly not only while mining but in the process of processing. Excessive mining dead rocks (connected with dilution) then separating in tails harms environment too as vast territories are required to place tailing pounds which negative influence is known.

The research are implemented in method of determining rational parameters of operation schedule to mine narrow vein heavy pitching deposits by means of compact load-haul dumpers, and in "Initial Standards" to design compact load-haul dumpers for mining narrow heavy pitching veins. The Standards are agreed with Institute of Geotechnical Mechanics of the National Academy of Sciences of Ukraine, approved and passed to the State Design Institute "Krivbassproject" to be applied.

REFERENCES

Korovyaka, E.A. 2003. *Control of Parameters of Face Space and Stowing Mass within Stopes of Narrow Heavy Pitching Veins*. Mining of Ore Deposits. Scientific and Technological Collection. Krivoy Rog, 82: 49-55.

Shirin, L.N., Korovyaka, E.A. & Shirin, A.L. 1998. *Model Analysis of Adaptive Capacity of Load-haul Dumpers to Mine Narrow Vein Deposits*. Inter-agency Collection of Scientific Papers of IGTM of the NAS of Ukraine, 6: 67-73.

Bartashevski, S.E., Strashko, V.A., Shirin, L.N. & Shumrikov, V.V. 2001. *Mathematical Models of Work-cycle Time of Ladleman Loading Machine*. Vibration in Methods and Technology, 3(19): 46-49.

Yevnevich, A.V. 1975. *Transport Machines and* Complexes. Moscow: Nedra: 415.

Poluyanski, S.A., Savitski, Yu.P., Strashko, V.A. & Voloshanyuk, S.N. 1981. *Calculations of Basic Technical Parameters and Efficiency of Mine Ladleman Loading Equipment*. – Kyiv.: Naukova Dumka: 76.

Semko, B.P. 1960. *Concerning Influence of Ladleman Loading Equipment on the Process of Bringing into Rock Pile*. Collection "Topics of Mine Transport": Gosgortechizdat, 4: 390-407.

Technical and Geoinformational Systems in Mining – Pivnyak, Bondarenko & Kovalevs'ka (eds)

The top caving system with roof fall for excavation of thick coal seams

M. Lubryka
"Jas-Mos" Coal Mine
J. Lubryka
Elgor+ Hansen Company, Kopex

ABSTRACT: The top caving system with roof fall is designed to excavation of thick seams. The solution assumes that the extracted coal from the top layer is recovered by the lifted up and pivoted tail canopy onto the retractable rear Armoured Face conveyor (AFC). The rear AFC AFC is installed behind bases of powered roof support units and is pulled on the floor. Hydraulic cylinders and chains are used as pulling members to hide the AFC under the tail canopy when waste rock is encountered. The "JAS-MOS" coal mine intends to apply that extraction method to the 510/1-2 seam. The seam deposited at the depth of 750 to 900 m and its thickness ranges from 9.6 to 13.6m. The top caving method should be supported by a longwall shearer, a system of powered roof support units with electrohydraulic control as well as a power supply and control system for the set of the longwall mining machinery with very high degree of reliability. Such a set of equipment cannot work without an advanced visualization system with the possibility of parameterization.

1 INTRODUCTION

Jastrzębie Coal Company SA (JSW plc.) has a number of seams, where many parts of them are of sizeable thickness. It is why the Managing Board of the company made the decision that application of the highly efficient top caving system to extraction of thick seams is a matter of crucial importance for further development of the company.

"Jas-Mos" coal mine intends to extract coal from the seam 510/1-2 in is part W2. The seam is deposited at the depth ranging from 750 to 900 m with its thickness from 10 to 13 m. Aiming to extract the seam with the optimum efficiency and to observe the stringent safety rules, the mine decided to consider top caving as a very promising option of mining operations.

"Jas-Mos" coal mine has developed the plan to extract that part of the seam with application of the longwall system with roof fall and with subdivision of the entire seam into two layers with the thickness of 3.5 m each. Therefore the seam with the thickness of 7 m is to be extracted from the overall bed thickness that varies from 10 to 13 m, as it was mentioned before.

Having considered all the circumstances, possible obstacles and difficulties with subdivision of the extraction process into layers as well as the wish to achieve higher efficiency of the seam excavation with simultaneous observance of all the standards and conditions intended to guarantee safety of surface facilities, the idea was put forward to apply the system of top caving under the areas that are chiefly used for agricultural purposes. It is the system that has not yet been used in the Polish mining industry and consists in longwall extraction with roof fall and advanced progress of the roof-adjacent layer in ahead.

The experience of both Russian and Chinese mining industry demonstrates that application of that system makes it possible to extract about 75% of coal deposited within the borders of longwall parcels with simultaneous minimization of indispensable roadway drivage jobs. Therefore the assumption could be made that the seam height to be extracted within borders of longwalls where the top cavity system is applied shall amount to 8-9 m.

2 CHARACTERISTIC PARAMETERS OF THE SEAM

Application of the top cavity system with roof fall is anticipated in the part of the W2 panel encircled from the north by the line of eastern drifts and by the fault area ~ 11.0 m from the south, by the ventilation roadway from the west and the border of the mining area from the east. The identified industrial resources of coal within the mentioned region amount to ca. 9.7 m. tons where the extractable re-

sources are estimated to 3.1 m. tons.

The considered part of the bed is made up of merely a single coal layer – the seam 510/1-2 with the thickness of 9.6-13.6 m. The coal is classified to the grades 35.2A, 35.2B and 37.1. Coal in that seam is brittle by its nature as its cohesion factor is estimated to $f \leq 0.5$.

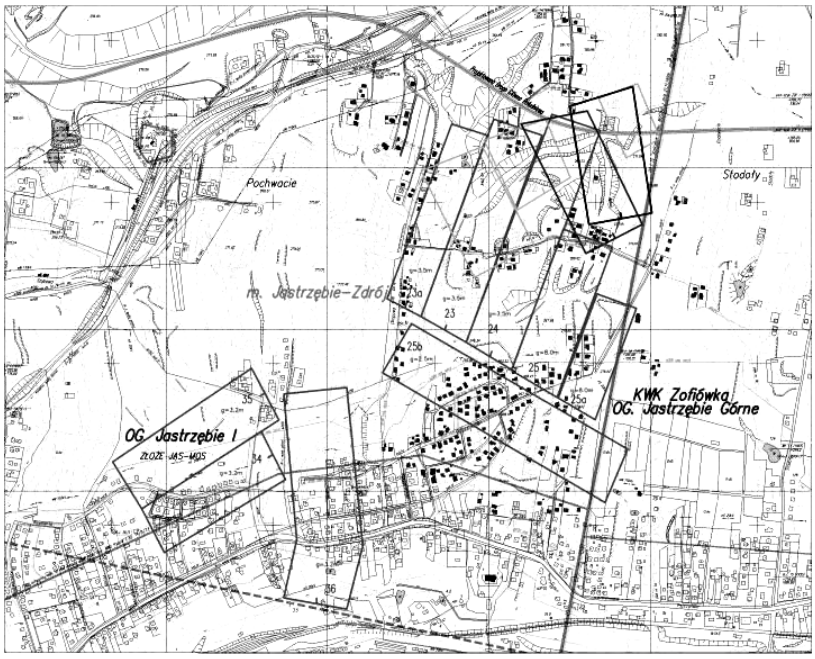

Figure 1. Part W2 of the seam 510/1-2.

The considered part of the bed represents the eastern, less steep wing of the geological anticline of Jastrzębie, with the central line sinking to the north-east direction and unduled. Inclination of coal strata in that wing averages to 16º/E.

The area features with many factors of both continuous tectonic effects (a tectonic fault and flexure) as well as non-continuous ones (normal and upthrown faults). The tectonic properties as well as formation and thickness of the seam are some of the essential factors that determine the seam development and extraction methods.

Major directions of the coal seam cleavage are nearly parallel to the central line of the anticline. The seam is directly covered by the layer of clay shale or mudstone, where the clay shale comprises local intrusions of sand. This roof-adjacent layer has the average thickness of 9.9 m and is loose and easily separable from the upper sandstone layer with the thickness of ca. 20 m. Upwards, within the neighbourhood of clay shale, the 508 seam can be found that approaches the 510/1-2 seam along the diagonal direction, where the both seam converge on the mining area of Jastrzębie Górne. In pace with mutual approaching of the both seams the sandstone layer represents still thinner and thinner wedge and completely disappears. Thickness of the 508 seam ranges from 0.0 m to 2.3 m. Upwards, above the 508 seam, a thick layer of sandy and gravelled deposits can be found (sandstone and pudding stone alternately) with the thickness of 75 to 80 m and with local intrusion of clay shale formations.

The floor of the considered seam is made up of mudstone (arenaceous shale).

Compression strength of the individual rock grades amounts to:

– sandstone – $R_c = 62 - 74$ MPa;

– clay shale (claycy stale) – $R_{c\,av.} = 21.4$ MPa;

– arenaceous shale (mudstone) – $R_{c\,av.} = 33.7 - 39$ MPa,

– coal – $R_c = 4.4 - 11.5$ MPa.

The slakeability factor is 0.8 for clay shale and 1.0 for arenaceous shale and sandstone.

The decline angle of strata within the considered region ranges from 5º to 25º/E and NE but locally the decline angle is as high as 30º/E.

Coal extraction used to be carried out from the

seam 505/1 that is deposited about 120 to 140 m above the considered seam 510/1-2. Nowadays the seam 505/2 is being extracted, about 110 to 130 m upwards.

The coal panel to be extracted may suffer from slips with the drops up to several meters and various directions of running. Rock in the regions of slips is brittle and cracked, conducive to falls or slides.

Hazards:

1st degree of water hazard.

4th category of methane hazard.

Class B of coal dust explosion hazard.

The seam in its W2 part is classified to the 1st degree of hazards due to rock bumps.

The seam is not rated to the class of rock that is conducive or hazardous in terms of methane or rock outbursts.

The southern part of that seam segment is built up with detached houses whilst the surface over central and northern areas is chiefly used for agricultural purposes.

For selection of the mining system that shall be applied to extraction of the seams 510/lłg, 510/1 and 510/1-2 in the part W-2 the following circumstances had to be considered:

– the need to conserve the land surface within the borders of the coal extraction area, in particular in the densely built-up southern part of the region;

– sophisticated geological conditions within the part of the seam that is to be extracted (substantial brittleness of coal, occurrence of considerable cleavage, presence of a loose shale layer with the thickness of several meters in the overlaying stratum of the seam), which present substantial obstacles to roadway driving operations;

– the need to achieve cost effectiveness of the mining operations with maximum possible extraction of the seam.

3 EXTRACTION SYSTEM

The roof fall system with advanced extraction of the roof-adjacent layer is dedicated to so called 'thick' seams. The solution assumes that the coal extracted from the top cavings is slid down on the partly lifted and pivoted tail canopy onto the rear Armoured Face Conveyor (AFC). The rear AFC is installed behind bases of powered roof support units and is pulled on the floor. Hydraulic cylinders and chains are used as pulling members to hide the AFC under the tail canopy when waste rock is excavated. When the powered roof support units are moved forward the rear AFC is left partly behind the tail canopy to enable more efficient loading of the extracted winning to the AFC. The hydraulically extended part of the tail canopy is provided with picks to disintegrate excessively large lumps of winning.

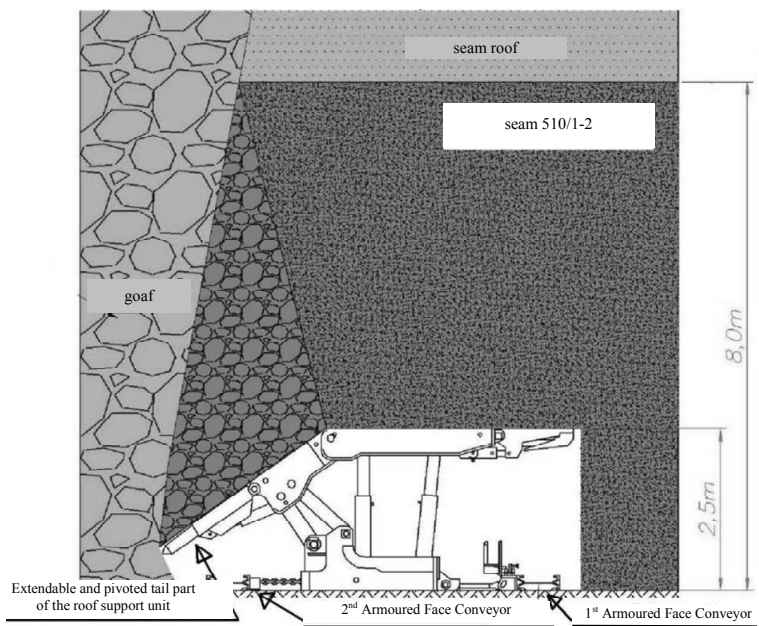

Figure 2. Essential components of the longwall appliances.

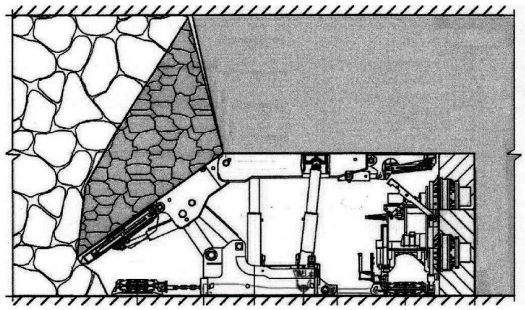

Figure 3. Use of a shearer to extraction of the floor layer of coal.

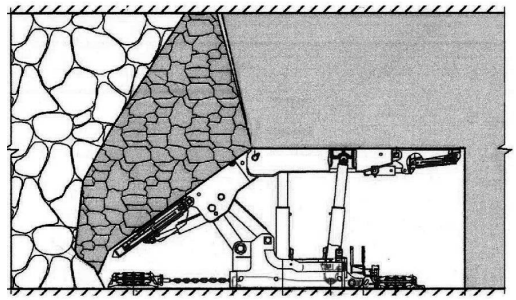

Figure 4. Advancing movement of the powered roof support unit with leaving the rear AFC immobile.

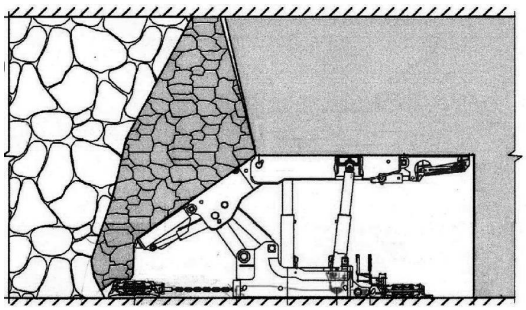

Figure 5. The first step associated with extraction and loading of the roof coal layer by controlling the extendable tail roof canopy.

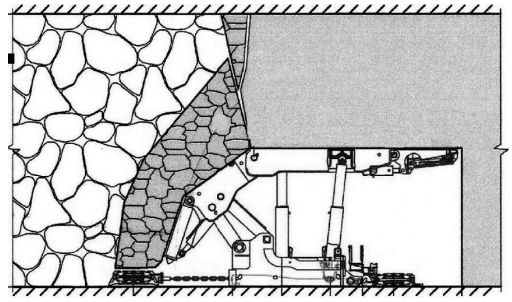

Figure 6. The second step associated with extraction and loading of the roof coal layer by controlling the pivoted part of the tail roof canopy.

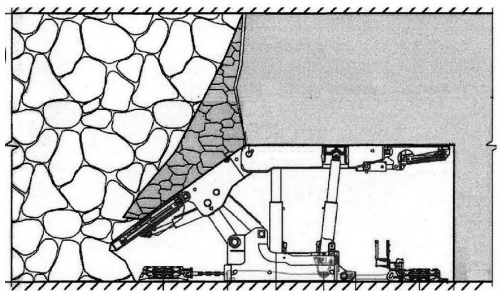

Figure 7. Final stage of extraction and loading of the roof coal layer.

Anticipated application of the innovative and experimental coal extraction method of top caving to excavate seams 510/łłg, 510/1 and 510/1-2 seams of the W-2 part entails a number of questions and wonderings. As the method has never been used in the Polish mining industry there are many doubts with regard to safety of the extraction method as well as to its effects to the land surface, in particular to these parts that are intensely built up with detached houses. Due to the aforementioned doubts the "Jas-Mos" coal mine made the decision to prepare an option of the top caving extraction method, where the seams 510/łłg, 510/1 and 510/1-2 seams of the W-2 part would be extracted with use of a single longwall that would serve as an field test to enable clarification of all doubts before major extraction of the entire W-2 part.

4 SHEARER

Current trends towards optimization of the entire process related to coal extraction and eventual improvement of its efficiency impose the need to use more productive and reliable equipment that make up the entire set of longwall machinery. As shearers represent the basic machines of longwall sets, their productivity and reliability are crucial for overall performance of mining operations. However, the designers of modern longwall shearers put main stress onto their reliability (Kostka).

Beside the advanced diagnostic system the shearer should be equipped with a positioning system to enable location of the machine within the

longwall as well as the functionality of the "pattern cut" with possibility of its automatic reproduction. Shearers should be designed is such a way that longwall extraction of coal should be automated as much as possible. In addition, the machine should be provided with a system of data transmission to the supervising system located in the main gate and on the coal mine surface.

The main stress is put to the reliability factor, which is achieved by application of equipment and components with the high MTBF (Mean Time Between Failures) factor.

The shearer operator should be enabled to select the source of control signals between the remote RF control and local wired control with use of dedicated devices. Selection of the RF control not only should enable remote control the shearer but also remote view of the monitored parameters and messages about emergency conditions. Such a solution absolves the operator from the need to walk each time to the central monitor, which is very important when overall length of shearers exceeds 14 m.

Worldwide manufacturers of shearers, such as ZZM from Zabrze, Poland, Joy or Eickoff offer the machines that demonstrate all the foregoing qualities.

5 CONTROL SYSTEM OF EQUIPMENT INCLUDED INTO THE LONGWALL EXTRACTION SET

Automatic control and mechanization are the most important factors of highly efficient coal extraction technology with use of longwall machinery and application of the top caving system with roof fall, where electrohydraulic control of powered roof support units is also a crucial component (Adamusiński 2010). The set of longwall machinery should be controlled from the operator station located in the main/tail gate. Operators of the control station are provided with visualization appliances to display current information about operational parameters of the longwall equipment and to adjust these parameters in the real time mode.

Innovative solutions for MV electric equipment of explosion-proof design have been developed by Elgor-Hansen to supply highly productive sets of extraction equipment. These solutions perfectly proved themselves for application in underground mining operations and made it possible to gain necessary experience. Simultaneous tracking of the most recent research and development solutions enabled the company in a short time to offer the equipment that not only guarantee the high degree of safety but also demonstrate the desired operational qualities. The systems form Elgor+Hansen are constantly improved and customized according to individual needs and requirements of customers.

The control system for the machinery of a highly productive extraction system with use of top caving and roof fall method is a really sophisticated and very complex solution intended to carry out a great number of functions, such as control, visualization, keeping records and diagnostics. Deployment of the controlled equipment in quite a large space suggests that the control system should be of the field type with use of industrial data transmission networks for local communication. The information shall be processed with use of the multi-level hierarchical structure, starting from the control level of individual components via parameterization of the equipment, diagnostic and record keeping functions, visualization and data storage up to the top level where the entire technological process is controlled.

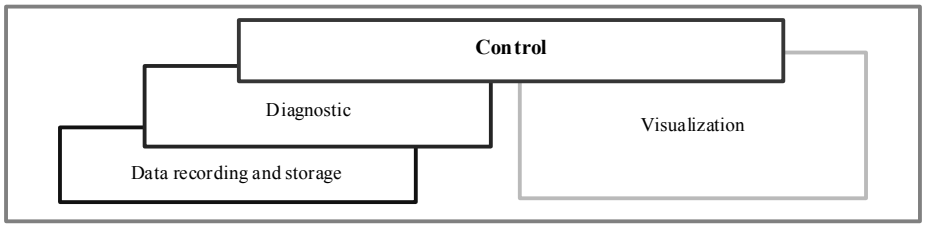

Figure 8. The tasks to be carried out by the control system for the set of extraction equipment with application of the top caving method with roof fall.

The control system for powered roof support units must be furnished with additional functionalities associated with application of the top caving system with roof fall. Such a system must be based on control modules installed on every unit of the longwall set. By appropriate configuration of the modules they should adhere to the operation mode selected for the entire system. Each control module receives values of measured parameters from components of the system. Therefore the operators, depending on the required configuration, should be capable to initiate individual, separate functions or to run the sys-

tem automatically.

In terms of operational applicability, the visualization system for the electric equipment of the longwall set should be structured into:

– local visualization;

– central visualization.

The local visualization shall cover only a single device, such as a compact power centre, a transformer unit or a single powered roof support unit. The visually presented information shall be restricted to a certain device, appropriately structured and organized to enable easy local diagnostics for the operator. When a need to adjust parameters of the device appears, the local visualization system should also make it possible. Additionally, on some cases the system of local visualization should enable local storage of operational information.

On contrary, the central visualization system shall cover all equipment incorporated into the set of extraction machinery. It will perform a large number of functions, including:

– visualization of the control system status;

– visualization of the shearer operation;

– visualization of the powered roof support system with regard to indications of the installed sensors and gauges;

– automatic advance of individual powered roof support units depending on indications of the installed sensors and gauges;

– adjustment of parameters that determine advancing operation of the longwall set;

– visualization of the equipment included into the train of electric appliances;

– visualization of the equipment included into the control system;

– parameterization of the control system;

– central data storage;

– viewing of historical information for maintenance purposes.

6 CONCLUSIONS

Extensive and detailed analyzes dedicated to extraction efficiency of 'thick' seams are carried out in a number of countries. Experience from extraction of 'thick' seams with use of the top caving system with roof fall acquired in Russia and China serve as a proof that the proposed technology is a cost-effective and technically justified method for efficient extraction of seam with the thickness ranging from 10 to 13 m. Additionally, the technology is supported by substantial economic benefits as it makes possible to extract 75% of resources deposited within boundaries of longwall panels with minimum amount of roadway drivage efforts. All in all, the technology offers the optimum extraction of seams with maintaining the most stringent safety requirements. The anticipated objectives can be achieved with use of highly efficient and reliable systems developed to control sets of longwall extraction machinery.

REFERENCES

Lubryka, M. 2003. *Assessment of financial efficiency achieved in investment projects at the "JAS-MOS" coal mine.* The School of Economy and Management in Mining Industry.

Lubryka, M. 2006. *Analysis of extraction opportunities for parts of seams with small sizes and irregular shapes with application of the "non-conventional" extraction methods.* Cracow: Proceedings of the School of Underground Mining. Symposiums and Conferences of PAN and AGH, 66.

Lubryka, M. 2007. *The determining aspects to seek for opportunities to sustain extraction of coking coal in the context of deposit exhaustion within the region of Jastrzębie town.* Power Engineering Policy. Vol. 10. Special Edition, 2.

Kostka, M. *The longwall shearer KSW-20008 in the aspect of modern power suppling, control and diagnostic technologies.* Zabrze.

Czechowski, A., Lubryka, J. & Lubryka, M. 2008. *The study of Control Software System and Visualization for Special Mining Machine.* 21st World Mining Congress & Expo 2008.

Lubryka, M. & Lubryka, J. 2010. *Control and power supply of highly efficient mining plow systems*. Advanced mining for sustainable development. International Mining Conference. Ha Long Vietnam.

Adamusiński, M., Morawiec, M., Jędruś, T. Lubryka, J. & Macierzyński, D. 2010. *Modern solutions for power supplying, control and automation system on the example of the highly efficient plow system supplied with 3.3 kV voltage at Zofiówka coal mine.* 13th National Conference of Mining Electric Systems.

Lubryka, M. & Lubryka, J. 2010. *Control and power supply of highly efficient mining plow systems.* Dnipropetrovs'k: Proceedings of the school of underground mining. New Techniques and Technologies in Mining – Bondarenko, Kovalevs'ka & Dychkov'kyy (eds) 2010 Taylor & Francis Group, London, ISBN 978-0-415-59864-4.

Lubryka, M. & Lubryka J. 2010. *Control and power supply of highly efficient mining plow systems.* International Forum and Contest for young scientists. The State Mining Institute of Sankt Petersburg: Journal of the Mining Institute.

Technical and Geoinformational Systems in Mining – Pivnyak, Bondarenko & Kovalevs'ka (eds)

Modeling of dynamic interaction of technological loading with elastic elements of sifting surfaces in mining and ore-dressing equipment

O. Dolgov
National Mining University, Dnipropetrovs'k, Ukraine

I. Dolgova
Prydneprovska academy of civil engineering and architecture, Dnipropetrovs'k, Ukraine

ABSTRACT: The subject matter is the research of dynamics of the rubber strings serving as the separation media in technological process. The rubber ribbon-strings used as the elements of sifting surfaces substantially differ from beams. Examining their motion as motion of the thin-walled bars, differential equations of their bending and torsion vibrations are developed. A mathematical problem is reduced to integration of the system of linear non-homogeneous differential equations at the given boundary conditions.

1 INTRODUCTION

The questions related to exploitation of self-cleaning sifting surfaces are closely associated with research of dynamic interaction of technological loading with elastic elements. Rubber ribbon-strings (RRS), used as such elements, on the geometrical parameters, behavior, constructional features essentially differ from beams. Many of them rather represent the thin-walled rods. Their structural features consist in possibility to sustain longitudinal elongations at torsion strains. Consequently, the longitudinal normal stresses, proportional to these strains, are reduced in each cross-section to system of balanced longitudinal forces. These, not examined in the theory of pure torsion additional stresses, arising owing to relative deplanation of cross-section, can reach rather great values.

The conditions of RRS work under the action of technological loading aggravate this circumstance and result in the necessity of account of these additional factors at theoretical research of their behavior for various operating regimes.

There is a fundamental concept of a bar centre line in the classic bending theory, based on the law of the plane sections. This is the line through the centroids of their transversal cross-sections. This basic concept of strength of materials, which in essence is Saint-Venant's principle, for thin-walled bars requires radical revision and specification.

If the bent element of a construction can be treated as a thin-walled rod, in considering of such element the concept of a line of bending takes on special significance. For the rods, which have in cross-section two axes of symmetry, this line coincides with centroids of cross-sections. For rods of any asymmetrical profile or a profile with one axis of symmetry, the line of centers of bending will not coincide with centroids of cross-sections. The teeth of RRS do not give possibility to consider a rod as an element with two axis of symmetry. Applying to such rods the classic theory of bending, which allows to consider only bending strains, it is necessary to accept for a rod axis not a line through centroids, but a line of centers of bending and to assume that the transversal loadings, causing a bending of a rod according to the law of plane sections, are applied at points of a line of the centers of bending. If transversal loading reduces to centroids such loading, except a bending, will cause as well torsion. The usual theory of a bending in this case becomes inapplicable (Vlasov 1959).

2 PROBLEM STATEMENT

The theory of thin-walled rods is based on the geometrical hypotheses; their main sense consists in the following:

– the rod in a plane of cross-section has a rigid (not deformable) profile;

– he shear strain of the middle surface, characterized by the right angle change between co-ordinate lines, is accepted equal to zero.

The sense of the first hypothesis consists in the fact that the elementary portion of the rod contained be-

tween its two cross-sections, is considered in the plane as absolutely rigid body. Then in a plane of cross-section, it possesses three degrees of freedom corresponding two linear and one angular displacement. At a deformation of an infinitesimal part from a plane of cross-section, it is considered as an elastic deformable body.

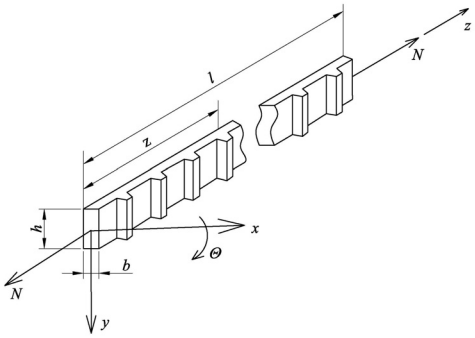

Figure 1. Design diagram of rubber ribbon-string.

The second hypothesis makes it possible to ignore right angle change between co-ordinate axes before and after deformation, i.e. to neglect right angle change between these axes as the geometrical factor, which does not have owing to smallness essential value for stresses in a rod.

Let us consider RRS, having unilateral teeth, and choose the co-ordinate system shown on the Figure 1. We will consider RRS under the action of technological loading and longitudinal eccentric force N. Let co-ordinates of a point of application of the force N are equal e_x and e_y.

Accepting aforementioned hypotheses and taking into account the quantities of corresponding components of disturbing forces, which are caused by the action of technological loading, we can obtain following differential equations of RRS vibrations:

$$
\begin{aligned}
&EJ_y\frac{\partial^4 u}{\partial z^4}-\rho J_y\frac{\partial^4 u}{\partial z^2\partial t^2}+\rho F\frac{\partial^2 u}{\partial t^2}-N\frac{\partial^2 u}{\partial z^2}+\rho Fa_y\frac{\partial^2\theta}{\partial t^2}+N\left(e_y-a_y\right)\frac{\partial^2\theta}{\partial z^2}=Q_x(z,t),\\
&EJ_x\frac{\partial^4 v}{\partial z^4}-\rho J_x\frac{\partial^4 v}{\partial z^2\partial t^2}+\rho F\frac{\partial^2 v}{\partial t^2}-N\frac{\partial^2 v}{\partial z^2}-\rho Fa_x\frac{\partial^2\theta}{\partial t^2}-N\left(e_x-a_x\right)\frac{\partial^2\theta}{\partial z^2}=Q_y(z,t),\\
&\rho Fa_y\frac{\partial^2 u}{\partial t^2}+N\left(e_y-a_y\right)\frac{\partial^2 u}{\partial z^2}-\rho Fa_x\frac{\partial^2 v}{\partial t^2}-N\left(e_x-a_x\right)\frac{\partial^2 v}{\partial z^2}+EJ_\omega\frac{\partial^4\theta}{\partial z^4}-\\
&-\rho J_\omega\frac{\partial^4\theta}{\partial z^2\partial t^2}+\rho Fr^2\frac{\partial^2\theta}{\partial t^2}-GJ_p\frac{\partial^2\theta}{dz^2}-N\left(r^2+2\beta_x e_x+2\beta_y e_y\right)\frac{\partial^2\theta}{\partial z^2}=M(z,t),
\end{aligned}
\tag{1}
$$

where u, v – displacements of the line of the centers of bending along coordinate axes x and y respectively; θ – angle of rotation of the RRS cross-section in plane xy; N – longitudinal force applied with eccentricity e_x and e_y; $Q_x(z,t)$, $Q_y(z,t)$, $M(z,t)$ – components of disturbing forces (technological loading); a_x, a_y – coordinates of the centre of bending; E, G – Yuong's and shear modulus respectively; J_x, J_y, J_ω – axial and sectorial moments of inertia; ρ – density of material; b – thickness of the RRS base; F – area of the cross-section of the base;

$$r^2=\frac{J_x+J_y}{F}+a_x^2+a_y^2;\ \beta_x=\frac{U_y}{2J_y}-a_x;$$

$$\beta_y=\frac{U_x}{2J_x}-a_y;\ U_x=\int_F y^3dF+\int x^2ydF;$$

$$U_y=\int_F x^3dF+\int_F y^2xdF.$$

It should be noted that at the action of the force N all equations in (1) are related, i.e., they define together with boundary conditions spatial bending and torsion vibrations.

Let us consider forced vibrations of ribbed RRS, which has in cross-section horizontal axis of symmetry ox, supported on diaphragms, rigid in xy plane and flexible in zy plane. Thus, mathematically the problem is reduced to the integration of simultaneous equations (1) at the given set boundary and initial conditions, assuming $a_x=0$.

3 PROBLEM SOLUTION

Let us consider the next boundary conditions:
at $z=0$, l, $u=v=\theta=0$,

$$\frac{\partial^2 u}{\partial z^2}=\frac{\partial^2 v}{\partial z^2}=\frac{\partial^2 \theta}{\partial z^2}=0. \quad (2)$$

Provided (2), solution can be represented in the form:

$$u(z,t)=\sum_{n=1}^{\infty}u_n(t)\sin\lambda_n z,\ v(z,t)=\sum_{n=1}^{\infty}v_n(t)\sin\lambda_n z,$$
$$\theta(z,t)=\sum_{n=1}^{\infty}\theta_n(t)\sin\lambda_n z, \quad (3)$$

where $\lambda_n=\frac{n\pi}{l}$, n – positive integer, l – length of RRS. Let us suppose that external loading can be expanded into Fourier's series:

$$Q_x(z,t)=f(t)\sum_{n=1}^{\infty}q_{xn}\sin\lambda_n z,$$
$$Q_y(z,t)=f(t)\sum_{n=1}^{\infty}q_{yn}\sin\lambda_n z, \quad (4)$$
$$M(z,t)=f(t)\sum_{n=1}^{\infty}m_{zn}\sin\lambda_n z,$$

where $f(t)$ – common function, which define the law of variation of external forces with time; q_{xn}, q_{yn}, m_{zn} – coefficients of Fourier's series.

By substituting expressions (3) and (4) into equations (1), we shall obtain for the n-th members:

$$EJ_y\lambda_n^4u_n+\rho\left(J_y\lambda_n^2+F\right)u_n''+\rho a_yF\theta''+$$
$$+N\lambda_n^2u_n-N\left(e_y-a_y\right)\lambda_n^2\theta=q_{xn}f(t),$$
$$EJ_x\lambda_n^4v_n+\rho\left(J_x\lambda_n^2+F\right)v_n''+N\lambda_n^2v+$$
$$+Ne_x\lambda_n^2\theta_n=q_{yn}f(t), \quad (5)$$
$$EJ_\omega\lambda_n^4\theta_n+\rho\left(J_\omega\lambda_n^2+Fr^2\right)\theta_n''+$$
$$+\rho a_yFu_n''-N\left(e_y-a_y\right)\lambda_n^2u_n+$$
$$+Ne_x\lambda_n^2v_n+\left[N\left(r^2+2\beta_xe_x+2\beta_ye_y\right)+GJ_p\right]\times$$
$$\times\lambda_n^2\theta=m_{zn}f(t).$$

The general solution of homogeneous equations corresponding to equations (5) can be obtained in the form of the simple harmonic vibrations:

$$u(t)=A\sin\left(k_nt+\alpha\right),\ v(t)=B\sin\left(k_nt+\alpha\right),$$
$$\theta(t)=C\sin\left(k_nt+\alpha\right). \quad (6)$$

By substituting expressions (6) into homogeneous equations and setting determinant of the coefficients of A, B and C equal to zero, we develop expressions for determination of natural frequencies:

$$\begin{vmatrix}C_{11} & 0 & C_{13}\\ 0 & C_{22} & C_{23}\\ C_{31} & C_{32} & C_{33}\end{vmatrix}=0, \quad (7)$$

where $C_{11}=J_{ny}\left(1-\frac{k_n^2}{k_{ny}^2}\right)+N$,

$$C_{13}=-\rho Fa_y\frac{k_n^2}{\lambda_n^2}-N\left(e_y-a_y\right),$$

$$C_{22}=J_{nx}\left(1-\frac{k_n^2}{k_{nx}^2}\right)+N,\ C_{23}=Ne_x,$$

$$C_{31}=-\rho Fa_y\frac{k_n^2}{\lambda_n^2}-N\left(e_y-a_y\right),\ C_{32}=Ne_x, \quad (8)$$

$$C_{33}=J_{n\omega}\left(1-\frac{k_n^2}{k_{n\omega}^2}\right)r^2+N\left(r^2+2\beta_xe_x+2\beta_ye_y\right),$$

$$J_{nx}=EJ_x\lambda_n^2,\ k_{nx}^2=\frac{EJ_x\lambda_n^4}{\left(J_x\lambda_n^2+F\right)\rho},$$

$$J_{ny}=EJ_y\lambda_n^2,\ k_{ny}^2=\frac{EJ_y\lambda_n^4}{\left(J_y\lambda_n^2+F\right)\rho},$$

$$J_{n\omega}=\frac{1}{r^2}\left(EJ_\omega\lambda_n^2+GJ_p\right),\ k_{n\omega}^2=\frac{EJ_\omega\lambda_n^4+GJ_p\lambda_n^2}{\left(J_\omega\lambda_n^2+Fr^2\right)\rho}.$$

Each value $\lambda_n=\frac{n\pi}{l}$, which characterizes according to solution (3) the mode shape, corresponds to compound bending and torsion vibrations.

After determining the natural frequencies from equations (7) the general integral of the system can be represented in the following form:

$$u_n(t)=\sum_{j=1}^{3} A_j \sin(k_{nj}t+\alpha_j),$$

$$v_n(t)=\sum_{j=1}^{3} B_j \sin(k_{nj}+\alpha_j), \qquad (9)$$

$$\theta_n(t)=\sum_{j=1}^{3} C_j \sin(k_{nj}t+\alpha_j).$$

Let us express arbitrary constants A_j and B_j through C_j, making use equations (5) and taking into account formulas (8):

$$B_j=-\frac{C_{23}^j}{C_{22}^j}C_j,\ A_j=-\frac{C_{13}^j}{C_{11}^j}C_j, \qquad (10)$$

where $C_{mn}^j=C_{mn}$ for each of three frequencies $k_{nj}(j=1,\ 2,\ 3)$.

Substituting formulas (10) into solutions (9), one can obtain:

$$u_n(t)=\sum_{j=1}^{3} \rho_{1j}C_j \sin(k_{nj}+\alpha_j),$$

$$v_n(t)=\sum_{j=1}^{3} \rho_{2j}C_j \sin(k_{nj}+\alpha_j), \qquad (11)$$

$$\theta_n(t)=\sum_{j=1}^{3} C_j \sin(k_{nj}+\alpha_j),$$

where $\rho_{1j}=\frac{C_{13}^j}{C_{11}^j}$; $\rho_{2j}=\frac{C_{23}^j}{C_{22}^j}$.

General integral (11) of the homogeneous system corresponding to equations (5) can be represented in other form:

$$u_n(t)=\sum_{j=1}^{3} \rho_{1j}\left(C_j \sin k_{nj}t+D_j \cos k_{nj}t\right),$$

$$v_n(t)=\sum_{j=1}^{n} \rho_{2j}\left(C_j \sin k_{nj}t+D_j \cos k_{nj}t\right), \qquad (12)$$

$$\theta_n(t)=\sum_{j=1}^{n} \left(C_j \sin k_{nj}t+D_j \cos k_{nj}t\right).$$

Expression for partial integral of nonhomogeneous equations (5) can be determined by the method of a variation of arbitrary constants or by method of initial parameters. Let us express six constants in expressions (12) in terms of displacements and speed at initial instant.

We have from formulas (12):

$$u_n(0)=\sum_{j=1}^{3} \rho_{1j}D_j\ ,\ v_n(0)=\sum_{j=1}^{3} \rho_{2j}D_j\ ,$$

$$\theta_n(0)=\sum_{j=1}^{3} D_j\ ,$$

$$u_n'(0)=-\sum_{j=1}^{3} \rho_{1j}k_{nj}C_j\ ,\ v_n'(0)=-\sum_{j=1}^{3} \rho_{2j}k_{nj}C_j\ , \qquad (13)$$

$$\theta_n'(0)=-\sum_{j=1}^{3} k_{nj}C_j.$$

By solving the system (13), one can obtain:

$$D_1=\frac{S_3S_6-S_1}{S_1S_4}u_n(0)-\frac{S_3}{S_1}v_n(0)+$$

$$+\frac{S_1S_2S_5-\rho_{11}S_1^2-S_2S_4}{S_4}\theta_n(0),$$

$$D_2=-\frac{S_6}{S_1}u_n(0)-\frac{S_4}{S_1}v_n(0)+\frac{S_2}{S_1}\theta_n(0), \qquad (14)$$

$$D_3=-\frac{S_5S_6-S_1}{S_1S_4}u_n(0)+$$

$$\frac{S_5}{S_1}v_n(0)-\frac{S_2S_5-\rho_{11}S_1}{S_4}\theta_n(0),$$

where $S_1=S_5S_6-S_4(\rho_{21}-\rho_{22})$,
$S_2=\rho_{11}S_6-\rho_{21}S_4$, $S_3=2\rho_{11}-\rho_{12}-\rho_{13}$,
$S_4=\rho_{11}-\rho_{13}$, $S_5=\rho_{11}-\rho_{12}$, $S_6=\rho_{21}-\rho_{23}$.

By analogy coefficients $C_j(j=\overline{1.4})$ can be written:

$$C_1=-\frac{S_3S_6-S_1}{k_{n1}S_1S_4}u_n'(0)+$$

$$+\frac{S_3}{k_{n1}S_1}v_n'(0)-\frac{S_1S_2S_5-\rho_{11}S_1^2-S_2S_4}{k_{n1}S_4}\theta_n'(0),$$

$$C_2=\frac{S_6}{k_{n2}S_1}u_n'(0)+\frac{S_4}{k_{n2}S_1}v_n'(0)-\frac{S_2}{k_{n2}S_1}\theta_n'(0), \qquad (15)$$

$$C_3=\frac{S_5S_6-S_1}{k_{n3}S_1S_4}u_n'(0)-\frac{S_5}{k_{n3}S_1}v_n'(0)+$$

$$+\frac{S_2S_5-\rho_{11}S_1}{k_{n3}S_4}\theta_n'(0).$$

Using formulas (14) and (15), one can determine

functions (12), which are factors of series (3), if initial conditions are known.

Let the displacements and speed of any particle at initial moment of time will be equal to zero and at instant t_1 the speeds are $u'_n(t_1)$, $v'_n(t_1)$, $\theta'_n(t_1)$. Then the law of motion can be written:

$$u_n(t) = \sum_{j=1}^{3} \rho_{1j} C_{1j} \sin k_{nj}(t - t_1),$$

$$v_n(t) = \sum_{j=1}^{3} \rho_{nj} C_{1j} \sin k_{nj}(t - t_1), \qquad (16)$$

$$\theta_n(t) = \sum_{j=1}^{3} C_{1j} \sin k_{nj}(t - t_1),$$

where C_{1j} are determined from formulas (15) at $t = t_1$.

Imparting of these velocities to the RRS points is equivalent to the action of instantaneous force. Let us express the speeds and accelerations through this force, assuming that it is known. If the force, which components are equal to $q_{xn} f(t_1)$, $q_{yn} f(t_1)$ and $m_{zn} f(t_1)$, acts rather small time Δt_1, it imparts accelerations $u''_n(t)$, $v''_n(t)$ and $\theta''_n(t)$.These accelerations are determined from equations (5), if assume in them at $t = t_1$, $u_n(t_1) = v_n(t_1) = \theta_n(t_1) = 0$.

Thus, for accelerations we have:

$$u''_n(t_1) = \frac{a_y F m_{zn} - \left(J_\omega \lambda_n^2 + F r^2\right) q_{xn}}{\rho\left[a_y^2 F^2 - \left(J_\omega \lambda_n^2 + F r^2\right)\left(J_y \lambda_n^2 + F\right)\right]} f(t_1),$$

$$v''_n(t_1) = \frac{q_{yn}}{\rho\left(J_x \lambda_n^2 + F\right)} f(t_1), \qquad (17)$$

$$\theta''_n(t_1) = \frac{a_y F q_{xn} - \left(J_y \lambda_n^2 + F\right) m_{zn}}{\rho\left[a_y^2 F^2 - \left(J_\omega \lambda_n^2 + F r^2\right)\left(J_y \lambda_n^2 + F\right)\right]} f(t_1).$$

Hence, the speeds $u'_n(t)$, $v'_n(t)$ and $\theta'_n(t)$ take the form of equations (17) if their right-hand parts multiply by Δt_1.

Substitution of the values of speeds into equations (15) and (16) yields the values of the functions $u_n(t)$, $v_n(t)$ and $\theta_n(t)$, which take part of expansion (3) for any moment of time after the action of a force.

If the series of impulses acts, the obtained results should be summed up. In the case of continuous action of impulses these sums turn into integrals. Thus, the gained expressions will be the solution of nonhomogeneous equations (5).

4 CONCLUSIONS

The proposed approach to research of dynamics of elastic elements of sifting surfaces allows choosing rational parameters and operating modes of the corresponding mining and ore-dressing equipment, in particular, rubber-string washing drums (Dolgov & Ravishin 1992). The described above algorithm allows calculating frequencies of RRS vibrations, forces of interaction of technological loading, contact time, etc.

The obtained results, in particular, show that the 10-percent relative extension substantially increases efficiency of a washing drum operating mode. The further increase in longitudinal strains leads to increase in efficiency factor of a mode, however, not so greatly. As one would expect, increase in axial stretching efforts, i.e., relative extension, causes the increase of the maximum force of interaction of technological loading, and decrease of a contact time. The analysis of the results, thus, leads to a conclusion that for used parameters a rational range of longitudinal strains of elastic elements of sifting surfaces of washing drum are 15-20%. As practice shows, the further increase in extension, and, as a result axial stretching efforts, leads to their intensive wear and falling out.

REFERENCES

Vlasov, V.Z. 1959. *Thin-walled elastic rods.* Moscow: Fizmatgyz: 508.

Dolgov, A.M. & Ravishin, V.P. 1992. *The rubber-string washing drum. Proceedings of Cracovian mineral processing conference*. Zacopane: 185-191

Technical and Geoinformational Systems in Mining – Pivnyak, Bondarenko & Kovalevs'ka (eds)

The system of the air cooling of deep mines

I. Shayhlislamova & S. Alekseenko
National Mining University, Dnipropetrovs'k, Ukraine

ABSTRACT: The system of air-cooling has been represented. It includes the method and the installation for the regulating of the thermal rate of the deep mines by means of redistribution of heat-moisture potential of mine air and installation for the thermal relaxation of mineworkers' organisms. The system suggested can be used in mines where inadmissibly high air temperatures occur in the mining and development faces as well as the low air temperature in the slope bottom of the air feeding shaft.

1 INTRODUCTION

The economic crises in our country, the complication of the mine industry restructuring, high electricity charges demand to think about the perspective of the mineral resources mining in the depth down to 1500-2000 m, the temperature of this field will be 50-75 °C and more, the temperature in the working face will raise to 45-50 °C. While passing deeper levels, the temperature and the moisture saturation of mine air increase because of the warm flows caused by the coal massif, the work of mechanisms, the oxidization and other reasons. The main source of heat releasing in mines is the coal massif whose heat release is above 50%.

Adverse climatic conditions cause heat-strokes, serious diseases and miners' efficiency decrease.

The analysis of thermal shock rate among mineworkers (Valutsina 2001) has shown certain dependence of the rate on the age. This dependence has been noticed for both acute and chronic heat exhaustion. It has been specified that the average age of mineworkers with acute overheating (AO) is 27.5 years meanwhile that with chronic overheating (CO) is 38,4 years old. In spite of the treatment taken 56.7% of workers with the AO have been found incapacitated for their profession under conditions of heating microclimate, among them 84% of patients with average severity and all the patients with serious acute heat exhaust. 74.2% of the patients with chronic overheating have also been found incapacitated for their profession after medical examination; thus, after the Medical Sanitation Expert Committee's reference, they have been employed in spheres with normal microclimatic conditions.

In the near future technological and economic reasons will not make it possible to normalize thermal conditions in mining and development high-temperature faces of deep level mines. Therefore, the issue may become even more urgent.

Thus, there is a great demand both to find new methods and technical equipment and to improve the existing ones, to improve microclimate in deep mines by using alternative energy sources. The wide range of the techniques giving the possibility to improve considerably and sometimes to normalize the climate conditions during mining in the deep mines has been developed at the Department of Aerology and Labour protection at the National Mining University.

2 THE MAJOR PART

A method and installation of mine air conditioning with preliminary heat moisture saturation of mine air have been developed for the regulating of the thermal rate (Patent 53467, 2006). The matter of the offered method of regulating thermal rate of workings with preliminary heat moisture saturation is the following. The heating of the mine air while moving along the workings from air-feeding shaft to working faces and preparatory faces is known to be accompanied by intensive moistening of the mine air therefore the relative humidity in all workings raises, as a rule, up to 95-100%. As a result, only one third of the value of heat increasing of the mine air is connected with its heating, while two thirds of the whole value of heat increase of the mine air is caused by moistening.

Under the natural thermal conditions in mines and pits (Figures 1) in slope-bottom air feeding shaft (SAFS), there is a zone of relative low thermal potential of mine atmosphere (LTP), particularly: the temperature of the air is usually 5-15 °C under the humidity 95-100%.

The harmful heat inflows move to the air in main line workings ($Q_e = 30 - 50$ kJ / kg) and the moisture inflows move to the air ($m_e = 10 - 20$ g / kg), as far as there is a great thermal head and a head of the proportioned pressing between the air and surrounding coal massif.

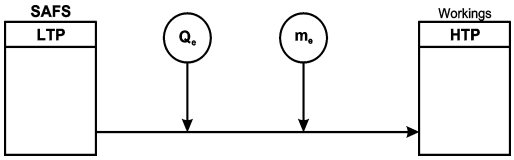

Figure 1. The scheme of the initial thermal potentials and inflows.

While getting saturated with heat and moisture in the main line workings, the air moves to the faces with inadmissibly high temperatures (35-40 °C) under the humidity 90-100%. As a result, a zone of high thermal moisture potential (HTP), unsuitable for safety and productivity of labour is formed.

The task is to reduce the harmful inflow of moisture to the air in the main line and field workings.

This effect can be achieved by "filling" that space in the air that will be taken by water vapour. It will be done with forced heating and moistening the air in the workings SAFS till the level that excludes the main part of moisture inflow to the air while moving to the working faces.

The technique solving this problem has been offered (Patent 53467, 2006). It is based on the forced reducing the temperature head and the head of the proportioned pressing of the water vapour between the mine air and surrounding coal massif, as well as the reducing the air temperature difference along the length of the working; as a result, the harmful inflows of heat and moisture will be reduced according to ventilation stream while moving from SAFS to faces.

To achieve this effect, one must remove the heat in quantity ΔQ out of the air which has reached the HTP zone (Figure 2) and transfer it to the LTP zone, filling the fresh ventilation stream with heat and moisture. The following results are to be achieved:

– the heat moisture potential of the HTP zone has been reduced and this space has been transformed into the space of RTP (reduced thermal potential), improving the microclimate of SAFS workings and faces;

– the heat moisture potential of the LTP zone has been increased and this zone is transformed into the ITP zone (increased thermal potential), improving the microclimate of SAFS workings;

– the temperature-moistening head between the mine air and surrounding coal massif in workings has been reduced, decreasing harmful inflows of heat ($Q_p \approx> 0$) and moisture ($m_p \approx> 0$) into the ventilation stream.

Thus, the positive effect of microclimate improvement in workings is to be achieved with heat massif exchange between the LTP and HTP zones.

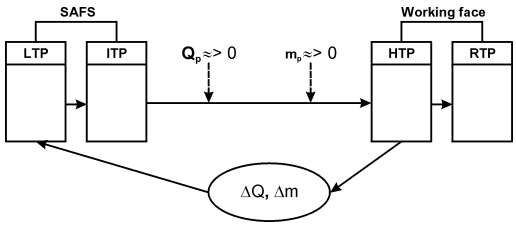

Figure 2. The scheme of exchanges of the heat potentials and inflows.

Figure 3 shows a quality temperature change of the mine air under the natural thermal mode (line *B*-*C*-C^I) and under the conditioning of the mine air with the method proposed (line $1-1^I-2-2^I-2^{II}$).

Point 1 (*B*) indicates the natural air temperature in workings of the slope bottom shaft before air-cooling. Point C characterizes the natural air temperature at the entrance of the mining, and the point C^I characterizes the natural air temperature at the exit of the faces.

The segment $1-1^I$ means the heating and moistening of the air in the air cooling in the slope-bottom workings. The segment 1^I-2 characterizes the air temperature change in main line workings under dispersal cooling.

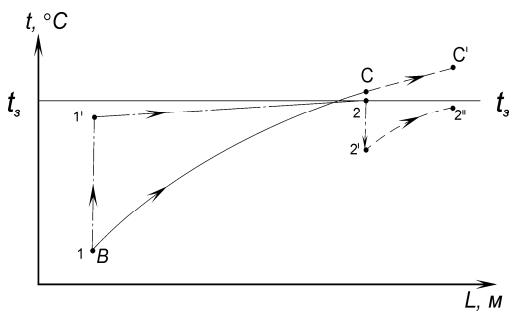

Figure 3. Qualitative change of mine air temperature.

Point 2 shows the air temperature in front of the air cooler. Point 2^I characterizes the temperature of conditioned air when leaving the air cooler. Tem-

perature difference between C and 2^{I} points indicates air cooling in mining fields workings of such type. Point 2^{II} indicates the temperature of conditioned air when leaving faces.

Under the natural thermal mode one can see intensive air temperature increase when it moves along workings from air feeding shaft to faces (*B-C-C*^{I} line) and provided the air is being conditioned according to the given method, air heating in main line workings occurs less intensive ($1^{I}-2$ line) than under the natural mode.

Due to the air preheating and humidification in a water cooler of evaporative type situated in slope bottom of air feeding shaft, there is certain decrease of the temperature head and the head of partial pressures of steam between ventilation stream and surrounding rock mass in workings which lead to mine sections. This results in reduction of heat and moisture inflow to the air mowing along workings.

Figure 4 shows the simplified scheme of a plant placement to control the heat mode in a sloping face of mine.

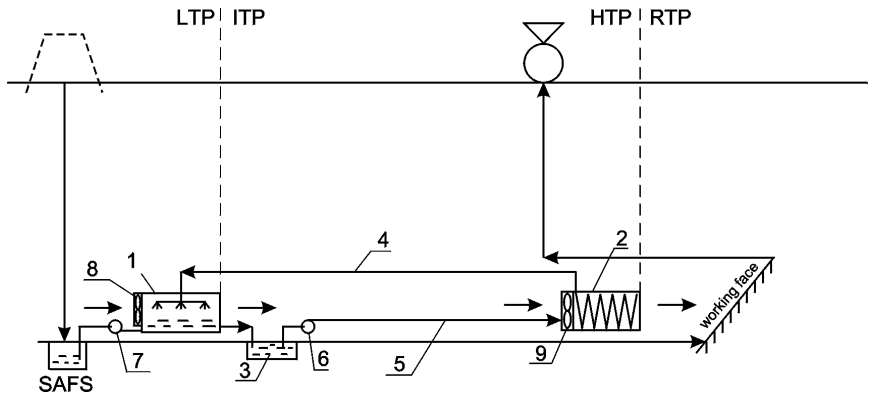

Figure 4. Simplified scheme of a plant placement in a mine.

The underground plant includes a hydraulically connected jet water cooler placed in the workings of pit-bottom (in the area of LTP) – 1, an air cooler of surface type – 2 situated near active working face (in the area of HTP), an accumulator of cooled water – 3 connected with the sump of air feeding shaft, circulating pipe-lines of heat-transfer agent – 4, 5 and pumps – 6, 7, fans – 8 and 9, and regulators of water and air consumption.

In water cooler 1two cross flows interact – the cold air and sprayed warm water – which results in the air being heated and moistened and water being cooled.

The cooled water from water cooler1 moves to the tank 3 (an accumulator of cooled water) then by means of pump 6 along pipe-line 5 it is fed into air cooler 2 where it is warmed due to the heat exchange with the air in the HTP zone. Cooled water from air cooler 2 along pipe-line 4 moves to water cooler 1 where it is cooled.

The cooled air leaving air cooler 1 is mixed with fresh ventilation flow, then it moves along main workings and gets into air cooler 2 where it is cooled and dried and after that moves to active working faces.

The plant provides continuous regulation of air heating and moistening dynamics in workings and faces within given limits without refrigerating machines. Due to this, costs as well as overheat and overcooling of miners reduce.

Cooling effect of the plant for mine air conditioning according to the given method is defined by two key factors:

– lower quantity of dangerous heat inflows and water steams to the ventilation stream from pit-bottom workings of air feeding shaft to the workings of mine sections;

– heat quantity carried from circulating water in the air cooler.

The overheating of miners occurs because heat production of their bodies is higher than emission of heat into the environment (cooling). It is known that human heat emission can be the result of convection, thermal radiation, moisture evaporation and conduction. This is convective heating of miners' bodies not cooling that occurs in high-temperature faces as the air temperature is higher than that of their skin. Radiant heat exchange of miners depends on the temperature and blackness degree of the surrounding surfaces, radiant flux geometry, skin temperature and external surface of working clothes. High radiating capacity of the working area is ex-

plained not only by high temperature and blackness degree of the surrounding surfaces, but also by the peak value of radiation angular coefficient as excavations are closed radiating systems. The heat radiation sources also include fresh rock and coal which have the temperature higher than the average temperature of the surrounding surfaces. As to the evaporation cooling of minors bodies, it is hampered because the air has a high saturation rate (about 90%) under these conditions, the sweat hardly evaporates but forms drops and a thin film which cover the skin and worsen convective heat exchange.

The analysis of possible heat exchange ways (heat production, convection, evaporation, radiation) does not provide the proper cooling of miners' bodies in high-temperature working faces which leads to the overheating and heat shock. Therefore it is necessary to look for the way out based on a partial (but acceptable) overheating of miners' bodies.

To cool miners in the development working faces from time to time, the *Relaxator* plant has been worked out (Patent 70653, 2007). The given technical solution can also be used to rescue workers overtaken by accidents in mine opening and having no possibility to go to the save zone, to protect mine workers temporarily and give the first aid.

The plant for protecting miners from overheating (Figure 5) includes: a screen in the form of a closed chamber – 1, an air quench system in the form of a perforated pipe – 2, a cold generator as a pneumatic turbine – 3 connected with a pipeline the external compressed air source, a catcher – 4 with a tray – 5 and an opening for the dried air exit – 6 which is connected with the wall passage and the chamber ceiling, and through them with the air quench system. In the front part of the chamber there are two openings for regulating condensate and discharge air emission. Moreover, the chamber has an independent compressed air source – 7, and the chamber itself is equipped with a hermetic door and is set on a chassis to make it possible to move. The chamber also has seats and sections for keeping insulating self-rescuer, respirators medical apparatus for providing the injured with the first aid.

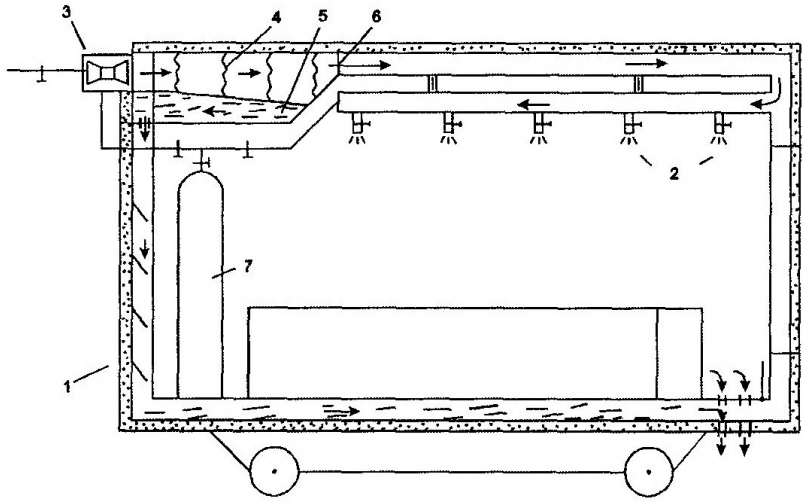

Figure 5. The *Relaxator* scheme.

The *Relaxator* works in the following way. The turbine 3 is connected to the pipe of the external source of the compressed air which enters the turbine through the high pressure pipeline. In the turbine 3 the compressed air dilates doing effective work of the wheel rotation. According to the first Thermodynamics Law, while advancing through the turbine the compressed air power budget decreases by the quantity of the work retracted from the turbine. This mechanical power is retracted from the turbine with the air flow in a different way. The decrease of the compressed air power budget is observed in its pressure and temperature decrease, relative humidity increase and condensation of part of steam. Moreover, the condensate is of a low temperature. The air used in the turbine 3 together with condensate drops goes to the catcher 4 where the condensate separates from the air. As a result, the air becomes dry saturated and through Exit 6 moves to the ceiling air passage and the chamber side walls while the condensate moves to the tray 5 of the catcher 4. While moving along the air passage the air cools the internal wall surface and

the chamber ceiling. At the same time the air is partly warmed while its relative humidity decreases considerably (down to 40-50% and lower). Therefore, the warm and dry air enters to the air quench system 2 and through the pipe branches it gets to the recreation area.

The condensate from the tray 5 of the catcher 4 gets to the back wall passage of the chamber. The turnback plates direct the condensate to the wall which is oriented to the middle of the chamber and is cooled by the condensate streaming down. After that the condensate gets to the floor passages, cools the floor and flows outside through the openings.

The auxiliary independent compressed air source 7 is used in the following cases: under absence or damage of the external source; under necessity of air consumption increase in the air quench system; while using the chamber as a shelter during accidents. For this purpose, the chamber has a section where extra self-rescuers are stored.

Therefore, the heat relaxation of mine workers in the chamber 1 is implemented in a complex way:

– by convection while blowing on the body with the air whose temperature is lower than the body surface temperature;

– by evaporating sweat form the external body surface and moisture from the respiratory tract internal surface while blowing on the body with dry air;

– by radiant heat exchange between the cold internal surface of the chamber and mineworkers' bodies (radiative cooling).

The use of all the main ways of the heat exchange of mineworkers' bodies in the *Relaxator* plant provides quick decrease of overheating, heat balance normalization which excludes heat shock risks, promotes the renewal of mineworkers' efficiency. Moreover, the *Relaxator* plant can provide efficient protection of mineworkers in case of emergency including high temperature protection during mine working fires.

The application of radiative cooling installations in high-temperature working faces allows decreasing the reduced radiant temperature by 10-15 °C and reduce mineworkers' radiant heating by 100-150 Watt. This radiative cooling effect can be compared to the convective cooling effect increase of the air flow provided the air is cooled down by 10-12 °C.

3 CONCLUSIONS

As for different mining conditions of deep mines the problem of thermal labour conditions normalizing in breakage and development faces must be solved in complex taking into consideration all means and components to improve microclimate. It will permit raising labour efficiency and reducing morbidity rate of miners.

The advantage of the method and mine air conditioning installation is absence of refrigerating machines and air conditioners using Freon. It increases safety of the plant, reduces costs connected with operation and service of underground devices, and simplifies considerably the servicing of the mine air conditioning plant. The method and plant for mine air conditioning provide the improvement of thermal labour conditions not only in workings and faces of mining sections but in pit-bottom workings where miners are always present.

The advantage of *Relaxator* plant is the ability to provide mineworkers' thermal relaxation in severe microclimatic conditions as well as efficient protection of mineworkers in case of emergency in production units including protection from the irrespirable atmosphere and heat shock protection.

REFERENCES

Valutsina, V.M., Tkachenko, L.N. & Ladariya, E.G. 2001. *The Frequency of thermal lesions of deep coal mine workers.* Journal of Hygiene and Epidemiology: Volume 5, #1: – 50-52.

Patent 53467 Ukraine, International Patent Classification 7 E21 F 3/00. *Mine air conditioning – the method and plant* / Muraveinik, V.I. Alekseenko, S.A., Shayhlislamova, I.A. and others; the patentee – the National Mining University. – #2002064680; applied 07.06.2002; published 15.12.2006, Bull. #12.

Patent 70653 Ukraine, International Patent Classification 2006 E21 F 3/00, E21 F 11/00. *Overheating protection installation* / Muraveinik, V.I., Alekseenko, S.A., Shayhlislamova ,I.A. & Korol, V.I.; the patentee – the National Mining University. – #20031211992; applied 22.12.2003; published 25.06.2007, Bull. #9.

Technical and Geoinformational Systems in Mining – Pivnyak, Bondarenko & Kovalevs'ka (eds)

Identifying method for abnormal values of methane release in mining level blocks

V. Okalelov, L. Podlipenskaya & Y. Bubunets
Donbass State Technical University, Alchevsk, Ukraine

ABSTRACT: We study the problem of identifying outliers in the time series of methane in the excavation sites of coal mines. The classification of outliers and methods for their diagnosis are designed. An algorithm that transforms a number of outliers in the modified series was described, which can be used to describe a longwall-analog and, accordingly, the forecast of methane release on a projected excavation area.

One of the most well-known in the theory and practice of various events forecasting is the analog approach. It is widely used in the prediction of methane release in the longwall. In this case we are talking about the forecast of only average values of methane release without regard to their pronounced dynamic character. In this connection there arose the necessity to improve existing methods of prediction to assess the dynamics of methane release in the longwall projected based on the data of longwall-analog (Okalelov 2008).

While solving this scientific and technical problem there arose the necessity to develop a method for analyzing time series of methane release in the active longwalls, aimed at establishing of causal relationships between forecasting performance and influencing factors (Podlipenskaya 2007).

The first stage of this analysis is to assess the reliability of the source data, which can be performed on the basis of a priori method comprising the following steps:

– assessment of the homogeneity of the study population;

– analysis of the distribution of the studied population characteristics;

– to identify logically significant causal relationships between the characters and phenomena.

Assessment of the homogeneity of the source data that characterize the dynamic process is recommended in the following sequence:

– identification and analysis of outliers;

– determination of the homogeneity degree of the totality by one or more essential characteristics;

– choosing the optimal selection variant of homogeneous populations.

In the statistical theory and practice there have been developed different approaches to assessing the degree of homogeneity (Sadovnikova 2007). The most difficult and controversial is the question of ways and criteria for the selection of homogeneous groups of objects within the original population.

Any researched population, along with the values of attributes, formed under the influence of factors directly characteristic of the object may contain attributes and values obtained under the influence of other factors that are not characteristic to the studied object. These values stand out sharply and, consequently, using this methodology of statistical analysis without studying these observations will result in serious errors.

Usually, outliers can be detected visually using a graphical representation of time series, but before you tweak the values found in this way, they should be subjected to quantitative and qualitative analysis.

Under the outliers of time series we understand the observation, which differs significantly from the rest of the observations set and localized in time (or other discrete variable number). We suggest classifying the outliers in relation to the symptoms associated with the processes of methane release at the excavation sites, operating at highly gas-bearing strata, as follows:

1) outliers of the first kind;
2) outliers of the second kind;
3) points of a structural shift.

The anomalous first-order (Figure 1) appears as a form of a strong change in the level indicator (jump or decline), followed by an approximate reconstruction of the previous level. Abnormality of this type is usually observed in a very narrow neighborhood of certain points of time axis.

At Figure 1, which characterizes methane release within a month in 17-th Orlovskaya longwall at "Molodogvardeiskaya" mine PC "Krasnodonugol", the outlier of the first kind can occur in the point which corresponds to the 8-th day.

Outlier of the second kind (Figure 2) is an atypical behavior of the indices at a visible interval of time axis.

At Figure 2, which characterizes methane release within 100 days the possible interval of outliers of the second kind is between 50-th and 60-th days.

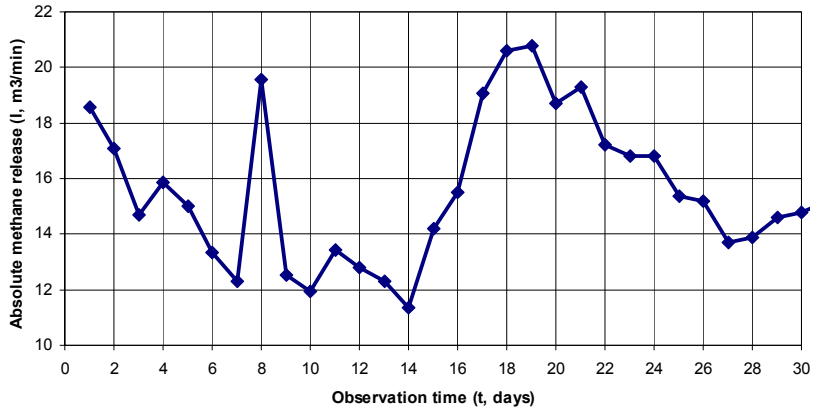

Figure 1. Methane release within a month in 17-th Orlovskaya longwall at "Molodogvardeiskaya" mine PC "Krasnodonugol".

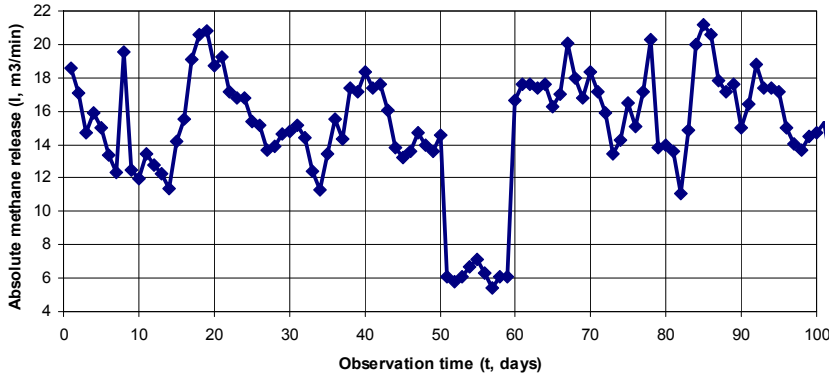

Figure 2. Methane release within 100 days in 17-th Orlovskaya longwall at "Molodogvardeiskaya" mine PC "Krasnodonugol".

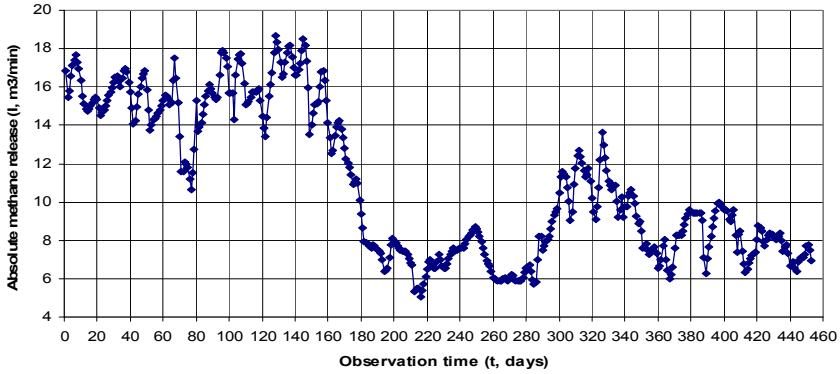

Figure 3. Methane release in 26-th Orlovskaya longwall at "Molodogvardeiskaya" mine PC "Krasnodonugol".

Points of the structural shift (Lukashin 2003) are those values of time series, in which there is an abrupt change in the behavior o whole time series. A similar case occurred in the 26th Orlovskaya longwall at "Molodogvardeiskaya" mine PC "Krasnodonugol" (Figure 3), where on the 162-th day of operation the ventilation scheme of excavation site has changed. Thus, $t = 162$ corresponds to the point of structural change.

Investigation of time series from the standpoint of causality shows that anomalously may be due to various reasons, which must be considered during accepting the decision on the rejection or correction of each individual outlier.

There are anomalous values, reflecting the objective process development, but very different from the general trend, as they show their extreme effects rarely. They do not always have to be excluded from the time series and may even be useful at the stage of studying the causal mechanism of the phenomenon. The presence of the peak values for the same time in different time series indicates, as a rule, the causal connection between the respective indices.

Some anomalous values appear due to single changes in the terms of the production process, such as changing the ventilation scheme. These values should not be excluded from consideration, and taken for "turning" (threshold) from which should be verified a mathematical model of time series for methane release. In the case of a single change of operational technological parameters it's rational to divide the original observations into several series.

Anomalous values arising from errors in measuring the indicator during recording and transmission the information, as well as the values associated with various catastrophic events do not influence the further course of events, the aggregation and disaggregation of indicators, etc., should be excluded from consideration anyway, as they distort the perception of the phenomenon nature and may have a significant impact on the conclusions obtained from analysis of a series containing such misrepresentations.

For the diagnosis of outliers of time series there were developed different criteria, for example, Irwin's method (Fedoseyev 1999). The idea of this method is that for all types or only for anticipated outliers value λ_t is calculated:

$$\lambda_t = \frac{y_t - y_{t-1}}{S_y}, \tag{1}$$

where y_t – current value of time series of methane release; y_{t-1} – previous value of time series of methane release; S_y – standard deviation of methane release.

$$S_y = \sqrt{\frac{\sum_{t=1}^{n}\left(y_t - \bar{y}\right)^2}{n-1}}. \tag{2}$$

$$\bar{y} = \frac{1}{n}\sum_{t=1}^{n} y_t. \tag{3}$$

If the module of calculated value λ_t exceeds the table level (Fedoseyev 1999), then level is considered abnormal and is replaced in the series by the appropriate calculated level.

In the introduced classification of types of anomaly time series values we propose a modification of the Irwin's criterion, which can be used both to diagnose outliers and identify the kind of anomaly.

Let the original dynamic range of indicators of methane excavation site is:

$$Y = \{y_1., y_2., \dots, y_{t-1}., y_t., y_{t+1}., \dots, y_n\}. \tag{4}$$

Let's consider an algorithm for recognizing outliers:

1. Calculation of numerical characteristics for the whole series on formulas (2-3).

2. Sequential computation of values, starting with $t > 2$:

$$\lambda_t = \frac{y_t - y_{t-1}}{S_y}. \tag{5}$$

3. Check a condition:

$$|\lambda_t| > \lambda_{kp}. \tag{6}$$

If condition (6) is not satisfied, then the point is not considered abnormal, and proceed to checking the next point (item 2).

If condition (6) holds, then the point y_t is declared abnormal, and proceeds to specify the kind of anomaly (item 4).

4. It is calculated $\lambda_{t+1} = \frac{y_{t+1} - y_t}{S_y}$ and also checked similar to (6) the condition:

$$|\lambda_{t+1}| > \lambda_{kp}. \tag{7}$$

If it holds, the composition is found:

$$\mu_t = \lambda_t \cdot \lambda_{t+1}. \tag{8}$$

Further variants are possible:

a) $\mu_t < 0$. Consequently, the point is anomalous

of the first order. It is taken away from a series, replacing by the arithmetic value of the close points. For more reliable replacement of anomalous value you can use more complex interpolation methods (Bahvalov 2007). Extracted anomalous point y_{t_k} together with its number t_k is put into the auxiliary unequidistant series of the first kind abnormal points $A_1 = \{y_{t_k}, k = 1, \ldots, m\}$, where m – the number of abnormal points of the first kind. Next, move to step 1, using the corrected value of the current point y_t.

b) $\mu_t > 0$. Hence, the point y_t may be anomalous of the second order, or is the beginning of a structural shift of the series. To determine the nature of the point go to the next item 5.

If condition (7) is not satisfied, then the conclusion is similar to case b) – the point y_t may be anomalous point of the second kind, or is the beginning of a structural shift of the series. Go to next item 5.

For convenience of presentation of test results on the anomaly, we introduce vector-indicator of outliers $\Psi = \{\psi_1., \psi_2., \psi_3\}$, whose components take values in a binary encoding 0 or 1 (Table 1).

Table 1. Values of vector-indicator of outliers.

Conditions	Values of indicators		ψ_t
	Condition is satisfied	Condition is not satisfied	
$\lvert\lambda_t\rvert > \lambda_{kp}$	1	0	ψ_1
$\lvert\lambda_{t+1}\rvert > \lambda_{kp}$	1	0	ψ_2
$\mu_t = \lambda_t \cdot \lambda_{t+1} < 0$	1	0	ψ_3

Then we can identify the points of the original series in the following combinations of indicators:

a) $\psi_t = \{0., \psi_2., \psi_3\}$ – means that the point is not anomalous (second and third components of the vector ψ_t can take values 0 or 1), in this case go to item 2 and check the next point;

b) $\psi_t = \{1., 1., 1\}$ – shows that the point is anomalous of the first kind;

c) indicators $\{1., 1., 0\}$, $\{1., 0, 1\}$, $\{1., 0., 0\}$ signal the possibility of appearing of the second kind anomaly or structural shift, then go to item 5.

5. Diagnosis of abnormality of the second kind, as well as a structural shift is performed online. Visualization of data in the form of the graphs allows you to check the hypothesis about the tested observation as the starting point of the anomalous data interval or the turning point to changing the structure of the series. Then, series is divided into specific intervals and through the variance analysis it is established a statistical difference between the intervals and the conclusion is made about the type of detected anomalies.

For further analysis if a point of structural shift is revealed the researches are made for each characteristic parts separately, but if there is an abnormality of the second kind, then to replace the outliers interval it is necessary to study the whole series (without anomalous points of the first kind), which will clarify the causes of the outliers interval, to establish the regularity of dynamic range in the absence of these causes and to make adequate replacement of points of anomalous interval.

Thus, we can conclude that the time series of methane release at the excavation site may contain outliers of various kinds. The proposed approach to identify the outliers in dynamic series describing the processes of methane release at the excavation site of a coal mine can be used to reconstruct the original series of methane release, and to establish cause-effect relationship between methane release and the influencing factors.

REFERENCES

Okalelov, V.N., Podlipenskaya, L.Ye., Bubunets, Y.V. & Dolgopyatenko, S.I. 2008. *Prognosis and control for dynamics of methane release in the breakage face*. Coal of Ukraine, 7: 21-24.

Podlipenskaya, L.Ye. & Bubunets, Y.V. 2007. *Dynamics investigation of methane release at the excavation site.* Alchevsk: DonSTU. Issue, 23: 56-66.

Sadovnikova, N.A.& Shmoilova, R.A. 2007. *Analysis of time series and prognosing.* Moscow: Issue 3: Studying-practical handbook. Publishing centre ЕАОИ: 272.

Lukashin, Yu. P. 2003. *Adaptive short-range forecasting methods of time series*. Moscow: Finances and Statistics: 416.

Fedoseyev, V.V., Garmash, A.N., Daiyitbegov, D.M., Orlova, I.V. & Polovnikov V.A. 1999. *Economic-mathematical methods and applied models.* Moscow: studying handbook for universities. UNITY: 391.

Bahvalov, N.S., Zhydkov, N.P. & Kobelkov, G.M. 2007. *Numeric methods. Moscow: studying handbook for students of phys.-math.* Specialized universities – 5-th edition. BIMOM. Knowledge laboratory: 637.

Technical and Geoinformational Systems in Mining – Pivnyak, Bondarenko & Kovalevs'ka (eds)

Research of dynamic processes in the deep-water pumping hydrohoists lifting two-phase fluid

Y. Kyrychenko, V. Kyrychenko & A. Romanyukov
National Mining University, Dnipropetrovs'k, Ukraine

ABSTRACT: A comprehensive methodology for the calculation of dynamics of the two-phase flows has been first developed. The methodology allows studying the whole spectrum of transient processes in the deep-water pump-based installations and provides the precision level needed for this class of problems. On the basis of the developed methodology a special HydroWorks 2p software is developed, allowing to define the parameters of transient processes in the deep-water pumping installations. Using the software it is defined that pressure oscillations and ensuing dynamic stresses often reach critical values, which may pose a risk in terms of efficiency of installation and violation of its integrity.

1 INTRODUCTION

Nowadays in Ukraine there is a shortage of some strategic non-ferrous metals extracted from the continental deposits in traditional way. In this regard, the further growth of mineral resources base in Ukraine is closely linked with the development of ore deposits of the World Ocean.

One of the most promising methods of transportation of solid minerals from the seabed is a pump-based hydrohoist (Fox 1981).

Decision of the of National Security and Defense Council on May 16, 2008 "On measures to ensure Ukraine's development as a maritime state" powered by Presidential Decree № 463/2008 of 20 May 2008, provides for the development of a new "National Programme for research and use of Azov-Black Sea and other regions' of the oceans resources in the years 2009-2034". Thus, development of technical means of lifting minerals from the seabed is one of the priority areas of research. This article focuses on the urgent problem of development of mineral potential of the World Ocean, the solution of which is directly linked to the development of effective methods of regulation and management of deep-water pump-based hydrohoists.

The lifting process of mineral raw materials on a basic watercraft associates with the solution of tasks of calculating the dynamics of two-phase (water and solids) flow, which is due to many transient processes accompanying the work of the pumping unit. Deep-water pumping hydrohoists (DPH) usually operate in non-stationary or quasi-stationary modes because of the long hydraulic paths and specific exploitation characteristics.

The existing methods of calculating the DPH mostly base on the idea of the mixture as a homogeneous fluid (Nigmatulin 1987). The authors of these methods tend to focus on the problems of water hammer giving the solid particles in the flow a passive role which means only increasing the density of the mixture (Kartvelishvili 1979; Makharadze 1986; Wallace 1972; Kyrychenko, Romanyukov, Tatur-evich 2009). This approach allows using simplified mathematical apparatus, based on the homogeneous model (Wallace 1972; Charny 1975) for calculations, which significantly reduces the accuracy of the results, because water and solid particles have different inertial properties. Obviously, such methods with acceptable for engineering calculations accuracy allow calculating the ground hydrotransport, which can be designed with appropriate safety margin. However, according to the authors of this paper, this approach is hardly acceptable for the calculation of such unique engineering facilities like DPH, because it does not take into account the specifics of marine mining equipment exploitation in difficult conditions of great depths.

The pipeline of DPH is the backbone of the entire subsea equipment. Because of the great length, mass and overall dimensions the pipeline is characterized by dangerous static longitudinal stresses (Kyrychenko 2001). When the carrier vessel moves, the pipeline takes a curved shape experiencing dynamic loads, caused by pitching, as well as various kinds of aerohydroelastic instability of the marine environment (aeolian vibration, galloping, flutter). It is also possible loss of the divergent stability of the pipeline and occurrence of parametric resonance due to interaction with the stationary and pulsating flow

of transported fluid. In addition, the processes associated with starting and stopping of pumping units in case of wrong management may be accompanied by the phenomenon of water hammer. These factors will inevitably give rise to additional dynamic stresses that may impair the integrity of the system.

Thus, one of the limiting factors of deep-water hydrohoists development is the lack of effective controlling systems, preventing of the abovementioned harmful effects. The development of such systems, in turn, is restrained by the lack of research results of unsteady modes and dynamic processes in the deep-water hydrohoists, as well as the mathematical description of the transitional processes and the lack of sufficiently accurate and physically grounded method for calculating the parameters of DPH and its software implementation. The controlling system must be capable of fast "tuning" of the current parameters in conditions of multivariate disturbing influences, which means to possess sufficient efficiency and performance.

Based on the above mentioned features, method of calculation of DPH must meet the following requirements:

– high accuracy due to the lack of safety margin;

– high integrity and efficiency, which means the possibility of studying the entire spectrum of nonstationary and transient processes in frames of a single mathematical apparatus, based on the differential equations of the same type;

Earlier the correct calculation of dynamic processes in hydrotransportation systems, pumping heterogeneous mixtures, was not possible mainly due to lack of adequate, physically grounded mathematical model, which would most fully take into account the specifics of deep-water hydraulics and all range of dynamic effects. Another reason is absence of the law of the speed of sound change in two-phase slurry (Wud 1934).

However, the authors of this paper have managed to obtain such mathematical model of two-phase fluid motion (Goman, Kyrychenko, Kyrychenko, 2008), the characteristic relations for it (Kyrychenko, Shvorak, Kyrychenko, Romanyukov, Taturevich 2011), and the speed of sound change laws (Goman, Kyrychenko, Kyrychenko 2008; Kyrychenko 2009). From now on, the possibility of developing an integrated method of calculating the dynamics of heterogeneous flows has been opened. This method will automatically provide the possibility of calculating the parameters of the full range of dynamic processes in the DPH from slow concentration waves that accompany the processes associated with the launch of the system to fast transients in different emergency situations.

2 FORMULATING THE PROBLEM

The aim of this paper is to develop a method for calculating the dynamics of two-phase flows in the pipelines of deep-water pumping systems for the study of nonstationary and transient processes.

Let us briefly discuss the main components of the methodology. In (Goman, Kyrychenko, Kyrychenko 2008) the flow of liquid and solid particles is reviewed. In the one-dimensional approximation, the equations describing the motion of two-phase flow obtained in (Goman, Kyrychenko, Kyrychenko 2008) look like:

$$(1-C_1)\frac{\partial p}{\partial t}-\rho_0 a_0^2\frac{\partial C_1}{\partial t}+\rho_0 a_0^2(1-C_1)\frac{\partial V_0}{\partial x}=0, \quad (1)$$

$$C_1\frac{\partial p}{\partial t}+\rho_1 a_1^2\frac{\partial C_1}{\partial t}+\rho_1 a_1^2 C_1\frac{\partial V_1}{\partial x}=0, \quad (2)$$

$$\left(1+\frac{C_1 k_1}{2}\right)\frac{\partial V_0}{\partial t}-\frac{C_1 k_1}{2}\frac{\partial V_1}{\partial t}+\frac{(1-C_1)}{\rho_0}\frac{\partial p}{\partial x}=\phi_0, \quad (3)$$

$$\left(\frac{\rho_1}{\rho_0}+\frac{k_1}{2}\right)\frac{\partial V_1}{\partial t}-\left(1+\frac{k_1}{2}\right)\frac{\partial V_0}{\partial t}+\frac{1}{\rho_0}\frac{\partial p}{\partial x}=\phi_1, \quad (4)$$

where

$$\phi_0=-(1-C_1)g\sin\alpha-\frac{\lambda}{2D}\frac{\rho_{mix}}{\rho_0}|V_{mix}|V_{mix}-$$

$$-\frac{3}{8}\left[\frac{C_1 C_{xs}}{R_1}|V_0-V_1|(V_0-V_1)\right],$$

$$\phi_1=-\frac{\rho_1}{\rho_0}g\sin\alpha+\frac{3}{8}\frac{C_{xs}}{R_1}|V_0-V_1|(V_0-V_1),$$

$$\frac{1}{a_1^2}=\frac{\rho_1}{K_1}+\frac{\rho_1}{F}\left(\frac{\partial F}{\partial p}\right),$$

$$\frac{1}{a_0^2}=\frac{1}{a_l^2}+\frac{\rho_0}{F}\left(\frac{\partial F}{\partial p}\right),\ a_l^2=\frac{K_l}{\rho_0},$$

$$K_1=\frac{E_1}{3(1-2\nu_1)},$$

$$\rho_{mix}=\rho_0^*+\rho_1^*=(1-C_1)\rho_0+C_1\rho_1,$$

$$V_{mix}=\frac{1}{\rho_{mix}}\left(\rho_0^* V_0+\rho_1^* V_1\right).$$

K_1, E_1, ν_1 – bulk modulus of elasticity, Young modulus and Poisson ratio of solid particles correspondingly; K_l – compression modulus of liquid;

a_l – sound velocity in pure unbounded liquid; R_1 – equivalent radius of solid particles; k_1 – a coefficient, which describes how virtual masses are affected by nonsphericity and concentration of solid particles; g – gravitational acceleration; α – pipeline canting angle; D – pipeline diameter; λ – Darcy coefficient; t – time; C_{xs} – solid particles resistance coefficient; C_i – phase bulk volume; p – pressure; ρ_i – phase real density; ρ_i^* – phase reduced density; V_i – phase velocity; x – longitudinal coordinate; sub-indices mean: "0" –water; "1" – solid particles; "m" – mixture.

It should be noted, that derivative of concentration C_1 enters only into continuity equations (1) and (2). Hence if we expresses the derivative $\frac{\partial C_1}{\partial t}$ from equation (2) and substitute it into equation (1), we get general continuity equation:

$$\rho_0 a_0^2 (1-C_1)\frac{\partial V_0}{\partial x} + \rho_0 a_0^2 C_1 \frac{\partial V_1}{\partial x} + \\ + \left[(1-C_1) + \frac{\rho_0 a_0^2 C_1}{\rho_1 a_1^2} \right] \frac{\partial p}{\partial t} = 0. \qquad (5)$$

Now the set of equations (1)-(4) can be divided into two subsets: first subset includes equations (3)-(5) and contains only V_0, V_1 and p derivatives, while derivative of concentration C_1 is absent. Second subset includes equation (2), contains C_1 time derivative and is connected with the first subset via derivatives of p and V_1. At the same time, first subset is connected with the second one only via concentration C_1 (but not via its derivative). Concentration enters into first subset both as a coefficient and implicitly through ϕ_0 and ϕ_1 variables.

Perturbation velocity in mixture and characteristic relations on the mach front can be derived from the first subset (3)-(5). Equation (2) is in fact an ordinary differential equation for calculating changes of concentration C_1 with time in every fixed point of pipeline (x) assuming that V_0, V_1 and p are already defined as functions of x in every time layer t.

If the transported liquid contains plenty of solid particles (pulp movement), wave movement in the pipeline has some peculiarities, caused by compressibility of solid particles, relative slip between solid and liquid phases (which is present in general case), different inertia of solid substance and transporting liquid etc.

We have to note, that the most complete expression for sound velocity in two-phase mixture D_0 is below:

$$D_0 = \frac{1}{\sqrt{\rho_y \left(\frac{(1-C_1)}{K_0} + \frac{C_1}{K_1} + \frac{1}{F}\frac{\partial F}{\partial p} \right)}}, \qquad (6)$$

where

$$\rho_y = \mu \cdot \rho_0, \quad \mu = \frac{A}{B},$$

$$A = \frac{\rho_1}{\rho_0}\left(1 + \frac{C_1 k_1}{2}\right) + \frac{k_1}{2}(1-C_1),$$

$$B = \frac{\rho_1}{\rho_0}(1-C_1)^2 + (2-C_1)C_1 + \frac{k_1}{2}.$$

Figure 1 shows the dependence of sound velocity on real bulk concentration of solid particles in slurry (hereinafter called slurry buld concentration) for various wave numbers of pipeline and spherical solid particles densities with diameter of 0.005 m. Comparing the depicted curves one can see that behavior of curves has little dependence on density of solid substance.

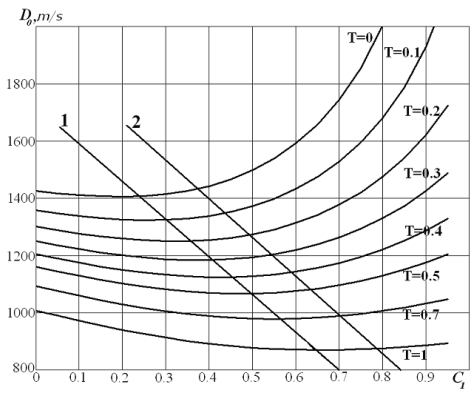

Figure 1. The dependence of perturbation velocity on concentration of solid substance in slurry at various pipeline parameters. ($C_2 = 0$; $\rho_1 = 1600$ kg / m^3; $K_1 = 4.5 \cdot 10^{10}$).

Analyzing mentioned relations several conclusions can be drawn. Sound velocity in slurry in general case depends on parameters of both slurry and pipeline. The competing influence of pulp and pipeline parameters defines three specific regions on the plot.

First region is located to the left from line 1 (Figure 1) $D_0 = -2124.7C_1 + 1630$ and corresponds to descending behavior of curves with increasing concentration of solid substance. This happens because increase of solid particles effective volume compressibility is outrunned by growth of pulp density.

The second region is located between the first line and the second line, defined by $D_0 = -2101.8C_1 + 1870$. Second region corresponds to quasi-constant speed velocity at fixed pipeline wave number. In the given range of solid substance concentrations, which is limited by lines 1 and 2, the slurry density is proportional to its volume compressibility. In this region sound velocity depends on pipeline wave number only. Such behavior significantly simplifies calculations, necessary for engineering methodology design. The first approximation of speed velocity is the following:

$$D_0 = -575T + 1415,$$

where $T = \frac{K_0 D}{E\delta}$ – pipeline wave number, δ – pipe wall thickness.

Third region is located to the right from line 2 and corresponds to ascending behavior of curves due to overrunning growth of effective volume compressibility of slurry comparing to increase of its density.

From Figure 2 one can conclude that decreasing of solid substance density leads to growth of speed of sound, if other factors are equal.

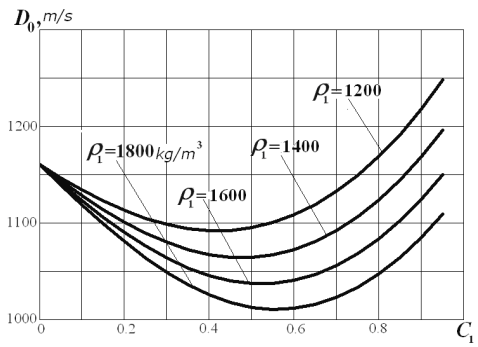

Figure 2. The dependence of sound velocity on solid substance concentration for various values of solid substance density ($C_2 = 0$; $T = 0.5077$; $K_1 = 4.5 \cdot 10^{10}$).

The obtained results lead us to reconsidering of a stereotypic statement, which claims that presence of solid substance in transporting liquid results in growth of sound velocity (Kyrychenko 2009).

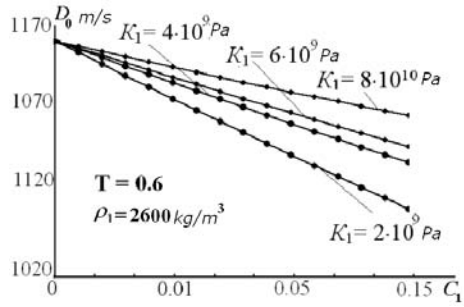

Figure 3. The dependence of sound velocity on solid substance concentration for various values of solid particles volume compressibility ($C_2 = 0$; $T = 0.5077$; $\rho_1 = 1600$ kg / m^3).

Speed of sound is also affected by volume compressibility of solid particles K_1 (Figure 3): higher volume compressibility leads to growth of sound velocity, if other factors are equal.

3 CHARACTERISTIC RELATIONS

Paper (Kyrychenko, Shvorak, Kyrychenko, Romanyukov, Taturevich 2011) shows, that for system (1)-(4) characteristic relations are fulfilled on the set of three characteristics:

$$dp + \mu\rho_0 D_0\left[(1-C_1)dV_0 + C_1 dV_1\right] - \\ - \frac{\mu\rho_0 D_0}{A}\psi dt = 0. \qquad (7)$$

$$-dp + \mu\rho_0 D_0\left[(1-C_1)dV_0 + C_1 dV_1\right] - \\ - \frac{\mu\rho_0 D_0}{A}\psi dt = 0. \qquad (8)$$

for following acoustic characteristics

$$\left(\frac{dx}{dt}\right)_1 = D_1 = D_0, \qquad (9)$$

$$\left(\frac{dx}{dt}\right)_2 = D_2 = -D_0. \qquad (10)$$

and $\left[(1-C_1)\left(1+\frac{k_1}{2}\right)+1+\frac{C_1 k_1}{2}\right]dV_0 -$

$$-\left[(1-C_1)\left(\frac{\rho_1}{\rho_0}+\frac{k_1}{2}\right)+\frac{C_1 k_1}{2}\right]dV_1 - \Omega_1 dt = 0, \qquad (11)$$

for characteristics like

$$D = 0, \qquad (12)$$

where

$D = x'(t)$ – mach front propagation velocity,

$$\psi = \varphi_l g \sin\alpha - \frac{\lambda \rho_{mix} |V_{mix}| V_{mix}}{2D\rho_0} \varphi_p +$$

$$+ \frac{3}{8} \frac{C_{xs}}{R_1} |V_0 - V_1| (V_0 - V_1) \varphi_1,$$

$$\varphi_l = -(1 - C_1)\varphi_p - C_1 \frac{\rho_1}{\rho_0} \left(1 + \frac{k_1}{2}\right),$$

$$\varphi_p = (1 - C_1)\frac{\rho_1}{\rho_0} + C_1 + \frac{k_1}{2},$$

$$\varphi_1 = C_1 (1 - C_1) \left(1 - \frac{\rho_1}{\rho_0}\right),$$

$$\Omega_1 = (1 - C_1) \left(\frac{\rho_1}{\rho_0} - 1\right) g \sin\alpha -$$

$$- \frac{\lambda \rho_{mix} |V_{mix}| V_{mix}}{2D_p \rho_0} - \frac{3}{8} \frac{C_{xs}}{R_1} |V_0 - V_1| (V_0 - V_1).$$

It has to be emphasized, that characteristic relations (7), (8) on acoustic characteristics represent relations between total differentials of p, V_0 and V_1 functions along these characteristics, but does not include differential of concentration C_1.

Characteristic condition (11) is fulfilled along $x = const$ lines, so differentials dV_0 and dV_1, which enter the expression, stand for increment of corresponding functions with time at every fixed section of pipeline.

It should be noted, that characteristic relation (11) does not contain differentials of concentration C_1.

Thereby in general case of liquid mixed with solid dispersed phase there are three families of characteristics, and along each of them a specific relation between the total differentials of unknown functions dp, dV_0 and dV_1 is fulfilled.

Concentration differential dC_1 does not enter into these characteristic relations. Concentration C_1 is to be obtained by solving differential equation (2), which is in fact an ordinary differential equation with respect to $\frac{\partial C_1}{\partial t}$. It allows us to use numerical integration using finite-difference schemes.

The obtained characteristic relations can be used as a basis for numerical calculation of non-stationary characteristic of hydromixture using integrated methodology, which represents a combination of characteristics technique for hydrodynamic parameters p, V_0 and V_1 and finite-difference technique for calculating the concentration C_1.

4 METHODOLOGY

Using the above results, let us construct a comprehensive methodology for calculating the dynamics of two-phase flows.

1. Specifying the initial data. In order to calculate the transients in the hydraulic system the following data is used:

– a scheme of hydraulic system (lengths of separate sections and sizes of pipelines; marks of the height of their docking sections; tilting angle of each section; location of major units and valvings of the system (pumps, check valves, gate valves, etc.), system performance, concentration of solid phase and its grain composition, marks of the receiving end output sections of the system);

– data of hydraulic calculation of the stationary mode (flow/pressure characteristics of pumps, their operating points; hydraulic slopes of pipes and pressure distribution throughout the system in stationary mode; operational velocities of components of the slurry; the coefficients of hydraulic and the coefficients of local losses in valvings, etc.

These hydraulic data serves as initial data for calculating non-stationary processes and the phenomena of water hammer in the hydraulic system, resulting from the abrupt change in mode of operation of one or more units or elements of the valve system (de-energizing of the pump or alarm failure, sudden complete or partial overlap of the valves; routine or emergency operation of check valves.

2. Calculation of unsteady hydraulic parameters begins with the partition of the entire pipeline to a finite number of computational elements of a length Δli, the ends of which Ai are reference points for determining the hydrodynamic parameters, and each unit of the hydraulic system is considered as a separate "zero" element, which has zero length, but has its own "input" Ak and "output" Ak +1 (Figure 4).

All the initial parameters of the slurry are determined at all points of Ai at time t0, at which the non-stationary process, which is to be calculated, arises. It is assumed that for each "zero" element (pumps, locking devices and other valvings) hydraulic law of this element (finite or differential equation defining the relationship between differential pressure upstream and downstream of this element and a flow rate of the mixture) is known.

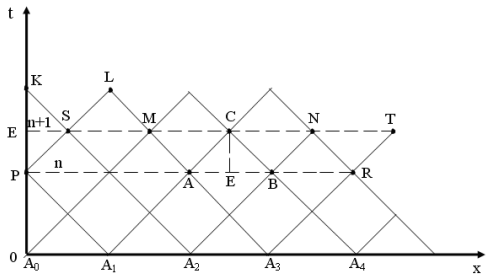

Figure 4. Scheme for using the combined method of characteristics for definition of the unsteady parameters of the slurry.

3. Calculation of unsteady hydraulic parameters goes as follows.

3.1. Determination of the initial distribution of pressure P_0, velocities V_0, V_1 and concentration of the solid particles C_1 in all the nodes $A_i^0\ \left(x_i^0, t=0\right)$.

3.2. Coordinates of the points A_i^1 of the new time layer, and new points of observation (x_i^1, t_i^1) are determined from the simultaneous solution of algebraic equations of the characteristics derived from equations (9), (10) by replacing the differentials by finite-difference relations.

$$x - x_A = \left(D_0\right)_A \left(t - t_A\right), \tag{13}$$

$$x - x_B = -\left(D_0\right)_B \left(t - t_B\right). \tag{14}$$

The coordinates x_i^1 for all zero elements remain the same. As for the distributed elements, the coordinates of the points of observation x_i^1 vary.

3.3. Calculation of pressure P and velocity of the carrier liquid V_0 and solids V_1 at the new time layer at all internal nodes A_i^1 is carried out by solving algebraic equations

$$p_C - p_A + \left(a_{00}\right)_A \left(V_{0C} - V_{0A}\right) +$$

$$+\left(a_{01}\right)_A \left(V_{1C} - V_{1A}\right) = \left(b_0\right)_A \left(t_C - t_A\right), \tag{15}$$

$$-\left(p_C - p_B\right) + \left(a_{00}\right)_B \left(V_{0C} - V_{0B}\right) +$$

$$\left(a_{01}\right)_B \left(V_{1C} - V_{1B}\right) = \left(b_0\right)_B \left(t_C - t_B\right), \tag{16}$$

$$\left(a_{10}\right)_E \left(V_{0C} - V_{0E}\right) +$$

$$+\left(a_{11}\right)_E \left(V_{1C} - V_{1E}\right) = \left(b_1\right)_E \left(t_C - t_E\right), \tag{17}$$

obtained by replacing the differentials by finite-difference relations in the equations of characteristics (7) (8) and (11). Here, the coefficients a_{ij} and b_i are determined by comparing equations (15)-(17) with equations (7), (8) and (11), respectively.

The concentration of solid phase is calculated using equation (2)

$$\left(C_1\right)_C = \left[\left(C_1\right)_E 1 - \left(\frac{1}{\rho_1 a_1^2}\left(\frac{\partial p}{\partial t}\right)_C + \right.\right.$$

$$\left.\left. + \left(\frac{\partial V_1}{\partial x}\right)_C\right)\left(t_C - t_E\right)\right], \tag{18}$$

where C_{1E} – expressed by interpolating the neighboring nodes A and B, and the derivative $\left(\frac{\partial V_1}{\partial x}\right)_C$ is determined using the values of V at the nodes adjacent to node C, using information from the previous calculation step. The velocity of disturbances propagation (the speed of the shock wave) D is calculated via the formula (6).

3.4. Calculation of hydrodynamic parameters in the boundary nodes (input and output section) as well as "zero" elements is based on the same equations (7), (8), (11) and (18) with appropriate boundary conditions or hydraulic law of each individual element.

3.5. The calculation of each new time layer is carried out by repeating the procedure described in item 3.3-3.4.

5 METHODOLOGY APPROBATION

Numerical experiment. Based on the stated methodology program complex HydroWorks 2p, intended for calculation of dynamics of two-phase flows, is developed. The complex is compatible to CAD-platform SolidWorks 2010/2011 and supports operating systems Windows Vista (x32, x64) and Windows 7 (x32, x64). User is offered two versions of installation package: add-in for SolidWorks and stand-alone application, allowing to work without SolidWorks installed. Application consists of the following units:

– The calculation dll unit, implementing the methodology. The library has an open API interface and can be integrated into other CAD/CAE-systems.

– Dll unit integrated into SolidWorks environment.

– Executable Windows application (.exe).

– Visualizer (dll). Forms reports, displays diagrams and tables.

Among the main functional capabilities, it is possible to select:

– construction of complex parametric pipeline systems;

– complete integration to SolidWorks;

– saving results in external formats (excel, word, txt).

Using the developed software, many numerical experiments have been conducted and the distribution of pressure, velocity and concentration for dynamic tasks in different statements obtained. As an example of the developed methodology usage, we present only the most typical results for the determination of the amplitudes of pressure waves in the pipeline of DPH. One embodiment of such hydrohoist DPH equipped with three electric submersible pumps H1-H3 (Figure 5).

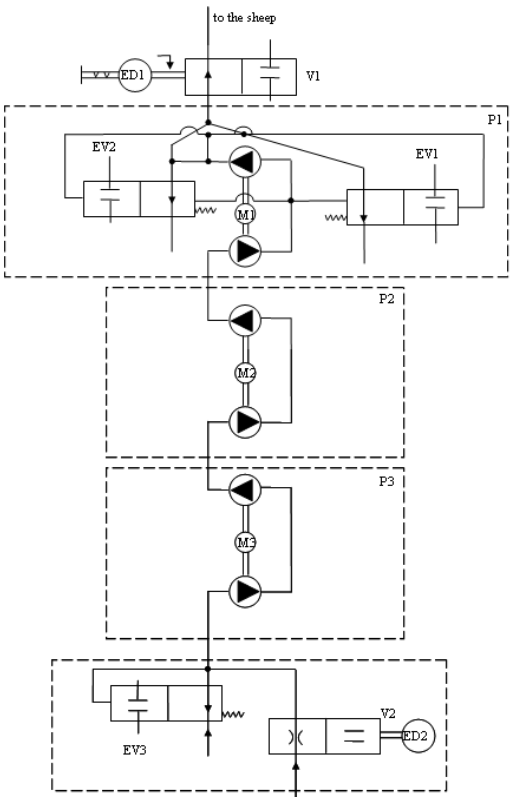

Figure 5. Hydraulic circuit of DPH.

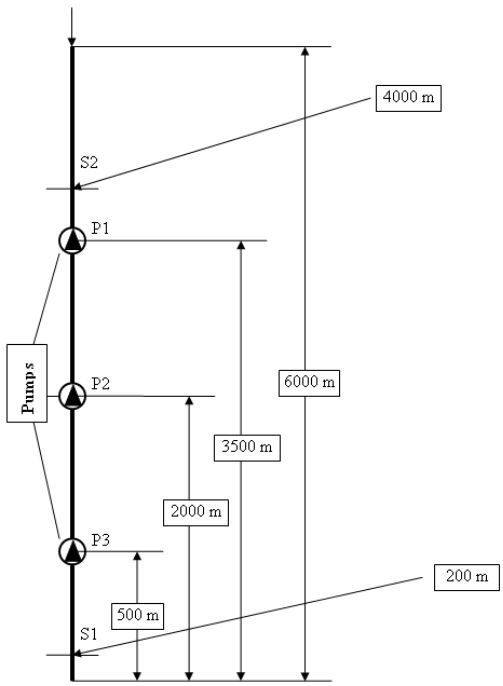

Figure 6. Arrangement of pumping units of DPH.

Slurry submission is conducted from depth of 6000 m. Pumps N1-N3 are installed sequentially in distances of 3500 m, 2000 m and 500 m from a seabottom accordingly (Figure 6) at the closed valves of emergency slurry escape (KAC1-KAC3) and open valves (KIII1, KIII2). Regulation of valves KSH1 and KIII2 is carried out by means of electric drives MSH1 and MIII2. Electric drives of pumping aggregates M1-M3 have possibility of regulation by means of the frequency shifter. It is admitted as well direct switching-on of electric drives in a vessel's network.

Valves of emergency slurry escape KAC1-KAC3 are installed parallel to pipeline.

Let us consider the routine sequential start of pumping units lifting up the water. This launch includes a step-by-step switching-on of the pumps, one after another, with some specified interval of time when filling out a pipeline with a homogeneous liquid.

For the first numerical experiment, step-by-step start-up of pumping units from H3 to H1 has been selected with the 5 seconds interval between launches. Alternative of step-by-step start-up of pumping aggregates is volley start-up when the power is simultaneously applied to all pumps. Re-

search was led taking into account connection of engines of all pumps to the frequency shifters, thus acceleration of shafts of the pumps till the rated speed in both cases happens in 5 seconds.

As control sections for research of dynamic parameters of DPH sections S1 (200 m) and S2 (4000) have been selected.

On Figure 7 diagrams of dependence between pressure of a slurry and time in section S1 are shown at volley and step-by-step start-up of pumping units under the conditions described above.

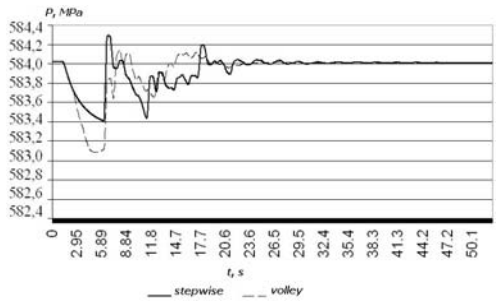

Figure 7. Dependence between pressure (P, MPa) and time (t, s) at stepwise and volley start of pumping units lifting up water in the section S1.

As seen from Figure 7, the amplitude of pressure fluctuations at step-by-step start of pumping units in the cross section S1 is very different from the same amplitude for the volley launch. The data obtained show that the maximum amplitude of pressure fluctuations for volley launch is observed at the first peak of oscillations and is equal to $9.17 \cdot 10^4$ Pa.

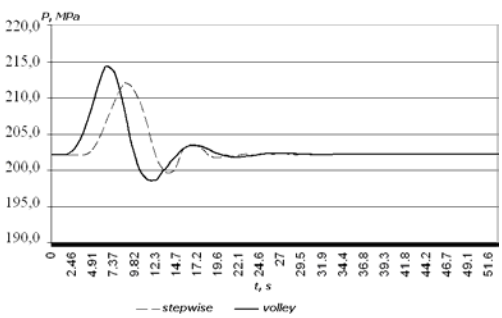

Figure 8. Dependence between pressure (P, MPa) and time (t, s) at stepwise and volley start-up of pumping aggregates lifting water in section S2.

For sequential start such maximum is much smaller ($6.08 \cdot 10^4$ Pa) and is observed in the first and the third peaks of pressure fluctuations due to the non-simultaneous occurrence of pressure waves in the pipeline and their subsequent superposition. The difference between the maximum deviations from the hydrostatic pressure in the cross section S1 for the volley and step-by-step launches is $3.09 \cdot 10^4$ Pa.

Figure 8 shows the dependence plots between the pressure of the slurry and time in the cross section S2 for the case of stepwise and volley run of the pumps.

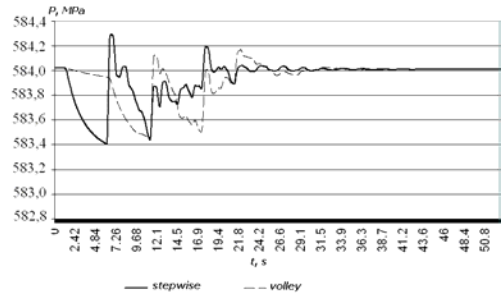

Figure 9. Dependence between pressure (P, MPa) and time (t, s) at stepwise start-up of pumping aggregates lifting water in section S1 with/without delay

Results of numerical experiment show that the maximum amplitude of pressure fluctuations of slurry for volley launch is observed at the first peak of oscillation and is $21.17 \cdot 10^5$ Pa and at stepwise start – $9.83 \cdot 10^5$ Pa, and also corresponds to the first peak of oscillations. At stepwise start of pumping units, system comes to its stationary mode more mildly, but at such start, it makes sense to delay acceleration time of the first pump's shaft to the rated speed to avoid high load on it at start-up (Figure 9, 10).

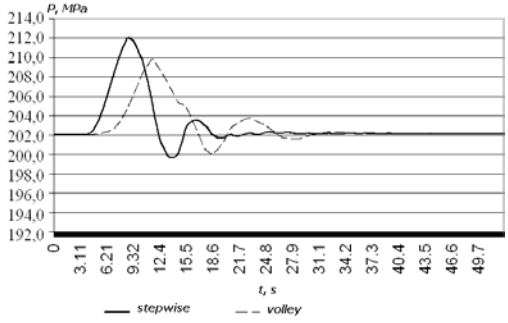

Figure 10. Dependence between pressure (P, MPa) and time (t, s) at stepwise start-up of pumping aggregates lifting water in section S2 with/without delay.

As seen from the numerical experiments, increasing the acceleration time of the pump has reduced

the pressure at the peaks of up to $5.58 \cdot 10^4$ Pa and $7.55 \cdot 10^5$ Pa in sections S1 and S2 respectively.

Of particular interest is the emergency shutdown of the system, when one or more of the pumps breaks down and abruptly closes section of the pipeline by its impeller. Typical feature of this transitional process is that at the time of the stop the pipeline is filled with liquid and solid particles and water hammer occurs in two-phase mixture (Figure 11, 12, 13).

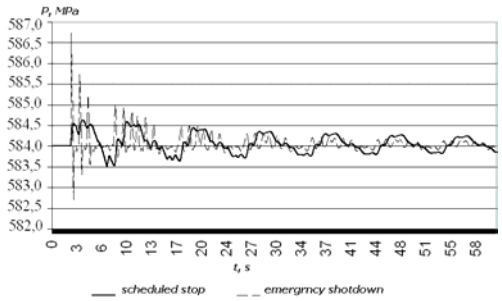

Figure 11. Dependence between pressure (P, MPa) and time (t, s) at an emergency shutdown of pumping units in section S1.

Figure 12 and 13 shows the transients at a scheduled stop of the system starting from the pump unit H1and ending with unit H3, and vice versa with the interval between power off pumps in 20 seconds in cross sections S1 and S3, respectively.

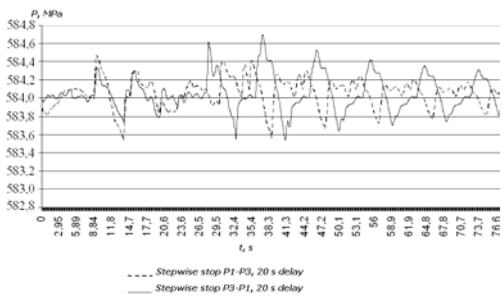

Figure 12. Dependence between pressure (P, MPa) and time (t, s) at a routine stop of pumping units in cross section S1.

In case of an emergency stop of the system, peak values of pressure several times exceed the corresponding values for routine stop. This can cause damage to both pumping units, and the pipeline with poorly predictable consequences. In case of a routine stop, the Figures 12 and 13 show that pressure oscillation amplitude at "bottom-up" algorithm of the pumps' stop is always much lower than the corresponding amplitude at "top down" case, which allows selecting the correct scheme of pumps' shutdown.

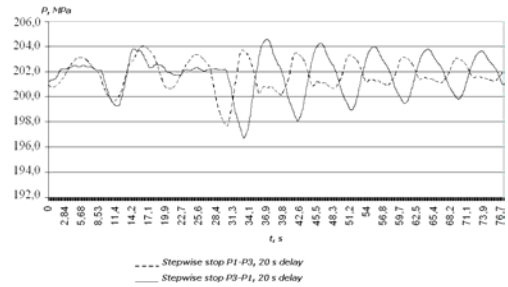

Figure 13. Dependence between pressure (P, MPa) and time (t, s) at a routine stop of pumping units in cross section S2.

Analyzing the obtained results for the three schemes of running the system, can be claimed that the maximum amplitude of pressure oscillation was observed in the case of volley launch of pumping units and reached $21.17 \cdot 10^5$ Pa. This is very unwanted in terms of possible damage to pumping equipment and pipelines in general, and also increases wear and reduces durability of the system elements. The lowest increase in pressure corresponds to step-by-step start-up of the system delaying the launch of the first pump reaching $7.55 \cdot 10^5$ Pa. It is not dangerous and does not create problems in terms of negative effects of water hammer. Such scheme ensures maximum efficiency of start/stop of the system and the risk of damage is minimal due to the avoidance of direct water hammer.

6 CONCLUSIONS

Based on the presented material the following scientific and practical results can be formulated. For the first time a comprehensive methodology of calculating the dynamics of two-phase flows has been developed, allowing quickly and with high accuracy study the full range of stationary and transient processes in the deepwater pumping installations within a single mathematical formalism.

Based on the foregoing, following can be concluded. The investigation of the issue showed that to date there is no method of calculation of nonstationary and transient processes in elements of DPH, taking into account the specifics of their operation in difficult conditions of great depths and providing sufficient accuracy for this class of problems.

Based on the developed methodology, software

package HydroWorks 2p is compiled, which allows to solve various problems associated with the two-phase flow and to determine the parameters of non-stationary and transitive modes in the deep-water mining installations. The developed complex is able to calculate the entire spectrum of transients from the launch of the system (pumping only water) up to the processes associated with the regulation and shutdown (operating with slurry).

Using this software package, different transients in deep-water pumping installations have been studied and the basic parameters of the systems depending on the time in different sections of the pipeline are obtained. It is established that the pressure oscillations caused by these dynamic stresses may reach critical values and significantly affect the efficiency of the installation up to the violation of its integrity.

Next stage of work is the use of the developed application HydroWorks 2p for different calculations of deepwater mining installations and making appropriate improvements and extensions to the existing software package.

REFERENCES

Fox, D. 1981. *Hydraulic analysis of unsteady flow in pipelines*. Moscow: Energoizdat.

Nigmatulin, R. 1987. *Dynamics of multiphase flows*. Moscow: Nauka.

Kartvelishvili, N. 1979. *Dynamics of pressure pipelines*. Moscow: Energiya.

Makharadze, L. 1986. *Nonstationary processes in the pressure hydrotransport systems and protection against water hammer*. Tbilisi: Metsniereba.

Wallace, H. 1972. *One-dimensional two-phase flows*. Moscow: Mir.

Kyrychenko, V., Romanyukov, A., Taturevich, A. 2009. *Study of parameters of water hammer under transient modes in deep-water hydrohoists*. Dnipropetrovsk: National Mining University. Research bulletin of NMU, 1.

Charny, I. 1975. *Unsteady motion of a real fluid in pipes*. Moscow: Nedra.

Kyrychenko, Y. 2001. *Scientific substantiation of the parameters of pipeline systems for minerals hydrohoisting.* Thesis of Doctor of Technical Sciences. Dnipropetrovs'k: National Mining University.

Wud, A. 1934. Sound waves and their application. Moscow, Leningrad: Gostekhizdat.

Goman, O., Kyrychenko, Y., Kyrychenko, V. 2008. *Development of multi-functional dynamic model of a multiphase flow in relation to airlift*. Dnipropetrovs'k: National Mining University. Research bulletin of NMU, 8.

Kyrychenko, Y., Shvorak, V., Kyrychenko, V., Romanyukov, A., Taturevich, A. 2011. *The issue of development of a numerical method for calculating the dynamics of multiphase flows.* Dnipropetrovs'k: National Mining University. Research bulletin of NMU, 2.

Goman, O., Kyrychenko, V., Kyrychenko, Y. 2008. *Determining the propagation velocity of pressure waves in the elements of deep-water hydrohoist*. Dnipropetrovs'k: National Mining University. Research bulletin of NMU, 9.

Kyrychenko, V. 2009. *Substantiation of the rational parameters of deep-water airlift taking into account the transitional processes*. Thesis of Candidate of Technical Sciences. Dnipropetrovs'k: National Mining University.

Technical and Geoinformational Systems in Mining – Pivnyak, Bondarenko & Kovalevs'ka (eds)

Electric stimulation of chemical reactions in coal

V. Soboliev, N. Bilan & A. Filippov
National Mining University, Dnipropetrovs'k, Ukraine
A. Baskevich
State higher educational institution "Ukrainian state chemical and technological university"

ABSTRACT: Experimental research has shown that a part of the solid phase of black coal transmuted into gas at action of the weak electric field. It is supposed, that destruction of the carbonaceous and hydrocarbonaceous chains leads to formation of the mobile components. The quantum-mechanical decision of a problem concerning chemical bonds stability of coal chain structure is given.

1 INTRODUCTION

Nowadays coal is exploited largely as energy fuel and technological raw materials for various productions. Coal as a natural nanosystem is becoming an object of the fundamental research. A number of the problems related to a task of coal origin still remains a riddle, and existing theories, versions, hypotheses are not convincing and, as a rule, are sated by paradoxes. Mechanisms, which form a variety of physical and chemical properties of coal, are also contradictory in the same way as the reasons of properties variation within a coal layer. Decision of these tasks is extremely important, especially for development of new technologies of controllable coal processing and making the most use of its power and chemical potential.

Development of new power-saving and ecofriendly technologies of coal treatment initiates necessity for creation of new ways of chemical bonds destabilization in coal components. The behaviour of the coal nanostructure especially at simultaneous action more than two physical parameters (pressure, temperature, electric field, magnetic field, and fluids) characteristic for natural processes of mineral formation has not been studied till now. Each of the numbered parameters could break balanced state in system, initiate development of various chemical processes and have considerable influence on chemical and physicotechnical properties of coal.

Up-to-date results in the field of physical mechanics of coal, which investigate its properties, reasons and mechanisms of unstable state origin in nanostructure, are obtained and applied for elaboration of technical, social and ecological projects in the coalmining industry (Soboliev 2003; Frolkov & Frolkov 2005; Alekseev 2010). Therefore, actuality of investigations of origin kinetics and new formed hydrocarbonaceous and carbonaceous phases growth, role of the surface in chemical reactions, dynamics of properties changing of coal organic mass in the process of coalification, quantum-mechanical regularities during formation of coal organic mass component composition under action of different physical fields is evident.

Investigations of the weak electric field influence on phase transition in coal have the greatest scientific interest because in nature tectonic activization is accompanied not only by complicated rocks deformation, but also by increasing of electrical and magnetic fields intensity.

2 FORMULATING THE PROBLEM

In (Soboliev 2003) there was suggested for the first time the mechanism of coal organic mass transition into gas as a result of action of pressure with shearing. Experiments confirmed it later (Frolkov & Frolkov 2005). The effect of mechanical energy transmutation into chemical one has been chosen as the mechanism of bonds destruction (Butyagin 1971). In recent times by investigations of structural and phase transformation in coal it is substantiated, that the part of coal mass transfers into gas in temperature range 300-400 K under action of the weak electric current (Soboliev, Chernay & Chernyak 2006). Thus, it is supposed, that transitions "coal → ga" under mechanical and electrophysical action are identical and could be described the unique physical mechanism.

The purpose is creation of physical and mathematical model, which would fulfil requirements of chemical bonds stability in coal components in case of electrophysical action.

Problems of carbonaceous-hydrogen chains stability were considered from the point of view of quantum-mechanical systems stability on the example of a typical carbonaceous-hydrogen chain

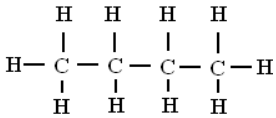

3 CALCULATION

For examination of a problem on stability of carbon-hydrogen molecules consisting of linearly arranged atoms of carbon, it is necessary to solve problems about movement of an electron in the field of two Coulomb fluctuating isotropic harmonic oscillators, and about movement in the field of N-Coulomb centres arranged linearly and about charges interaction with a chain of atoms.

Common energy of the given carbon-hydrogen chain consists:

$$E = E_0 + W_1 + W_2 ,$$

where E_0 – interaction energy of particles in the decision of a two-centric problem, W_1 and W_2 – disturbances caused by oscillating movement of Coulomb centres and atoms of a chain.

For the solution a Schrodinger equation in ellipsoidal coordinates

$$\left\{\frac{4}{R^2\left(\lambda^2-\mu^2\right)}\left[\frac{\partial}{\partial\lambda}\left(\lambda^2-1\right)\frac{\partial}{\partial\lambda}+\frac{\partial}{\partial\lambda}\left(1-\mu^2\right)\frac{\partial}{\partial\lambda}+\right.\right.$$

$$\left.\left.+\frac{4}{R^2\left(\lambda^2-1\right)\left(1-\mu^2\right)}\frac{\partial^2}{\partial\varphi^2}\right]\right\}\psi+$$

$$+2\left[E+U(\lambda,\mu)\right]\psi=0 \qquad (1)$$

where it is necessary that variables λ, μ were parted and the requirement satisfied:

$$U(\lambda,\mu,\varphi)=\frac{\Phi_1(\lambda)+\Phi_2(\mu)}{\lambda^2-\mu^2}.$$

Potentials, which allow the equation (1) to be parted:

– a Coulomb potential

$$U_{coul}(\lambda,\mu,\varphi)=\frac{2}{R}\left[\frac{Z_1}{\lambda+\mu}+\frac{Z_2}{\lambda-\mu}\right];$$

– harmoniously fluctuating Coulomb potentials $U_{fluct}(\lambda,\mu,\varphi)=\frac{R^2\omega^2}{8}\left(\lambda^2+\mu^2\right)$, where ω is frequency of the basic oscillations of carbon atoms.

Calculation of energy of diatomic molecule C-C ground states was carried out under the formula

$$E_{k,\Lambda,n}=\frac{\left\langle\psi_{k,\Lambda,n}\left|H_0\right|\psi^*_{k,\Lambda,n}\right\rangle}{\left\langle\psi_{k,\Lambda,n}\left|\psi^*_{k,\Lambda,n}\right\rangle\right.},$$

where H_0 – Hamiltonian of a two-centric problem

$$H_0=\frac{4}{R^2\left(\lambda^2-\mu^2\right)}\left[\frac{\partial}{\partial\lambda}\left(\lambda^2-1\right)\frac{\partial}{\partial\lambda}+\frac{\partial}{\partial\lambda}\left(1-\mu^2\right)\frac{\partial}{\partial\lambda}+\right.$$

$$\left.+\frac{4}{R^2\left(\lambda^2-1\right)\left(1-\mu^2\right)}\frac{\partial^2}{\partial\varphi^2}\right],$$

where $\psi_{k,\Lambda,n}$ – wave function of a two-centric problem, k,Λ,n – main quantum numbers.

Energy of diatomic molecule C-C:

$$E=E_{\frac{1}{2},0,0}+E_{e-e}+\frac{Z_1Z_2}{R},$$

where

$$E_{\frac{1}{2},0,0}=\frac{4\left[\frac{1}{2}\left(a-Z^+\right)+e^{4a}\cdot E_i(-4a)\cdot\left(a^2-a\cdot Z^+-\frac{1}{4}a\right)\right]}{R^2\left[\frac{1}{2a}-\frac{4}{3}a\cdot e^{4a}\cdot E_i(-4a)\right]};$$

$$E_{e-e}=\left\langle\psi_{det}\left|\frac{1}{r_{1,2}}\right|\psi_{det}\right\rangle=\frac{4}{R\left[\frac{1}{2a}-\frac{4}{3}a\cdot e^{4a}\cdot E_i(-4a)\right]^2}\left[\left(\frac{3}{40a^2}+\frac{1}{20a^2}\right)(C+ln\,2a)+e^{8a}E_i^2(-8a)\times\right.$$

$$\left.\times\left(\frac{3}{40a^2}+\frac{11}{20a}+\frac{7}{5}+\frac{8a}{15}\right)+e^{4a}E_i^2(-8a)\frac{4a^2}{15}+e^{4a}E_i^2(-4a)\left(-\frac{3}{20a^2}+\frac{1}{2a}-\frac{1}{5}\right)+\frac{1}{8a}-\frac{1}{10}\right].$$

For a finite linear chain of atoms in length R, a charge of the first atom designates Z_a and a charge of N^{th} one – Z_b. In ellipsoidal coordinates (λ,μ,φ):

$$\lambda = \frac{r_a + r_b}{R};\ \lambda = \frac{r_a - r_b}{R},$$

where r_a – distance from an electron to the first atom; and r_b is the same one to N^{th} atom accordingly.

The operator of potential energy $U(\lambda,\mu,\varphi)$ of N – Coulomb centres system arranged along a line is expressed in the following way:

$$U(\lambda,\mu,\varphi) = \frac{2}{R}\left[\frac{Z_1}{\lambda+\mu} + \frac{Z_2}{\lambda-\mu}\right] + \sum_{i=2}^{n-1}\frac{2Z_i}{R(\lambda+\mu)}\times$$

$$\times\left[1 - \frac{1 + 2\lambda\mu + \frac{4i\lambda\mu}{N-1} + \frac{4i^2}{(N-1)^2}}{(\lambda+\mu)^2}\right]^{-\frac{1}{2}}.$$

Last equation show that the potential consists of a Coulomb potential plus disturbance:

$$W_2 = \sum_{i=2}^{N-1}\frac{2Z_i}{R(\lambda+\mu)}\left[1 - \frac{1 + 2\lambda\mu + \frac{4i\lambda\mu}{N-1} + \frac{4i^2}{(N-1)^2}}{(\lambda+\mu)^2}\right]^{-\frac{1}{2}}.$$

In case of $R_1 = R_2$ last expression becomes:

$$W_1 = Z^+\sum_{i=1}^{\infty}(-1)^i\frac{a^i R^{i-1}}{i!}\left[2I_{i+1} + \frac{2E_i(-4a)}{3}\right] +$$

$$+ Z^-\sum_{i=1}^{\infty}(-1)^i\frac{a^i R^{i-1}}{i!}\left[2I_2 + \frac{2E_i(-4a)}{3}\right] +$$

$$+ Z^+\sum_{j=1}^{\infty}\sum_{i=4}^{\infty}(-1)^{i+j+1}\frac{a^{i+2j}R^{i+j}}{(8+32(i+j-4))}\times$$

$$\times\left[\frac{2I_{i-1}}{(2+(i+j)+1)} + \frac{2E_i(-4a)}{(2(i+j)+3)}\right],$$

where $Z^{\pm} = Z_1 + Z_2$, $I_i = \int_1^{\infty}\frac{\lambda^i e^{-a(\lambda-1)}}{\lambda+1}d\lambda$.

To submit the influence of the third Coulomb centre on separately chosen chemical bond, the third centre is presented as some disturbance, which operates on it. Then it is possible to express a Hamiltonian in a view:

$$H_0 = -\frac{h^2}{2M_1}\Delta\vec{R}_1 - \frac{h^2}{2M_2}\Delta\vec{R}_2 - \frac{h^2}{2M_3}\Delta\vec{R}_3 +$$

$$+ \frac{Z_1Z_2}{\left|\vec{R}_2 - \vec{R}_1\right|} + \frac{Z_1Z_3}{\left|\vec{R}_3 - \vec{R}_1\right|} + \frac{Z_3Z_2}{\left|\vec{R}_3 - \vec{R}_2\right|},$$

where H_0 – Hamiltonian of interaction of three particles; Φ – full wave function of a temporary Schrodinger equation.

Taking into account the estimation and using two Coulomb centres as the base, the disturbance caused by influence of the third centre is expresses in Neumann decomposition:

$$W_3 = \frac{2Z_3}{R}\sum_{p=0}^{\infty}\sum_{m=-p}^{p}(-1)^m(2p+1)\left[\frac{(p-|m|)!}{(p+|m|)!}\right]\times$$

$$P_p^{|m|}(\lambda_<)Q_p^{|m|}(\lambda_>)P_p^{|m|}(\mu_3)Q_p^{|m|}(\mu_3)e^{im(\varphi-\varphi_3)},$$

where $\lambda_3 = \frac{R_2+R_3}{R_1}$; $\mu_3 = \frac{R_2-R_3}{R_1}$; $\lambda_{<,>}$ – major or smaller quantities; $P_p^{|m|}(\lambda_<)$ and $Q_p^{|m|}(\lambda_>)$ – associated functions of Legendre I and II sorts.

Then a problem of three particles taking into account disturbance energy will be following:

$$E_0(R_1,R_2,R_3) = \frac{\langle\psi|H+W|\psi^*\rangle}{\langle\psi|\psi^*\rangle} + E_0(R_1) + \sum_{i=1}^{N}\frac{4aZ_i}{R_i\left[\frac{1}{2a} - \frac{4a}{3}e^{4a}E_i(-4a)\right]}\times$$

$$\times\left\{Q_0^0(\lambda_3)\left[\frac{2}{3}e^{4a}E_i(-4a) - \frac{1}{4a^2}\right] - \frac{1}{8a^2e^{2a(\lambda_3-1)}}[P_2(\lambda_3)P_2(\mu_3)-1]\times\right.$$

$$\left.\times\left[e^{2a(\lambda_3+1)}E_i(-2a(\lambda_3+1)) - e^{2a(\lambda_3+1)}E_i(-2a(\lambda_3-1))\right] - Q_2(\lambda_3)P(\mu_3)\left[\frac{2}{3}e^{4a}E_i(-4a) +\right.\right.$$

$$+\left(\lambda_3^2-1\right)e^{2a(\lambda_3-1)}E_i\left(-2a(\lambda_3-1)\right)+e^{-2a(\lambda_3-1)}\left(\frac{1}{2a}-\frac{1}{4a^2}-\frac{\lambda_3}{2a}\right)+\frac{1}{4a^2}\Bigg]+$$

$$+Q_0(\lambda_3)P_2(\lambda_3)P_2(\mu_3)\Bigg[\left(\lambda_3^2-1\right)e^{2a(\lambda_3+1)}E_i\left(-2a(\lambda_3+1)\right)-\left(\frac{1}{2a}-\frac{1}{4a^2}-\frac{\lambda_3}{2a}\right)\Bigg]e^{-2a(\lambda_3-1)}\times$$

$$\times P_2(\lambda_3)P_2(\mu_3)\cdot\left[e^{4a}E_i(\lambda_3+1)E_i\left(-2a(\lambda_3+1)\right)+\frac{1}{2a}e^{-2a(\lambda_3-1)}\right]\Bigg\}.$$

4 DISCUSSION AND CONCLUSION

Calculation of C-C bond energy revealed that the presence of a superfluous electron results in "anti-bonding" of the chemical bond (Figure 1, curve 2). Moreover, the chemical bond practically ceases in case of influence on it more than two electrons (Figure 1, curve 3).

Figure 2 shows that interaction of a positive electric charge with C-C chemical bond increases the distance between atoms and accordingly reduces bond energy and its stability.

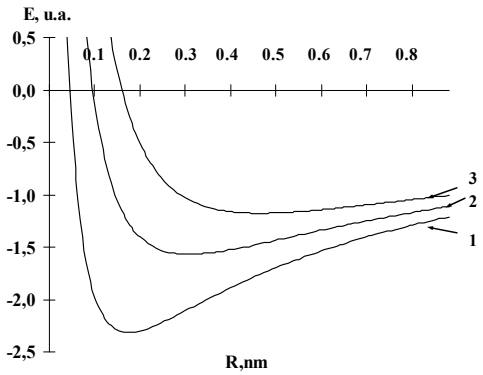

Figure 1. Influence of "superfluous" electrons on bond energy of the next atoms of a carbon molecule: 1 – energy of unperturbed bond C-C; 2 – bond energy C-C taking into account influence on it of a superfluous electron; 3 – bond energy C-C taking into account influence on it of two superfluous electrons.

Experimental research on the weak electric field influence on coal structure was carried out for substantiation of above-mentioned calculation. Destructive processes accompanying by formation of movable components (radicals, gas) take place while weak electric current passing. An electronic paramagnetic resonance (EPR) showed the high concentration of paramagnetic centres about $6.5\cdot10^{19}$. The analysis of X-ray diffractograms testifies unequivocally that a degree of coal amorphism is getting higher after electric current passing.

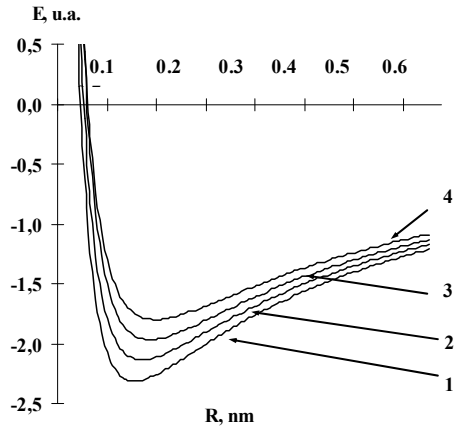

Figure 2. Changing of bond energy from charge $Z=2$, which is at a distance H from the centre of this bond: $1-H=6$; $2-H=5$, $3-H=4$; $4-H=3$.

According to infrared spectroscopy (IRS), destruction of bridge aliphatic chains is confirmed by decline of an optical density of bands 2920 and 2860 sm^{-1} corresponding to the valence and deformation oscillations of bonds C-H in structures, which contain CH_2 -groups. Destruction of oxygen-methylene bridges is accompanied by break of CH_3-methanal groups, which related with them (the band 1370 sm^{-1} decreases). Besides, growth of bands 1025 and 1080 sm^{-1} on infrared spectrum, which is typical for primary ($-CN_2ON$) and secondary ($>CHOH$) alcoholic groups, points to destruction.

By results of action electrical stimulation of chemical processes in coal is similar to mechanochemical activation; however in case of mechanochemical activation process of coal transition into gas is accompanied by high-speed decomposition of coal.

Quantum-mechanical estimation of influence of exterior elementary electric charges on a chemical bond stability testify to an energy drop between atoms of carbon and bond breaking in case of "superfluous" electrons increase, which is confirmed by EPR and IRS data.

REFERENCES

Soboliev, V.V. 2003. *To the Question about Nature of Outburst Coal Formation*. Collection of scientific works of NMU, 17. V.1: 374-383.

Frolkov, G.D. & Frolkov, A.G. 2005. *Mechanochemical Conception of Outburst in Coal Layers*. Coal, 2: 18-22.

Alekseev, A.D. 2010. *Physics of Coal and Minin*g. Kyiv: Naukova dumka: 424.

Butyagin, P.Yu. 1971. *Kinetics and Nature of Mechanochemical Reactions*. Successes of Chemistry. V.40: 1935-1959.

Soboliev, V.V., Chernay, V.V. & Chernyak, S.A. 2006. *Role of Electric Current in Stimulation of Destructive Processes in coal*. Bulletin of Higher educational institutions. The Northern Caucasians region. Techn. Sciences. Appendix, 9: 45-51.

Technical and Geoinformational Systems in Mining – Pivnyak, Bondarenko & Kovalevs'ka (eds)

Substabtiation of the parameters of elements of mine vent systems while exploiting bedded deposits of horizontal occurence

V. Golinko, O. Yavors'ka & Y. Lebedev
National Mining University, Dnipropetrovs'k, Ukraine

ABSTRACT: The results of research aimed at increasing efficiency of vent systems of mines and pits are given. There is a substantiation of parameters of such elements of mine vent systems as vertical mine working (mine shafts, holes, holes cluster) built on the area of mining works to remove outgoing air stream at mine with horizontal layer occurrence on comparatively small depth. Economic and mathematical model is developed on which basis formula for determining optimal parameters of vertical mine workings is obtained. Transfer from optimal parameters of elements of mine vent system to rational ones is substantiated.

1 INTRODUCTION

Reducing the way of air current movement through mine ventilation network can be definitely the only way of economic solution of the ventilation problems while exploiting large mine field.

Analysis of the research results and recommendations for Donbass coal mines shows that using mine ventilation network with vertical mine working for removing outgoing air stream (fresh air supply) within mining allows to reduce considerably the way of air current movement through the ventilation network, to reduce depression of ventilation network, to increase the amount of incoming air, to decrease ventilation loss etc. As a rule, use of such ventilation networks without necessary scientific and economic grounding results in decrease of ventilating efficiency.

2 FORMULATING THE PROBLEM

While exploiting deposits with 70-100 m occurrence of horizontal seam (for example, Podmoskovya and Nikopol basins) it is possible to use direct-flow ventilation with moving air taken away at a flank of mine field near mine workings. Such ventilation networks can be implemented only under condition of consecutive vertical shaft sinking (air shaft or hole) within stoping. It helps take into account dynamics of mining and remove return ventilation current straight in the area of mining instead of transporting contaminated air through the whole ventilation network in the opposite direction. In such a way it is possible to reduce considerably air flow path, to increase the scheme reliability, and to decrease ventilation loss. While advancing mining air shafts or holes are being liquidated with new ones replacing them.

Under advance mining protective pillar are left, the scheme of mine working ventilation is done in the following way. Fresh air is supplied to the face through central and air shafts, and then through airway and gate road. Outgoing air current is removed up to the surface through airway and hole. When mining operations approach to the hole the latter is sealed and outgoing air current is removed through a newly built air hole (n is the number of air shafts or holes built consecutively from the surface to a drift within the mining period with L length).

To put the ventilation schemes into operation it is important to know such parameters as quantity of return air shafts or holes, their location in the scheme and diameter or section. The matter is that the parameters influence greatly capitalized expenses while constructing ventilation schemes under conditions of high concentration of stoping.

3 BASIC UNIT

To calculate optimal values d and n, corresponding to the minimum of total expenditures, the economic and mathematical model of total expenditures is obtained (Golinko, Yavors'ka & Lebedev 2009).

$$f(n,d)=1.9\cdot 10^3\cdot d\cdot l\cdot n+\frac{lkQ^3T\alpha P}{2\cdot S^3}+$$

$$+\frac{lkQ^3T\alpha P}{2\cdot S^3 n}+\frac{6.5lkQ^3T\alpha_h}{2\cdot d^5}, \quad (1)$$

where l – length of air hole, m; d is diameter of hole, m; k – coefficient, taking into account annual cost of electricity for the system; Q – consumption, m^3/s; T is period of pillar mining, years; α – coefficient of aerodynamic resistance of the mine working; P – perimeter of mine working, m; S – cross-section area of mine working, m^2; α_h – coefficient of aerodynamic resistance of a hole.

The obtained model is dynamic one as it reflects dynamics of the process of ventilating boundary area of slope mine while removing outcoming air through consecutively built ventilation holes. It often turns that values of such a parameter as the quantity of ventilation holes or shafts determined according to the obtained expression (Golinko, Yavors'ka & Lebedev 2009) are not whole numbers that is why they need to be rounded. Herewith total given expenditures increase to some extent. If function is symmetrical, rounding to the near whole number is allowable. In this case costs transforming from the parameters expected values to the whole ones increase equally. If the function is asymmetrical, and total expenditures increase differently while deviating from expected value either side rounding to the near hole can result in ungrounded increase in total expenditures.

Consider function of total expenditures (1) for ventilation and hole construction throughout the mine working. After examining the function as for extreme point we get:

$$\frac{\partial f(d)}{\partial d}=1.9\cdot 10^3\cdot l\ n-\frac{32.5\cdot lkQ^3T\alpha_h}{d^6}=0$$

Whence

$$d=0.5\cdot\sqrt[6]{\frac{k\alpha_h Q^3 T}{n}}. \quad (2)$$

One may not take into account the second term in function (1), as it can not influence d and n parameters. Hence, taking into account (2) we have:

$$f(n)=\frac{LkQ^3T\alpha P}{2\cdot S^3}\frac{1}{n}+$$
$$+1.16\cdot 10^3\cdot n^{5/6}\cdot l\cdot\sqrt[6]{kQ^3T\alpha_h}. \quad (3)$$

If we set

$$a=\frac{LkQ^3T\alpha P}{2\cdot S^3}. \quad (4)$$

$$b=1.16\cdot 10^3\cdot l\ \sqrt[6]{kQ^3T\alpha_{скв}}. \quad (5)$$

We get

$$f(n)=\frac{a}{n}+bn^{0.81}. \quad (6)$$

Optimal amount of ventilation holes corresponding to minimum of function is determined from the expression

$$n_o=\left(1.23\cdot\frac{a}{b}\right)^{0.55}. \quad (7)$$

On the basis of (7), we get

$$a=0.81\cdot bn_o^{1.81}. \quad (8)$$

$$b=1.23\cdot\frac{a}{n_o^{1.81}}. \quad (9)$$

Under optimum quantity of ventilation holes with taking into account (8) and (9), the expression (6) is

$$f(n_o)=2.23\cdot a\frac{1}{n_o}=1.81\cdot bn_o^{0.81}. \quad (10)$$

Having divided expression (6) by (10) we get:

$$f\left(\frac{n}{n_o}\right)=0.45\cdot\frac{n_o}{n}+0.55\cdot\frac{n^{0.81}}{n_o^{0.81}}. \quad (11)$$

If we set $n/n_0=\delta$, we get:

$$f(\delta)=\frac{0.45}{\delta}+0.55\cdot\delta^{0.81}. \quad (12)$$

The expression is the function of fractional variation of total costs for ventilation and ventilation holes construction if their optimum quantity no is replaced by rational n.

Function graph (12) is given in Figure 1 on which basis at optimum value of no it is possible to write

$$f(\delta)=0.45\cdot\delta_o^{-1}+0.55\cdot\delta_o^{0.81}=1. \quad (13)$$

Let Δ is deviation of function value (1) from optimum

$$f(\delta)-f(\delta_o)=\Delta f(\delta_o). \quad (14)$$

If we put function value (12) into equation (11) taking into account (10) we get

$$0.45\cdot\delta^{-1}+0.55\cdot\delta^{0.83}=1+\Delta. \quad (15)$$

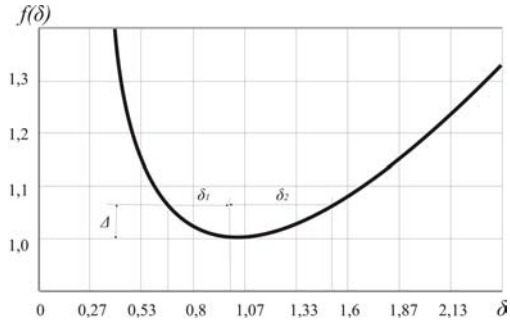

Figure 1. Change of relative expenses under deviation from optimum.

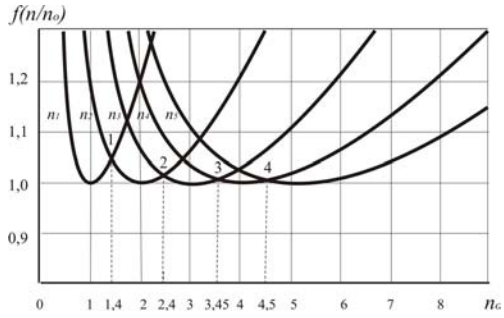

Figure 2. Graphs of function (11) for neighbouring n_o values.

Taking value Δ, and solving equation (15) we find that two quantitatively different values δ_1 and δ_2 correspond to each Δ value. It shows that function of total costs is asymmetrical. Thus transition to the near whole, while obtaining fractional value n_o, can lead to groundless cost increase. Correlation between optimum fractional and rational integral number of holes can be expressed by the inequation $n < n_o < n+1$. It means that more or less integral values n correspond to each optimum value. Rational one is the value transition to which will cause less cost increase. Graph of function (11) shows that for neighbouring goal objectives of n and $n+1$, shown in Figure 2, it can be seen that each interval from n up to $n+1$ contains such value as n_Δ. If we take any of the two neighbouring integral values n or $n+1$ instead of n_Δ it can result in similar increase of total costs. Therefore if in the process of determination n_o we will see that $n_o < n_\Delta$, it is necessary to take less value of the integral. And visa versa, if $n_o > n_\Delta$ then it is more.

Develop a formula for calculating n_Δ. It is obvious that ratio $f(n)/f(n+1)=1$ occurs for neighbouring integral values n and $n+1$. Taking into account this ratio and basing on expressions (6) and (8) we obtain

$$\frac{f(n)}{f(n+1)} = \frac{0{,}81\cdot\dfrac{n_\Delta^{1.81}}{n} + n^{0.81}}{0.81\cdot\dfrac{n_\Delta^{1.81}}{n+1} + (n+1)^{0.81}} = 1 . \qquad (16)$$

Whence

$$n_\Delta = 1.124\cdot\left[n(n+1)^{1.81} - (n+1)n^{1.81}\right]^{0.55} . \qquad (17)$$

Table 1 gives rounding intervals determined from the expression (17).

If calculation results show that $n_o < n_\Delta$, it is necessary to take less neighbouring integral n; if $n_o > n_\Delta$, it is more.

Table 1. Rounding intervals for transition of value of no parameter to rational ones.

Rational Values	1	2	3	4	5	6	7
n_Δ	1.41	2.45	3.48	4.5	5.5	6.54	7,56
Rounding Intervals	0.7-1.41	1.41-2.45	2.45-3.48	3.48-4.5	4.5-5.5	5.5-6,54	6.54-7.56

4 CONCLUSIONS

1. Economic and mathematical model is developed on which basis formula for determining optimal parameters of vertical mine workings is obtained.

2. Transfer from optimal parameters of elements of mine vent system to rational ones is substantiated.

REFERENCES

Golinko, V.I., Yavors'ka, E.A & Lebedev, Y.Y. 2009. Estimation *of efficiency of vent networks of manganese mines*. Materials of International Research and Practice Conference "School of Underground Mining": 167-184.

Technical and Geoinformational Systems in Mining – Pivnyak, Bondarenko & Kovalevs'ka (eds)

Ennobling of salty coals by means of oil agglomeration

V. Beletskyi
Donetsk national technical university, Donetsk, Ukraine

T. Shendrik
Ukrainian academy of sciences, Donetsk, Ukraine

ABSTRACT: The phenomenon of coal modification at oil agglomeration has been studied, specifically, changing of its structure and physical-chemical properties of surface. It was established: agglomeration process of coal with size 0-1(3) mm is accompanying by direct adhesive contact of "coal-oil" on 75-80% from external surface of coal. The high power chemical bonds are formed together with physical bondes in the interphase zone. This modification leads to the increasing hydrophobicity of coal surface and the contrastance of mosaic liophylic-liophobic picture; internal surface of coal is hydrophobized by diffusing oil agent into pores and fissures. Infiltration phenomenon intensifies this process since light fractions of a binder penetrate into micropores of coal substance; the changes in supermolecular structure of coal organic mass (COM) have been revealed in oil agglomeration process. The experience carried out on low rank salty coals of Western Donbas.

1 INTRODUCTION

Perspective of exhausting natural reserves of petrol and gas and increase of coal consumption have conditioned an increasing interest of the world scientists to coal technologies. Special attention is given today to the study of special processes of coal preparation and ennobling, and this opens new possibilities of processing of low grade raw materials to conditional ecologically clear products (Ding & Erten 1989).

During past ten years the process of coal selective oil agglomeration is quickly developed. The interest to this problem is considerable not only from specialists in fossils ennobling, but also coal chemists, heat-power engineers, transport workers (Biletskyi, Sergeev & Papushyn 1986; Shrauti & Arnold 1995; Wheelock etc. 1994; Mishra Surendra & Klimpel Richard 1989). The oil agglomeration is considered by us as a perspective high efficient substance of preparing low quality coal to coking, burning, pyrolysis and also as polyfunctional process of coal preparation to its liquefaction. Besides, some investigators have demonstrated advantages of utilization the techniques and technologies of oil agglomeration in main hydrotransport systems of energetic and coking coal (Beletskyi, Papayani, Svitly & Vlasov 1995; Rigbi, Jones & Meiwaring 1982).

Universality and technological parameters of oil pelleting allow to use it for processing of low grade coals, in particular, oxidized, with high ash, and high salt content (salty coals).

The goals of our investigation were: to study the structural changes of coal organic mass (COM) at its oil agglomeration; to estimate the efficiency of oil pelleting using for obtaining ecologically suitable coal products.

2 EXPERIMENTAL

Primary raw materials and reagents. Energetic and coking coals from Donetsk (UKRAINE) are of different rank with ash content from 10 to 14%, have been investigated (Biletskyi, Sergeev & Papushyn 1986). Special attention was given to salty coals (SC) of Novomoskovskoe deposit, Western Donbas. The some characteristics of this sample are, %: $W^a = 21.4$; $A^d = 9.9$; $C^{daf} = 72.8$; $H^{daf} = 5.0$; $V^{daf} = 42.6$. Na_2O content in ash is 11.6%. The furnace residual oil (mazut M100), oil of oiling charge (OOC) and polymer of benzene department of coke-chemical production have been used (as reagents-binders).

Parameters of oil agglomeration process: Agglomeration process has been carried out in the laboratory granulator of impeller type at solid : liquid $= 1:3$, $pH = 7$, $t = 18 - 20\,^{\circ}\mathrm{C}$, frequency of impeller rotation $1500\ \mathrm{min}^{-1}$, concentration of binder was from 3-5 to 25-30 mass. %, size of coal particles were from 0 to 200 mn.

Methods of investigation:

– Optical microscopy of agglomerates (microscope NEOPHOT-21);

– Electron parametric resonance (radiospectrometer RE-1306);

– IR-spectrometry (Specord IR-75, Perkin-Elmer);

– X-Ray diffractometry (DRON-UM-1.5);

– Photocolorimetric studying of coal surface.

3 RESULTS AND DISCUSSION

Microscopic investigations of coal-oil structures anshliffs (flocules, agglomerates, granules) allowed to select 4 principal structure types of coal aggregates (Figure 1):

I – *pellicle* – compact formations, with thin broad pellicles of oil-binder between individual grains of coal.

II – *meniscus* – structures with concave meniscus of binder between coal grains on aggregates surface.

III – *powdered* – when binder drops filled with coal grains.

IV – *bridge* – friable formations of coal grains, which are bonding with oil-binder "bridges".

With photocolorimetric methods (using methylene blue solution) (Kolbanovskaya 1959) has been established the part of coal grains surface, which are cowed with a binder for the I type structures consist of 57-79%, II – 86-95 %, III – 100%, IV – 40-44%. This case on the coal grains surface of I type oxipellicle ("white border" around coal grain) can be kept; it doesn't exist in III rd type of granules (Figure 2).

However, for salty coals that high parameters are achieved only at special treatment of raw material with oil agent.

In general, the salty coal has a hydrophilic surface and it is agglomerated by apolar agent with difficulty. To increase its agglomeration capacity, we have worked out a number of steps.

Firstly, this is oil treatment of coal (with mazut M100, for exemple) during the crushing process (Patent 1514404).

Secondly, for salty coal agglomeration, it is recommended to use aromatized agents which contain functional oxygen groups in the side links (Biletskyi 1986).

Thirdly, the agglomeration process itself should be carried out in conditions of increased turbulance of water-coal-oil mixture ($Re > 3000$) and Solid: Liquid = 1:1(3). Without special treatment of coal surface, cowing with the binder is fluctuated between 0-5% only. This fact can be interpretated as a low natural ability of SC to agglomeration.

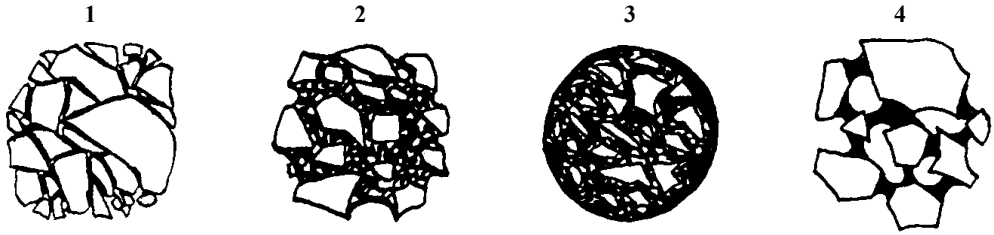

Figure 1. Oil-coal agglomerates (×5 times).

I type

(a) (b)

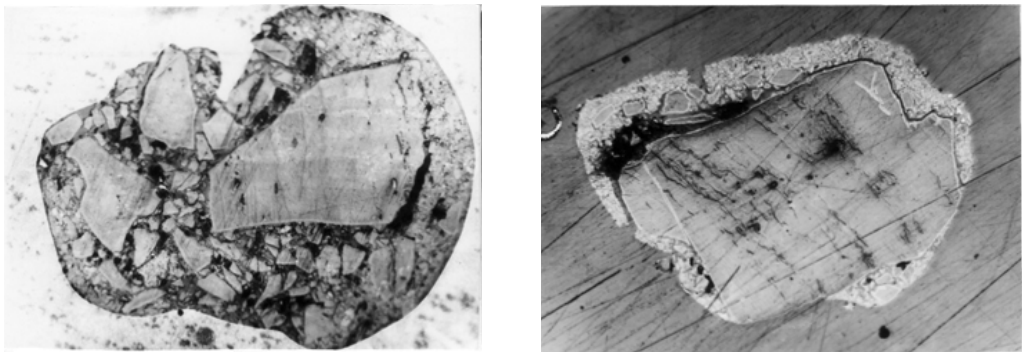

III type

(c) (d)

Figure 2. Anshlifs of granules: I type (a, b) – × 600; III type (c, d) – × 400.

Microscopic investigations allow to confirm a penetration of a binder in pores and fissures of coal substances (Figure 3). It is obviously, that this process is accompanied by infiltration phenomena, during which light fractions of binder penetrate into micropores and more heavy ones remain on surface of coal grains. The last one promotes the formation of border solvate layer of binder on coal surface.

Figure 3. Anshlifs of oil-coal granules with the penetration of oil into coal substance × 600.

As the result, the cohesion of binder pellices is arised, and the stability of aggregates (agglomerates, granules) is increased.

Paramagnetic characteristics of samples were determined on serial radiospectrometer RE-1306 at wave length $\lambda = 3.2$ sm in air. Mn^{+2} in a lattice of MgO was the internal standard.

The obtained data for constituents of agglomerate, intermediate and end products are shown in Table 1. It is seen, that the first addition of oil agent (I stage of process) did not influence on nature and paramagnetic centers (PMC) concentration significantly.

Oil-agent M 100 is more complex, because its three types of PMC are characterized. They are very differed from one another (Figure 4).

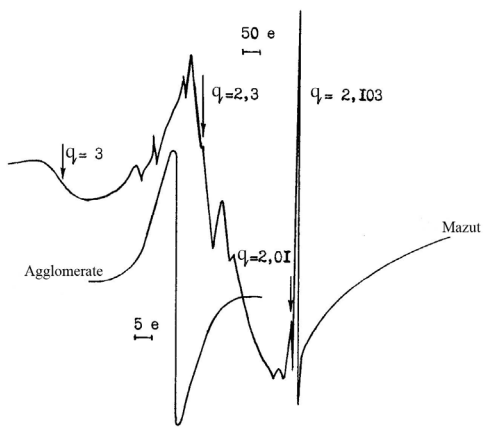

Figure 4. ERS-spectra of M100 and agglomerate, which has been obtained on the basis of salty coal (Novomoskovskoe deposit, Western Donbas).

Table 1.

Sample	ΔH , Gs	g -factor	N , spin / g
Initial coal	4.6	2.0035	$8.9 \cdot 10^{17}$
Coal +5% mazut:			
In air	4.6	2.0036	$8.9 \cdot 10^{17}$
In vacuums	4.9	2.0036	$9.8 \cdot 10^{17}$
Mazut:			
Signal 1	4.6	2.0031	$9.7 \cdot 10^{16}$
Signal 2	12.4	2.0169	$9.7 \cdot 10^{16}$
Signal 3	320	4	$9.7 \cdot 10^{16}$
Agglomerates:			
Agglomerate – 23	4.8	2.0035	$1.4 \cdot 10^{16}$
Agglomerate – 29	5.1	2.0035	$4.8 \cdot 10^{16}$

Table 2.

Sample	Oxygen-containing groups, mg-ekv / g			Na – contain, mg-ekv / g		Heat of combustion Q , MJ / kg
	OH	$COOH$	$O=N=O$	in coal	in ash	
Initial coal	1.60	0.20	9.3	0.30	4.08	24.3
A-23	2.44	0.11	7.1	0.10	1.77	28.2
A-29	2.40	0.10	6.5	0.10	1.88	28.6

Literature data analysis allowed to classify signal I (at $g = 2.0031$ and $\Delta H = 4.6$ e.) as π -polyconjugated systems (Berlin 1972), signal II (with $g \sim 3-4$ and $\Delta H = 320$ e.) as ferrum-containing paramagnetic structures (Ingram 1972), but signal III (with $g \sim 2.017$ and $\Delta H \sim 12$ e.), perhaps, as radicals of peroxide ($R-O-O$) or $R-S-S$ (Butuzova, Saranchuk & Shendrik 1985) types.

PM-characteristics of agglomerates A-23 (% of mazut) and A-29 (% of mazut), as it was expected, are more similar to same of parent coal, excluding PMC concentration. The last one is lower. It is testified about chemical interaction between coal and oil, or, at any rate, about sharply change of intermolecular interactions into COM. Evidently in this case, the important role belongs to water, as a strong hydrolyzing agent .

If it is so, the changes in supermolecular organization of COM and in active oxygen-containing group's composition must take place. As has been established (Table 2), in the agglomeration process of SC carboxyl and quinone groups decreasing and phenol hydroxyl increasing happened. Besides, the significant lessen of sodium concentration takes place, that is to say, desalting raw material to conditional level (Na_2O in ash < 2 %).

Evidently the annihilation of ERS signal II of M 100 (g -factor ~ 3-4; $H \sim 320$ e.) and quinone concentration decreasing, are connected between one and another. We admit, that formation of helate complexes take place here, the central ion is Fe^{3+}, and the ligands are electron donor quinone structures.

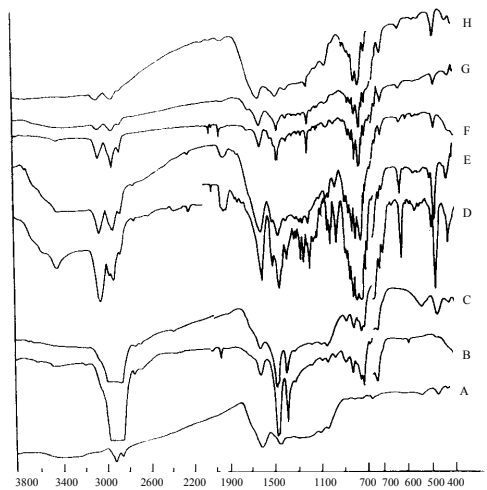

Figure 5. IR-spectra of oil-coal aggregates and their components: A – coal of mine "Inskaja", sort G; B – M100; C – agglomerate "M100-coal"; D – OOC; E – agglomerate "OOC-coal"; F – polymer; G – aggregate "polymer-coal"; H – same agglomerate after 10-days keeping on air.

The phenol groups increasing can be explained with particular quinones reduction by proton donor structures of oil or by hydrolysis of salt form (phenolates) during agglomeration process, which include the water treatment stage.

The decreasing of free carboxyl groups concentration may be explained with their particular substitution by metal or strong H -bonds formation (IR-spectra, Figure 5).

These conclusions are confirmed by IR-data and X-Ray investigations, which we are going to be published in the next article.

4 CONCLUSIONS

During oil agglomeration of coals radical changes of physic-chemical surface characteristics of coal substances take place. They are caused by interphase interaction "coal-oil". That is why it can wait sufficiently different technological properties of agglomerated coals and parent coals.

REFERENCES

Ding, Y. & Erten, M. 1990. *Selective flocculation versus oil agglomeration in removing sulfur from ultra fine coal*. Proc. and Util. High Sulfur Coals III: 3 rd. Int. Conf. Ames. Iowa: 255-264. Amsterdam.

Biletskyi, V.S., Sergeev, P.V. & Papushyn Yu.L. 1986. *Theory and practice of coal selective agregation*. Donetsk: Gran: 264.

Shrauti, S.M. & Arnold, D.W. 1995. *Recovery of waste fine coal by oil agglomeration*. Fuel. V.74 (3): 54-465.

Wheelock, T.D. etc. 1994. *The role of air in oil agglomeration of coal at a moderate shear rate*. Fuel. V.73 (7): 1103-1107.

Ed. Mishra Surendra K., Klimpel Richard R. 1989. *Fine coal processing.* N.J.: Park Ridge. Noyes Publ.: 450.

Beletskyi, V.S., Papayani, F.A., Svitly, J.G. & Vlasov, J.F. 1995. *Hydraulic Transport of Coal in Combination With Oil Granulation.* 8-th Int. Conference on Transport and Sedimentation of Solids Particles: Prague: D6.

Rigbi, G.R., Jones, C.V. & Meiwaring, D.E. 1982. *Slurry pipeline Studeson the BHP-BPA 30-tonne per hour demonstration plant*. 5-th Int. Conf. on the Hydraulic Transport of Solids in Pipes. Johannesburg: D1.

Kolbanovskaya, A.S. 1959. *Colors methods for determination of bitume adhesion with mineral materials*. Moscow: Avtotransizdat: 32.

Patent 1514404 USSR. BO3B7 100. The manner of salty coal processing V.S. Biletskyi, A.T. Elichevitch, Yu.N. Potapenko. Institute polytechnic of Donetsk. #4352939 23-03, declared 29.12.87, published 15.10.89, bul. #38.

Biletskyi, V.S. 1986. *Technological basis of rational using of oil granulation for dewatering and ennobling of hydraulical transported coals.* Ph.D. thesis. Institute polytechnic of Donetsk: 202.

Berlin, I.K. 1972. *Chemistry of polyconjugated systems*. Moscow: Mir: 272.

Ingram, E. 1972. *ERS in biology*. Moscow: Mir: 296.

Butuzova, L.F., Saranchuk, V.I. & Shendrik T.G. 1985. Water *role in themochemical destruction process of coals*. In book Geotecnological problems of fuel-energetic resources of Ukraine. Kyiv: Naukova Dumka: 108-113.

Technical and Geoinformational Systems in Mining – Pivnyak, Bondarenko & Kovalevs'ka (eds)

Features of the resources of the hard coal covering in thin coal-seams in Poland

A. Krowiak
Central Mining Institute, Katowice, Poland

ABSTRACT: The results of analyses of features of geological resources of the hard coal, in majority of mine located in Poland, were presented, according to adopted arbitrarily criteria. All active mines of the hard in the Silesia voivodship were provided with analysis. Apart from analysis there was only one mine stayed – "Bogdanka" in the Lublin Voivodeship. Thin coal seams are defined as the medium thickness in the range from 0.6 up to 1.6 m in the context of this analysis. The following diameters of analyses were accepted: type of coal, division into ranges of the average depth of covering of coal seams, the division into ranges of the average inclination of seams, associative criteria of the average depth of covering and the medium thickness of coal seams and associative criteria for average depth of covering, the average of the calorific value and the average of contents of sulphur. The analysis of concentrations and automatic neural networks were applied in methods of calculation.

1 INTRODUCTION

Described analysis concerns resources of the hard coal covering in active mines in Poland, located in the Silesian Voivodeship.

It is embracing almost 100% of all mines of the hard coal in Poland, apart from one mine "Bogdanka" in the Lublin Voivodeship. The Silesian voivodship is on the South of country. Coal seams are defined as the medium thickness from 0.6 up to 1.6 m.

Over 10 billion ton of the hard coal covering in thin coal- seams are in resources of analysed mines. In Poland, over 30 years ago, it was resigned from their exploitation, having thicker seams at their disposal. It comes back to idea of exploitation of thin coal-seams at present, because thick seams in some mines undergo exhaustion, which threatens these mines the closure with reason of exhaustion of resources.

It is a next argument for the return to the exploitation of thin coal-seams, that many of them, incurring little investments relatively, it is possible to exploit from mine horizon's already made available. Building new mineshafts and new levels of the output in mines is an alternative what requires very big investments.

This analysis concerns geological resources. On this stage of the works, associated with the identification of thin coal-seams, it isn't possible to settle which of them are already now available for the economically justified exploitation. It requires further research works and design. Nevertheless, accepting theoretically, that at least 10% of these resources are available, right away to efficient economical exploitation, we have over 1 billion the tone of coal at our disposal. It is An equivalent of 10 of year's production of the hard coal in Poland.

The analysis was carried out an analysis under the following criteria: type of coal, division into ranges of the average depth of covering of coal-seams, the division into ranges of the average inclination of seams, associative criteria of the average depth of covering and the medium thickness of seams and associative criteria for average depth of covering, the average of the calorific value and the average of contents of sulphur. Chosen criteria of diameters of analysis were chosen arbitrarily. The last diameter of analysis is being taken back to quality parameters of coal, taking into account its calorific value and the content of sulphur.

2 METHOD OF ANALYSIS

For aims of analysis a system of Cartesians coordinates was created in the n- dimension's space, which one kind of variables describing features of a given coal seam corresponds to every of axes in. It is possible to describe every of lines of the set of primary data in the form of the vector in the n-dimensions space, for which coordinates of the top appoint values of individual variables for. For the entire set of primary data we will receive, so, very bulk of vectors located in this space, fastened in the beginning of the system of coordinates.

A method of concentrations and automatic neural networks were used to the further data handling

(Cichosz 2000; Tadeusiewicz 1993). The application of the method of concentrations allows for assigning subsets being characterized by resemblance of variables with reason of oneself (Everitt 2001). For individual sections of analysis, from the entire set of primary data, subsets described only by analysed variables were created.

Automatic neural networks are computer programs imitating learning processes appearing in the human mind in their action. In this particular case a peculiar type of the net was exploited – Kohonena networks, and a STATISTICA program was a tool of the realization 9.0 version (Dokumentacja 2010). Primary data obtained from mines were a base of to do analyse (Materiały źródłowe 2010).

3 STRUCTURE OF RESOURCES ACCORDING TO THE CRITERION OF THE TYPE OF COAL

The criterion of types of coal was applied in this diameter of analysis. It was assumed that giving a few types of coal in characteristics of resources meant that they are in these resources quoin of different types in this analysis.

According to classification in accordance with Polish Norms the following types of coal were distinguished: Type 31 – flame coal; Type 32 – fiery – flame coal; Type 33 – fiery coal; Type 34 – fiery – cooking coal; Type 35 – orto – cooking coal; Type 36 – meta – cooking coal; Type 37 – semi – cooking coal.

In the Table 1 a structure of resources was given according to the criterion of types of coal. In figure 6 a structure of reserves according to the criterion of the type of coal for the whole tested resources was described.

In resources with the whole coals of the following types have large stakes: Type 31 – 2 946 517 th. tone i.e. 27.06% whole of stores; Type 32 – 1 683 001 th. tone i.e. 15.46% whole of stores; Type 31, 32 – 1 267 695 th. tone i.e. the 11.64% whole of stores and the Type 32, 33, 34 – 1 042 487 th. tone i.e. 9.57% whole of stores.

Table 1. Structure of sources according to the criterion of types of coal.

Id.	Types of coals	Size of resources [thousands of ton]	% of participation in resources with the whole
1	Type 31	2 946 517	27.6
2	Type 32	1 683 001	15.46
3	Type 33	70 201	0.64
4	Type 34	648 717	5.96
5	Type 35	537 166	4.93
6	Type 36	4 202	0.04
7	Type 37	37 633	0.35
8	Type 31,32	1 267 695	11.64
9	Type 32,33	445 191	4.09
10	Type 32,34	624 489	5.74
11	Type 32,35	18 820	0.17
12	Type 33,34	256 514	2.16
13	Type 33,35	13 375	0.12
14	Type 34,35	811 447	7.45
15	Type 35,36	23 729	0.22
16	Type 35,37	69 252	0.64
17	Type 36,37	5 478	0.05
18	Type 31,32,33	30 960	0.28
19	Type 31,32,34	57 766	0.53
20	Type 32,33,34	1 042 487	9.57
21	Type 32,34,35	35 494	0.33
22	Type 33,34,35	84 125	0.77
23	Type 34,35,37	5 475	0.05
24	Type 35,36,37	1 913	0.02
25	Type 31,32,33,34	70 959	0.65
27	Type 32,33,34,35	95 713	0.88
	TOTAL	10 888 319	

Source: own study.

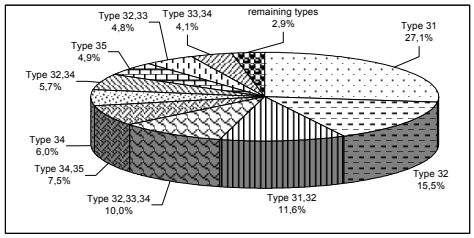

Source: own study.

Figure 1. Structure of resources according to the criterion of types of coal.

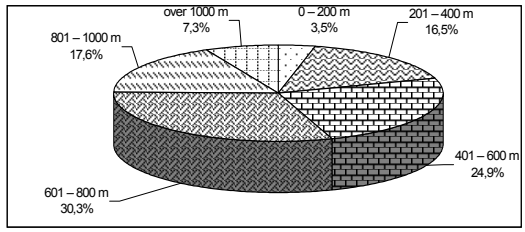

Source: own study.

Figure 2. Structure of resources according to the criterion of the average depth of covering of coal seams.

4 STRUCTURE OF RESOURCES ACCORDING TO THE CRITERION OF IDENTITY FOR RANGES OF THE AVERAGE DEPTH OF COVERING OF COAL SEAMS

In this diameter of analysis a criterion of identity was applied for ranges of the average depth of covering of restores. In analysis the following ranges of the average depth of covering were accepted: 0 – 200 m, 201 – 400 m, 401 – 600 m, 601 – 800 m, 801 – 1000 m, over 1000 m.

In the Table 2 a structure of resources was given according to the criterion of identity for ranges to the depth of covering of coal seams, and in picture 2 graphically this structure of resources was described.

In resources with the whole the largest reserves of coal are appearing in ranges of the average depth of covering: in the range from 601 up to 800 m – 3 299 842 thousands tone i.e. the 30.31% whole of stores and in the range from 401 up to 600 m – 2 708 947 thousands tone i.e. 24.88%.

Table 2. Structure of resources according to the criterion of the average depth of covering of coal seams.

Id.	Ranges of the depth of covering	Size of resources [thousands of ton]	% of participation in resources with the whole
1	0-200 m	381 258	3.50
2	201-400 m	1 791 386	16.45
3	401-600 m	2 708 947	24.88
4	601-800 m	3 299 842	30.31
5	801-1000 m	1 910 948	17.55
6	over 1000 m	795 938	7.31
	TOTAL	10 888 319	

Source: own study.

5 STRUCTURE OF RESOURCES ACCORDING TO THE CRITERION OF THE MEDIUM THICKNESS OF COAL SEAMS

In this diameter of analysis a criterion of ranges of the medium thickness of coal seams was applied. The following ranges of the medium thickness of seams were accepted: 0.6 up to 0.8 m; 0.81 to 1.0 m; 1.01 up to 1.2 m; 1.21 up to 1.4 m; 1.41 to 1.6 m and above 1.6 m. In the range resources above of the average thicknesses 1.6 m are finding underground oneself resources about the variable of thicknesses, in which the lower limit of the thickness is located in a range 0.6 up to 1.6 m.

In Table 3 a structure of sources was given according to the criterion of ranges to the medium thickness of decks, and in Figure 3 a graphical illustration of this structure was described.

Table 3. Structure of resources according to the criterion of ranges of the medium thickness of coal seams.

Id.	Ranges of the medium thickness of coal seams	Size of resources [thousands of ton]	% of participation in resources with the whole
1	0.6 to 0.8 m	821 037	7.54
2	0.81 to 1.0 m	4 120 405	37.84
3	1.01 to 1.2 m	3 492 662	32.08
4	1.21 to 1.4 m	1 577 880	14.49
5	1.41 to 1.6 m	500 760	4.60
6	over 1.6 m	375 575	3.45
	TOTAL	10 888 319	

Source: own study

The largest resources of coal are located in ranges of the medium thickness of seams: in the range 0.81 to 1.0 m – 4 120 405 thousand of ton that presents 37.84% of whole of resources and in the range 1.01 up to 1.2 m – 3 492 662 thousand of ton that presents 32.08% of whole of resources.

6 THE STRUCTURE OF RESOURCES ACCORDING TO CRITERION OF THE AVERAGE INCLINATION OF COAL SEAMS

It was applied a criterion of ranges of average inclination of coal seams as well as the resources selection into the capital groups and then its division into the particular coal mines that are within those groups in this diameter of analysis .

The following ranges of average inclination of seams were accepted: 0° to 5°; 6° to 10°; 11° to 15°; 16° to 20°; 21° to 25°; above 25°.

In Table 4 a structure of resources was given according to the criterion of ranges of average inclination of coal seams, and in Figure 4 a graphical illustration of this structure was described.

The largest coal resources are located in range of average inclination of seams: in range 0° to 5° – 4 559 024 thousand tone i.e. the 41.87% whole of stores and in range 6° to 10° – 3 829 225 thousand tone i.e. the 35.17% whole of stores.

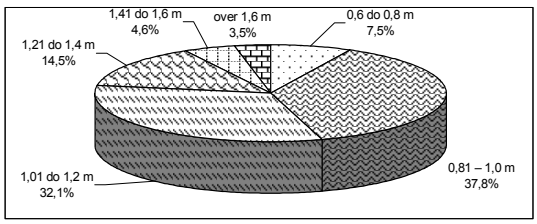

Source: own study.

Figure 3. Structure of resources according to the criterion of ranges of the medium thickness of coal seams.

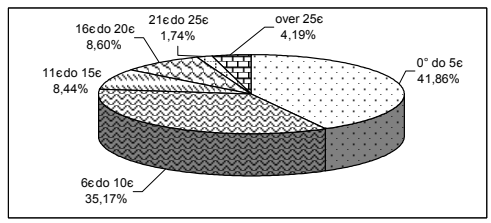

Source: own study.

Figure 4. The structure of resources according to criterion of ranges the average inclination of coal seams.

Table 4. Structure of resources according to the criterion of ranges of average inclination coal-seams.

Id.	Ranges of average inclination of coal seams	Size of resources [thousands of ton]	% of participation in resources as total
1	0° to 5º	4 559 024	41.86
2	6º to 10º	3 829 225	35.17
3	11º to 15º	918 671	8.44
4	16º to 20º	936 025	8.60
5	21º to 25º	189 195	1.74
6	above 25º	456 179	4.19
	SUM	10 888 319	

Source: own study.

7 STRUCTURE OF RESOURCES ACCORDING TO ASSOCIATIVE CRITERIA OF THE AVERAGE DEPTH OF COVERING AND THE MEDIUM THICKNESS OF COAL SEAMS

It was applied the associative criteria of the average depth of covering of coal seams and the average of thickness of these seams as well as the resources selection into the capital groups and then its division into the particular coal mines that are within those groups in this diameter of analysis. The following ranges of the average depth of covering of seams were accepted: 0 up to 200 m; 201 up to 400 m; 401 up to 600 m; 601 up to 800 m; 801 up to 1000 m; over 1000 m.

The following ranges of the medium thickness of coal seams were accepted: 0.6 up to 0.8 m; 0.81 up to 1.0 m; 1.01 up to 1.2 m; 1.21 up to 1.4 m; 1.41 to 1.6 m and the over 1.6 m. The seam of the thickness over 1.6 m were ranked among thin coal seams about the diversified thickness, which the lower limit of the thickness is located in a range from 0.6 up to 1.6 m.

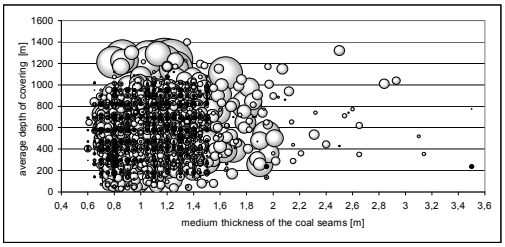

Source: own study.

Figure. 5. Structure of resources according to associative criteria of ranges of the average depth of covering and ranges of the average of thickness of seams appointed according to real values.

The structure of resources according to the associative criterion of ranges to the medium thickness and the average depths of covering of stores was given in Table 5. The illustration of structure of resources appointed according to real values was showed on Figure 5 and on Figure 6 appointed according to ranges of value.

The largest resources of coal are located in the ranges of the medium thickness of coal seams and the average depths of covering: in the range of the thickness 0.81 up to 1.0 m and the range of the depth of covering 601 to 800 m – 1 590 812 thousand ton i.e. the 14.61% whole of stores.

Table 5. The structure of resources according to associative criteria of ranges of average depth covering as well as the ranges of average of thickness seams.

Ranges of the average depth of covering of seams	Ranges of medium thicknesses of coal seams [m]						SUM
	0.6-0.8	0.81-1.0	1.01-1.2	1.21-1.4	1.41-1.6	over 1.6	
Absolute values [thousands of ton]							
0 to 200 m	66 599	126 630	100 305	58 386	9 992	4 619	1 791 386
201 to 400 m	114 000	650 579	509 224	301 317	102 503	113 763	2 712 548
401 to 600 m	227 235	1 113 775	879 427	332 538	83 671	75 902	3 314 569
601 to 800 m	228 071	1 590 812	997 034	260 852	134 432	43 368	375 575
801 to 1000 m	87 468	509 240	641 519	439 086	153 989	79 646	1 910 948
over 1000 m	37 664	129 368	365 153	185 701	16 173	58 278	792 337
SUM	821 037	4 120 404	3 492 662	1 577 880	500 760	375 576	10 888 319
Percentage share in the whole of resources							
0 to 200 m	0.61	1.16	0.92	0.54	0.09	0.04	3.36
201 to 400 m	1.05	5.98	4.68	2.77	0.94	1.04	16.46
401 to 600 m	2.09	10.22	8.08	3.05	0.77	0,70	24.91
601 to 800 m	2.65	14.61	9.16	2.40	1.23	0.40	30.45
801 to 1000 m	0.80	4.68	5.88	4.03	1.41	0.73	17.53
over 1000 m	0.35	1.19	3.35	1.71	0.15	0.54	7.29
SUM	7.55	37.84	32.07	14.50	4.19	3.45	100

Source: own study.

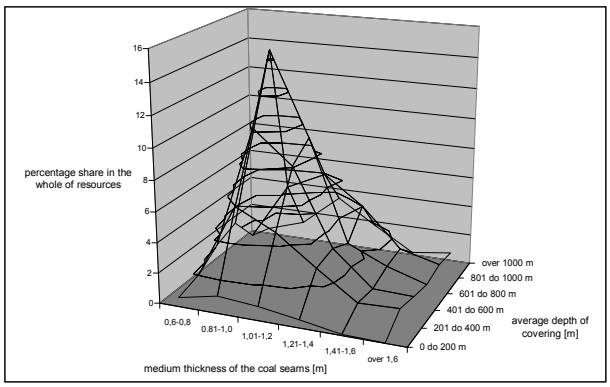

Source: own study.

Figure 6. Structure of resources according to associative criteria of ranges of the average depth of covering and ranges of the average of thickness of coal seams appointed according to ranges of value.

8 STRUCTURE OF RESOURCES ACCORDING TO ASSOCIATIVE CRITERIA OF THE AVERAGE DEPTH OF COVERING, OF THE MEDIUM CALORIFIC VALUE AND THE AVERAGE CONTENT OF SULPHUR

It was applied the associative criteria of the average depth of covering of coal seams, of the medium calorific value and the average content of sulphur in as well as the resources selection into the capital groups and then its division into the particular coal mines that are within those groups in this diameter of analysis.

The following ranges of the average depth of covering of coal seams were accepted: 0 up to 200 m; 201 up to 400 m; 401 up to 600 m; 601 up to 800 m; 801 up to 1000 m; over 1000 m. The following ranges of the medium calorific value were accepted: to 18.0 kJ / kg; 18.01 to 22.0 kJ / kg; 22.01 to 26.0 kJ / kg; 26.01 to 30.0 kJ / kg and above 30.0 kJ / kg.

The following ranges of the average content of sulphur were accepted: to 0.4%; 0.41 to 1.0%; 1.01 to 1.6%; 1.61 to 2.2% and above 2.20%.

The structure of resources for the whole of stores according to the associative criterion of ranges to the average depth of lying of decks, for the medium calorific value and the average content of sulphur was given in Table 6.

Structure of resources was set according to real values, based on adopted criteria, for stores with the whole, for different ranges contents of sulphur were described appropriately: on Figure 7 – for the range to 0.4%; on Figure 8 – for the range from 0.41 to 1.0%; on Figure 9 – for the range from 1.01 to 1.6%; on Figure 10 – for the range 1.61 to 2.2% and on Figure 11 for the content above 2.21%.

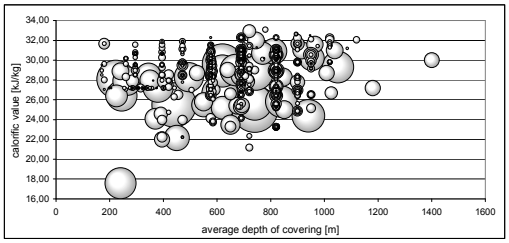

Source: own study.

Figure 7. Structure of resources according to associative criteria of the average depth of covering and the medium calorific value appointed according to real values – for the content of sulphur in coal to 0.4%.

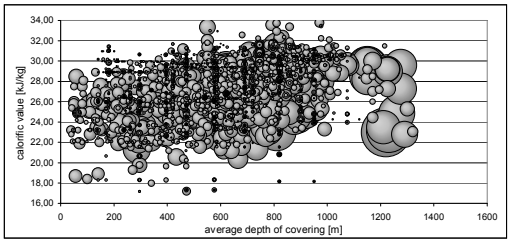

Source: own study.

Figure 8. Structure of resources according to associative criteria of the average depth of covering and the medium calorific value appointed according to real values – for the content of sulphur in coal from 0.41 to 1.0%.

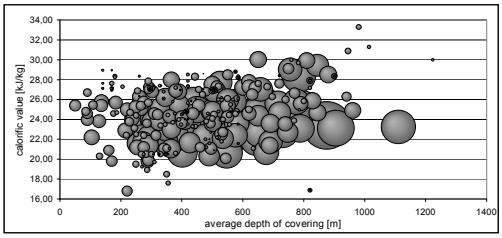

Source: own study.

Figure 9. Structure of resources according to associative criteria of the average depth of covering and the medium calorific value appointed according to real values – for the content of sulphur in coal from 1.01 to 1.6%.

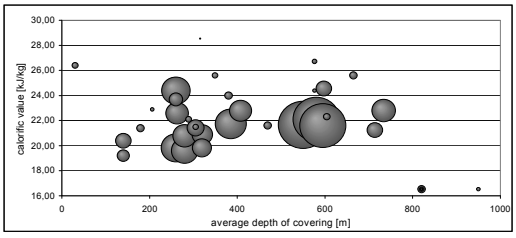

Source: own study.

Figure 10. Structure of resources according to associative criteria of the average depth of covering and the medium calorific value appointed according to real values – for the content of sulphur in coal from 1.61 to 2.2%.

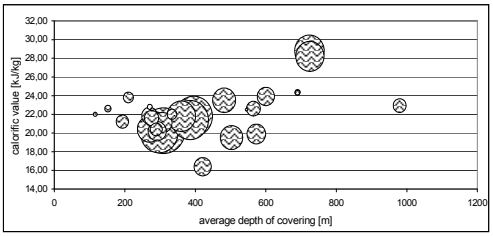

Source: own study.

Figure 11. Structure of resources according to associative criteria of the average depth of covering and the medium calorific value appointed according to real values – for the content of sulphur in coal above 2.2%.

Table 6 (a). Structure of resources according to associative criteria of ranges of the average depth of covering of coal seams, ranges of the medium calorific value and ranges of the average content of sulphur – real value.

Ranges of the average depth of coal seams	Ranges of medium calorific values [kJ / kg]					SUM
	to 18.0	18.01-22.0	22.01-26.0	26.01-30.0	over 30.0	
Absolute values [thousands of ton]						
	Content of sulphur to 0.4%					
0 to 200 m	0	0	0	795	1 029	1 824
201 to 400 m	7 205	0	7 958	51 961	3 501	70 625
401 to 600 m	0	0	29 068	40 385	6 215	75 668
601 to 800 m	359	0	40 796	86 381	22 231	149 767
801 to 1000 m	0	0	27 412	35 155	34 294	96 861
over 1000 m	0	0	0	14 765	4 521	19 286
SUM	7 564	0	105 234	229 442	71 791	414 031
	Content of sulphur from 0.41 to 1.0%					
0 to 200 m	21 390	0	150 094	109 751	3 003	284 238
201 to 400 m	1 746	66 949	633 341	225 984	3 335	931 355
401 to 600 m	3 729	30 901	811 865	772 411	50 173	1 669 079
601 to 800 m	0	61 804	807 316	1 436 642	219 145	2 524 907
801 to 1000 m	0	5 141	343 304	1 040 425	225 986	1 614 856
over 1000 m	0	0	252 743	453 791	28 092	734 626
SUM	26 865	164 795	2 998 663	4 039 004	529 734	7 759 061
	Content of sulphur from 1,01 to 1.6%					
0 to 200 m	0	8 839	49 573	5 249	0	63 661
201 to 400 m	4 303	114 902	308 134	59 163	0	486 502
401 to 600 m	0	131 210	510 559	83 504	0	725 273
601 to 800 m	0	82 262	383 555	112 732	9 000	587 549
801 to 1000 m	640	0	148 367	42 358	2 059	193 424
over 1000 m	0	0	37 752	228	446	38 426
SUM	4 943	337 213	1 437 940	303 23	11 505	2 094 835
	Content of sulphur from 1.61 to 2.2%					
0 to 200 m	0	12 425	0	1 087	0	13 512
201 to 400 m	0	0	161 694	42	0	161 736
401 to 600 m	0	127 259	80 385	586	0	208 230
601 to 800 m	0	6 823	18 064	0	0	24 887
801 to 1000 m	3 046	0	0	0	0	3 046
SUM	3 046	146 507	260 143	1 715	0	411 411
	Content of sulphur above 2.2%					
0 to 200 m	0	2 688	608	0	0	3 296
201 to 400 m	0	137 611	3 557	0	0	141 168
401 to 600 m	4 625	13 386	16 304	0	0	34 297
601 to 800 m	0	0	800	26 659	0	27 459
801 to 1000 m	0	0	2761	0	0	2 761
SUM	4 625	153 667	24 030	26 659	0	208 981
TOTAL	47 043	802 182	4 826 010	4 600 054	613 030	10 888 319

Source: own study

The complete resources of coals with the content of sulphur meeting the appropriate ranges, representing the following participations : to 0.40% – 3.801% i.e. 414 031 thousands of ton; from 0.41 to 1.0% – 71.266% i.e. 7 759 061 thousands of ton; from 1.01 to 1.6% – 9.263% i.e. 2 094 835 thousands of ton; from 1.61 to 2.2% – 3.787% i.e. 411 411 thousands of ton; above 2.2% – 1.882 % i.e. 208 981 thousands of ton.

The complete resources of the coals with the calorific value meeting the appropriate ranges representing the following participations : to 18 kJ / kg – 0.439% i.e. 47 043 thousands of ton; from 18.01 to 22.0 kJ / kg – 7.373% i.e. 802 182 thousands of ton; from 22.01 to 26.0 kJ / kg – 44.306% i.e. 4 826 010 thousands of ton; from 26.01 to 30.0 kJ / kg – 42.257% i.e. 4 600 054 thousands of ton; above 30.0 kJ / kg – 5.624% i.e. 613 030 thousands of ton.

The maximum participation in the whole of resources carrying out 13.19% i.e. 1 436 642 thousand tons possess the resources fulfilling the following criteria: the content of sulphur the range from 0.41 to 1.0%; calorific value in range from 26.01 to 30.0 kJ / kg as well as depth of covered in range since 601 to 800 m.

Table 6 (b). Structure of resources according to associative criteria of ranges of the average depth of covering of coal seams, ranges of the medium calorific value and ranges of the average content of sulphur – percentage shares.

Ranges of the average depth of coal seams	Ranges of medium calorific values [kJ / kg]					SUM
	to 18.0	18.01-22.0	22.01-26.0	26.01-30.0	over 30.0	
Percentage shares in the whole of resources						
	Content of sulphur to 0.4%					
0 to 200 m	0	0	0	0.0073	0.0095	0.017
201 to 400 m	0.07	0	0.073	0.48	0.0322	0.655
401 to 600 m	0	0	0.27	0.37	0.0571	0.698
601 to 800 m	0.003	0	0.375	0.793	0.20	1.371
801 to 1000 m	0	0	0.25	0.32	0.31	0.880
over 1000 m	0	0	0	0.14	0.04	0.180
SUM	0.073	0.000	0.968	2.111	0.649	3.801
	Content of sulphur from 0.41 to 1.0%					
0 to 200 m	0.20	0	1.38	1.01	0.028	2.618
201 to 400 m	0.016	0.61	5.82	2.08	0.031	8.557
401 to 600 m	0.034	0.28	7.46	7.09	0.46	15.324
601 to 800 m	0	0.57	7.41	13.19	2.01	23.180
801 to 1000 m	0	0.047	3.15	9.56	2.08	14.837
over 1000 m	0	0	2.32	4.17	0.26	6.750
SUM	0.250	1.507	27.54	37.1	4.869	71.266
	Content of sulphur from 1.01 to 1.6%					
0 to 200 m	0	0.081	0.46	0.048	0	0.589
201 to 400 m	0.04	1.06	2.83	0.54	0	4.470
401 to 600 m	0	1.21	4.69	0.77	0	6.670
601 to 800 m	0	0.76	3.52	1.04	0.083	5.403
801 to 1000 m	0.006	0	1.36	0.39	0.019	1.775
over 1000 m	0	0	0.35	0.0021	0.0041	0.356
SUM	0.046	3.111	13.210	2.790	0.106	19.263
	Content of sulphur from 1,61 to 2,2%					
0 to 200 m	0	0.114	0	0.010	0	0.124
201 to 400 m	0	0	1.49	0.00039	0	1.490
401 to 600 m	0	1.17	0.74	0.0054	0	1.915
601 to 800 m	0	0.063	0.166	0	0	0.229
801 to 1000 m	0.028	0	0	0	0	0.028
SUM	0.028	1.347	2.396	0.016	0.000	3.787
	Content of sulphur above 2.2 %					
0 to 200 m	0	0.025	0.0056	0	0	0.031
201 to 400 m	0	1,26	0.0033	0	0	1.263
401 to 600 m	0.042	0.123	0.151	0	0	0.316
601 to 800 m	0	0	0.0073	0.24	0	0.247
801 to 1000 m	0	0	0.025	0	0	0.025
SUM	0.042	1.408	0.192	0.240	0.000	1.882
TOTAL	0.439	7.373	44.306	42.257	5.624	100.00

Source: own study

CONCLUSIONS

The analysis of characteristic feature of coal seams, covering in Poland in thin seams, show that they are then the resources, in majority, very attractive to future exploitation. It is possible even to propose a thesis, that they are more attractive than, many thin coal seams exploited for decades in the Ukraine. The mining of Ukraine, with success, exploits such coal seams, then it is logic that it should also be back to their mining utilization in Poland

REFERENCES

Cichosz, P. 2000. *Systemy uczące się*. Warszawa: WNT.

Dokumentacja programu. 2010. STATISTICA v. 9.0.

Everitt, B.S., Landau, S. & Leese, M. 2001. – *Cluster analysis*. Londyn, Arnold, New York, Oxford: University Press.

Tadeusiewicz, R. 1993. *Sieci neuronowe.* Warszawa: AOW RW.

Materiały źródłowe Kompanii Węglowej S.A., Katowickiego Holdingu Węglowego S.A., Jastrzębskiej Spółki Węglowej S.A. oraz Południowego Koncernu Węglowego. 2010.

Technical and Geoinformational Systems in Mining – Pivnyak, Bondarenko & Kovalevs'ka (eds)

Bolt-pneumatic support for development workings with big cross-section

V. Buzilo, O. Koshka & A. Yavors'kyy
National Mining University, Dnipropetrovs'k, Ukraine

ABSTRACT: The article is concerned with problems of construction of underground workings with big cross-section. The paper is dedicated to questions of integrity face assurance and non-admission of its caving during construction of workings in soft rock, because otherwise great difficulties concerned with support and saving of their integrity occur. The results of theoretical, laboratorial and field observations of ways and means of support of faces of workings with big cross-section by bolt-pneumatic support are shown.

1 INTRODUCTION

While dealing workings with big cross-section, in underground passaging, in particular, big exposures of soft rock without support are not admitted. During construction of Kiev underground, in particular, the tunnelling was done the entry way of 1 m wide and 2 m high. The traditional technology of using steel beams and wooden laggings for face support is known to be high cost and labor intensive (Buzilo 2005).

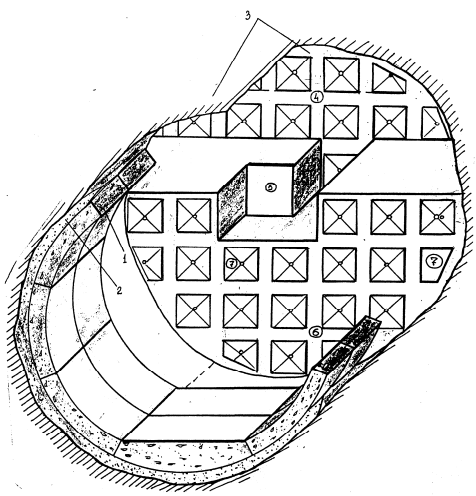

Figure 1. The technology of working with the application of bolt-pneumatic support: 1 − permanent support (lining); 2 − cement-and-sand grout slurry; 3 − rock mass; 4 − mined-out and bolted upper level; 5 − entry way being mined; 6 − lover level; 7 − bolt-pneumatic support.

The application of bolt-pneumatic support (BPS) with its soft shell of any size allows to keep face development with the entry way providing the whole area support. The suggested scheme of developing and supporting is shown in Figure 1.

The bolt-pneumatic support consists of a bolt, a soft shell and a face plate. To press properly onto the face, the soft shell must have a support. The main idea of the suggested supporting method is following: the soft shell with a face plate is held by a bolt. As the bolts the screw-in, drive, auger-type, spade, and other bolt kinds determined for soft rocks can be used here. In this context the bolt length is to be of the size with its working part located off possible caving rock zone.

The soft shell size is designed with the bolt-pneumatic support application technology and the proper holding power. Being made of metallic profile the face plate provides hard pressure of the soft shell filled with the compressed air to the rock.

2 DETERMINING OF THE BPS PARAMETERS OF FACE DEVELOPMENT WHILE WEDGE BLOCKS CAVING

While valuing the BPS holding power and the soft shell parameters we will proceed from the information about maximum caving blocks formed in the development face according to the full-scale researching data and results of theoretical research dealt with the determining of stress-train state zone in front of the moving face.

The analysis of the caving variants observed during building underground passages in clays shows that the wedge-shaped and prismatic blocks dumps are the most probable. Just for them we are to determine the BPS optimal parameters.

2.1 *Pull-out in a bolt*

While caving rock forming block is similar to wedge of dimensions D_B, L_B and a height H_B (Figure 2).

Under the boundary force balance the block is affected by the interbalanced forces system: the block weight $\vec{G}$, the reaction of unbroken rock massive $\vec{R}$, rock-to-rock friction force $\vec{F}_{TP} = f\vec{R}$, in which f – is rock-to-rock friction coefficient, and $\vec{F}$ – resultant force of shell elements.

The system balance condition is the following:

$$\vec{G} + \vec{R} + \vec{F}_{TP} + \vec{F} = 0 \qquad (1)$$

or in vertical or horizontal projections:

$$G = R\sin\alpha + fR\cos\alpha\ ;\ R\cos\alpha = F + fR\sin\alpha\ , \qquad (2)$$

where $tg\,\alpha = L_B / H_B$ (see Figure 2). Resulting:

$$R = G/\left(\sin\alpha + f\cos\alpha\right). \qquad (3)$$

$$F = G\left(1 - ftg\,\alpha\right)/\left(f + tg\,\alpha\right). \qquad (4)$$

If we know clay rock specific γ, we may get block weight:

$$G = \gamma H_B L_B D_B / 2\ . \qquad (5)$$

Resulting formulas (4), (5) allow to value total loading on a bolt when forming caving block near face surface, the block form is shown on Figure 2.

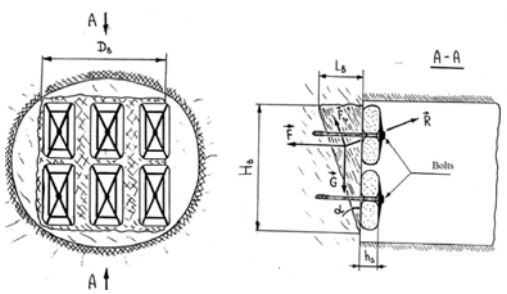

Figure 2. Design model of bolt-pneumatic support when edge blocks caving.

Joining formulas (4) and (5), we get

$$F = \gamma D_B H_B^2 \frac{1 - f\,L_B / H_B}{2\left(1 + f\,L_B / H_B\right)}. \qquad (6)$$

An average clay specific weight under natural conditions $\gamma = 19.3$ kN / m^3, so

$$F[\kappa N] = 9.65 D_B H_B^2 \frac{1 - f\,L_B / H_B}{1 + f\,L_B / H_B}\ . \qquad (7)$$

The most unacceptable conditions for support loading appear to be when rock-to-rock friction is ignorable, what allows to get maximal total loading on support for given block caving dimensions.

$$F_{max}\left(H_B, D_B\right) = 9.65 D_B H_B^2\ , \text{kN} \qquad (8)$$

Then for a caving block of $H_B = 8$ m, $D_B = 6$ m:

$$F_{max}\,(8\text{ m}, 6\text{ m}) = 463, \text{ kN} \qquad (9)$$

If caving block requires n soft shells, so an average force affecting a bolt makes:

$$P_3 = F_{max}\left(H_B, D_B\right)/n = 9.65 D_B H_B^2 / n\ , \text{kN} \qquad (10)$$

and with $H_B = 8$ m, $D_B = 6$ m

$$P_3(n) = 463 / n\ , \text{kN} \qquad (11)$$

The plot of maximal load P_3 on a bolt against a number of shells ensuring caving block support is shown on Figure 3. For $n = 40$, in particular, $P_3(40) = 12$ kN. If a caving block surface is covered by fewer shells load on a bolt grows and makes in this example:

$$P_3(30) = 15 \text{ kN};\ P_3(20) = 23 \text{ kN}$$

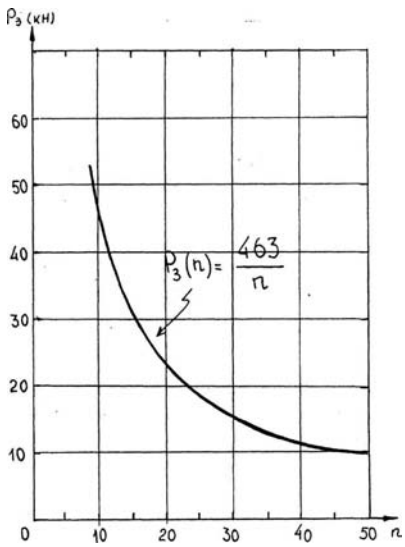

Figure 3. The plot of support load against shells number for a block dimensioning $H_B = 8$ m, $D_B = 6$ m ($\gamma = 19.3$ кN / m^3).

Formulas (8-11) allow to determine extreme load on bolt depending on caving block size and soft shells number, and, thus to make requirements for supporting power bolts used. Computations made on the ground caving data and the before obtained results have the right to claim that specific supporting power of bolts used is to be not less than 20 kN.

The obtained results help to solve the opposing problem: according to given bolt supporting power $P_{3,max}$ and limit block size we are to determine a proper number of soft shells.

$$n = int\left[\frac{\gamma D_B H_B^2}{2P_{3,max}}\left(\frac{1 - f\,L_B / H_B}{1 + f\,L_B / H_B}\right)\right]. \qquad (12)$$

2.2 *Determining a bolt length*

In determining a bolt length we ground on that it may have non-working part equals inrush depth in the considering cross-section $\ell_x = H_x\,tg\,\varphi = L_B H_x / H_B$, where H_x – distance from block base to observing bolt, ℓ_P – working part ensuring real bolt fastening with pinning strength at break $P_{3,max}$ and a value of bolt cross-section parameter S_T:

$$\ell_P = P_{3,max} / (\sigma_T S_T). \qquad (13)$$

where σ_T – clay fluidity limit at a bolt surface. A full length of bolt ℓ_a makes a value:

$$\ell_a = \ell_x + \ell_p = L_B H_x / H_B + P_{3,max} / (\sigma_T S_T). \qquad (14)$$

For the above considered matter with $P_3 = 20$ kN, $S_T = 0.051$ m^2: $\ell_a = 2.8$ m.

2.3 *Pressure in a soft shell*

To determine surplus internal pressure in a soft shell cavity ensuring a proper value F of all BPS shells pull to face surface we are to consider a design model in Figure 4.

In Figure 4 a ℓ_s и b_0 – soft shell initial length and width (in the plan), r_c – butt end corner radius, forming when come pressing of a face plate and a shell under pressure P and depending on compression value h_s.

Suppose d_a and h_a – are diameter and height of a collar, ensuring a hole in the shell centre.

On condition of inextensible of soft-shell fabrics we may determine length ℓ_s and width b_s of area contacting soft shell with a rock:

$$\ell_s = \ell_0 - h_s\,;\; b_s = b_0 - h_s\,. \qquad (15)$$

Butt end corner radius r_c is proportional to a compression value h_s and can be defined by formula $r_c = k \cdot h_s / 2$, where k – proportion coefficient.

In Figure 4 b one can see

$$d_p = h_s - h_a + d_a\,. \qquad (16)$$

Now we can deduce soft shell-rock contact area S_k:

$$S_k = b_s \ell_s - (1 - \pi/4) r_c^2 - \pi d_p^2 / 4\,.$$

or provided $k \approx 1$, we get:

$$S_k = (\ell_0 - h_s)(b_0 - h_s) - \left((1 - \pi/4) k^2 h_s^2 + \pi (h_s - h_a + d_a)^2 / 4\right). \qquad (17)$$

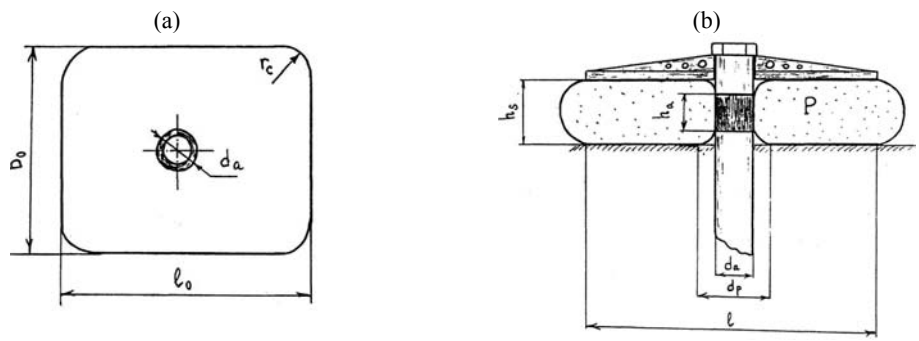

Figure 4. Design scheme of a soft shell of bolt-pneumatic support.

If n – is a total sum, number of the soft shells covering inrush area, so surplus pressure P in any shell cavity can be calculated by the formula:

$$P = \frac{F}{nS_k} = \frac{\gamma D_B H_B^2}{2nS_k}\left(\frac{1 - f\,L_B / H_B}{1 + f\,L_B / H_B}\right). \qquad (18)$$

Formula (17) for soft shell contact area can be simplified provided that for really applied soft shell $h_a \approx h_s$ and $k \approx 1$. Resulting:

$$S_k = (\ell_0 - 2r_c)(b_0 - 2r_c) - \\ -\left((1-\pi/4)d_p^2 + \pi d_a^2/4\right). \quad (19)$$

Technologically bearable support values of h_s make: 1) $h_s = 0.07$ m; 2) $h_s = 0.15$ m. Then accordingly we have: 1) $d_a \approx h_s/2$; 2) $d_a \approx h_s$ and equation (19) for both cases:

$$S_k\ (h_s = 0.07\ \text{m}) \approx b_0\ell_0 - h_s(b_0 + \ell_0) + 7\pi h_s^2/16, \\ S_k\ (h_s = 0.15\ \text{m}) \approx b_0\ell_0 - h_s(b_0 + \ell_0). \quad (20)$$

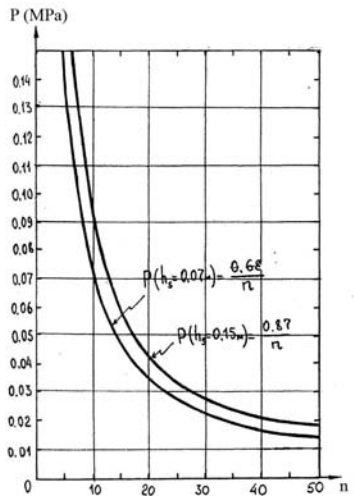

Figure 5. The dependence of surplus pressure in a soft shell cavity on soft shells number covering wedge block.

When applying soft shells with parameters $\ell_0 = 0.94$ m; $b_0 = 0.85$ m resulting from (20)

$$S_k\ (h_s = 0.07\ \text{m}) \approx 0.68\ \text{m}^2, \\ S_k\ (h_s = 0.15\ \text{m}) \approx 0.53\ \text{m}^2. \quad (21)$$

Using values F_{max} from (15) and S_k from (21) and substituting them into equation (18), we will find dependence of a surplus internal pressure in a soft shell cavity on their number under above considered caving block parameters:

$$P\ (h_s = 0.07\ \text{m}) = 0.68/n\ \text{, MPa} \\ P\ (h_s = 0.15\ \text{m}) = 0.53/n\ \text{, MPa} \quad (22)$$

The dependence diagrams provided by formulas (22), are given on Figure 5. In particular, with $h_s = 0.15$ m и $n = 40$ we have $P = 0.022$ MPa; and with $h_s = 0.07$ m и $n = 40$, $P = 0.07$ MPa.

3 DETERMINING OF SUPPORT PARAMETERS WHEN PRISMATIC BLOCKS CAVING

3.1 *Pull-out in a bolt*

Another type of block caving has a form approximate to the rectangular prism under the angle $(\pi/2 - \alpha)$ to the face line. As a rule, such blocks are formed in the face top near roof of working (Figure 6). The block balance condition is of the kind:

$$F = G(tg\,\alpha - f)/(1 + f\,tg\,\alpha), \quad (23)$$

where the block weight G is calculated by the formula:

$$G = \gamma H_B L_B D_B \cos\alpha. \quad (24)$$

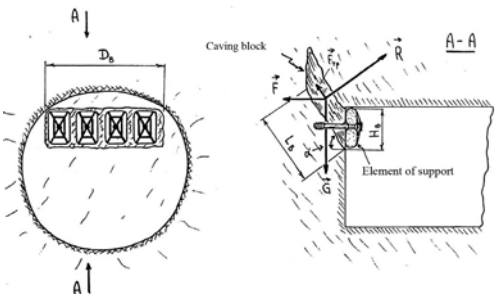

Figure. 6. Design model of BPS when prismatic blocks caving.

Joining formulas (23) and (24), resulting:

$$F = \frac{\gamma H_B L_B D_B \cos\alpha(\sin\alpha - f\cos\alpha)}{(\cos\alpha + f\sin\alpha)}. \quad (25)$$

There we do simplifications analogical to (8) resulting:

$$F_{max}(H_B, L_B, D_B) = \gamma H_B L_B D_B \sin^2\alpha$$

or when $\varphi \approx \pi/3$

$$F_{max}(H_B, L_B, D_B) = 2.6 H_B L_B D_B\ \text{, kN} \quad (26)$$

For the block dimensioning $D_B = 1.5$ m,

$H_B = 6$ m, $L_B = 6$ m, we have:

F_{max} (6 m, 6 m, 1.5 m) ≤ 140 , kN

3.2 *Pressure in the soft shell*

Surplus pressure in the soft shell cavity is calculated by the formula analogical (18):

$$P = \frac{F}{nS_k} = \frac{\gamma L_B D_B H_B \cos\alpha(\sin\alpha - f\cos\alpha)}{nS_k(\cos\alpha + f\sin\alpha)}. \quad (27)$$

that for the above-mentioned case ($h_s = 0.15$ m) becomes $P = 0.26/n$, MPa, with:

$$n \le int\left(\frac{H_B D_B}{b_0 \ell_0}\right). \quad (28)$$

The dependence diagram (27) is shown in Figure 7. In particular, for $n = 10$, we have $P = 0.026$ MPa, and for $n = 6$ – $P = 0.04$ MPa.

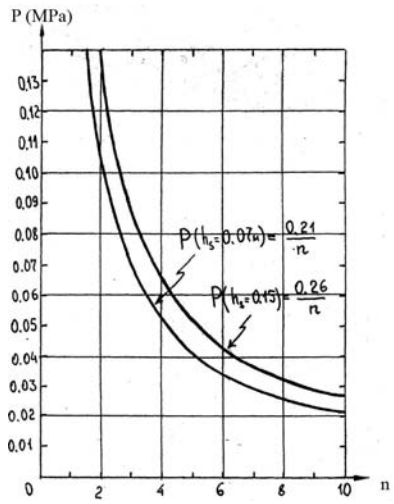

Figure 7. The plot of surplus pressure in the soft shells cavity against the shell number covering prismatic block of dimensions, when $D_B = 1.5$ m, $H_B = 8$ m, $L_B = 6$ m.

The designs made according to the described technique for bolt-pneumatic support for development in clays showed that BPS shall have the following values: shells number $n = 24$; pressure in a soft shell $P = 0.04$ MPa; pull in a bolt $P_a = 30$ кN, a bolt length $\ell_a = 2.8$ m.

4 THE RESULTS OF BPS TESTING UNDER THE FIELD OBSERVATIONS CONDITIONS

The BPS passed its industrial verification during building of the "Pecherskaya" station, zone #221. The wedge-shaped, drive and screw-in bolts were tested. The pull-out value was determined by the appliance PA-3.

For the wedge-shaped bolts installation the blast-holes of 36 mm in diameter and 1.5 m length were drilled. The drilling of one blast-hole with its further clearing took 3 minutes. The average pull-out value of the wedge-shaped bolt according to the testing results made 18 kN.

The drive bolts were made of drilling bars with the cross-section hexahedron-shaped and were mounted with the pneumatic hammer and the hydraulic prop HP-3. The drilling bar was hammered on the depth of 1 m during 1.2 minutes. The average pull-out value of the drive-bolt is – 13 кN.

The tested drive bolt parameters are given on Table 1.

The symbols used in the table 1 are the following (look at Figure 8): $S_n = \pi nt(d + 2h)$ – the surface area of the cylinder traversing the bolt thread; $S_0 = \pi h(d + h)$ – the area of one turn surface exposed face; $S_L = \pi d^2(L - nt)/4$ – the bolt surface area between the face and the threaded initial part; $S_c = \pi(d + 2h)^2/4$ – the bolt pipe cross-section area; $S = S_n + S_0 + S_L$ – the bolt surface total area.

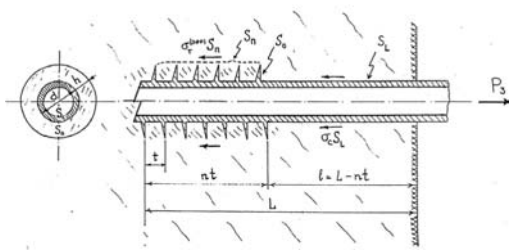

Figure 8. The scheme of drive bolt installing in the massive.

Figure 9 shows experimentally made diagrams of functional dependence of average resistance force F_c against the bolt penetration into the massive on the penetration depth (when driving bolts every 5-10 turns the force, level and depth of entry way were marked).

Table 1. The drive bolts parameters.

No of bolt	Diameter d (m)	Pace of a thread t (mm)	Height a thread h (mm)	Number of turns n	Penetration depth L (m)	$S_n \cdot 10^3$ (m^2)	$S_o \cdot 10^3$ (m^2)	$S_L \cdot 10^3$ (m^2)	$S \cdot 10^3$ (m^2)
1	0.065	0.02	0.08	9	1.00	4.58	1.885	2.725	50.360
2	0.033	0.02	0.08	6	1.52	6.20	1.030	1.265	8.495
3	0.049	0.02	0.08	9	1.20	36.8	1.433	1.923	40.150
4	0.033	0.03	0.08	9	1.00	41.6	1.030	0.700	43.330
5	0.033	0.02	0.08	9	1.15	27.7	1.030	0.825	29.560

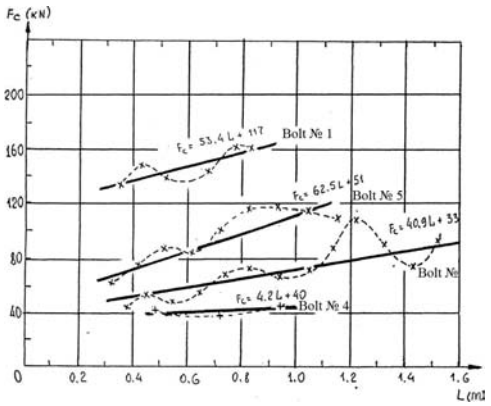

Figure 9. Functional dependence of average resistance force on penetration depth: −x−x− the results of measurements; _____ the lines of regression.

The data of drive bolts supporting power are given in the Table 2 and in the Figure 10.

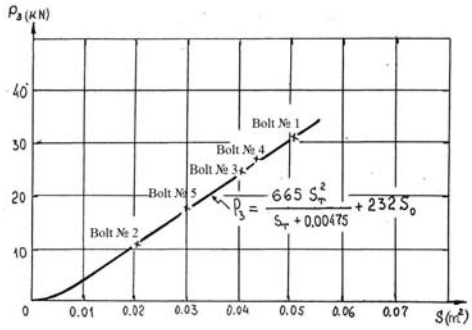

Figure 10. The plot of the drive bolt supporting power against the lateral surface area.

To compare various bolts by their supporting power in Table 3 one can find values of their specific supporting power, i.e. ratio of extreme load P_3 to the total surface resisting shift S.

Table 2. The bolts pull-out values.

No of bolt	$S_n \cdot 10^3$ (m^2)	$S_o \cdot 10^3$ (m^2)	$S_L \cdot 10^3$ (m^2)	$S \cdot 10^3$ (m^2)	P_3 (кН)
1	4.58	1.885	2.725	50.360	31
2	6.2	1.030	1.265	8.495	11
3	36.8	1.433	1.923	40.150	25
4	41.6	1.030	0.200	43.330	27
5	27.7	1.030	0.825	29.560	18

Table 3.The bolts compared of their supporting power.

No of bolt	$S \cdot 10^3$, m^2	P_3 / S, MN / м^2
1	50.360	0.616
2	8.495	1.295
3	40.150	0.623
4	43.330	0.623
5	29.560	0.609
bar	69.000	0.232

5 THE INDUSTRIAL VERIFICATION OF BOLT-PNEUMATIC SUPPORT (BPS) OF FACE

The BPS verification was done in the distilling tunnels of mines #221 and #225 of "Kyivmetrostroy" in accordance with the approved program and testing methodology.

The BPS verification was conducted in the workings of 5.5-8.5 m in diameter. The bolts of friction, screw-in, face plates and the soft shell were tested aiming at setting BPS parameters, defining applica-

tion efficiency and the bolt and soft shell labour productivity.

The bolt was mounted in the massive with its protruding part coated with soft shell and face plate both were fixed with the washer and nut. The bolt length made not less than 2.8 m while maximal "depth" of inrush could reach 2.3 m.

Being rectangular-shaped, dimensioning 850-940 mm with 20 mm width, the soft shell consisted of cap rock made of kapron fabrics and hermetic camera.

The grummet of 80 mm wide and the hole of 40-50 mm in diameter was set in the centre of the soft shell. The noise-piece with the stopper for compressed air fit-and-discharge was set in the lower lateral side.

The air for soft shell was given from mine manifold through the pressure regulator set on working pressure of 0.02-0.03 MPa. With the working pressure of 0.03 MPa in the soft shell the support section ensures the spread strength of 2.5 tons enough for holding and fastening the caving block dimensioning $6 \times 6 \times 2.3$ m. The face plate provided fast and reliable fastening to the bolt. The achieved time for the face plate and soft shell setting, fastening the bolt and filling in with compressed air made 1.5-2 minutes. The tests proved the BPS working capability and expediency of its application when working with big cross-section in soft rocks.

The BPS design Ukrainian and Russian patents defended (Petrenko 1992; Petrenko 1994; Buzilo 1994).

6 CONCLUSIONS

1. For the considered geological conditions there were determined the BPS parameters – the bolt's supporting power $P \geq 20$ кN, the bolt's length $\ell_a = 2.8 - 2.9$ m and the maximal surplus pressure in the soft shell cavity up to $P_{max} = 0.04$ MPa.

2. The dependence allowing to determine the extreme load in the BPS bolt by the dimension of the block rocks detached from the massive and the soft shells number can be obtained.

3. The dependence of surplus pressure in the pneumatic shell of support on the bolt's fastening strength and its contact area with the surface support or face has been found.

4. Using full-scale research data there has been defined the dependence of bolt's pull-out value on its depth penetration into the massive with clay.

5. There was determined the holding power of wedge-shaped bolt, hammer bolt and some drive bolts. The drive bolt of 33 mm in diameter and thread height of 12 mm appears to have the biggest supporting power ($P_3 = 30$ кN) and it is to be recommended for the application along with BPS under industrial conditions.

REFERENCES

Buzilo, V., Rahutin, V. & Serdyuk, V. 2005. *Potential for use of pneumatic constructions in underground mining*. International Mining Forum. New Technologies in Underground Mining. Safety and Sustainable Development. Poland: Taylor & Francis Group: 83-86.

Patent of Ukraine #93010056. 1992. *The method of temporary support of permanent mine workings within the zone of active rock pressure* / Petrenko, V.I., Rahutin, V.S., Kalinichenko, G.F., Buzilo, V.I. and others. (Ukraine). - Application date 02.12.1992.

Patent of Ukraine #94020546. 1994. *Method of face mining and support while mining in soft rocks* / Petrenko, V.I., Rahutin, V.S., Kalinichenko, G.F., Buzilo, V.I. and others. (Ukraine). - Application date 02.12.1994.

Patent #3849 (RF). 1994. *Method of temporary support of soft rocks and its performing mechanism* / Buzilo, V.I., Rahutin, V.S., Kalinichenko, G.F., Likhman, S.N. and others. (Ukraine). – Publication date. 27.12.94. Bul. #6-1.

Technical and Geoinformational Systems in Mining – Pivnyak, Bondarenko & Kovalevs'ka (eds)

About the influence of intense fracturing on the stability of horizontal workings of Eastern Donbass mines

P. Dolzhikov & N. Paleychuk
Donbass State Technical university, Alchevsk, Ukraine

ABSTRACT: The article presents the results of mine researches of stability of workings, as well as analytical studies of the parameters intensely fractured zones. Produced by typing parts of development workings out of the zones affected by coal-face works and by tectonic disturbance in terms of stability and fracture parameters. According to researches the classification of the various zones of workings.

1 INTRODUCTION

One of the main components that determine the economic and technological efficiency of underground coal mining is the state of development workings. On the state of the underground workings is influenced a lot of geological, technological and operational factors. To one of the most influential factors fracturing of rock massif is included. Analysis of domestic and foreign research in the field of geomechanics and mine buildings (Malinin 1970; Parchevskiy & Simanovich 1966; Erofeev 1977) shows that are currently under intense fracturing, basically, means the number of fissures per unit length or area of rock massif (Shashenko & Pustovoytenko 2004). However, this definition refers to an already formed system of fissures, primarily as a result of tectonic processes, i.e. to the natural and the tectonic fracturing types. In turn, according to (Dolzhikov, Paleychuk & Kobzar 2010), under intense refers to a fracturing, which is characterized by an to increase in the number and parameters of fissures over a fixed period of time in a certain direction of space. This definition is the technological fracture corresponds more.

In this regard, the influence of intensive technological fracturing on the state of development workings is actual.

2 FORMULATING THE PROBLEM

In the framework developed in the current classification of rock outcrops on the stability (Melnikov 1988), is put a sign of "bias rocks U ", which is a consequence of the geomechanical processes in rock massif around the workings. With the last one can only state what type of stability are those of certain rocks. This option is most reasonably be used during the building, before the installation of permanent roof supports. Since the period of exploitation there is an interaction roof supports with the rock massif, define about the sustainability of workings on the basis only the displacement of rocks is not correct for several reasons. In the first, in the hard rocks (sandstones, siltstones) of the investigated region at bias of rocks 0.5 m exploitation of working can be performed in accordance with the appointment, without prejudice to the processes, convenience and safety. However, there are cases when in a small bias of rocks (up to 0.3 m) was emergency state of roof supports, and the working of required repairs. Secondly, it is unclear how to classify the parts of workings with different values the bias of rocks and the state of roof supports, on the basis of what evidence to produce a comparison of different parts with the same values the bias, but in a different exploitation state. Thirdly, the need not only refers to the rocks of various categories of stability, but also to produce prediction in space and time of an emergency condition of the latter.

Thus, for qualitative assessment of the operational status of the development workings is necessary to classify their various parts on the intensity of fracturing in combination with other factors.

3 RESEARCH OF THE DEVELOPMENT OF FRACTURING IN WORKINGS

The object of investigation were selected horizontal development workings of seams h_8 and h_{10} of mines "Komsomolskaya" and "Partizanskaya" SE "Antratcite", as well as mine name V.V. Vakhrusheva SE "Rovenkiantratcite". Host rocks of coal seams in the region represented by siltstones, power m which in

the researched mines were in the range 4.7-9.5 m, and the temporary compressive strength σ_c perpendicular to the bedding planes was 53.7-64.2 MPa, by sand shale with $m = 2.8$-16.2 m, $\sigma_c = 67.5$-71 MPa, by mudstone with $m = 7$-24.6 m, $\sigma_c = 73$-96.8 MPa and by sandstones with $m = 9$-38 m, $\sigma_c = 135.7$-178 MPa. Angles to the dip of rocks in the studied workings were $\alpha = 2 \div 19^\circ$ in the depth range $H = 694 \div 1115$ m.

Due to the fact that the length of some of the workings up to 3 km in assessing their operational status of their total length was divided into plots of 40 m. The stability measure our ω_S, defined as the ratio of the actual minimum to project of area cross-section in part of working, as well as with index ω_N calculated as the ratio of the number of able-bodied frame of metal roof supports to their total number at a length of 40 m (Dolzhikov, Paleychuk & Kobzar 2010). The study found that between sustainability indicators ω_N and ω_S depend on, so for convenience of calculation in what follows, we use the index ω_N, as it is a quantitative characteristic of stability and allows you to visually compare the operational status of various parts of workings, while the figure ω_S – qualitative characteristic reflecting the change in cross-sectional area of workings after making the displacement of rocks. An analysis of the extent and nature of the deformation of rock massif and permanent roof supports in the mines SE "Antratcite" and SE "Rovenkiantratcite" meaningfully measure ω_N identified four types of the most characteristic zones: the value of indicator less than 0.5 – Zone I-type, with $\omega_N = 0.5 \div 0.65$ – Zone II-type, with a value $\omega_N = 0.651 \div 0.8$ – Zone III-type, and parts of workings with $\omega_N > 0.8$, respectively, Zone IV-type.

To determine the change of the sustainability indicator ω_N depending on the density of fractures of the rocks massif over a fixed period of time (1 month), during the year were instrumental investigations. With the help of photo planimetry method determines the initial value of fissures density λ, then determined the increment of the number of fissures on 1 m of working over time at different parts. The greatest interest is the intensity of fracturing, at which a qualitative transition part of working from the zones of the previous generation to the next zone types.

Results of the research of fracturing in horizontal development workings, lifetime over 5 years, outside the zone of influence of coal-face works and tectonic disturbance the for conditions of the seam h_{10} are shown in Figure 1.

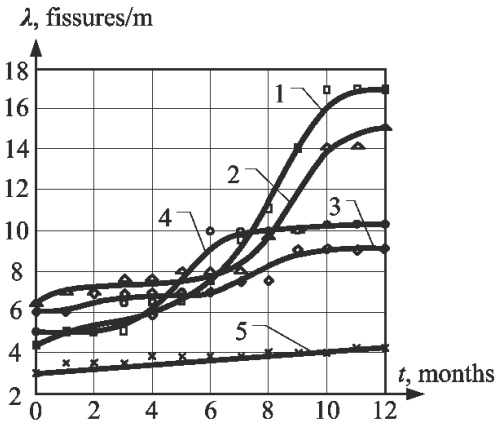

Figure 1. Graph of fissured in time zones of various types of development workings of seam h_{10}.

In Figure 1, line 5 corresponds to the zone IV-type at the end of the research. Curve 3 corresponds to the zone type II (the value of sustainability indicator $\omega_N = 0.6$) transition which occurred at the 8-th month of researches; up to this indicator ω_N, was 0.75 (Zone III type). On part of workings, represented by curve 4 in the current year indicator ω_N changed from 0.825 (May 2009) to 0.575 (April 2010). The transition from zone IV to zone III type occurred in the second month of research, and from zone III to zone II type – on the fifth. In the zones represented by curves 1 and 2 the value of the index ω_N were respectively 0.825 and 0.7 at baseline and 0.375, 0.45, after a year. On the part of working, which is characterized by curve 1, the indicator ω_N changed from 0.825 to 0.75 in the fourth month of researches, from 0.725 to 0.575 in the sixth, with 0.55 to 0.375 in the eighth. On part of working, the development of fissures roughness, which reflected the curve 2, the initial value of sustainability index was 0.7; the seventh month dropped to 0.64, while the tenth was reduced to 0.45.

Curves 1-5 are approximated by least squares corresponding functions of the form:

$$\lambda(t)_1 = 4.093 + 1.505t - 0.646t^2 + \\ + 0.115t^3 - 0.004t^4;\ R^2 = 0.85; \quad (1)$$

$$\lambda(t)_2 = 6.214 + 1.212t - 0.458t^2 + \\ + 0.065t^3 - 0.002t^4;\ R^2 = 0.78; \quad (2)$$

$$\lambda(t)_3 = 5.786 + 1.028t - 0.345t^2 + $$

$$+ 0.047t^3 - 0.002t^4;\ R^2 = 0.73; \quad (3)$$

$$\lambda(t)_4 = 5.205 - 1.033t + 0.583t^2 -$$

$$- 0.064t^3 + 0.002t^4;\ R^2 = 0.79; \quad (4)$$

$$\lambda(t)_5 = 3.261 + 0.011t;\ R^2 = 0.83, \quad (5)$$

where $\lambda(t)_1$, $\lambda(t)_2$, $\lambda(t)_3$, $\lambda(t)_4$, $\lambda(t)_5$ – density of fissures in time for the parts of workings represented by curves 1-5; (fissures / m) / mo.; t – commit time, the corresponding value of fissures density array, mo.

For dependencies (1)-(5) the accuracy of constant coefficients is 0,001. The choice of this value due to the necessity of appropriate accuracy of the approximation polynomial dependencies for subsequent determination of the intensity of fracturing.

Variation of density of cracks in time curves 1-4 corresponding approximated by polynomial dependences. Then, knowing the time at which there was a qualitative shift parts of workings of the bands previous to the zone of subsequent types, determine the intensity of fractures in these areas at which this transition occurred.

Because at the part, characterized by a direct 5 with time indicator of stability is not changed, for further research, this area are not interesting.

Intensity change of the x by function $y = f(x)$, provided that this function is continuous and differentiable at each point is defined as the first-order derivative:

$$v = f'(x) = \frac{dy}{dx}. \quad (6)$$

Thus, the expression for determining the intensity of fracturing in areas represented by curves 1-4, can be written accordingly:

$$v_1 = 1.505 - 1.292t + 0.345t^2 - 0.017t^3; \quad (7)$$

$$v_2 = 1.212 - 0.916t + 0.195t^2 - 0.009t^3; \quad (8)$$

$$v_3 = 1.028 - 0.69t + 0.141t^2 - 0.008t^3; \quad (9)$$

$$v_4 = -1.033 + 1.166t - 0.192t^2 + 0.008t^3. \quad (10)$$

The time at which the transition was detected parts of workings of the zones II-nd in the band I-th type for curves 1 and 2 is 8 and 10 months respectively. The intensity of fracturing in the transition zone of I-type is:

$$v_1 = 1.505 - 1.292 \cdot 8 + 0.345 \cdot 8^2 -$$

$$- 0.017 \cdot 8^3 = 4.5, \text{ (fissures / m) / mo}; \quad (11)$$

$$v_2 = 1.212 - 0.916 \cdot 10 + 0.195 \cdot 10^2 -$$

$$- 0.012 \cdot 10^3 = 2.51 \text{ (fissures / m) / mo.} \quad (12)$$

Similarly, we calculated the value of the intensity of fracturing in the transition parts in Zone II-nd and III-rd types. The results are shown in Table 1.

Table 1. Calculated values of the intensity of fracturing in zones of various types for the conditions of seam h_{10}.

Parameters	Types of zones							
	I-th type		II-th type				III-th type	
Number of curve	1	2	1	2	3	4	1	4
Commit time, the transition zone of this type, t, mo.	8	10	6	7	8	5	4	2
The density of fissures, λ, fissures / m	11	14	8	8	10	8	6	5
The intensity of fracturing, ν, (fissures / m) / mo.	4.5	2.51	2.5	1.2	0.95	1.0	0.8	0.6

Analysis of the dependences shows that, in the seams h_{10} most intensive development of fissures occurs in the moment of transition the part of working from the zone of II-nd in the zone of I-type, but less intense – in the transition zone of the IV-rd in the zone III-type.

In the graphs in Figure 2 shows the results of mine researches of fracturing in time for the conditions of seam h_8.

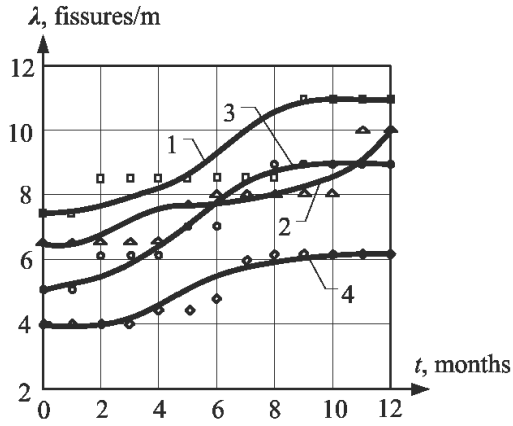

Figure 2. Graph of fissured in time zones of various types of development workings of seam h_8.

A curve 1 and 2 corresponds to the zone of I-th type at the end of the research. On zone, characterized by curve 1, the indicator ω_N changed from 0.825 to 0.7 at the fifth month research, from 0.7 to 0.5 in the seventh, with 0.5 to 0.45 in the tenth. In local areas of working, the development of fissured which affects the curve 2, the initial value of sustainability index was 0.875, the fifth month dropped to 0.675, was 0.55 at the eighth and the eleventh had fallen to 0.375. Curve 3 corresponds to the zone II-type, (value of the index of stability $\omega_N = 0.65$) transition which occurred at the 6-th month of studies, up to this figure ω_N site generation, representation, curve 3, was 0.775 (Zone III-rd type). In section, represented by curve 4 in the current year figure ω_N changed from 0.9 to 0.75. The transition from zone IV-th zone III-first type occurred in the third month of studies, and from the zone of the III-rd in the zone II-type – on the fifth.

Curves 1-4 well approximated by the corresponding polynomial dependence:

$$\lambda(t)_1 = 7.193 + 1.370t - 0.501t^2 + $$

$$+ 0.068t^3 - 0.0025t^4;\ R^2 = 0.82; \quad (13)$$

$$\lambda(t)_2 = 6.609 - 0.592t + 0.312t^2 -$$

$$- 0.041t^3 + 0.002t^4;\ R^2 = 0.88; \quad (14)$$

$$\lambda(t)_3 = 5.086 + 0.129t + 0.078t^2 - 0.005t^3;$$

$$R^2 = 0.91; \quad (15)$$

$$\lambda(t)_4 = 4.102 - 0.336t + 0.130t^2 - 0.007t^3;$$

$$R^2 = 0.78. \quad (16)$$

By the method of determining the intensity of fracturing for the seam h_{10} similar calculations were performed for the seam h_8. The results of calculations are summarized in Table 2.

Table 2. Calculated values of the intensity of fracturing in zones of various types for the conditions of seam h_8.

Parameters	Types of zones								
	I-th type		II-th type				III-th type		
Number of curve	1	2	1	2	3	4	1	2	4
Commit time, the transition zone of this type, t, mo.	10	11	7	8	6	5	5	5	4
The density of fissures, λ, fissures / m	11	7	8.75	8	7	4.5	8	7	4
The intensity of fracturing, v, (fissures / m) / mo.	1.75	2.0	0.9	0.62	0.5	0.4	0.2	0.39	0.35

As follows from the results in the seam h_8 the most intensive development of fissured was observed in the transition parts of the workings of the zones II-nd in the band I-type, but less intense – in the transition sections of the workings of zones IV-th zone in the III-th type .

Comparative analysis of results shows that the nature of fracture in time for the consideration seams is different. This fact is due to the substantial difference of deformation and strength properties of host rocks. However, the most intensive development of fractures observed in the transition parts of workings in the zone I-th type of seams conditions h_{10} and h_8.

Based on these calculations, as well as analysis of field researches, zones I-th type can be described as intensely fractured, zone II-type – as a zone of active development of fissures, III-first type – the zone activation of fissures, and zone IV-type – as a zone of potential development of fracture.

4 DEVELOPMENT OF CLASSIFICATION PARTS OF MINE WORKINGS

The basis of the developed classification is laid features of the intensity of fracturing v in zones of different types of seams h_8 and h_{10}. For the most complete description of the operational status of development workings in the classification were also used parameters such as time compression strength σ_c perpendicular to the bedding planes of rocks, the average power of rocks m, averaged over the length of the parts of the offset value of displacement of rocks U, density of fissures massif λ, as well as the values indicators ω_N and ω_S, which were obtained and analyzed as a result of the mine field researches. Along with this, the most important parameter is likely inrushes, which determines the degree of development of accident and the need to be repaired of working.

Table 3. Classification zones of development workings.

Parameters	Marking of zones			
	I-th type	II-th type	III-th type	IV-th type
Sustainability indicator, ω_N	$\omega_N < 0.5$	$0.5 \le \omega_N \le 0.65$	$0.65 \le \omega_N \le 0.8$	$\omega_N > 0.8$
Sustainability indicator, ω_S	$\frac{< 0.6}{< 0.65}$	$\frac{0.6 \div 0.72}{0.64 \div 0.74}$	$\frac{0.73 \div 0.85}{0.75 \div 0.84}$	$\frac{> 0.85}{> 0.84}$
The temporary roof rock strength, σ_c; MPa	$\frac{50 \div 90}{80 \div 160}$	$\frac{50 \div 80}{110 \div 153}$	$\frac{62.5 \div 85}{92 \div 168}$	$\frac{72 \div 97}{110 \div 180}$
Power roof rocks, m; m	$\frac{5 \div 13}{5 \div 20}$	$\frac{7 \div 14}{7.7 \div 25}$	$\frac{8.5 \div 20}{10 \div 28}$	$\frac{13.6 \div 25}{13 \div 38}$
Density of fracturing, λ; fissures / m	$\frac{11 \div 20}{7 \div 13}$	$\frac{7.5 \div 10}{4.5 \div 8.75}$	$\frac{5 \div 8}{4 \div 8}$	$\frac{3 \div 7}{1 \div 5}$
The mean value of the displacement of rocks, U; m	$\frac{> 0.65}{> 0.5}$	$\frac{0.46 \div 0.65}{0.34 \div 0.5}$	$\frac{0.16 \div 0.45}{0.15 \div 0.33}$	$\frac{\le 0.15}{\le 0.14}$
The intensity of fracturing, ν, initiating the transition zone of this type; (fissures / m) / mo.	$\frac{>2.5}{>1.0}$	$\frac{0.95 \div 2.5}{0.4 \div 1.0}$	$\frac{0.4 \div 0.94}{0.2 \div 0.39}$	--
Probability of inrushes, $P(A)$; %	87	30	2.8	0.5

By generalizing the materials mining and analysis was the classification of the zones, which is shown in Table 3. In the numerator are given values parameters for the seam h_{10}, and the denominator – for the formation h_8.

The main practical advantage of the proposed classification is the ability to predict changes in the workings of sustainability indicators, as well as the probability inrushes in bed h_8 and h_{10} Eastern Donbass mines based on the values density and intensity of the fractured edge of a rock massif that will allow efficient use of interventions to prevent inrushes and increase the stability of development workings.

5 CONCLUSIONS

1. For a characterization of the fracture of rocks, in addition to parameters such as disclosure and the density of fissures, it is advisable to use a parameter of intensity, which corresponds to the rate of fracturing is one of the criteria for determining the probability inrushes at the local areas of workings.

2. The researches established the values of density and intensity of fracturing for mining and geological conditions of seams h_{10} and h_8 deep mines of the Eastern Donbass, in which there is a change of stability parts of workings and there is a qualitative shift from one zone to another zone type.

3. The developed classification parts of workings

contains the quantitative (indicator ω_N) and qualitative (indicator ω_S) stability characteristics which depend primarily on the intensity of fracturing.

4. The advantage of the developed classification is the ability to predict changes in the indices of stability depending on the intensity of fracturing and other factors.

REFERENCES

Malinin, S.I. 1970. *Geologichyeskiye osnovy prognoza povedyeniya porod v gornykh vyrabotkakh po razvedochnym dannym.* Seriya: Gorno-geologichyeskaya. Moscow: Nyedra, 192.

Parchevskiy, L.Ya. & Simanovich, A.M. 1966. *Issledovaniye vliyaniya porodnykh polos na sostoyaniye podgotovityelnykh vyrabotok.* Kommunarsk: Donbasskiy gorno-metallurgichyeskiy institut: 168.

Erofeev, B.N. 1977. *Prognozirovaniye ustoychivosti gornykh vyrabotok*. Alma-Ata: Nauka: 81.

Shashenko, A. N. & Pustovoytenko, V.P. 2004. *Mekhanika gornykh porod.* Uchyebnik dlya VUZov. Kyiv: Novyi druk: 400.

Dolzhikov, P.N, Paleychuk, N.N. & Kobzar, Yu. I. 2010. *Isslyedovaniye osobennostey usloviy ekspluatatcyi arochnykh ramnykh kryepey v zonakh intensivnoy tryeshchinovatosti*. Zbornik nauchnykh trudov. Dnipropetrovs'k: Natcionalnyi Gornyi Universityet: 4, T. 1., 280.

Melnikov, N.I. 1988. *Provedyeniye i kreplyeniye gornykh vyrabotok.* Moscow: Nyedra: 336.

Technical and Geoinformational Systems in Mining – Pivnyak, Bondarenko & Kovalevs'ka (eds)

The nature and prediction of regional zones for development of dynamic phenomena in the mines of the Donets Coal Basin

A. Antsiferov & V Kanin
UkrNIMI NAS of Ukraine, Donetsk, Ukraine

M. Dovbnich & I. Viktosenko
National Mining University, Dnipropetrovs'k, Ukraine

ABSTRACT: The main notions of method and results of regional zones prediction for development of dynamic phenomena in mines of the Donets Coal Basin are considered. Researches on the basis of geological environment mechanical stresses estimation caused by the Earth equilibrium state disturbances on gravimetric data are executed. A detailed comparison of computed stress fields with gas-dynamic phenomena occurred during mining of seams in A.F. Zasyadko mine was made. The authors are convinced that in investigation of dynamic phenomena in geologic environment, independently of their scale – earthquakes, rock bursts, gas-dynamic phenomena and others – the most important element is study of all whole factors, starting from planetary and ending by local ones, which result in disturbance of equilibrium state of the planet and cause occurrence of mechanical stresses in the outer shells of the Earth.

1 INTRODUCTION

The Donets Coal Basin is the main fuel-energy region of Ukraine. For its development inestimable human resources have been used. For that reason human losses, sometimes accompanying coal production, are very appreciable. Accident prevention in mining is the main industrial-functional problem of coal producers that requires the most careful attention and science knowledge.

In coal mines of the Donets Coal Basin, as, it must be said, in any other coal regions where coal is produced underground, at all times there has long been risk of dynamic phenomena in mine workings. In the first instance the risk is due to dynamic phenomena - sudden outbursts.

Sudden coal, rock and gas outbursts are in the form of avalanche-like collapse of the breast part of coal (rock) mass as a result of which considerable material resources are spent and people die. Generally sudden outbursts occur after some preparation period duration of which is determined by several factors:

– *geological one* connected with a series of geological processes at all stages of coal deposit formation;

– *human-induced one* connected with changes in geomechanical condition of rock mass surrounding mine working as a result of advance mining of the neighboring seams;

– *technological one* connected with changes in gas-dynamic mode of the breast part of the seam in the process of its mining under the influence of different methods and techniques of rock mass impact;

– *current one* connected with energy state of the breast part of rock mass at a time.

And if three latter factors are determined mainly by the human-induced impact on rock mass being mined, geological factor is of purely natural origin. One of the most important characteristics that determine the role of geological factor is tectonic stresses. Specifically, in conditions of the Donets Coal Basin these are stresses arising in deformation of sedimentation mass during movement of the basement blocks. By its nature the natural component of the mechanism of dynamic phenomena in mine workings in many respects is similar to earthquake generating mechanism. Actually dynamic phenomena can be considered as a step-like process of coal-rock mass discontinuity during mining that disturbs natural stress state, which in its turn is determined both by weight of overlying rocks and by tectonic processes that took place and are taking place within rock mass. In these circumstances the type of dynamic phenomenon is determined by the properties of rock mass itself.

2 FORMULATING THE PROBLEM AND METHOD

Stress-deformed state of subsurface is one of the key factors in the nature of occurrence of multiscale dynamic phenomena. In general case in any point of rock mass stress state is determined by the weight of overlying rocks and tectonic factors, and in case of mining it is also determined by redistribution of stresses around mine working. The features of spatial distribution of tectonic stresses are more complex than those of lithostatic ones. Using the terms of exploration geophysics we can say that lithostatic stresses are normal and tectonic stresses are anomalous. It is important to distinguish tectonic stresses arising under the effect of planetary factors and stresses due to secondary deformation processes in subsurface, e. g. crustal block movements, folding and faulting. More over, it is important to realize that it is the case of stress field change with time. We can speak like that about recent stresses and paleo-stresses acted in geological past that have been relaxed partially or completely so far. The defining role in maintaining considerable level of recent tectonic stresses is plaid by neo-tectonic activity within any given territory. In this connection one of the topical problems in research into geologic causes for occurrence of dynamic phenomena in mine workings is prediction of geodynamically active zones.

Basically, idea to research into zones for development of dynamic phenomena within the Donets Coal Basin attracting information on neo-tectonic activity is not new. In the beginning of 1960-s of XX century G.A. Konkov (Konkov 1962) put forward a concept of grouping coal and gas outbursts into linear zones. His research was based on comprehensive analysis of coal and gas outburst distributions and idea of their connection with recent tectonic movements. In his works G.A. Konkov identified a number of zones striking northeast which, on his judgment, corresponded to the regions of the strongest movements. Later G.A. Konkov's ideas have found their development in the works of V.S. Vereda et al. (Vereda et al. 1968), who also identified regional gas-dynamic zones striking northeast, supposing that regional outburst-prone zones reflect increased tectonic stresses in coal-bearing sediments of the Donets Coal Basin connected with increased recent ground surface deformations. V.A. Privalov (Panova et al. 2009) in his research showed tectonic nature of zones of bursting liability in the Donets Coal Basin, specifically their connection with shear dislocations.

The authors of this work also hold to an opinion on the confinedness of dynamic phenomena in mine workings to geodynamically active zones of tectonosphere and suppose that research into stress fields is the most important stage in identifying geodynamically active zones in prediction of the zones for development of geodynamic phenomena in mine workings.

The objective of this work is to consider main points of the method and the results of prediction of the regional zones for development of dynamic phenomena in the mines of the Donets Coal Basin.

The basis for the proposed approach is the model of the rotating Earth equilibrium state proposed by K.F. Tyapkin and called *geoisostasy*, which is well covered in geological references (Tyapkin 1980 & Tyapkin 1985). Today computation algorithms for tectonosphere stress fields due to disturbance of the Earth equilibrium state are developed based on the analysis of geoid anomalies (Dovbnich 2008).

In previous work (Dovbnich & Demyanets 2009) it was shown that geodynamically active zones of tectonosphere manifest themselves in stress anomalies attributable to disturbance of the Earth equilibrium state. First and for most such zones, on the assumption of sufficient value of stresses acting therein, manifest themselves as seismically active (Demyanets & Dovbnich 2010). Elements that are tectonic basis for seismo-generating structures find their reflection in the stresses under consideration.

3 RESULTS

In conditions of the Donets Coal Basin computations for estimation of subsurface stress state attributable to disturbance of the Earth equilibrium state were made based on ground gravity survey data on a 1:200,000 scale and a digital terrain model. For the most part of the territory of the region, based on the author's method (Dovbnich & Demyanets 2009; Demyanets & Dovbnich 2010), geoid anomalies were reconstructed by ground gravity data – Faye gravity anomalies on 4x4 km grid (Figure 1). The obtained geoid anomalies served as the basis for computation of stress fields at the territory under investigation.

In order to determine position of the estimated stress fields in tectonics and geodynamics of the investigated region and also the influence of multiscale and multi-depth processes on the disturbance of the equilibrium state we divided stress fields into local and regional components. Comprehensive analysis of the estimated stress fields, tectonics of the Priazovsky block of Ukrainian Shield (US) and junction zone of US and Donets Coal Basin allows us to suggest that the regional stress field component reflects mainly block structure of crystalline basement which is in multi-stress state. Taking into account that dynamic phenomena in mines are con-

fined to sedimentation mass of the Donets Coal Basin it becomes evident that we should look for their connection with the local stress field component attributable to the disturbance of equilibrium state, which, on the authors' opinion, reflects mainly deformation processes in sedimentation mass. At the same time, confinedness of stress field local anomalies to gradient zones of regional anomalies is being clearly identified that speaks for their genesis in the course of development of fault-block crystalline basement.

Theoretic prerequisites for connection of dynamic phenomena, zones of migration and accumulation of hydrocarbons in coal-rock mass with the features of subsurface stress state allows us to use stress fields, attributable to disturbance of the Earth's equilibrium state, as additional predicted criterion in solving the problem of prediction of regional zones for development of dynamic phenomena in mine workings. The working assumption for such constructions can be the following statement. *Regional zones for development of dynamic processes shall be determined by the degree of deformation processes occurring in sedimentation mass, which in their turn find their reflection in the local component of stress field attributable to disturbance of the Earth's equilibrium state.*

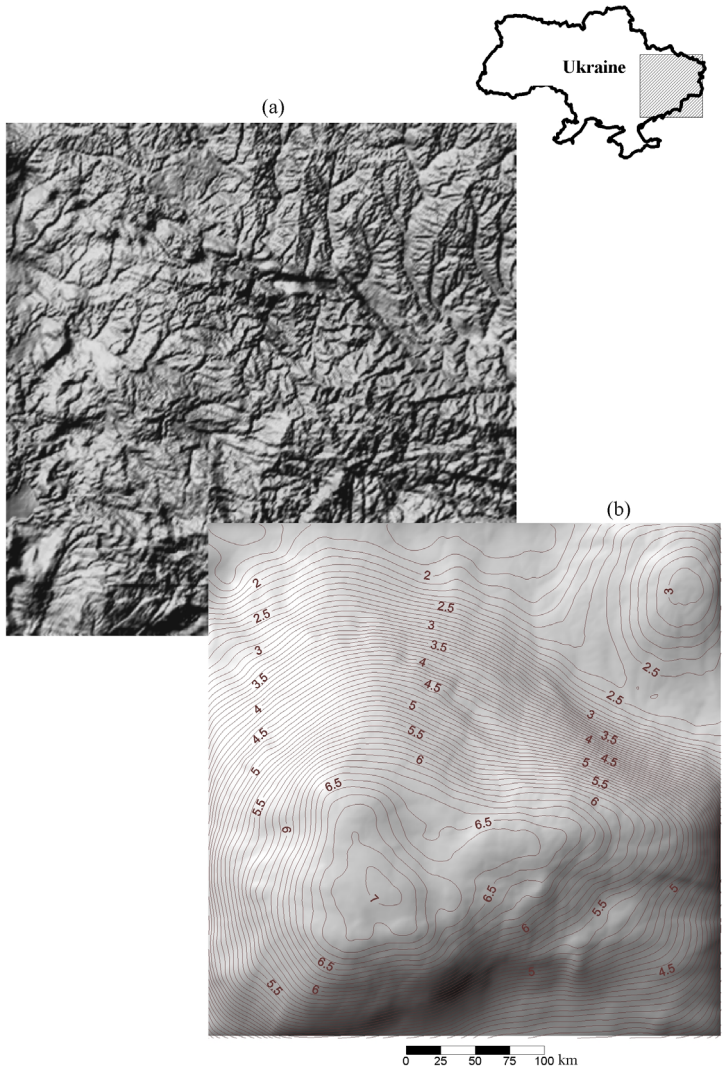

Figure 1. Light-shadow map of Faye gravity anomalies (a) and the result of reduction of geoid anomalies (b), m.

Stress field integral characteristic that reflects the whole of deformation phenomena can be energy of elastic deformations, which computation is not difficult if stress tensor is known. According to the above working assumption this characteristic can be considered as indicator of stored by coal-rock mass elastic energy related to its deformation.

As a case study of our constructions we consider predicted map of the regional zones for development of dynamic phenomena constructed on the basis of the local component of the energy of elastic deformations (Figure 2).

Comparison of the identified zones with the regional stress field component and localized boundaries of the basement blocks allows us to state the key role in their genesis of the movements of crystalline basement, both in geological past and recent ones.

During our investigations we made a more detailed comparison of the estimated stress fields with gas-dynamic phenomena occurred when extracting seams m_3, l_4, l_1 and k_8 at A.F. Zasydko Mine (Figure 3).

The Mine is methane super-hazard, prone to sudden coal, rock and gas outbursts and prone to coal dust explosibility (Antsiferov et al. 2009). Immense tragedy related to the operation of Ukrainian coal mines over the whole of the post-war history were three explosions that took place on 18.11.07, 01.12.07 and 02.12.07 at A.F. Zasydko Mine and took lives of 106 miners, tens of mine workers were hospitalized.

In tectonic terms the mine field is located in the south part of the Kalmius-Toretskaya depression, on the elevated flank of the Vetkovskaya flexure. Here Carboniferous deposits have gentle north-east dip with angles 7-25°. The mine field on the west is limited by the Vetkovsky and Panteleimonovsky Faults with amplitudes 35-55 m. At present coal seams m_3, l_4, l_1 and k_8 are being developed at the depth 1200-1400 m.

At the first stage of our research we made comparison of gas-dynamic phenomena occurred when extracting seams m_3, l_4, l_1 and k_8 with local stress fields estimated by ground gravity survey data on a 1:200,000 scale on 1x1 km grid (Figure 4).

As it is evident from the Figure 4, gas-dynamic phenomena within the Mine can be divided into two groups: 1 – majority of the phenomena is confined to the anomaly of intensive shear stresses; 2 – less of the phenomena is confined to the impact zone of the Vetkovsky Overlap Fault and is related to the anomaly of compressive stresses.

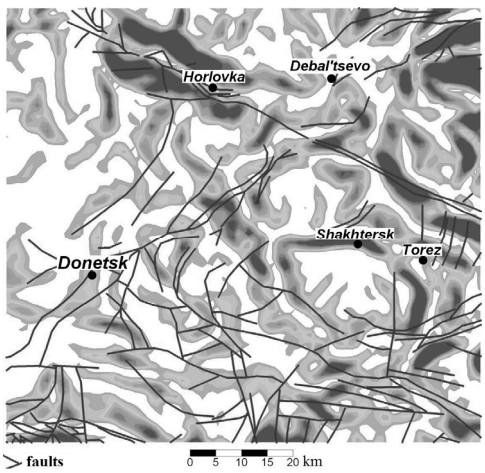

Figure 2. Fragment of the prediction map of the regional zones for development of dynamic phenomena.

Figure 3. Comparison scheme of lay-out of in-seam l_1 workings with the main faults: 1 – gas-dynamic phenomena, 2 – predicted zones of methane accumulation (Goncharenko et al. 2007), 3 – faults.

The most part of the zones of methane accumulation predicted by a set of independent methods (Goncharenko et al. 2007) is also related to the anomaly of intensive shear stresses. We think that formation of regions of methane transition into free state, development of the ways of its natural migration and occurrence of the zones of methane accumulation are closely related to the increase in cavity space and coal-rock mass permeability under the effect of mechanical stresses of tectonic nature.

It should be noted that in case of the effect of shear stresses fracture opening and reservoir formation occur, gas drainage of coal-rock mass will be much lower than that of fracture opening under the effect of tension stresses. Thus we can state that within the limits of A.F. Zasyadko Mine, in addition to the human-induced component that has decisive influence on the development of gas-dynamic phenomena, of considerable importance is natural stress state of coal-rock mass responsible for both confinedness of dynamic phenomena to geodynamically active zones and development in coal-rock mass of conditions favorable for their occurrence, in particular, formation of the zones of methane accumulation (Viktosenko et al. 2011).

At the second stage of our research, for more complete analysis of deformation processes in sedimentation mass, we employed trend-analysis for the surface of coal seam m_3 within the limits of mine field as a result of which a map of local folding that complicates close monoclinal bedding of this seam (Figure 5) was obtained. This folding is the difference of the seam surface and its approximating surface which is 3rd order polynomial.

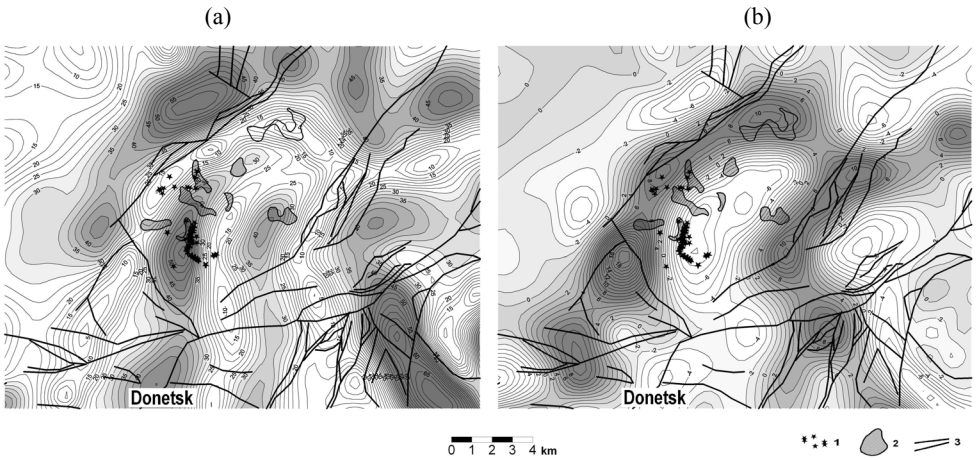

Figure 4. Comparison scheme of gas-dynamic phenomena at A.F. Zasydko Mine with the local stresses (kPa): shear stresses (a), compression-tension stresses (b); 1 – gas-dynamic phenomena, 2 – predicted zones of methane accumulation (Goncharenko et al. 2007), 3 – faults.

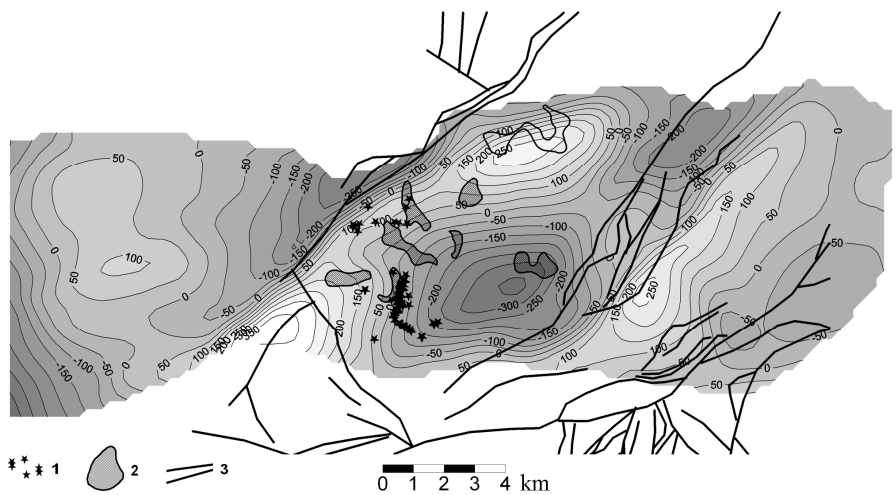

Figure 5. Comparison map of local folding of the seam m_3 with gas-dynamic phenomena: 1 – gas-dynamic phenomena, 2 – predicted zones of methane accumulation (Goncharenko et al. 2007), 3 – faults.

Comparing a map of local folds with dynamic phenomena and predicted zones of methane accumulation we see that majority of them is confined to the gradient zone of local folds, the nature of which is closely connected with the processes that find their reflection in the anomalies of intensity of the local shear stresses. These regularities dramatically confirm the fact of confinedness of gas-dynamic phenomena to the zones of seam kinks (Zabigailo et al. 1974).

Regularities identified within the limits of A.F. Zasyadko Mine field confirm previously made suggestions on the connection of certain components of stress field, attributable to disturbance of the Earth's equilibrium state, with deformation processes in sedimentation mass and reflection therein of the zone of development of dynamic phenomena.

5 CONCLUSIONS

It is important to realize that this characteristic is unique, but not exclusive, that determines geologic factor of the occurrence of dynamic phenomena in mine workings. Only comprehensive consideration of stress fields, tectonics, and features of coal seam hypsometry, depth of occurrence of coal seams, metamorphism intensity and other factors will allow improving reliability of such constructions.

Prediction on the fields of operating mines and those being built of stressed areas, potentially prone to gas-dynamic phenomena, will allow making early control improving mine safety and substantially reducing costs on non-hazardous areas thus improving efficiency of mine practice.

Most interesting opportunities are being afforded in integration of the proposed in this work approach with GPS monitoring. In this case the territory of the Donets Coal Basin shall be covered by stationary operating grid of GPS profiles on which their elevations are determined in one and the same points. Thus uplift velocity-anomalous relaxation areas shall be identified under which existence of anomalous subsurface stress is assumed. By so doing, on the one hand, stress fields connected with disturbance of equilibrium state and maps of recent movements could be independent indicators mutually complementing each other. And on the other hand, employment of information on stress state will allow optimizing grid of GPS receivers. As a result of such integration we propose generating a map of stress-deformed state of the Donets Coal Basin paying special attention exclusively to the stressed areas potentially prone to gas-dynamic phenomena. Geochemical investigations at the hazardous areas shall be conducted with the aim of determining isotopic composition of combustible gases escaping into mine workings and generating maps of distribution of subsurface gases.

Also promising in such anomalous zones is geomechanical modeling of deformation processes in sedimentation mass in order to estimate stress-deformed state followed by geologic interpretation. Today seismic survey is the only geophysical method that allows, on one hand, making detailed structural constructions of formation studied, where total deformations experienced by geologic environment during its development (from accumulation of sediments to manifestation of recent neotectonics) find their reflection, and, on the other hand, based on the analysis of elastic wave propagation velocity and density of geologic environment to give correct enough information related to subsurface elastic properties (Kozlov, 2006). As consequence, we have information required to estimate subsurface stress-deformed state due to the deformation processes therein. In recent years researches repeatedly noticed in their works a possibility to study stress-deformed state on the basis of subsurface structural velocity models by seismic data in solving problems of petroleum and coal geology (Kozlov, 2006, Dovbnich et al. 2009 & Dovbnich et al. 2008).

The authors argue that in research of subsurface geodynamic phenomena, regardless of their scale – earthquakes, rock bursts, gas-dynamic phenomena and others, the most important element is study of the whole of factors, beginning from planetary and ending with local ones that lead to disturbance of global equilibrium state and contributing to the occurrence of mechanical stresses in the outer shells of the Earth.

REFERENCES

Konkov, G.A. 1962. *On the connection of the newest and recent tectonic movements with methane-bearing and outburst-prone zones in conditions of the Donets Coal Basin.* Reports of the Academy of Sciences of the USSR, 3: 670-673.

Vereda, V.S. & Yurchenko, B.K. 1968. *On the correlation of the Donets Coal Basin gas-dynamic zones, coal fracturing and thermal behavior with recent tectonic movements.* Recent movements of the Earth's crust. Moscow: Nedra. Volume 4: 80-89.

Panova, O.A., Pryvalov, V.A., Izart, A., Alsaab, D. & Antsiferov, A.V. 2009. *Geodynamical Events (Coal-and-Gas Outbursts) in the Donets Basin.* EAGE 71th Conference and Technical Exhibition, Expanded Abstract: 222.

Tyapkin, K.F. 1980. *New rotational hypothesis of structure formation and geoisostasy.* Geophysical Journal, 5: 40-46.

Tyapkin, K.F. 1985. *New model of geoisostasy and tectonogenesis.* Geological Journal, 6: 1-10.

Dovbnich, M.M. 2008. *Disturbance of geoisostasy and stress state of tectonosphere.* Geophysical Journal, 4: 123-132.

Dovbnich, M.M. & Demyanets, S.N. 2009. *Tectonosphere stress fields attributable to geoisostasy and geodynamics of the Azov Sea-Black Sea region.* Geophysical Journal, 2: 107-116.

Demyanets, S.N., Dovbnich, M.M. 2010. *Satellite and Ground Gravimetry - The Innovative Approaches in Studying the Earthquake Nature and Prognosis.* EAGE 72th Conference and Technical Exhibition, Expanded Abstract: 582.

Antsiferov, A.V., Golubev, A.A., Kanin,V.A., Tirkel, M.G., Zadara, G.Z., Uziyuk, V.I., Antsiferov, V.A. & Suyarko, V.G. 2009. *Gas content and methane resources of Ukrainian coal basins.* Volume 1. Donetsk: Veber: 456.

Goncharenko, V.A., Svistun, V.K., Gerasimenko, T.V. & Malinovsky, A.K. 2007. *Prospects for integrated geologic-geophysical prediction of methane accumulation zones at coal deposits of the Donets Coal Basin*. Naukovy visnik of the National Mining University, 4: 73-77.

Viktosenko, I.A., Dovbnich, M.M. & Kanin, V.A. 2011. *Regional Zoning of Dynamic Phenomena in Mines – The Innovative Approaches in Gravimetry*. EAGE 73th Conference and Technical Exhibition, Expanded Abstract: 281.

Zabigailo, V.E., Shirokov, A.Z., Bely, I.S., Kudelsky, V.V., Mossur, E.A. & Rudometov, B.P. 1974. *Geological factors of bursting liability of rocks in the Donets Coal Basin*. Kyiv: Naukova dumka: 270.

Kozlov, E.A. 2006. *Subsurface models in exploration seismology*. Tver: GERS: 480.

Dovbnich, M.M., Soldatenko, V.P. & Bobylev, A.A. 2009. *Estimation of stress-deformed state on the basis of structural velocity models: new opportunities in solving petroleum geology problems*. Seismic exploration technologies, 2: 12-18.

Dovbnich, M.M., Soldatenko, V.P. & Bobylev, A.A. 2008. *Estimation of stress-deformed state of coal-rock mass on the basis of structural velocity models*. Geotechnical mechanics: Interdepartmental collection of scientific papers of the Institute of Geotechnical Mechanics of the National Academy of Sciences of Ukraine. Dnipropetrovs'k: Issue, 80: 97-101.